THE UNIVERSITY OF CALGARY

Theory and Numerical Solutions of Wave Propagation in Non-linear Thermoelastic Materials

by

David Viet Dang Tran

A THESIS

SUBMITTED TO THE FACULTY OF GRADUATE STUDIES

IN PARTIAL FULFILLMENT OF THE REQUIREMENTS FOR THE

DEGREE OF MASTER OF SCIENCE IN MECHANICAL ENGINEERING

DEPARTMENT OF MECHANICAL ENGINEERING

CALGARY, ALBERTA

JUNE, 1990

National Library of Canada
Bibliothèque nationale du Canada

Canadian Theses Service
Service des thèses canadiennes

Ottawa, Canada
K1A 0N4

ISBN 0-315-61938-4

THE UNIVERSITY OF CALGARY

FACULTY OF GRADUATE STUDIES

The undersigned certify that they have read, and recommend to the Faculty of Graduate Studies for acceptance, a thesis entitled, "Theory and Numerical Solution of Wave Propagation in Non-linear Thermoelastic Materials", submitted by David Viet Dang Tran in partial fullfillment of the requirements for the degree of Master of Science.

Manasa Singh

Dr. M.C. Singh , Supervisor
Department of Mechanical Engineering

M. Epstein

Dr. M. Epstein
Department of Mechanical Engineering

Richard D. Rowe

Dr. R.D. Rowe
Department of Mechanical Engineering

R.S. Dhaliwal

Dr. R.S. Dhaliwal
Department of Mathematics and Statistics

June 25, 1990

ABSTRACT

In this thesis, the problem of one-dimensional coupled thermoelastic waves propagating in non-linear elastic materials under dynamic input at the boundary is examined. Along with the Gibbs free energy, continuum thermodynamics is applied for obtaining the equation of conservation of energy as well as a new model of the constitutive law. The investigation of the behavior of waves propagating in thermoelastic materials is considered from two different points of view namely waves in conductors and waves in non-conductors.

For a conductor, the modified Fourier's law of heat conduction is employed to eliminate the infiniteness of the thermal wave speed which cannot be accepted on physical grounds. New approaches of the characteristic method and the finite element method are applied to study the features at the leading wavefront and to obtain the solutions of the unknowns in the disturbed region .

For a non-conductor, the system of governing equations is reduced by the absence of heat flux. Simple waves and shock waves involved in the problem are analysed by a graphical method. Three different numerical methods are employed for comparing the results: the first based on the method of characteristics, the second based on the finite element method and the third based on the group theoretic technique. The use of similarity coordinates in the location of the wavefront is also investigated.

Finally, discussions on the dynamic response of thermoelastic materials under either mechanical impact or thermal impact are briefly given.

ACKNOWLEDGEMENTS

I wish to express my deepest gratitude to Dr. M.C. Singh, Department of Mechanical Engineering, University of Calgary, for his constant encouragement and guidance throughout the preparation of this thesis.

It is a pleasure to acknowledge the help which I have received from Dr.Epstein who read over the thesis and suggested many improvements of the text and style.

Special thanks go to my fiancée, Hau Chung, and my friends, Dat Le and David Kyejo, for their co-operation, encouragement, patience and support throughout the course of this investigation.

Finally, the financial assistance rendered by the Department of Mechanical Engineering and the financial support received by my supervisor from the Natural Sciences and Engineering Research Council of Canada (NSERC) are gratefully acknowleged.

Kính biếu Bố Mẹ

Trần Đăng Khôi

Trần Thị Cậy

Dedicated to my parents

TRAN DANG KHOI

and

TRAN THI CAY

TABLE OF CONTENTS

	Page
APPROVAL PAGE	(ii)
ABSTRACT	(iii)
ACKNOWLEDGEMENT	(iv)
DEDICATION	(v)
TABLE OF CONTENTS	(vi)
LIST OF TABLES	(x)
LIST OF FIGURES	(xi)
NOMENCLATURE	(xxii)
CHAPTER	
1. INTRODUCTION	1
1.1 BASIC CONCEPTS OF WAVE PROPAGATION	1
1.2 EVOLUTION OF WAVE PROPAGATION IN A THERMOELASTIC MEDIUM	1
1.2.1 Uncoupled Transient Analysis	4
1.2.2 Coupled Transient Analysis	5
1.2.3 Classical Heat Conduction Analysis	7
1.2.4 Modified Heat Conduction Analysis	8
1.3 OBJECTIVES AND ORGANIZATION OF THE THESIS	10
2. THEORY OF NON-LINEAR THERMOELASTIC MATERIALS	13
2.1 EQUATION OF MOTION	14
2.2 THERMODYNAMIC PRELIMINARIES	16
2.2.1 Basic Concepts	16
2.2.2 Continuum Thermodynamics	17
2.2.3 Energy Equation	19

TABLE OF CONTENTS (cont'd)

	Page
2.2.4 Irreversible Process	20
2.3 DYNAMIC COUPLED THERMODYNAMIC EQUATION	25
2.4 MODIFIED HEAT CONDUCTION EQUATION	27
2.5 STRESS-STRAIN-TEMPERATURE RELATION	29
2.6 EQUATION OF WAVE PROPAGATION IN NON-LINEAR THERMOELASTIC MATERIALS	34
3. CONDUCTOR AND NON-CONDUCTOR	37
PART A: BASIC EQUATIONS AND JUMP CONDITIONS FOR CONDUCTING MATERIALS	37
3.1 SPEED OF WAVE PROPAGATION	38
3.2 JUMP CONDITIONS AT THE WAVEFRONTS	47
PART B: BASIC EQUATIONS AND JUMP CONDITIONS FOR NON-CONDUCTING MATERIALS	52
3.3 SIMPLE WAVES	58
3.4 SHOCK WAVES	60
3.4.1 Shock Velocity	60
3.4.2 Shock Amplitude Equations	62
4. NUMERICAL METHODS FOR CONDUCTING MATERIALS	66
4.1 THE METHOD OF CHARACTERISTICS	66
4.1.1 Diamond-Shaped Network	67
4.1.2 Rectangular-Shaped Network	69
4.1.3 Combination Network	70
4.2 NUMERICAL COMPUTATION BY THE CHARACTERISTIC METHOD	72
4.2.1 Grid Points Along the Leading Wavefront	75

TABLE OF CONTENTS (cont'd)

		Page
4.2.2	Grid Points Along the Ot-Axis	80
4.2.3	Interior Grid Points	85
4.3	FINITE ELEMENT METHOD	90
4.3.1	Interior Grid Points	95
4.3.2	Grid Points Along the Ot-Axis and Next to the Leading Wavefront	101
4.3.3	Grid Points Along the Leading Wavefront	104
5.	NUMERICAL METHODS FOR NON-CONDUCTING MATERIALS	106
5.1	THE METHOD OF CHARACTERISTICS	107
5.1.1	Grid Points Along the Front Path	108
5.1.2	Grid Points Along the Ot-Axis	115
5.1.3	Interior Grid Points	116
5.2	THE FINITE ELEMENT METHOD	119
5.2.1	Interior Grid Points	119
5.2.2	Grid Points Along the Ot-Axis and Next to the Front Path	120
5.2.3	Grid Points Along the Front Path	123
5.3	THE SIMILARITY METHOD	123
5.3.1	Construction of the Group of Transformations	125
5.3.2	Independent Absolute Invariants of Group G_6^A	130
5.3.3	Similarity Representation for Basic Equations	136
5.3.4	Similarity Analysis of the Wavefront	138

TABLE OF CONTENTS (cont'd)

	Page
5.3.5 Similarity and Jump Conditions	140
6. NUMERICAL SIMULATIONS	144
6.1 SOME REMARKS OF NUMERICAL SIMULATIONS	144
6.1.1 Stability Condition	144
6.1.2 Computer Implementation	146
6.2 BOUNDARY CONDITIONS	151
6.3 DATA OF THERMOELASTIC MATERIAL PROPERTIES	152
6.4 RESULT REPRESENTATION	152
7. DISCUSSIONS AND CONCLUSION	208
7.1 DISCUSSIONS OF RESULTS	208
7.1.1 For Conducting Materials	206
7.1.2 For Non-Conducting Materials	212
7.2 CONCLUSION	214
7.3 SUGGESTIONS FOR FURTHER WORK	216
REFERENCES	217
APPENDICES	228
A DETERMINING THE UNKNOWNS AT THE ORIGIN FOR THE CASE OF CONDUCTING MATERIALS	228
B DETERMINING THE MASS MATRIX AND STIFFNESS MATRIX FOR A FINITE ELEMENT SCHEME	231

LIST OF TABLES

Table		Page
6.1	PROPERTIES OF THREE DIFFERENT CONDUCTING MATERIALS: STEEL, CAST IRON AND COPPER AT ROOM TEMPERATURE ($20^{o}C$)	153
6.2	PROPERTIES OF TWO DIFFERENT NON-CONDUCTING MATERIALS: RUBBER AND LEATHER AT ROOM TEMPERATURE ($20^{o}C$)	154

LIST OF FIGURES

Figure		Page
3.1	CHARACTERISTIC CURVES PASSING THROUGH POINT E_I^J - THE CASE OF CONDUCTING MATERIALS	44
3.2	PROPAGATING SURFACE OF DISCONTINUITY D(t)	48
3.3	CHARACTERISTIC CURVES PASSING THROUGH POINT E_I^J - THE CASE OF NON-CONDUCTING MATERIALS	57
3.4	STRESS-STRAIN DIAGRAM WITH $n > 1$	59
3.5	CONFIGURATION OF SIMPLE WAVES	59
3.6	STRESS-STRAIN DIAGRAM WITH $n < 1$	61
3.7	FORMATION OF SHOCK WAVES	61
4.1	DIAMOND-SHAPED MESHES	67
4.2	IRREGULAR MESHES	68
4.3	RECTANGULAR MESHES	69
4.4	COMBINATION MESHES	71
4.5	THREE DIFFERENT TYPES OF GRID POINTS IN THE DISTURBED REGION	75
4.6	CHARACTERISTIC CURVES PASSING THROUGH BOUNDARY GRID POINTS - THE CASE OF CONDUCTING MATERIALS	81
4.7	CHARACTERISTIC CURVES PASSING THROUGH INTERIOR GRID POINTS - THE CASE OF CONDUCTING MATERIALS	86
4.8	A FLOW DIAGRAM FOR COMPUTING UNKNOWNS AT POINT A_J^J ALONG THE LEADING WAVEFRONT	91
4.9	A FLOW DIAGRAM FOR COMPUTING UNKNOWNS AT POINT C_0^J ALONG THE Ot-AXIS WITH $v(0,t)$ AND $\theta(0,t)$ PRESCRIBED	92

LIST OF FIGURES (cont'd)

Figure		Page
4.10	A FLOW DIAGRAM FOR COMPUTING UNKNOWNS AT INTERIOR GRID POINT E_I^J	93
4.11	LINEAR BASIC FUNCTION OF THE FINITE ELEMENT METHOD	96
4.12	A FLOW DIAGRAM FOR THE NUMERICAL COMPUTATION BASED ON THE FINITE ELEMENT METHOD	105
5.1	TREATMENT OF POINTS ALONG THE SHOCKFRONT	113
5.2	CHARACTERISTIC CURVES PASSING THROUGH THE BOUNDARY GRID POINTS - THE CASE OF NON-CONDUCTING MATERIALS	116
5.3	CHARACTERISTIC CURVES PASSING THROUGH THE INTERIOR GRID POINTS - THE CASE OF NON-CONDUCTING MATERIALS	118
6.1	INTERMEDIATE GRID POINTS	146
6.2	A FLOW DIAGRAM OF THE CHARACTERISTIC AND THE FINITE ELEMENT SCHEMES AT THE FIRST STEP OF COMPUTATION	148
6.3	A FLOW DIAGRAM OF THE CHARACTERISTIC SCHEME	149
6.4	A FLOW DIAGRAM OF THE FINITE ELEMENT SCHEME	150
6.5	STRESS-STRAIN DIAGRAM OF A COPPER ROD AT ROOM TEMPERATURE	155
6.6a	STRESS RESPONSE OF THREE TYPES OF COPPER RODS TO $v(0,t) = -0.5$ m/s AND $\theta(0,t) = 0$. (BY THE XTIC METHOD)	156
6.6b	VELOCITY RESPONSE OF THREE TYPES OF COPPER RODS TO $v(0,t) = -0.5$ m/s AND $\theta(0,t) = 0$. (BY THE XTIC METHOD)	156

LIST OF FIGURES (cont'd)

Figure		Page
6.6c	TEMPERATURE RESPONSE OF THREE TYPES OF COPPER RODS TO $v(0,t) = -0.5$ m/s AND $\theta(0,t) = 0$. (BY THE XTIC METHOD)	157
6.6d	HEAT FLUX RESPONSE OF THREE TYPES OF COPPER RODS TO $v(0,t) = -0.5$ m/s AND $\theta(0,t) = 0$. (BY THE XTIC METHOD)	157
6.7a	STRESS RESPONSE OF THREE TYPES OF COPPER RODS TO $v(0,t) = -0.5$ m/s AND $\theta(0,t) = 0$. (BY THE F.E METHOD)	158
6.7b	VELOCITY RESPONSE OF THREE TYPES OF COPPER RODS TO $v(0,t) = -0.5$ m/s AND $\theta(0,t) = 0$. (BY THE F.E METHOD)	158
6.7c	TEMPERATURE RESPONSE OF THREE TYPES OF COPPER RODS TO $v(0,t) = -0.5$ m/s AND $\theta(0,t) = 0$. (BY THE XTIC METHOD)	159
6.7d	HEAT FLUX RESPONSE OF THREE TYPES OF COPPER RODS TO $v(0,t) = -0.5$ m/s AND $\theta(0,t) = 0$. (BY THE XTIC METHOD)	159
6.8a	STRESS RESPONSE OF A STEEL ROD ($n = 1.012$) TO $v(0,t) = -0.5$ m/s AND $\theta(0,t) = 0$.	160
6.8b	VELOCITY RESPONSE OF A STEEL ROD ($n = 1.012$) TO $v(0,t) = -0.5$ m/s AND $\theta(0,t) = 0$.	160
6.8c	TEMPERATURE RESPONSE OF A STEEL ROD ($n = 1.012$) TO $v(0,t) = -0.5$ m/s AND $\theta(0,t) = 0$.	161

LIST OF FIGURES (cont'd)

Figure		Page
6.8d	HEAT FLUX RESPONSE OF A STEEL ROD ($n = 1.012$) TO $v(0,t) = -0.5$ m/s, $\theta(0,t) = 0$.	161
6.9a	STRESS RESPONSE OF A CAST IRON ROD ($n = 1.2074$) TO $v(0,t) = -0.5$ m/s, $\theta(0,t) = 0$.	162
6.9b	VELOCITY RESPONSE OF A CAST IRON ROD ($n = 1.2074$) TO $v(0,t) = -0.5$ m/s, $\theta(0,t) = 0$.	162
6.9c	TEMPERATURE RESPONSE OF A CAST IRON ROD ($n = 1.2074$) TO $v(0,t) = -0.5$ m/s, $\theta(0,t) = 0$.	163
6.9d	HEAT FLUX RESPONSE OF A CAST IRON ROD ($n = 1.2074$) TO $v(0,t) = -0.5$ m/s, $\theta(0,t) = 0$.	163
6.10a	STRESS RESPONSE OF A COPPER ROD ($n = 1.047$) TO $v(0,t) = -0.5$ m/s, $\theta(0,t) = 0$.	164
6.10b	VELOCITY RESPONSE OF A COPPER ROD ($n = 1.047$) TO $v(0,t) = -0.5$ m/s, $\theta(0,t) = 0$.	164
6.10c	TEMPERATURE RESPONSE OF A COPPER ROD ($n = 1.047$) TO $v(0,t) = -0.5$ m/s, $\theta(0,t) = 0$.	165
6.10d	HEAT FLUX RESPONSE OF A COPPER ROD ($n = 1.047$) TO $v(0,t) = -0.5$ m/s, $\theta(0,t) = 0$.	165
6.11a	STRESS RESPONSE OF A STEEL ROD ($n = 1.012$) TO $v(0,t) = -120 \times t^{0.2}$ m/s AND $\theta(0,t) = 0$.	166
6.11b	VELOCITY RESPONSE OF A STEEL ROD ($n = 1.012$) TO $v(0,t) = -120 \times t^{0.2}$ m/s AND $\theta(0,t) = 0$.	166
6.11c	TEMPERATURE RESPONSE OF A STEEL ROD ($n = 1.012$) TO $v(0,t) = -120 \times t^{0.2}$ m/s AND $\theta(0,t) = 0$.	167

Figure		Page
6.11d	HEAT FLUX RESPONSE OF A STEEL ROD (n = 1.012) TO $v(0,t) = -120 \times t^{0.2}$ m/s AND $\theta(0,t) = 0$.	167
6.12a	STRESS RESPONSE OF A CAST IRON ROD (n = 1.2074) TO $v(0,t) = -120 \times t^{0.2}$ m/s AND $\theta(0,t) = 0$.	168
6.12b	VELOCITY RESPONSE OF A CAST IRON ROD (n = 1.2074) TO $v(0,t) = -120 \times t^{0.2}$ m/s AND $\theta(0,t) = 0$.	168
6.12c	TEMPERATURE RESPONSE OF A CAST IRON ROD (n = 1.2074) TO $v(0,t) = -120 \times t^{0.2}$ m/s AND $\theta(0,t) = 0$.	169
6.12d	HEAT FLUX RESPONSE OF A CAST IRON ROD (n = 1.2074) TO $v(0,t) = -120 \times t^{0.2}$ m/s AND $\theta(0,t) = 0$.	169
6.13a	STRESS RESPONSE OF A COPPER ROD (n = 1.047) TO $v(0,t) = -120 \times t^{0.2}$ m/s AND $\theta(0,t) = 0$.	170
6.13b	VELOCITY RESPONSE OF A COPPER ROD (n = 1.047) TO $v(0,t) = -120 \times t^{0.2}$ m/s AND $\theta(0,t) = 0$.	170
6.13c	TEMPERATURE RESPONSE OF A COPPER ROD (n = 1.047) TO $v(0,t) = -120 \times t^{0.2}$ m/s AND $\theta(0,t) = 0$.	171
6.13d	HEAT FLUX RESPONSE OF A COPPER ROD (n = 1.047) TO $v(0,t) = -120 \times t^{0.2}$ m/s AND $\theta(0,t) = 0$.	171
6.14a	STRESS RESPONSE OF A STEEL ROD (n = 1.012) TO $\sigma(0,t) = 20$ MPa AND $\theta(0,t) = 0$.	172
6.14b	VELOCITY RESPONSE OF A STEEL ROD (n = 1.012) TO $\sigma(0,t) = 20$ MPa AND $\theta(0,t) = 0$.	172
6.14c	TEMPERATURE RESPONSE OF A STEEL ROD (n = 1.012) TO $\sigma(0,t) = 20$ MPa AND $\theta(0,t) = 0$.	173

Figure		Page
6.14d	HEAT FLUX RESPONSE OF A STEEL ROD (n = 1.012) TO $\sigma(0,t)$ = 20 MPa AND $\theta(0,t)$ = 0.	173
6.15a	STRESS RESPONSE OF A CAST IRON ROD (n = 1.2074) TO $\sigma(0,t)$ = 20 MPa AND $\theta(0,t)$ = 0.	174
6.15b	VELOCITY RESPONSE OF A CAST IRON ROD (n = 1.2074) TO $\sigma(0,t)$ = 20 MPa AND $\theta(0,t)$ = 0.	174
6.15c	TEMPERATURE RESPONSE OF A CAST IRON ROD (n = 1.2074) TO $\sigma(0,t)$ = 20 MPa AND $\theta(0,t)$ = 0.	175
6.15d	HEAT FLUX RESPONSE OF A CAST IRON ROD (n = 1.2074) TO $\sigma(0,t)$ = 20 MPa AND $\theta(0,t)$ = 0.	175
6.16a	STRESS RESPONSE OF A COPPER ROD (n = 1.047) TO $\sigma(0,t)$ = 20 MPa AND $\theta(0,t)$ = 0.	176
6.16b	VELOCITY RESPONSE OF A COPPER ROD (n = 1.047) TO $\sigma(0,t)$ = 20 MPa AND $\theta(0,t)$ = 0.	176
6.16c	TEMPERATURE RESPONSE OF A COPPER ROD (n = 1.047) TO $\sigma(0,t)$ = 20 MPa AND $\theta(0,t)$ = 0.	177
6.16d	HEAT FLUX RESPONSE OF A COPPER ROD (n = 1.047) TO $\sigma(0,t)$ = 20 MPa AND $\theta(0,t)$ = 0.	177
6.17a	STRESS RESPONSE OF A STEEL ROD (n = 1.012) TO $\sigma(0,t) = 5 \times t^{0.2}$ GPa AND $\theta(0,t)$ = 0.	178
6.17b	VELOCITY RESPONSE OF A STEEL ROD (n = 1.012) TO $\sigma(0,t) = 5 \times t^{0.2}$ GPa AND $\theta(0,t)$ = 0.	178
6.17c	TEMPERATURE RESPONSE OF A STEEL ROD (n = 1.012) TO $\sigma(0,t) = 5 \times t^{0.2}$ GPa AND $\theta(0,t)$ = 0.	179

Figure		Page
6.17d	HEAT FLUX RESPONSE OF A STEEL ROD (n = 1.012) TO $\sigma(0,t) = 5 \times t^{0.2}$ GPa AND $\theta(0,t) = 0$.	179
6.18a	STRESS RESPONSE OF A CAST IRON ROD (n = 1.2074) TO $\sigma(0,t) = 5 \times t^{0.2}$ GPa AND $\theta(0,t) = 0$.	180
6.18b	VELOCITY RESPONSE OF A CAST IRON ROD (n = 1.2074) TO $\sigma(0,t) = 5 \times t^{0.2}$ GPa AND $\theta(0,t) = 0$.	180
6.18c	TEMPERATURE RESPONSE OF A CAST IRON ROD (n = 1.2074) TO $\sigma(0,t) = 5 \times t^{0.2}$ GPa AND $\theta(0,t) = 0$.	181
6.18d	HEAT FLUX RESPONSE OF A CAST IRON ROD (n = 1.2074) TO $\sigma(0,t) = 5 \times t^{0.2}$ GPa AND $\theta(0,t) = 0$.	181
6.19a	STRESS RESPONSE OF A COPPER ROD (n = 1.047) TO $\sigma(0,t) = 5 \times t^{0.2}$ GPa AND $\theta(0,t) = 0$.	182
6.19b	VELOCITY RESPONSE OF A COPPER ROD (n = 1.047) TO $\sigma(0,t) = 5 \times t^{0.2}$ GPa AND $\theta(0,t) = 0$.	182
6.19c	TEMPERATURE RESPONSE OF A COPPER ROD (n = 1.047) TO $\sigma(0,t) = 5 \times t^{0.2}$ GPa AND $\theta(0,t) = 0$.	183
6.19d	HEAT FLUX RESPONSE OF A COPPER ROD (n = 1.047) TO $\sigma(0,t) = 5 \times t^{0.2}$ GPa AND $\theta(0,t) = 0$.	183
6.20a	STRESS RESPONSE OF A STEEL ROD (n = 1.012) TO $v(0,t) = 0$. AND $\theta(0,t) = -5\ ^{o}K$.	184
6.20b	VELOCITY RESPONSE OF A STEEL ROD (n = 1.012) TO $v(0,t) = 0$. AND $\theta(0,t) = -5\ ^{o}K$.	184
6.20c	TEMPERATURE RESPONSE OF A STEEL ROD (n = 1.012) TO $v(0,t) = 0$. AND $\theta(0,t) = -5\ ^{o}K$.	185

LIST OF FIGURES (cont'd)

Figure		Page
6.20d	HEAT FLUX RESPONSE OF A STEEL ROD ($n = 1.012$) TO $v(0,t) = 0.$ AND $\theta(0,t) = -5\ ^{\circ}K$.	185
6.21a	STRESS RESPONSE OF A CAST IRON ROD ($n = 1.2074$) TO $v(0,t) = 0.$ AND $\theta(0,t) = -5\ ^{\circ}K$.	186
6.21b	VELOCITY RESPONSE OF A CAST IRON ROD ($n = 1.2074$) TO $v(0,t) = 0.$ AND $\theta(0,t) = -5\ ^{\circ}K$.	186
6.21c	TEMPERATURE RESPONSE OF A CAST IRON ROD ($n = 1.2074$) TO $v(0,t) = 0.$ AND $\theta(0,t) = -5\ ^{\circ}K$.	187
6.21d	HEAT FLUX RESPONSE OF A CAST IRON ROD ($n = 1.2074$) TO $v(0,t) = 0.$ AND $\theta(0,t) = -5\ ^{\circ}K$.	187
6.22a	STRESS RESPONSE OF A COPPER ROD ($n = 1.047$) TO $v(0,t) = 0.$ AND $\theta(0,t) = -5\ ^{\circ}K$.	188
6.22b	VELOCITY RESPONSE OF A COPPER ROD ($n = 1.047$) TO $v(0,t) = 0.$ AND $\theta(0,t) = -5\ ^{\circ}K$.	188
6.22c	TEMPERATURE RESPONSE OF A COPPER ROD ($n=1.047$) TO $v(0,t) = 0.$ AND $\theta(0,t) = -5\ ^{\circ}K$.	189
6.22d	HEAT FLUX RESPONSE OF A COPPER ROD ($n = 1.047$) TO $v(0,t) = 0.$ AND $\theta(0,t) = -5\ ^{\circ}K$.	189
6.23a	STRESS RESPONSE OF A STEEL ROD ($n = 1.012$) TO $\sigma(0,t) = 1$ Pa AND $\theta(0,t) = -5^{\circ}K$.	190
6.23b	VELOCITY RESPONSE OF A STEEL ROD ($n = 1.012$) TO $\sigma(0,t) = 1$ Pa AND $\theta(0,t) = -5^{\circ}K$.	190
6.23c	TEMPERATURE RESPONSE OF A STEEL ROD ($n = 1.012$) TO $\sigma(0,t) = 1$ Pa AND $\theta(0,t) = -5^{\circ}K$.	191

LIST OF FIGURES (cont'd)

Figure		Page
6.23d	HEAT FLUX RESPONSE OF A STEEL ROD ($n = 1.012$) TO $\sigma(0,t) = 1$ Pa AND $\theta(0,t) = -5^{\circ}K$.	191
6.24a	STRESS RESPONSE OF A CAST IRON ROD ($n = 1.2074$) TO $\sigma(0,t) = 1$ Pa AND $\theta(0,t) = -5^{\circ}K$.	192
6.24b	VELOCITY RESPONSE OF A CAST IRON ROD ($n = 1.2074$) TO $\sigma(0,t) = 1$ Pa AND $\theta(0,t) = -5^{\circ}K$.	192
6.24c	TEMPERATURE RESPONSE OF A CAST IRON ROD ($n = 1.2074$) TO $\sigma(0,t) = 1$ Pa AND $\theta(0,t) = -5^{\circ}K$.	193
6.24d	HEAT FLUX RESPONSE OF A CAST IRON ROD ($n = 1.2074$) TO $\sigma(0,t) = 1$ Pa AND $\theta(0,t) = -5^{\circ}K$.	193
6.25a	STRESS RESPONSE OF A COPPER ROD ($n = 1.047$) TO $\sigma(0,t) = 1$ Pa AND $\theta(0,t) = -5^{\circ}K$.	194
6.25b	VELOCITY RESPONSE OF A COPPER ROD ($n = 1.047$) TO $\sigma(0,t) = 1$ Pa AND $\theta(0,t) = -5^{\circ}K$.	194
6.25c	TEMPERATURE RESPONSE OF A COPPER ROD ($n = 1.2074$) TO $\sigma(0,t) = 1$ Pa AND $\theta(0,t) = -5^{\circ}K$.	195
6.25d	HEAT FLUX RESPONSE OF A COPPER ROD ($n = 1.047$) TO $\sigma(0,t) = 1$ Pa AND $\theta(0,t) = -5^{\circ}K$.	195
6.26a	STRESS RESPONSE OF A STRING OF A RUBBER-LIKE MATERIAL ($n = 1.6$) TO $v(0,t) = -0.5$ m/s .	196
6.26b	VELOCITY RESPONSE OF A STRING OF A RUBBER-LIKE MATERIAL ($n = 1.6$) TO $v(0,t) = -0.5$ m/s .	196
6.26c	STRAIN RESPONSE OF A STRING OF A RUBBER-LIKE MATERIAL ($n = 1.6$) TO $v(0,t) = -0.5$ m/s .	197

LIST OF FIGURES (cont'd)

Figure		Page
6.26d	TEMPERATURE RESPONSE OF A STRING OF A RUBBER-LIKE MATERIAL ($n = 1.6$) TO $v(0,t) = -0.5$ m/s .	197
6.27a	STRESS RESPONSE OF A STRING OF A RUBBER-LIKE MATERIAL ($n = 1.6$) TO $v(0,t) = -5 \times t^{0.2}$ m/s .	198
6.27b	VELOCITY RESPONSE OF A STRING OF A RUBBER-LIKE MATERIAL ($n = 1.6$) TO $v(0,t) = -5 \times t^{0.2}$ m/s .	198
6.27c	STRAIN RESPONSE OF A STRING OF A RUBBER-LIKE MATERIAL ($n = 1.6$) TO $v(0,t) = -5 \times t^{0.2}$ m/s .	199
6.27d	TEMPERATURE RESPONSE OF A STRING OF A RUBBER-LIKE MATERIAL ($n = 1.6$) TO $v(0,t) = -5 \times t^{0.2}$ m/s .	199
6.28a	STRESS RESPONSE OF A STRING OF A RUBBER-LIKE MATERIAL ($n = 1.6$) TO $\sigma(0,t) = 0.5 \times t^{0.2}$ MPa .	200
6.28b	VELOCITY RESPONSE OF A STRING OF A RUBBER-LIKE MATERIAL ($n = 1.6$) TO $\sigma(0,t) = 0.5 \times t^{0.2}$ MPa .	200
6.28c	STRAIN RESPONSE OF A STRING A RUBBER-LIKE MATERIAL ($n = 1.6$) TO $\sigma(0,t) = 0.5 \times t^{0.2}$ MPa .	201
6.28d	TEMPERATURE RESPONSE OF A STRING OF A RUBBER-LIKE MATERIAL ($n = 1.6$) TO $\sigma(0,t) = 0.5 \times t^{0.2}$ MPa .	201
6.29a	STRESS RESPONSE OF A STRING OF A LEATHER-LIKE MATERIAL ($n = 0.7545$) TO $v(0,t) = -0.5$ m/s .	202
6.29b	VELOCITY RESPONSE OF A STRING OF A LEATHER-LIKE MATERIAL ($n = 0.7545$) TO $v(0,t) = -0.5$ m/s .	202
6.29c	STRAIN RESPONSE OF A STRING OF A LEATHER-LIKE MATERIAL ($n = 0.7545$) TO $v(0,t) = -0.5$ m/s .	203

LIST OF FIGURES (cont'd)

Figure		Page
6.29d	TEMPERATURE RESPONSE OF A STRING OF A LEATHER-LIKE MATERIAL ($n = 0.7545$) TO $v(0,t) = -0.5$ m/s .	203
6.30a	STRESS RESPONSE OF A STRING OF A LEATHER-LIKE MATERIAL ($n = 0.7545$) TO $v(0,t) = -5 \times t^{0.2}$ m/s .	204
6.30b	VELOCITY RESPONSE OF A STRING OF A LEATHER-LIKE MATERIAL ($n = 0.7545$) TO $v(0,t) = -5 \times t^{0.2}$ m/s .	204
6.30c	STRAIN RESPONSE OF A STRING OF A LEATHER-LIKE MATERIAL ($n = 0.7545$) TO $v(0,t) = -5 \times t^{0.2}$ m/s .	205
6.30d	TEMPERATURE RESPONSE OF A STRING OF A LEATHER-LIKE MATERIAL ($n = 0.7545$) TO $v(0,t) = -5 \times t^{0.2}$ m/s .	205
6.31a	STRESS RESPONSE OF A STRING OF A LEATHER-LIKE MATERIAL ($n = 0.7545$) TO $\sigma(0,t) = 0.5 \times t^{0.2}$ MPa .	206
6.31b	VELOCITY RESPONSE OF A STRING OF A LEATHER-LIKE MATERIAL ($n = 0.7545$) TO $\sigma(0,t) = 0.5 \times t^{0.2}$ MPa .	206
6.31c	STRAIN RESPONSE OF A STRING OF A LEATHER-LIKE MATERIAL ($n = 0.7545$) TO $\sigma(0,t) = 0.5 \times t^{0.2}$ MPa .	207
6.31d	TEMPERATURE RESPONSE OF A STRING OF A LEATHER-LIKE MATERIAL ($n = 0.7545$) TO $\sigma(0,t) = 0.5 \times t^{0.2}$ MPa .	207

NOMENCLATURE

Roman Letters

Symbol	Meaning
$\bar{\bar{a}}_i$	Elastic Constant tensors
$\bar{b}$	Body force
C_σ	Specific heat at constant stress
C_v	Specific heat at constant volume
C_i^+	Characteristic curve having a positive slope
C_i^-	Characteristic curve having a negative slope
$[C_1],[C_2]$	Assembled stiffness matrix
$D(t)$	Singular surface
$\frac{D}{Dt}$	Material derivative
e	Internal energy per unit mass
e_M	Elastic energy density
e_T	Thermal energy density
E	Young's modulus
$\bar{F}$	Total applied force
$\bar{g}$	Temperature gradient
G	Gibbs free energy per unit mass
h_I	Distance between two nodes (I-1) and I
K	Coefficient of thermal conductivity
$[K_1]$	Elemental mass matrix
$[K_2]$	Elemental stiffness matrix
$[K_1]_i$	Submatrix of elemental mass matrix $[K_1]$

Symbol	Meaning
$[K_2]_i$	Submatrix of elemental stiffness matrix $[K_2]$
m_1	Number of dependent variables
$\underline{m}_2$	Number of independent variables
M_L	Linear momentum
$[M_1],[M_2]$	Assembled mass matrix
n	Material parameter of non-linearity
$\tilde{n}$	Normal unit vector to the surface ∂R^*
$\underset{\sim}{N}$	Normal unit vector to the surface $D(t)$
p	Number of physical parameters
$\bar{p}$	Traction force
$\bar{q}$	Heat flux vector per unit surface area
$Q(t)$	Time function of heat flux q in the finite element scheme
r	Internal heat supply per unit time per unit mass
$R_i(x,t)$	Residual errors in the Galerkin's scheme
$S(t)$	Time function of stress σ in the finite element scheme
t	Time
t_{G_1}, t_{H_1}	Positions in time of two points G_1 and H_1 along the wavefront
T	Absolute temperature at time t
T_o	Reference temperature
$\bar{u}$	Displacement vector

Symbol	Meaning
$\underset{\sim}{U}$	Vector denoting the totality of the primary dependent variables (conductors)
$\underset{\sim}{U}_t$	Partial derivative of $\underset{\sim}{U}$ with respect to t
$\underset{\sim}{U}_x$	Partial derivative of $\underset{\sim}{U}$ with respect to x
$\underset{\sim}{U}_2$	Vector denoting the totality of the primary dependent variables (non-conductors)
$\underset{\sim}{U}_{2t}$	Partial derivative of $\underset{\sim}{U}_2$ with respect to t
$\underset{\sim}{U}_{2x}$	Partial derivative of $\underset{\sim}{U}_2$ with respect to x
$\bar{v}$	Particle velocity vector
$\dot{v}$	Derivative of particle velocity v with respect to t
V_a	Wave speed in an adiabatic state
V_e	Speed of purely elastic wave
V_f	Speed of wavefront
V_i	Speed of wavelets
V_M	Uncoupled mechanical wave speed
V_o	Parameter of velocity impact
V_s	Sound speed
$V(t)$	Time function of particle velocity v in the finite element scheme
$W(R^*)$	Working rate of the body R^* with respect to time
$w_i(x)$	Test function in the finite element scheme
$\bar{x}$	Position of a particle in a reference configuration
$\bar{X}$	Position of a particle in the Cartesian coordinates
X_w	Location of the wavefront

Greek Letters

Symbol	Meaning
α	Coefficient of thermal expansion
δ	Parameter
δ_{ij}	Kronecker delta-symbol
$\Delta(t)$	Time function of temperature difference θ in the finite element scheme
Δt	Time increment
Δx	Spatial increment
$\bar{\bar{\varepsilon}}$	Total strain tensor
$\bar{\bar{\varepsilon}}_M$	Mechanical strain tensor
$\bar{\bar{\varepsilon}}_T$	Thermal strain tensor
$\dot{\varepsilon}$	Derivative of axial strain with respect to t
ε_x	Derivative of axial strain with respect to x
η	Similarity coordinate
η_w	Location of the wavefront in the similarity coordinate
θ	Temperature difference
θ_o	Parameter of temperature impact
λ_i	Eigenvalues
λ'	First Lamé constant
μ	Modulus of elasticity
μ'	Second Lamé constant
ν_c	Courant-Friedrichs-Léwis number
ξ_1,ξ_2	Damping factors

Symbol	Meaning
ρ	Mass density
$\bar{\bar{\sigma}}$	Total stress tensor
σ_{ij}	Stress tensor in Cartesian coordinates
σ_o	Parameter of stress impact
τ_o	Thermal relaxation time
$\phi_i(x)$	Linear basis function in the finite element scheme
ψ	Helmholtz free energy
ψ_o	Hemlholtz free energy at the reference state
$\underset{\sim}{\ell}^{(1)}, \underset{\sim}{\ell}^{(2)}, \ldots, \underset{\sim}{\ell}^{(7)}$	Eigenvectors
$\mathcal{S}$	Entropy per unit mass
$\nabla\theta$	Gradient of temperature difference

ABBREVIATIONS

CFL	Courant-Friedrichs-Léwy
FDM	Finite difference method
F.E	Finite element
PDEs	Partial differential equations
XTIC	Characteristic

CHAPTER 1
INTRODUCTION

1.1 BASIC CONCEPTS OF WAVE PROPAGATION

In recent years, the subject of wave propagation in elastic solids has seen a dramatic growth. The subject has attracted investigators who possess strong background in applied science, mathematics, and engineering. Besides the intricacy and challenge of the wave theory, the practical determination of the dynamic response of materials becomes more attractive due to its wide range of applications in connection with important problems arising from resource exploration, earthquake phenomena, artificial explosives, etc.

The nature of wave propagation is best explained in a picture of an ocean with the rollers sweeping onto the beach from the open sea, or in terms of a simplest body such as a stretched elastic string. With a suddenly applied force or heat on a body, the initiation of displacement will travel outward from the point of application. It is said there is a propagating wave in the body [1.1].

1.2 EVOLUTION OF WAVE PROPAGATION IN A THERMOELASTIC MEDIUM

The early work on elastic waves received its impetus from the view prevalent until the mid-nineteenth century, that *light* could be considered as a wave propagating in the elastic ether.

With regard to the works especially dealing with the propagation of waves in elastic solids, a number of earlier references are given in the book by Kolsky [1.2]. Furthermore, a review article which contains most of the contributions to the field until 1964 was given by Miklowitz [1.3].

The theory of stress waves in perfectly elastic solids is well developed as a mathematical consequence of Hooke's law and the equations of motion. A one-dimensional wave in linear elastic materials is generally governed by a simple partial differential equation whose solution can be determined by using different methods for the solution of linear partial differential equations. Several papers and monographs [1.4-1.7] have dealt with linear elastic waves.

The problem of elastic wave becomes more complicated when a body is no longer a perfect elastic medium. Due to encumbrance of geometrical complications to display the essential aspects of motion of a continuum as well as to describe the governing system of non-linear equations, some authors have presented the characteristic features of wave motion in the body in one-dimensional geometry. The speed of non-linear waves is not constant but may vary from point to point in the medium; the shock occurs whenever its wavelets converge.

About 300 years ago, the first non-linear law of elasticity was introduced by Leibnitz (1690) when observing the experimental data from a tensile test in a gut string. In 1695, Bernoulli proposed a parabolic law in contrast to the experiment of Hooke (1678) who suggested a linear law for the relationship between stress and strain in an elastic medium. In the nineteenth century, experimenters [1.8] also demonstrated that Hooke's law was only an approximation applied to many kinds of solids including metals.

Several papers dealing with one-dimensional wave propagation in non-linear elastic medium were published recently. Frydrychowicz and Singh [1.9] have considered the propagation of disturbances along a thin elastic rod whose constitutive law is in the form of a power law. Elzanowski and Epstein [1.10] have assumed a quadratic form for stress-strain relations to examine the decay and growth of the amplitude shock waves.

Early experimental evidence concerning the phenomenon of deformation-induced heating was reported by Joule (1859) [1.11] who studied thermal effects of tension on various solids. His results persuaded researchers to pay more attention to the deformation-induced heating of materials .

Thermoelasticity, as indicated by the name itself, concerns the effects of heat on stresses and deformations in an elastic medium and vice versa, the effects on temperature distribution caused by the elastic deformation. The internal energy, therefore, becomes a function of the deformation and the temperature. The thermoelastic processes are coupled and not totally reversible because of the dissipation of energy taking place during heat transfer, especially during heat conduction. Strictly speaking, the actual process of thermoelastic deformation of a body is a non-equilibrium process whose irreversibility is due to the temperature gradient. A medium which is characterized by a reversible elastic process and an irreversible thermal process will hereafter be called a *thermoelastic medium* [1.12].

After World War II, thermo-mechanical waves played a special rolè to fulfill the requirements of high technology for the design of steam and gas turbines, jet motors, rockets, high-speed aircraft, nuclear reactors and so on [1.13].

The earliest work regarding the effects of temperature in the formulation of elasticity problems is that of Duhamel-Newman on the foundation of the constitutive equations of the linear theory of thermoelasticity valid for the general type of anisotropic materials [1.14]. Even so, their simple theorem is insufficient in the presence of thermal gradients. A more rigorous and satisfactory analysis can be achieved only by applying the fundamental laws of thermodynamics since the relation of stress-strain-temperature can be explicitly established with the aid of thermodynamic laws.

The literature on the theory of thermoelastic waves is too vast to be reviewed here. One of the recent works on this field is due to Boley [1.15] who successfully made a general review of the subject of thermal effects in solids and structures up to 1984.

The stages involved in analyzing propagation of disturbances in a thermoelastic medium generally consist of the following categories: (i) uncoupled transient analysis, (ii) coupled transient analysis, (iii) classical heat conduction analysis, and (iv) modified heat conduction analysis.

1.2.1 Uncoupled Transient Analysis

In this category, effects of inertia have been taken into account in thermoelastic problems, however, the coupling between mechanical and thermal fields is neglected. The first attempt to examine inertia effects in a dynamic problem of thermoelasticity is apparently due to Danilovskaya [1.16] who reconsidered the Duhamel's hypothesis (1837), referred to as the conventional quasi-static approach. According to Duhamel, inertia terms could be neglected in the governing field equations when the time rate of temperature change was slow enough so that these terms would not be significant. Danilovskaya's investigation showed that the stress distribution can be obtained in an elastic half space even though its boundary is subjected to a thermal impact. Since the appearance of her first paper, inertia terms became more meaningful in many thermoelastic problems.

Later, Nowacki [1.17] was regarded as a particular contributor in this subject for his achievements of several close-to-exact solutions to the uncoupled dynamics of three-dimensional thermoelastic problems with a time-dependent heat source in the interior of a medium.

Sternberg and Chakravorty [1.18] carried Danilovskaya's solution further by applying a ramp-type heating to the boundary. Meanwhile Michaels [1.19] determined the relation between heating rates and the magnitude of induced stresses in a slender rod subjected to thermal heating at one end. Various cases of the distribution of temperature and stress in a thin thermoelastic rod are also investigated by many other research workers [1.20, 1.21, 1.22,1.23].

1.2.2 Coupled Transient Analysis

Unlike the uncoupled transient problem, the coupled transient problem takes into account the coupling term representing the interaction between thermal and mechanical fields in the governing equations. Uncoupled analysis is, of course, impossible if problems are examined in which the details of the propagation and decay of disturbances in solids are important.

One of the first application of coupled theory is due to Sneddon [1.24] who attempted to calculate the distribution of temperature and stress in a linear thermoelastic thin rod suffered by mechanical or thermal disturbances at the boundary.

Dillon [1.25] obtained the solutions of dynamic response of a long slender thermoelastic bar subjected to three different kinds of boundary conditions: (i) a step function in temperature, (ii) a step function in strain, and (iii) constant velocity impact. By assuming the coupling parameter as unity, he was able to convert directly the Laplace transformed solutions. The final solutions showed a remarkable deviation from the uncoupled solutions.

Nickell and Sackman [1.26] applied the variational method for the approximated solution of fully coupled initial-boundary value problems in linear thermoelasticity. As an illustration, they considered two types of boundary problem in one-dimension: (i) rapid heating of a half-space through a thermally conducting boundary layer, and (ii) gradual heating of the boundary surface of the half-space. They also emphasized that the variational principles derived in their earlier paper [1.27] can even apply to complicated problems along with inhomogeneous, anisotropic continuum in any dimensions.

By means of perturbation series in the coupling parameter, Soler and Brull [1.28] aimed to solve the governing equations through a simple set of perturbation techniques which is admissible (sufficiently small coupling parameter) and approximated results were in excellent agreement with exact solutions.

Recently, with the advance of modern computational facilities, Ting and Chen [1.29] adopted the finite element method to improve the sophisticated formulation of field theories and to obtain solutions of some boundary value problems. Three different types of temperature boundary condition were employed: (i) a sudden surface heating, (ii) a convective surface heating, and (iii) a ramp-type surface heating. The comparisons among uncoupled solutions, coupled solutions and analytical solutions were also illustrated.

1.2.3 Classical Heat Conduction Analysis

Problems which belong to this category have characteristic features as follows:

(i) The conventional Fourier's law of heat conduction in solids remains valid.

(ii) The set of basic equations of uncoupled or coupled thermoelasticity is composed of a mixed hyperbolic-parabolic type.

(iii) The infinite speed of a thermal wave and the finite speed of mechanical wave can be predicted.

Besides the aforementioned articles, numerous papers dealing with this subject are classified by:

a. *Neglecting the coupling effect*: Gładysz [1.30] applied the same theory used by Sternberg and Chakravorty for a closed-form solution to a plane wave propagation problem for a half-space whose boundary was subjected to uniform time-dependent heating. Fan et al [1.31] applied the finite element method to the uncoupled dynamic problem of thermoelasticity. The method was employed for the prediction of temperature and stress fields of an axi-symmetric object made of alloy steel. The analytical solutions obtained compared well with the experimentally measured data.

b. *Including the coupling effect*: Hetnarski [1.32] considered the propagation of spherical stress and temperature waves.

The solutions were obtained by him in the form of a series of functions of the coupling parameter.

With the help of Laplace transform technique, Achenbach [1.33] studied the wave motion in one and three-dimensional problems by subjecting the boundaries to stress and temperature impact. By the same method, Daimaruya and Ishikawa [1.34] discussed the coupled thermoelastic wave problems in one-dimension. They examined the problems under two types of boundary conditions: (i) a constant velocity impact with adiabatic conditions over the boundary plane, and (ii) a sudden strain with constant temperature. The discontinuity at the wavefront was also determined in the above two papers. Further work can be observed in the one-dimensional problem of Dhaliwal and Shanker [1.35] who obtained the numerical solutions of the infinite thermoelastic cylindrical hole along with two types of boundary conditions, namely (i) step input of stress and zero temperature, and (ii) step input of temperature and zero stress, at one end of the cylinder. Many other articles [1.36,1.37] have also treated similar problems.

1.2.4 Modified Heat Conduction Analysis

In this case, the heat conduction equation based on the Fourier's law in the governing equations must be modified so that the infinite speed of thermal wave is no longer valid. Recent experiments performed on solid helium by Ackerman et al [1.38], Ackerman and Overton [1.39] and on sodium fluoride by Jackson and Walker [1.40] have confirmed that the thermal wave (or second sound) with a finite velocity does indeed occur in solids.

These observations have led to a strong agreement for modifying the heat conduction equation from the parabolic type to a hyperbolic one. The short time called the thermal relaxation time is taken into account to establish a steady-state heat conduction whenever a temperature gradient is suddenly generated in a solid. As a result, a wave-type equation for heat transport is obtained by the *ad hoc* addition of an adjusted term in the classical Fourier form.

With a new form of the modified Fourier's law of heat equation, many papers relating to the problems of waves propagating in thermoelastic materials have been published.

Nayfeh [1.41] was seeking the solutions of the wave motion in a two-dimensional homogeneous, isotropic elastic solid subjected to time-dependent temperature and temperature gradient line-load which are suddenly applied to the free surface of the half-space. The extensive work of studying the distribution of stress and temperature fields due to the application of an instantaneous heat source in an unbounded medium is also presented by the same author [1.42]. Further investigations can be found in Chandrasekharaiah's article [1.43]. In the context of the linearized Green-Lindsay thermoelastic theory [1.44], he considered one-dimensional disturbances in a thermoelastic half-space whose plane boundary is subjected to a step in strain or temperature. His recent work [1.45] which contains a bibliographical review of the relevant literature dealing with the existence of finite speed for the propagation of thermal waves during the past twenty years is also noticeable.

1.3 OBJECTIVES AND ORGANIZATION OF THE THESIS

In the above discussion of thermoelastic waves, most of the authors have assumed that the stress-strain relation for the thermoelastic materials obeys Hooke's law, and the problems may be solved in a framework of linearized approximation. However, real solids may not be perfectly elastic as observed from experiments of stretching a rubber band or a thin copper wire. Thus, the linearized theory seems to be unsuitable for these kinds of materials. To fill the gap between the problem of non-linear elastic waves and the problem of linear thermoelastic waves, this thesis will study thermo-mechanical waves in non-linear elastic materials with the following assumptions:

(i) The materials are assumed to be isotropic and homogeneous.

(ii) The thermal strain is linear due to the effect of temperature field T which differs only slightly from the reference temperature T_o, i.e. $\left|\frac{T-T_o}{T_o}\right| \ll 1$. The thermal and mechanical properties are then kept constant throughout the investigation.

(iii) Only the mechanical strain is a non-linear function of stress.

(iv) The total strain, being the sum of thermal and mechanical strain, is very small as compared with unity.

For the sake of analysis, this dissertation is organized into seven chapters whose salient features are summarized in the following:

In Chapter 2, a general theory of non-linear thermoelasticity is developed on the basis of thermodynamic laws and the internal state variables. The equation of conservation of energy, as well as a new model of the constitutive relation of stress-strain-temperature is constructed by the use of the Gibbs free energy. Approximated formulae for thermal relaxation time τ_o are also given with a brief discussion.

In Chapter 3, a semi-infinite non-linear thermoelastic material is examined in one-dimension. The governing basic equations along with the prescribed auxiliary conditions for a conductor and for a non-conductor are fully expressed. Simple waves and shock waves are examined in the case of non-conducting materials. A new set of equations used to obtain a path of the shockfront and unknowns along and across it is presented. Jump conditions are also determined in each kind of materials.

In Chapter 4, the development of two computational algorithms for the numerical solutions to the system of equations describing the wave motion in conductors is presented. The first algorithm is based on the numerical method of characteristics while the second employs the generalized Galerkin scheme. A new kind of grid points namely *combination grid points* is proposed to study the features at the leading wavefront and to obtain the approximate solutions of unknowns in the disturbed region.

Chapter 5 presents three methods of computation to obtain the solutions from the set of equations along with its auxiliary conditions given in Part B of Chapter 3. The first two methods, namely the characteristic method and the finite element method are similar to the ones discussed in Chapter 4. The third one is based on the similarity analysis. The application of the group theoretic technique in this case is considered as a new aspect of this method applying to a thermoelastic material . A new approach of treating shock waves is also introduced.

In Chapter 6, numerical representations of the wave propagating in non-linear thermoelastic solids are divided into two categories:

(i) The dynamic response of elastic conducting materials such as steel, cast iron and copper.

(ii) The dynamic response of elastic non-conducting materials such as rubber and leather.

In chapter 7, the thesis is closed with discussions of the results.

Conclusions and suggestions for further work are also presented.

CHAPTER 2
THEORY OF NON-LINEAR THERMOELASTIC MATERIALS

This chapter is devoted to the theory of non-linear thermoelasticity based on the application of thermodynamic principles to the process of deformation. The examination makes use of the basic hypotheses which underline all investigations regarding continuous media, and concepts which arise from two different disciplines, namely mechanics and thermodynamics. Although the theory of linear thermoelasticity is well developed in the literature [2.1-2.6], it can not be properly applied to materials which have nonlinear stress-strain relations even when sustaining small deformations. Within the elastic range, the linearized theory is not applicable to highly non-linear materials. The purpose of this chapter is to develop a stress-strain-temperature relation for a non-linear thermoelastic material which is assumed to be homogeneous and isotropic .

Let coordinates be referred to a fixed rectangular Cartesian coordinate system. In general, $\bar{X}$ indicates a point in the material by giving its position vector in the reference configuration, while $\bar{x}$ in the function $\hat{x}(\bar{X},t)$ expresses the motion in its position vector at time t. For the sake of simplicity, we use the same system to describe both the original and the deformed configurations of the body.

The particle displacement vector $\bar{u}$ is defined by:

$$\bar{u} = \bar{x} - \bar{X} \quad . \tag{2.1}$$

With the assumption of infinitesimal deformation, the geometrically linear strain tensor $\bar{\bar{\varepsilon}}$ can be expressed as:

$$\bar{\bar{\varepsilon}} = \frac{\partial \bar{u}}{\partial \bar{x}} \quad . \tag{2.2}$$

2.1 EQUATION OF MOTION

Based on the Newton's second law of motion which states that *the material rate of change of the linear momentum of a body is equal to the resultant of applied forces acting on the body* [1.14], the equation of motion is derived. Assuming that at an instant of time t, a continuous medium R^* bounded by a closed surface ∂R^* contains the linear momentum:

$$\bar{M}_L = \int_{R^*} \rho \bar{v} d\mathcal{V} \quad . \tag{2.3}$$

If the body is subjected to external forces which are now separated into the surface traction $\bar{p}$ and the body force per unit volume $\bar{b}$, the resultant force is:

$$\bar{F} = \int_{\partial R^*} \bar{p} da + \int_{R^*} \bar{b} d\mathcal{V} \quad . \tag{2.4}$$

According to Cauchy's formula, the surface traction $\bar{p}$ is defined by:

$$\bar{p} = \bar{\bar{\sigma}} . \hat{n} \quad , \tag{2.5}$$

where $\bar{\bar{\sigma}}$ is considered as the symmetric stress tensor [2.7], and $\hat{n}$ is the normal unit vector directed outward from the surface da which is an element of the surface ∂R^*.

Replacing $\bar{p}$ in equation (2.4) by the right-hand side of (2.5) and transforming into a volume integral by Gauss's theorem, we have:

$$\bar{F} = \int_{R^*} (\mathrm{div}\ \bar{\bar{\sigma}} + \bar{b})\ d\mathcal{V} \quad . \tag{2.6}$$

According to Newton's second law:

$$\frac{D}{Dt} \bar{M}_L = \bar{F} \quad . \tag{2.7}$$

where $\frac{D}{Dt}$ denotes material time derivative [1.14].

Substituting equations (2.3) and (2.6) into equation (2.7), and applying the transport theorem to the left-hand side term, we have :

$$\int_{R^*} \left[\frac{\partial}{\partial t} (\rho\bar{v}) + \frac{\partial}{\partial \bar{x}} (\rho\bar{v}.\bar{v}) \right] d\mathcal{V} = \int_{R^*} (\mathrm{div}\ \bar{\bar{\sigma}} + \bar{b})\ d\mathcal{V} \quad . \tag{2.8}$$

Since this equation must hold for any arbitrary region of R^*, the integral on the two sides must be equal. Thus:

$$\frac{\partial}{\partial t} (\rho\bar{v}) + \frac{\partial}{\partial \bar{x}} (\rho\bar{v}.\bar{v}) = \mathrm{div}\ \bar{\bar{\sigma}} + \bar{b} \quad . \tag{2.9}$$

The left-hand side of (2.9) can be written as:

$$\bar{v} \left(\frac{\partial \rho}{\partial t} + \mathrm{div}(\rho\bar{v}) \right) + \rho \left(\frac{\partial \bar{v}}{\partial t} + \bar{v}\ .\ \mathrm{grad}(\bar{v}) \right) \quad . \tag{2.10}$$

The first parenthesis vanishes on account of the equation of continuity:

$$\frac{\partial \rho}{\partial t} + \mathrm{div}(\rho\bar{v}) = 0 \quad , \tag{2.11a}$$

hence

$$\rho \frac{D\bar{v}}{Dt} = \mathrm{div}\ \bar{\bar{\sigma}} + \bar{b} \quad , \tag{2.11b}$$

where

$$\frac{D\bar{v}}{Dt} = \frac{\partial \bar{v}}{\partial t} + \bar{v} \cdot \text{grad}(\bar{v}) \quad . \tag{2.11c}$$

The equation (2.11b) is recognized as the Eulerian equation of motion of the body, where ρ is mass per unit volume, and $\bar{v}$ is the particle velocity vector defined by:

$$\bar{v} = \frac{\partial \bar{u}}{\partial t} \quad . \tag{2.12}$$

2.2 THERMODYNAMIC PRELIMINARIES

2.2.1 Basic Concepts

The theory of thermoelasticity is concerned with questions of equilibrium of bodies treated as thermodynamic systems whose interaction with the environment is confined to mechanical work, heat exchange or external forces. Thus, it forms a part of the thermodynamic field.

Before discussing about the laws of thermodynamics a brief summary of the basic structure of the classical theory of thermodynamics is given here.

A thermodynamic system is defined as a material body consisting of a large number of particles and interacting with the environment. The state of a thermodynamic system is composed of a number of macroscopic quantities known as the *thermodynamic variables* or the *state variables*, each of which describes a different property of the system. If a certain state variable can be expressed in terms of a set of other state variables, then the variable is called a *state function* and the relationship is considered as an *equation of state*.

For a given system, if the values of the state variables are independent of time, the system is said to be in *thermodynamic equilibrium*. Whereas if the state variables vary with time, the system is said to *undergo a process*. Furthermore, the system is said to be *homogeneous* if the state variables do not depend on space coordinates.

Generally, thermodynamic processes are divided into two types. The first is known as *thermodynamics of reversible process* which is assumed to be in equilibrium with the surroundings without any change in the environment whereas the second is known as *thermodynamics of irreversible process* in which it is impossible for the thermodynamic system to go back to its initial state without some change taking place in the environment.

Besides, the system is said to be *adiabatic* if there is no energy exchange with the surroundings in the form of heat.

2.2.2 Continuum Thermodynamics

The concept of internal variables was first introduced into thermodynamics by Onsager [2.8, 2.9]. The application to continuum thermodynamics was then focused on by Eckart [2.10], Biot [2.11, 2.12], Coleman and Mizel [2.13]. Based on the previous publications [2.11, 2.12] in which the concept of generalized free energy was introduced, Biot [2.14] formulated the general laws of thermoelasticity in a variational form along with a minimum entropy production principle. Coleman and Mizel [2.13] derived a set of necessary and sufficient conditions for the validity of the Clausius-Duhem inequality in the continuum sufficiently closed to equilibrium. They assumed that in the constitutive equations, the basic independent variables are taken to be the temperature, the temperature gradient, the strain and the velocity gradient.

Further, Coleman and Gurtin [2.15] studied various types of dynamical stabilities of the thermodynamics of non-linear materials with internal state variables. The investigations of Coleman and his co-workers have had strong effects of the development of the models of constitutive relations for thermoelastic materials. This is because those models are easily correlated with the microstructural changes associated with the physical deformation mechanisms.

In linearized theory, many authors [2.16-2.19] have adopted the stress-strain-temperature relation in the general form:

$$\sigma_{ij} = 2\mu' \varepsilon_{ij} + \delta_{ij} \left[\lambda' \varepsilon_{kk} - (3\lambda' + 2\mu')\, \alpha\theta\right] \quad , \qquad (2.13)$$

where σ_{ij} is a stress tensor and is obtained from derivation of Helmholtz free energy ψ with respect to strain tensor ε_{ij}.

Helmholtz free energy ψ expressed as a function of independent internal variables ε_{ij} and θ is given as follows [1.13,2.1]:

$$\psi = \psi_o + \frac{\lambda'}{2} \varepsilon_{kk}^2 + \mu' \varepsilon_{ij}\varepsilon_{ij} - (3\lambda' + 2\mu')\, \alpha\, (T-T_o)\, \varepsilon_{kk} + \text{higher terms} \qquad (2.14)$$

where ψ_o is the free energy at the reference state, λ', μ' are Lamé elastic constants, α is the coefficient of linear thermal expansion, θ is the temperature excess over a reference absolute temperature T_o, and δ_{ij} is the Kronecker delta-symbol.

In linear thermoelasticity, the higher terms in equation (2.14) are neglected. And even though these terms are included to define a non-linear stress-strain-temperature relation as such the relation cannot be widely used in application. This is because, in equation (2.14), the elastic constants of order higher than the third are yet unknown (and the third order elastic constants are known only for some materials) [2.20].

The above correlation between stress and free energy is mainly developed from two basic laws of thermodynamics, namely the first law and the second law.

2.2.3 Energy Equation

According to the first law of thermodynamics which asserts that [2.21]:

$$\int_{R^*} \rho\bar{v} \cdot \frac{D\bar{v}}{Dt}\, d\mathcal{V} + \frac{D}{Dt}\int_{R^*} \rho e\, d\mathcal{V} = W(R^*) - \int_{\partial R^*} \bar{q}\cdot\tilde{n}\, da + \int_{\partial R^*} \rho r\, d\mathcal{V} \; , \tag{2.15}$$

in which the rate of work $W(R^*)$ of the body R^* at time t is defined by [2.7]:

$$W(R^*) = \int_{R^*} \bar{\bar{\sigma}} \cdot \frac{D\bar{\bar{\varepsilon}}}{Dt}\, d\mathcal{V} + \int_{R^*} \bar{v} \cdot (\mathrm{div}\bar{\bar{\sigma}} + \bar{b})\, d\mathcal{V} \quad . \tag{2.16}$$

Substitution of equation (2.11b) into equation (2.16) gives:

$$W(R^*) = \int_{R^*} \bar{\bar{\sigma}} \cdot \frac{D\bar{\bar{\varepsilon}}}{Dt}\, d\mathcal{V} + \int_{R^*} \rho\bar{v} \cdot \frac{D\bar{v}}{Dt}\, d\mathcal{V} \quad . \tag{2.17}$$

Applying the Gauss's theorem, the second term on the right-hand side of equation (2.15) can be expressed as:

$$\int_{\partial R^*} \bar{q}\cdot\tilde{n}\, da = \int_{R^*} \mathrm{div}\,\bar{q}\, d\mathcal{V} \quad . \tag{2.18}$$

Substituting equations (2.17, 2.18) into equation (2.15) and simplifying, we obtain:

$$\int_{R^*} \left\{ \rho \frac{De}{Dt} - \left(\bar{\bar{\sigma}} \cdot \frac{D\bar{\bar{\varepsilon}}}{Dt} - \text{div } \bar{q} + \rho r \right) \right\} d\mathcal{V} = 0 \quad . \qquad (2.19)$$

The above equation applies to any arbitrary small region of the medium. It follows that the integrand of (2.19) is identically zero at every point of the medium. Thus, the local equivalent of the first law of thermodynamics can be written as:

$$\rho \frac{De}{Dt} = \bar{\bar{\sigma}} \cdot \frac{D\bar{\bar{\varepsilon}}}{Dt} - \text{div } \bar{q} + \rho r \quad , \qquad (2.20)$$

where e is the internal energy per unit mass, r is the internal heat supply per unit time per unit mass and $\bar{q}$ is the heat flux vector.

2.2.4 Irreversible Process

The actual process of thermoelastic deformation of a body subjected to the external forces and non-uniform heating can be expressed by the Clausius-Duhem inequality or the second law of thermodynamics which states that [2.21]:

$$\frac{D}{Dt} \int_{R^*} \rho \mathcal{S} d\mathcal{V} - \int_{R^*} \frac{\rho r}{T} \, d\mathcal{V} + \int_{\partial R^*} \frac{1}{T} \, \bar{q} . \hat{n} \, da \geq 0 \quad . \qquad (2.21)$$

Applying the Gauss's theorem to the last term of (2.21) yields:

$$\int_{R^*} \left\{ \rho \frac{D\mathcal{S}}{Dt} - \frac{\rho r}{T} + \text{div} \left(\frac{\bar{q}}{T} \right) \right\} d\mathcal{V} \geq 0 \ , \qquad (2.22)$$

from which the following local version of the Clausius-Duhem inequality is expressed as:

$$\rho \frac{D\mathcal{S}}{Dt} - \frac{\rho r}{T} + \text{div} \left(\frac{\bar{q}}{T} \right) \geq 0 \ , \qquad (2.23a)$$

or

$$\rho T \frac{D\mathcal{S}}{Dt} \geq \rho r - \text{div}\ \bar{q} + \frac{\bar{q}}{T} \cdot \bar{g} \quad , \tag{2.23b}$$

where

$$\bar{g} = \text{grad}\ T \quad , \tag{2.24}$$

and $\mathcal{S}$ is internal entropy production per unit mass.

The second law of thermodynamics represented by the inequality (2.23b) explains that the rate of increase in the entropy stored in the body R^* exceeds the sum of entropy flux through the surface ∂R^* and entropy supply inside R^*. The Clausius-Duhem inequality also plays a dual role in inducing *a priori* restrictions on constitutive relations.

2.2.5 Internal State Variables

In an elastic and homogeneous material, it is usually assumed that the internal energy e, the Helmholtz free energy ψ, the stress $\bar{\bar{\sigma}}$, the specific entropy $\mathcal{S}$ and the heat flux $\bar{q}$ are state functions of the state variables strain $\bar{\bar{\varepsilon}}$, the temperature T and the temperature gradient $\bar{g}$ [2.4].

However, in this thesis, we take the strain $\bar{\bar{\varepsilon}}$ as a state function, the stress $\bar{\bar{\sigma}}$ and temperature T as the independent variables, and employ the Gibbs free energy G instead of Helmholtz free energy ψ.

Such a choice of strain as a function of stress and temperature is practically based on two reasons:

(i) The constitutive relation obtained may be similar to those found from the experiments [1.8].

(ii) In testing materials, the stresses are often easier to control than the strain and much of the published data for heat capacity are based on the constant stress tests.

The above approach has been employed by Schapery [2.22] and Lubiner [2.23], and yields a constitutive equation which expresses strain in terms of stress and temperature histories. Chang and Cozzarelli [2.24] have also used it to develop the constitutive relation for a non-linear thermoviscoelastic material.

In the light of above discussion, we assume the equations of state of a thermoelastic material as follows:

$$\bar{\bar{\varepsilon}} = \hat{\bar{\bar{\varepsilon}}} \, [\bar{\bar{\sigma}}(\bar{x},t),\ T(\bar{x},t),\ \bar{g}(\bar{x},t)] \ , \tag{2.25a}$$

$$e = \hat{e} \, [\bar{\bar{\sigma}}(\bar{x},t),\ T(\bar{x},t),\ \bar{g}(\bar{x},t)] \ , \tag{2.25b}$$

$$G = \hat{G} \, [\bar{\bar{\sigma}}(\bar{x},t),\ T(\bar{x},t),\ \bar{g}(\bar{x},t)] \ , \tag{2.25c}$$

$$\mathcal{S} = \hat{\mathcal{S}} \, [\bar{\bar{\sigma}}(\bar{x},t),\ T(\bar{x},t),\ \bar{g}(\bar{x},t)] \ , \tag{2.25d}$$

$$\bar{q} = \hat{\bar{q}} \, [\bar{\bar{\sigma}}(\bar{x},t),\ T(\bar{x},t),\ \bar{g}(\bar{x},t)] \ , \tag{2.25e}$$

where G denotes the Gibbs free energy and is defined by [2.25]:

$$G = e - \mathcal{S}T - \frac{\bar{\bar{\sigma}} \cdot \bar{\bar{\varepsilon}}}{\rho} \quad . \tag{2.26}$$

Rearranging the terms in equation (2.20) gives:

$$\bar{\bar{\sigma}} \ . \ \frac{D\bar{\bar{\varepsilon}}}{Dt} = \mathrm{div}\ \bar{q} + \rho\dot{e} - \rho r \quad . \tag{2.27}$$

Adding equation (2.27) to inequality (2.23b) yields:

$$\rho\dot{e} - \rho T \cdot \frac{D\mathscr{S}}{Dt} - \bar{\bar{\sigma}} \cdot \frac{D\bar{\bar{\varepsilon}}}{Dt} + \frac{\bar{q}}{T} \cdot \bar{g} \le 0 \quad . \qquad (2.28)$$

From equation (2.26):

$$e = G + \mathscr{S}T + \frac{\bar{\bar{\sigma}}.\bar{\bar{\varepsilon}}}{\rho} \quad . \qquad (2.29)$$

Taking material derivative on both sides of equation (2.29) and then substituting the result into equation (2.28), we have:

$$\rho \frac{DG}{Dt} + \rho\mathscr{S} \frac{DT}{Dt} + \frac{D\bar{\bar{\sigma}}}{Dt} \cdot \bar{\bar{\varepsilon}} + \frac{\bar{q}}{T} \cdot \bar{g} \le 0 \quad . \qquad (2.30)$$

Since the Gibbs free energy function is a state function, its material derivative is obtained from equation (2.25c) as:

$$\frac{DG}{Dt} = \frac{\partial\hat{G}}{\partial\bar{\bar{\sigma}}} \cdot \frac{D\bar{\bar{\sigma}}}{Dt} + \frac{\partial\hat{G}}{\partial T}\frac{DT}{Dt} + \frac{\partial\hat{G}}{\partial\bar{g}} \cdot \frac{D\bar{g}}{Dt} \quad . \qquad (2.31)$$

Replacing $\frac{DG}{Dt}$ in the inequality (2.30) by the right-hand side terms of the equation (2.31), we arrive at the following form:

$$\left(\rho \frac{\partial\hat{G}}{\partial\bar{\bar{\sigma}}} + \bar{\bar{\varepsilon}}\right) \cdot \frac{D\bar{\bar{\sigma}}}{Dt} + \rho \left(\frac{\partial\hat{G}}{\partial T} + \mathscr{S}\right) \frac{DT}{Dt} + \rho \left(\frac{\partial\hat{G}}{\partial\bar{g}}\right) \cdot \frac{D\bar{g}}{Dt} + \frac{\bar{q}}{T} \cdot \bar{g} \le 0 \ . \qquad (2.32)$$

By the same token, taking material derivative on both sides of equation (2.29) and substituting into equation (2.20) wherein $\frac{DG}{Dt}$ is eliminated by means of the equation (2.31), we obtain:

$$\left(\rho \frac{\partial\hat{G}}{\partial\bar{\bar{\sigma}}} + \bar{\bar{\varepsilon}}\right) \cdot \frac{D\bar{\bar{\sigma}}}{Dt} + \rho \left(\frac{\partial\hat{G}}{\partial T} + \mathscr{S}\right) \frac{DT}{Dt} + \rho\left(\frac{\partial\hat{G}}{\partial\bar{g}}\right) \cdot \frac{D\bar{g}}{Dt} + \rho \frac{D\mathscr{S}}{Dt} T + \operatorname{div} \bar{q} - \rho r = 0 \quad . \qquad (2.33)$$

The proceeding equations must retain their validity for all conceivable thermoelastic processes involving the constitutive relations

(2.25). Since the expressions appearing in the parentheses in equations (2.32, 2.33) do not depend upon $\frac{D\bar{\bar{\sigma}}}{Dt}$, $\frac{DT}{Dt}$ and $\frac{D\bar{g}}{Dt}$, the expressions must vanish identically. This leads to the consequent conditions:

$$\rho \frac{\partial \hat{G}}{\partial \bar{\bar{\sigma}}} + \bar{\bar{\varepsilon}} = 0 \; , \tag{2.34a}$$

$$\frac{\partial \hat{G}}{\partial T} + \mathcal{S} = 0 \; , \tag{2.34b}$$

$$\frac{\partial \hat{G}}{\partial \bar{g}} = 0 \; . \tag{2.34c}$$

Equation (2.34c) confirms that the Gibbs free energy function is independent of the temperature gradient $\bar{g}$. Furthermore, the strain $\bar{\bar{\varepsilon}}$ and the entropy $\mathcal{S}$ are correlated to G in the terms of stress $\bar{\bar{\sigma}}$ and temperature T through equations (2.34a) and (2.34b). Without loss of any generality, strain $\bar{\bar{\varepsilon}}$, internal energy e and entropy $\mathcal{S}$ can be expressed as functions which are independent of the temperature gradient $\bar{g}$.

Thus, in the internal state variables, the constitutive equations of a homogeneous, isotropic and non-linear thermoelastic materials can be represented by:

$$\bar{\bar{\varepsilon}} = \hat{\bar{\bar{\varepsilon}}} \, (\bar{\bar{\sigma}}, T) \; , \tag{2.35a}$$

$$e = \hat{e} \, (\bar{\bar{\sigma}}, T) \; , \tag{2.35b}$$

$$G = \hat{G} \, (\bar{\bar{\sigma}}, T) \; , \tag{2.35c}$$

$$\mathcal{S} = \hat{\mathcal{S}} \, (\bar{\bar{\sigma}}, T) \; , \tag{2.35d}$$

$$\bar{q} = \hat{\bar{\bar{q}}} \, (\bar{\bar{\sigma}}, T, \bar{g}) \; . \tag{2.35e}$$

The remaining terms in equations (2.32) and (2.33) are written as:

$$\frac{\bar{q}}{T} \cdot \bar{g} \leq 0 \ , \tag{2.36a}$$

$$\rho T \frac{D\mathcal{S}}{Dt} + \text{div } \bar{q} - \rho r = 0 \ . \tag{2.36b}$$

The inequality (2.36a) tells us that heat cannot flow in the direction of increasing temperature.

2.3 DYNAMIC COUPLED THERMODYNAMIC EQUATION

Unlike the uncoupled theory, the coupled theory takes into account the coupling effect between the stress and temperature fields during the thermodynamic process. Even though the coupling parameters of certain types of materials are very small as compared with unity [2.26], the disagreements between the two theories can be possible not only because of their distinct formulae [2.1] but also their physical features at the wavefront [2.27, 2.28].

The distinctions between the coupled and uncoupled solutions of a linear thermoelastic material can be summarized in the following:

(i) In both cases the velocity of the elastic wavefront is constant as the wave propagates in the medium. However, in coupled theory, the stress and strain discontinuities at the front decrease exponentially [2.29] as the wavefront propagates, whereas, the uncoupled theory predicts no change in those mechanical discontinuities at the wavefront.

(ii) In the coupled theory, the mechanical state interacts with the thermal state, and the discontinuities of the first or second derivatives of the temperature may take place at the wavefront. But in the uncoupled theory the temperature and its derivative are continuous everywhere since the temperature is explicitly calculated from the Fourier equation and is not influenced by the mechanical disturbance.

Even though it seems practically admissible to ignore the effects of coupling, as compared with those of internal heat generation and heat exchange with the surrounding [2.6], we are still interested in the coupled theory because of its acceptable physical phenomenon which is concluded from the experiment [2.30], and having some attractive effects on problems of wave propagation.

The coupled thermoelastic equation composed of both thermal term and mechanical term is deduced from the first law of thermodynamics.

The equations (2.34a,b) can be rewritten as:

$$\bar{\bar{\varepsilon}} = -\rho \left(\frac{\partial \hat{G}}{\partial \bar{\bar{\sigma}}} \right) , \tag{2.37}$$

$$\mathcal{S} = - \left(\frac{\partial \hat{G}}{\partial T} \right) . \tag{2.38}$$

The material derivative of equation (2.38) is:

$$\frac{D\mathcal{S}}{Dt} = - \left(\frac{\partial^2 \hat{G}}{\partial T^2} \frac{DT}{Dt} + \frac{\partial^2 \hat{G}}{\partial T \partial \bar{\bar{\sigma}}} \cdot \frac{D\bar{\bar{\sigma}}}{Dt} \right) . \tag{2.39}$$

Since the strain $\bar{\bar{\varepsilon}}$ is a function of stress $\bar{\bar{\sigma}}$ and temperature T, the partial derivative of both sides of equation (2.37) with respect to temperature T yields:

$$\frac{\partial \bar{\bar{\varepsilon}}}{\partial T} = - \rho \frac{\partial^2 \hat{G}}{\partial T \partial \bar{\bar{\sigma}}} \quad . \tag{2.40}$$

Introducing equation (2.40) into equation (2.39), making use of (2.36b) and rearranging the equation results in:

$$\text{div } \bar{q} - \rho \left(\frac{\partial^2 \hat{G}}{\partial T^2} \frac{DT}{Dt} \right) T + T \frac{\partial \bar{\bar{\varepsilon}}}{\partial T} \cdot \frac{D\bar{\bar{\sigma}}}{Dt} - \rho r = 0 \quad . \tag{2.41}$$

By definition, the specific heat at constant stress C_σ is given by [2.31]:

$$C_\sigma = T \left(\frac{\partial \mathcal{S}}{\partial T} \right)_{\bar{\bar{\sigma}}} = - T \left(\frac{\partial^2 \hat{G}}{\partial T^2} \right)_{\bar{\bar{\sigma}}} \quad . \tag{2.42}$$

Replacing the term $\left(- \frac{\partial^2 \hat{G}}{\partial T^2} \right)$ in equation (2.41) by C_σ leads to:

$$\text{div } \bar{q} + \rho C_\sigma \frac{DT}{Dt} + T \frac{\partial \bar{\bar{\varepsilon}}}{\partial T} \cdot \frac{D\bar{\bar{\sigma}}}{Dt} - \rho r = 0 \quad . \tag{2.43}$$

The equation (2.43) is also called the equation of conservation of energy since it is derived from the first law of thermodynamics.

It is mentioned that $\frac{D}{Dt}(\ \ )$ denotes the material derivative of a variable and is defined by [2.25]:

$$\frac{D}{Dt}(\ \ ) = \frac{\partial}{\partial t}(\ \ ) + \bar{v} \cdot \text{grad}(\ \ ) \quad , \tag{2.44a}$$

which, under the approximation of small velocities, is the same as the partial derivative with respect to time t. Thus, we can assume that:

$$\frac{D}{Dt}(\ \ ) = \frac{\partial}{\partial t}(\ \ ) = (\dot{\ }) \quad . \tag{2.44b}$$

2.4 MODIFIED HEAT CONDUCTION EQUATION

According to the classical Fourier's law (1822), the speed of thermal disturbances propagating in the body is infinity. However, this is an inadmissible physical phenomenon and the enormous speed of thermal waves cannot be achieved instantaneously since thermal energy is carried by molecular motions and proceeds with a finite speed [2.32]. An objection against Fourier's law can be made on the basis of general physical principles from which it is clear that neither heat nor temperature disturbances can propagate faster than the velocity of *light*. Such a paradox can be eliminated by an appropriate generalization of Fourier's law.

From a mathematical point of view, the finite thermal wave speed would be attained if the classical Fourier's law which leads to a partial differential equation of parabolic type could be modified so that it becomes an equation of hyperbolic type without much change in the behaviour of its solutions so far as practical problems of thermoelasticity are concerned.

For an isotropic medium, the Fourier's law is expressed by [2.33]:

$$\bar{q} = - K\nabla\theta \ , \qquad (2.45)$$

where K is a positive constant , called the coefficient of thermal conductivity, $\nabla\theta$ is the temperature gradient and θ denotes the change in the absolute basic temperature T_o.

The modified form of the Fourier's law of heat conduction, usually referred to as the well-known Maxwell-Cattaneo equation, is of the form:

$$\tau_o \frac{\partial \bar{q}}{\partial t} + \bar{q} = - K\nabla\theta \quad , \tag{2.46}$$

where τ_o is the *thermal relaxation time*, a constant which is measured in seconds and characterizes the second sound velocity. The physical meaning of τ_o is interpreted as the time required to establish steady-state heat conduction in a volume element when a temperature difference is suddenly produced on the element. The term of $\tau_o \frac{\partial q}{\partial t}$ in equation (2.46) is the so-called *thermal inertia* [2.34].

Based on the above modified Fourier's equation (2.46), several aspects of thermoelastic waves in solids have been examined by numerous authors such as Norwood and Warren [2.35], Popov [2.36], Sawatzky and Moodie [2.37]. Also, Lebon and Lambermont [2.38] attempted to derive the generalized equation of heat conduction from the point of view of basic continuum thermodynamics.

If it is agreed that the speed of heat propagation may not exceed the sound speed V_s , then a formula for the relaxation time τ_o can be assumed to be [2.6] :

$$\tau_o = \frac{K}{\rho C_v V_s^2} \quad , \tag{2.47}$$

where C_v is the specific heat at constant volume. The other term of τ_o that was defined by Chester [2.39] and Maurier [2.40] is:

$$\tau_o = \frac{3K}{\rho C_v V_s^2} \quad . \tag{2.48}$$

Values of relaxation time for some materials can be found in the table from Francis [2.41] and, generally, τ_o is in the range from 10^{-14} second to 10^{-10} second [1.45]. Moreover, an experimental procedure for investigating the influence of the magnitude of τ_o has been proposed by Mengi and Turhan [2.42] as well.

2.5 STRESS-STRAIN-TEMPERATURE RELATION

The development of constitutive law forms an important part of this thesis since it expresses the characteristic non-linearity of the materials which are brought into the investigation of wave propagation. The various models of the non-linear constitutive relations have been contributed by many authors.

For a slightly non-linear isotropic material Dillon [2.43] expanded the Helmholtz free energy ψ into a power series in strain invariants and temperature increments:

$$\psi = a_2 II + a_3 III + a_5^2 I + a_6^3 I + a_7^2 \theta + a_8 I\theta + a_9 I\ II + a_{10}^2 I\theta + a_{11} II\theta + a_{12}\theta^3 + a_{13} I^2\theta + a_{14} I^4 + a_{15} II^2 + a_{16} I\ II \quad , \qquad (2.49)$$

where

$$I = \varepsilon_{ii} \ , \qquad (2.50a)$$

$$II = \frac{1}{2} (\varepsilon_{ii}\varepsilon_{jj} - \varepsilon_{ij}\varepsilon_{ij}) \ , \qquad (2.50b)$$

$$III = \det (\varepsilon_{ij}) \ , \qquad (2.50c)$$

are the invariants of strain tensor ε_{ij} in the Cartesian system and a_k ($k = 2,3,5...$) are elastic constants.

The stress is then defined as:

$$\Sigma_{ij} = \rho \frac{\partial \psi}{\partial \varepsilon_{ij}} \quad . \qquad (2.51)$$

By the same token, Jekot [2.44] introduced the free energy function ψ

accounting for the non-linear thermal effects in the form of:

$$\psi(T,I_{(i)}) = a_0(T) + a_1(T)I_{(1)} + a_2(T)I_{(2)} + a_3(T)I_{(3)} + a_4(T)I_{(1)}^2 + a_5(T)I_{(1)}I_{(2)} + a_6(T)I_{(1)} + \ldots \quad , \tag{2.52}$$

where $I_{(i)}$, $i = 1,2,3$ are the Green tensor invariants and the coefficients $a_k(T)$, $k = 0,1,2,\ldots,6$ depend on temperature.

However, equations (2.49) and (2.52) are not widely used in practical computations since the numerical values of their higher elastic constants (third order and up) are as yet unknown. Because of that reason, most solutions of thermoelastic problems have been solved in the framework of linearized approximations of Hooke's law.

In contrast to their work, here we expand the Gibbs free energy function $\hat{G}$ into a Taylor series in the neighborhood of its natural state (i.e. when $\bar{\bar{\sigma}} = 0$, $T = T_o$):

$$\hat{G}(\bar{\bar{\sigma}},T) = \hat{G}(0,T_o) + \frac{\partial\hat{G}(0,T_o)}{\partial\bar{\bar{\sigma}}} \cdot \bar{\bar{\sigma}} + \frac{\partial\hat{G}(0,T_o)}{\partial T}\,\theta + \frac{1}{2}\left[\frac{\partial^2\hat{G}(0,T_o)}{\partial\bar{\bar{\sigma}}^2} \cdot \bar{\bar{\sigma}}^2 + 2\,\frac{\partial^2\hat{G}(0,T_o)}{\partial\bar{\bar{\sigma}}\partial T} \cdot \bar{\bar{\sigma}}\theta + \frac{\partial^2\hat{G}(0,T)}{\partial T^2}\,\theta^2\right] + \frac{1}{6}\left[\frac{\partial^3\hat{G}(0,T_o)}{\partial\bar{\bar{\sigma}}^3} \cdot \bar{\bar{\sigma}}^3 + 3\,\frac{\partial^3\hat{G}(0,T_o)}{\partial\bar{\bar{\sigma}}^2\partial T} \cdot \bar{\bar{\sigma}}^2\theta + 3\,\frac{\partial^3\hat{G}(0,T_o)}{\partial\bar{\bar{\sigma}}\partial T^2} \cdot \bar{\bar{\sigma}}\theta^2 + \frac{\partial^3\hat{G}(0,T_o)}{\partial T^3}\,\theta^3\right] + \text{higher order terms} \quad , \tag{2.53}$$

where $\theta = T - T_o$ is the temperature difference.

At the natural state, the constant $\hat{G}\,(0,T_o)$ may be assumed to be zero. From the definition of strain given by equation (2.37) we have:

$$\bar{\bar{\varepsilon}}\,(\bar{\bar{\sigma}},T) = -\rho \left\{ \frac{\partial \hat{G}(0,T_o)}{\partial \bar{\bar{\sigma}}} + \frac{\partial^2 \hat{G}(0,T_o)}{\partial \bar{\bar{\sigma}}^2} \cdot \bar{\bar{\sigma}} + \frac{1}{2}\frac{\partial^3 \hat{G}(0,T_o)}{\partial \bar{\bar{\sigma}}^3} \cdot \bar{\bar{\sigma}}^2 + \frac{\partial^2 \hat{G}(0,T_o)}{\partial \bar{\bar{\sigma}}^2 \partial T}\,\theta + \frac{\partial^3 \hat{G}(0,T_o)}{\partial \bar{\bar{\sigma}}^2 \partial T} \cdot \bar{\bar{\sigma}}\theta + \frac{1}{2}\frac{\partial^3 \hat{G}(0,T_o)}{\partial \bar{\bar{\sigma}} \partial T^2}\,\theta^2 \right\} . \tag{2.54}$$

From equation (2.42), the specific heat at constant stress yields:

$$C_\sigma = -T \left\{ \frac{\partial^2 \hat{G}(0,T_o)}{\partial T^2} + \frac{\partial^3 \hat{G}(0,T_o)}{\partial T^3}\,\theta + \frac{\partial^3 \hat{G}(0,T_o)}{\partial \bar{\bar{\sigma}} \partial T^2} \cdot \bar{\bar{\sigma}} \right\} . \tag{2.55}$$

The constant of specific heat which is assumed to be independent of the temperature θ and stress tensor $\bar{\bar{\sigma}}$ may be incorporated into the equation by taking:

$$\frac{\partial^3 \hat{G}(0,T_o)}{\partial T^3} = \frac{\partial^3 \hat{G}(0,T_o)}{\partial \bar{\bar{\sigma}} \partial T^2} = 0 \quad . \tag{2.56}$$

Furthermore, the total strain $\bar{\bar{\varepsilon}}$ is simply composed of the mechanical strain $\bar{\bar{\varepsilon}}_M$ and the thermal strain $\bar{\bar{\varepsilon}}_T$, i.e.:

$$\bar{\bar{\varepsilon}} = \bar{\bar{\varepsilon}}_M + \bar{\bar{\varepsilon}}_T \quad , \tag{2.57}$$

in which $\bar{\bar{\varepsilon}}_T$ can be approximated in the linear form [2.20]:

$$\bar{\bar{\varepsilon}}_T = \alpha\theta \quad , \tag{2.58}$$

where α denotes the coefficient of linear thermal expansion for isotropic materials. Thus, without loss of generality, we may assume that:

$$\frac{\partial^3 \hat{G}(0,T_o)}{\partial \bar{\bar{\sigma}}^2 \partial T} = 0 \quad . \tag{2.59}$$

Following the constraints expressed by equations (2.56) and (2.59), the total strain $\bar{\bar{\varepsilon}}$ can be written as:

$$\bar{\bar{\varepsilon}}\ (\bar{\bar{\sigma}},T) = \bar{\bar{a}}_1 + \bar{\bar{a}}_2.\bar{\bar{\sigma}} + \bar{\bar{a}}_3.\bar{\bar{\sigma}}^2 + \alpha\theta \quad , \tag{2.60}$$

where $\bar{\bar{a}}_i$, i = 1,2,3 are elastic constant tensors and are defined by:

$$\bar{\bar{a}}_1 = -\rho \frac{\partial \hat{G}(0,T_o)}{\partial \bar{\bar{\sigma}}} \quad , \tag{2.61a}$$

$$\bar{\bar{a}}_2 = -\rho \frac{\partial^2 \hat{G}(0,T_o)}{\partial \bar{\bar{\sigma}}^2} \quad , \tag{2.61b}$$

$$\bar{\bar{a}}_3 = -\frac{1}{2}\rho \frac{\partial^3 \hat{G}(0,T_o)}{\partial \bar{\bar{\sigma}}^3} \quad , \tag{2.61c}$$

$$\alpha = -\rho \frac{\partial^2 \hat{G}(0,T_o)}{\partial \bar{\bar{\sigma}} \partial T} \quad . \tag{2.61d}$$

At the reference state, $\bar{\bar{\sigma}} = \theta = \bar{\bar{\varepsilon}} = 0$ leads to $\bar{\bar{a}}_1 = 0$. The equation (2.60) becomes:

$$\bar{\bar{\varepsilon}}\ (\bar{\bar{\sigma}},T) = \bar{\bar{a}}_2.\bar{\bar{\sigma}} + \bar{\bar{a}}_3.\bar{\bar{\sigma}}^2 + \alpha\theta \quad . \tag{2.62}$$

Because of this dèliberate emphasis on the non-linear relation of stress and strain, we will consider only one-dimensional thin medium in which the primary stress is the axial one. Equation (2.62) is then expressible in one-dimension as:

$$\varepsilon(\sigma,T) = a_2\sigma + a_3\sigma^2 + \alpha\theta \quad , \tag{2.63}$$

where ε and σ represent for normal strain and normal stress, respectively, a_2 and a_3 are elastic constant.

The quadratic expression in equation (2.63) has an equivalent form such that:

$$a_2\sigma + a_3\sigma^2 \simeq \left(\frac{\sigma}{\mu}\right)^n \quad . \tag{2.64}$$

Substituting the equivalence (2.64) into (2.63) yields:

$$\varepsilon(\sigma,T) = \left(\frac{\sigma}{\mu}\right)^n + \alpha\theta \ , \tag{2.65}$$

where μ is the modulus of elasticity and n is the parameter of non-linearity. When n equals unity, a linear relation is obtained as a result.

2.6 EQUATIONS OF WAVE PROPAGATION IN NON-LINEAR THERMOELASTIC MATERIALS

With the aid of the corresponding equation (2.44b), equation of motion (2.11b) wherein the body force $\bar{b}$ is neglected, and equation of conservation of energy (2.43), are stated in one-dimension as:

$$\frac{\partial\sigma}{\partial x} = \frac{\partial v}{\partial t} \quad , \tag{2.66}$$

$$\frac{\partial q}{\partial x} + \rho C_\sigma \frac{\partial T}{\partial t} + T\frac{\partial \varepsilon}{\partial T}\frac{\partial \sigma}{\partial t} - \rho r = 0 \quad . \tag{2.67}$$

In order to remain in the realm of an elastic region, we may assume that the change of temperature θ is small as compared with the reference temperature T_o, i.e. $\left|\frac{\theta}{T_o}\right| \ll 1$, this leads to $T \simeq T_o$ [2.5].

Differentiating equation (2.65) with respect to temperature T, we have:

$$\frac{\partial \varepsilon}{\partial T} = \frac{\partial \varepsilon}{\partial \theta} = \alpha \quad . \tag{2.68}$$

The equation (2.67) then yields:

$$\frac{\partial q}{\partial x} + \rho C_\sigma \frac{\partial \theta}{\partial t} + \alpha T_o \frac{\partial \sigma}{\partial t} = 0 \ , \tag{2.69}$$

where the internal heat supply r is neglected.

By taking derivative on both sides of equation (2.2) with respect to time t and on both sides of equation (2.12) with respect to x when these equations are in one-dimensional form, the compatibility equation is obtained as:

$$\frac{\partial \varepsilon}{\partial t} = \frac{\partial v}{\partial x} \quad . \tag{2.70}$$

The equations (2.65) and (2.70) can be combined to yield:

$$\frac{\partial v}{\partial x} = \frac{\partial}{\partial t}\left\{\left(\frac{\sigma}{\mu}\right)^n + \alpha\theta\right\} \quad . \tag{2.71}$$

In general, the system of equations being necessary to investigate one-dimensional wave motion in non-linear thermoelastic materials is summarized as follows:

Equation of Motion: $$\frac{\partial \sigma}{\partial x} = \rho \frac{\partial v}{\partial t} \ , \tag{2.72a}$$

Constitutive relation: $$\frac{\partial v}{\partial x} = \frac{\partial}{\partial t}\left\{\left(\frac{\sigma}{\mu}\right)^n + \alpha\theta\right\} \ , \tag{2.72b}$$

Modified heat conduction: $$\tau_o \frac{\partial q}{\partial t} + q = - K \frac{\partial \theta}{\partial x} , \quad (2.72c)$$

Conservation of energy equation: $$\frac{\partial q}{\partial x} + \rho C_\sigma \frac{\partial \theta}{\partial t} + \alpha T_o \frac{\partial \sigma}{\partial t} = 0 . \quad (2.72d)$$

It is also mentioned that the presence of the last term in equation (2.72d) is regarded as a sign of coupling existing between thermal and mechanical fields. The existence of coupling implies that the solution of the system (2.72) must proceed simultaneously. The last term is neglected if the interaction of thermal and mechanical energy is ignored.

In the above, the constitutive relation (2.65) is developed on the basis of principles of thermodynamics based on Gibbs free energy. This form is not seen by the author in the literature. The results, thus, are only compared by numerical solutions of the system (2.72) solved by different methods as seen in the following chapters.

CHAPTER 3
CONDUCTOR AND NON-CONDUCTOR

In this chapter we consider the behavior of one-dimensional waves propagating in elastic bodies which are divided into two types:

(i) elastic conducting materials

(ii) elastic non-conducting materials.

In practice, solids are usually classified as metals or non-metals. From experiment, we conclude that the first kind of materials has much higher coefficients of thermal conductivities than the second one. Due to impurities, the real solids; commercial building materials, being conglomerates of various solid constituents of different conductivities, display variations of thermal conductivities. This depends on the thermal properties of the constituents as well as on the level of their porosity. However, to limit the scope of this thesis, the solids have been assumed to be homogeneous and isotropic. The thermal properties are, therefore, kept unchanged through the course of investigation.

By definition, a solid is termed a non-conductor if its coefficient of thermal conductivity $K = 0$, and a definite conductor or conductor simply called for $K \neq 0$.

PART A: BASIC EQUATIONS AND JUMP CONDITIONS FOR CONDUCTING MATERIALS

Most metallic materials are considered as conducting materials since they have high thermal conductivities and allow energy to transfer from hot to cold regions of substances easily by molecular interaction. The heat flux then always exists along with the wave propagating in the medium.

Considering a semi-infinite thin rod of non-linear thermoelastic material which is assumed to be initially at rest and at uniform temperature T_o, the system (2.72) can be written in the following form:

$$\rho \frac{\partial v}{\partial t} - \frac{\partial \sigma}{\partial x} = 0 \quad , \tag{3.1a}$$

$$\frac{n}{\mu^n} \sigma^{n-1} \frac{\partial \sigma}{\partial t} + \alpha \frac{\partial \theta}{\partial t} - \frac{\partial v}{\partial x} = 0 \quad , \tag{3.1b}$$

$$\tau_o \frac{\partial q}{\partial t} + q + K \frac{\partial \theta}{\partial x} = 0 \quad , \tag{3.1c}$$

$$\alpha T_o \frac{\partial \sigma}{\partial t} + \rho C_\sigma \frac{\partial \theta}{\partial t} + \frac{\partial q}{\partial x} = 0 \quad . \tag{3.1d}$$

3.1 SPEEDS OF WAVE PROPAGATION

The equations (3.1) are recognized as a hyperbolic system of four quasi-linear partial differential equations for the set of unknowns $\{v, \sigma, \theta, q\}$ and can be written in a general form as:

$$[A_1]\, \underset{\sim}{U}_t + [A_2]\, \underset{\sim}{U}_x = \underset{\sim}{A}_3 \quad , \tag{3.2}$$

in which:

$$\underset{\sim}{U} = [v \quad \sigma \quad \theta \quad q]^T \quad , \tag{3.3a}$$

$$\underset{\sim}{U}_t = \frac{\partial \underset{\sim}{U}}{\partial t} = [v_t \quad \sigma_t \quad \theta_t \quad q_t]^T \quad , \tag{3.3b}$$

$$U_x = \frac{\partial \underset{\sim}{U}}{\partial x} = [v_x \quad \sigma_x \quad \theta_x \quad q_x]^T \quad , \tag{3.3c}$$

$$[A_1] = \begin{bmatrix} \rho & 0 & 0 & 0 \\ 0 & \frac{n}{\mu^n}\sigma^{n-1} & \alpha & 0 \\ 0 & 0 & 0 & \tau_o \\ 0 & \alpha T_o & \rho C_\sigma & 0 \end{bmatrix} , \tag{3.3d}$$

$$[A_2] = \begin{bmatrix} 0 & -1 & 0 & 0 \\ -1 & 0 & 0 & 0 \\ 0 & 0 & K & 0 \\ 0 & 0 & 0 & 1 \end{bmatrix} , \tag{3.3e}$$

$$\underset{\sim}{A}_3 = [0 \quad 0 \quad -q \quad 0]^T , \tag{3.3f}$$

where the superscript 'T' denotes the transpose of a matrix.

It is also noted that the matrix $[A_1]$ is non-singular since:

$$\det [A_1] = \rho\tau_o \left(\alpha^2 T_o - \frac{n}{\mu^n}\sigma^{n-1}\rho C_\sigma\right) \neq 0 \quad . \tag{3.4}$$

After premultiplying the system (3.2) by $[A_1]^{-1}$, it is expressible in a new form as:

$$\underset{\sim}{U}_t + [B_1]\underset{\sim}{U}_x = \underset{\sim}{B}_2 , \tag{3.5}$$

where:

$$[B_1] = [A_1]^{-1}[A_2] , \tag{3.6a}$$

$$\underset{\sim}{B}_2 = [A_1]^{-1}\underset{\sim}{A}_3 , \tag{3.6b}$$

$[A_1]^{-1}$ is the inverse of matrix $[A_1]$ and is obtained as:

$$[A_1]^{-1} = \begin{bmatrix} \frac{1}{\rho} & 0 & 0 & 0 \\ 0 & \rho C_\sigma \gamma & 0 & -\alpha\gamma \\ 0 & -\alpha T_o \gamma & 0 & \beta\gamma \\ 0 & 0 & \frac{1}{\tau_o} & 0 \end{bmatrix} . \qquad (3.7a)$$

The matrix $[B_1]$ and vector $\underset{\sim}{B}_2$ are found to be:

$$[B_1] = \begin{bmatrix} 0 & -\frac{1}{\rho} & 0 & 0 \\ -\rho C_\sigma \gamma & 0 & 0 & -\alpha\gamma \\ \alpha T_o \gamma & 0 & 0 & \beta\gamma \\ 0 & 0 & \frac{K}{\tau_o} & 0 \end{bmatrix} , \qquad (3.7b)$$

$$\underset{\sim}{B}_2 = [0 \quad 0 \quad 0 \quad -\frac{q}{\tau_o}]^T , \qquad (3.7c)$$

where:

$$\beta = \frac{n}{\mu^n} \sigma^{n-1} , \qquad (3.8a)$$

$$\gamma = \frac{1}{\beta\rho C_\sigma - \alpha^2 T_o} . \qquad (3.8b)$$

The characteristic curves along which the canonical equations are valid are governed by the characteristic equation [3.1]:

$$\det ([B_1] - \lambda[I]) = 0 , \qquad (3.9)$$

in which λ's are eigenvalues and [I] is the unit matrix (4×4). The matrix $([B_1] - \lambda[I])$ is given by:

$$([B_1] - \lambda[I]) = \begin{bmatrix} -\lambda & -\frac{1}{\rho} & 0 & 0 \\ -\rho C_\sigma \gamma & -\lambda & 0 & -\alpha\gamma \\ \alpha T_o \gamma & 0 & -\lambda & \beta\lambda \\ 0 & 0 & \frac{K}{\tau_o} & -\lambda \end{bmatrix} . \quad (3.10)$$

The determinant of (3.10) yields:

$$\lambda^4 - \lambda^2 \left(\frac{K\beta\gamma}{\tau_o} + C_\sigma \gamma\right) + \frac{K\gamma}{\rho\tau_o} = 0 \quad . \quad (3.11)$$

Let:

$$V_e^2 = \frac{1}{\beta\rho} \quad , \quad (3.12)$$

which is considered as the speed of purely elastic waves.

Dividing both sides of equation (3.11) by $(V_e)^4$ and simplifying, we have:

$$\left(\frac{\lambda}{V_e}\right)^4 - \left(\gamma_1 + \beta_1 + 1\right) \left(\frac{\lambda}{V_e}\right)^2 + \gamma_1 = 0 \quad . \quad (3.13)$$

The eigenvalues are then obtained as:

$$\lambda_i = \pm V_e \left\{ \frac{(\gamma_1+\beta_1+1) \pm \sqrt{(\gamma_1+\beta_1+1)^2 - 4\gamma_1}}{2} \right\}^{1/2} , \quad (3.14)$$

where:

$$i = 1,2,3,4 \quad ,$$

$$\gamma_1 = \frac{K\gamma}{\tau_o}\,\rho\beta^2 \quad , \tag{3.15a}$$

$$\beta_1 = \alpha^2 T_o \gamma \quad . \tag{3.15b}$$

It is also apparent that the eigenvalues λ's strongly depend on the stress σ. Thus, we can write:

$$\lambda_i = \hat{\lambda}_i(\sigma) \tag{3.16}$$

The above equation (3.13) has the same form as obtained by Achenbach [2.29] for a linear thermoelastic material. However, those parameters V_e, γ_1, β_1 are no longer constant but are functions of the unknown stress σ in this case.

For investigating the wave motion in particular materials, the eigenvalues represented by equation (3.14) are to be real. This leads to the conditions :

$$(\gamma_1 + \beta_1 + 1)^2 - 4\gamma_1 > 0 \quad , \tag{3.17a}$$

$$(\gamma_1+\beta_1+1) - \sqrt{(\gamma_1+\beta_1+1)^2 - 4\gamma_1} > 0 \quad . \tag{3.17b}$$

We can prove without difficulty that the above inequalities are satisfied only when both values of γ_1 and β_1 are positive. Since both γ_1 and β_1 are functions of γ, equations (3.15), we have:

$$\gamma = \frac{1}{\beta\rho C_\sigma - \alpha^2 T_o} > 0 \quad . \tag{3.18}$$

Making use of the value of β from equation (3.8a), we obtain :

$$\frac{n}{\mu^n} \sigma^{n-1} \rho C_\sigma > \alpha^2 T_o \quad . \tag{3.19}$$

The above inequality gives:

$$|\sigma| > \left\{ \frac{\mu^n \alpha^2 T_o}{n \rho C_\sigma} \right\}^{\frac{1}{n-1}} \quad ; \quad n \neq 1 \quad . \tag{3.20}$$

The absolute stress σ is employed here to confirm that the conditions (3.17) hold without taking the direction of stress into consideration. A sign convention from which a tensile stress propagating in the opposite direction of the rod is considered positive and a compressive stress propagating in the same direction as the rod is considered negative, is assumed to hold. It is also noted that when $n = 1$, the condition (3.20) does not exist.

For eigenvalues λ_i to be real, the stress σ can not be arbitrary but must be constrained by the inequality (3.20).

The wave speed is defined by:

$$V_i = \lambda_i = \frac{dx^i}{dt} \ , \tag{3.21}$$

where dx^i is a distance which the wave having speed V_i propagates in a time interval dt; and $\frac{dx^i}{dt}$ is referred to as the slope of the characteristic curve C_i as shown in Figure 3.1.

Thus, along the characteristic curve C_1^+, the wave has its own speed which is presented as follows:

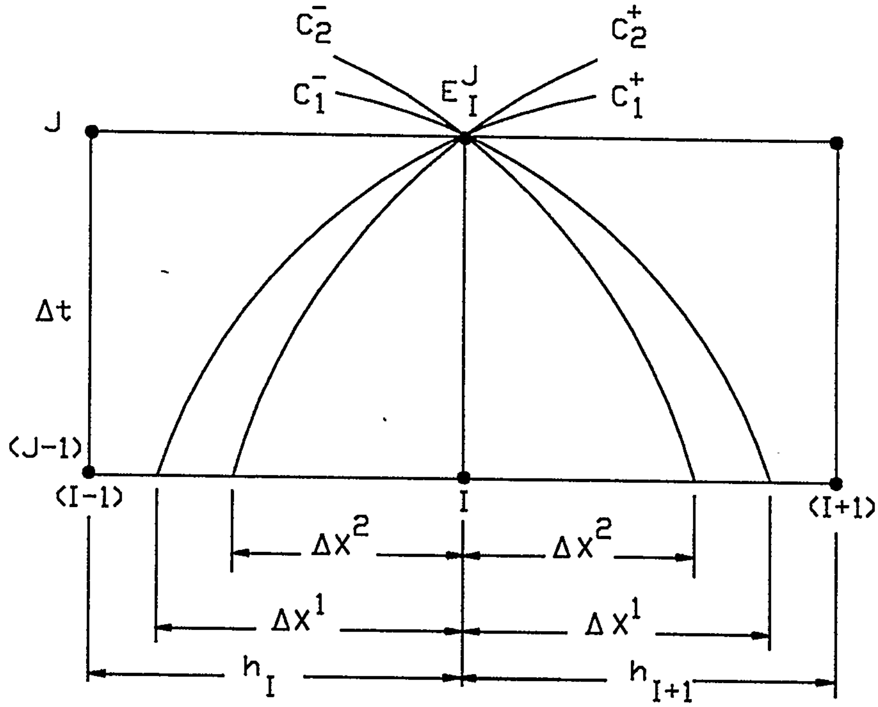

FIG. 3.1 CHARACTERISTIC CURVES PASSING THROUGH POINT E_I^J - THE CASE OF CONDUCTING MATERIAL

$$V_1 = \frac{dx^1}{dt} = \lambda_1 = V_e \left\{ \frac{(\gamma_1+\beta_1+1) + \sqrt{(\gamma_1+\beta_1+1)^2 - 4\gamma_1}}{2} \right\}^{1/2} . \quad (3.22a)$$

Similarly,

- along the characteristic curve C_2^+:

$$V_2 = \frac{dx^2}{dt} = \lambda_2 = V_e \left\{ \frac{(\gamma_1+\beta_1+1) - \sqrt{(\gamma_1+\beta_1+1)^2 - 4\gamma_1}}{2} \right\}^{1/2} , \quad (3.22b)$$

- along the characteristic curve C_2^-:

$$V_3 = \frac{dx^3}{dt} = \lambda_3 = -V_e \left\{ \frac{(\gamma_1+\beta_1+1) - \sqrt{(\gamma_1+\beta_1+1)^2 - 4\gamma_1}}{2} \right\}^{1/2} , \tag{3.22c}$$

- along the characteristic curve C_1^-:

$$V_4 = \frac{dx^4}{dt} = \lambda_4 = -V_e \left\{ \frac{(\gamma_1+\beta_1+1) + \sqrt{(\gamma_1+\beta_1+1)^2 - 4\gamma_1}}{2} \right\}^{1/2} . \tag{3.22d}$$

Comparing the wave speeds given by the expressions on the right-hand side of equations (3.22), we have:

$$V_4 = -V_1 , \tag{3.23a}$$

$$V_3 = -V_2 . \tag{3.23b}$$

For an adiabatic process , i.e. when the material is considered as a non-conductor, only one positive wave propagates in the medium with a speed:

$$V_a = V_e \sqrt{\beta_1+1} . \tag{3.24}$$

This is because the term γ_1 in equations (3.22) no longer exists due to the negligible value of thermal conductivity K which is very close to zero at the reference state. A further study of wave motion in non-conductors will be discussed later in this chapter.

When $\beta_1 = 0$ (uncoupled case), the two positive wave speeds are given by:

$$V_M = V_e \left\{ \frac{(\gamma_1+1) + \sqrt{(\gamma_1+1)^2 - 4\gamma_1}}{2} \right\}^{1/2} , \qquad (3.25a)$$

$$V_T = V_e \left\{ \frac{(\gamma_1+1) - \sqrt{(\gamma_1+1)^2 - 4\gamma_1}}{2} \right\}^{1/2} . \qquad (3.25b)$$

where V_M and V_T denote the uncoupled mechanical wave speed and uncoupled thermal wave speed, respectively.

The expressions under the roots in equations (3.25) lead to two following cases:

(i) If the value of γ_1 is less than unity, the leading wave is essentially a mechanical wave whereas the lagging wave is essentially a thermal wave, i.e.:

$$V_1 > V_M > V_T > V_2 \quad . \qquad (3.26)$$

Also, when $\gamma_1 < 1$, we have:

$$V_M = V_e \quad , \qquad (3.27a)$$

and

$$V_T = V_e \sqrt{\gamma_1} \quad . \qquad (3.27b)$$

For a real root, γ_1 is always positive for which from equations (3.15) and (3.8b) :

$$\beta\rho C_\sigma - \alpha^2 T_o > 0 \quad . \qquad (3.28)$$

Since the value of α is very small as compared to unity, we may assume that the amount of $\alpha^2 T_o$ is insignificant in the inequality (3.28). The uncoupled thermal wave speed is then given by:

$$V_T = \sqrt{\frac{K}{\rho C_\sigma \tau_o}} \quad . \tag{3.29}$$

It is obvious that when the thermal relaxation time τ_o reaches zero as proposed by the classical Fourier's law, the speed of thermal wave is infinity.

(ii) If the value of γ_1 is greater than unity, the situation is reversed, i.e.

$$V_T = V_e \sqrt{\gamma_1} \quad , \tag{3.30a}$$

$$V_M = V_e \quad , \tag{3.30b}$$

which confirm that the leading wave must be thermal and the lagging wave must be mechanical.

3.2 JUMP CONDITIONS AT THE WAVEFRONTS

In quasi-linear equations, smooth solutions do not necessarily exist for all time. After a finite time, a smooth solution may cease to be smooth and later on tend to a discontinuity which behaves quite differently from the smooth wave. The location of the points having discontinuous solutions is called the wavefront. By definition, in x-t coordinates, the wavefront is a curve which separates the disturbed region from the undisturbed region or separates the disturbed region from the region having an additional disturbance [3.2].

Let R^+, ∂R^+ and R^-, ∂R^- denote the portions of a body R^* with surface ∂R^* situated ahead and to the rear with respect to a singular surface D at time t as shown in Figure 3.2 . The unit normal $\tilde{N}$ of the surface is pointing from R^+ to R^-. The limit of f(x,t) across D(t) is expressed by:

$$\|f\| = f^{-} - f^{+} \neq 0 \quad . \tag{3.31}$$

The variable f(x,t) may be a scalar, vector, or tensor over the present configuration. If $\|f\|$ is normal to the singular surface D(t) , the discontinuity is said to be longitudinal , whereas it is said to be transversal when $\|f\|$ is tangential to D(t).

For a partial differential equation of the form:

$$\frac{\partial \underset{\sim}{U}}{\partial t} + \frac{\partial}{\partial_x} \underset{\sim}{F} (\underset{\sim}{U}) + \underset{\sim}{B} (\underset{\sim}{U}) = 0 \quad , \tag{3.32}$$

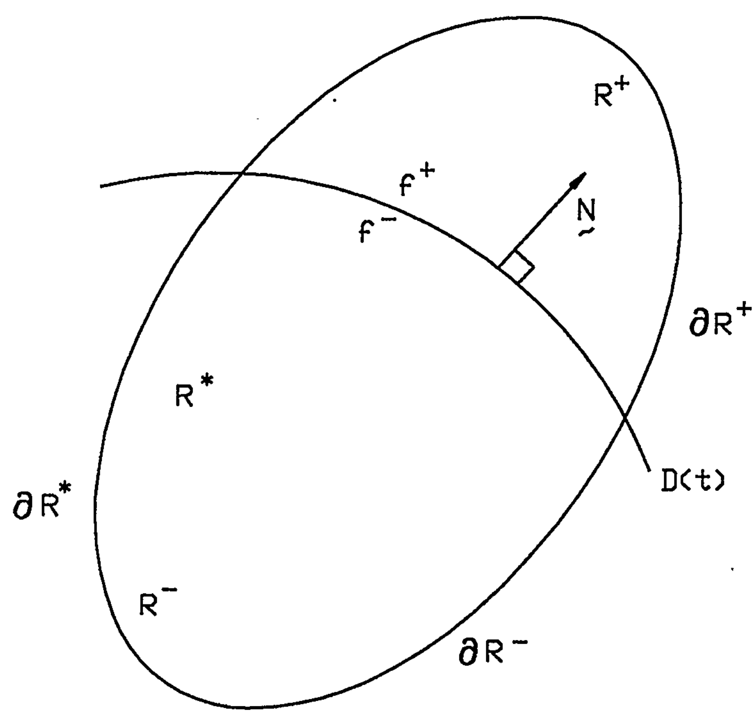

FIG. 3.2 PROPAGATING SURFACE OF DISCONTINUITY D(t)

the corresponding jump condition across a surface of discontinuity, according to Kosinski's theorem [3.3,3.4] is given by:

$$V_f \, \| \underset{\sim}{U} \| = \| \underset{\sim}{F} \| \quad , \tag{3.33}$$

where the bracket " $\| \; \|$ " thereafter denotes the jump, and V_f is the intrinsic velocity of the wavefront.

In order to apply the Kosinski's theorem, the equation of motion (3.1a), the modified equation of heat conduction (3.1c), and the coupled energy equation (3.1d) are written respectively in the form:

$$\frac{\partial}{\partial t} (\rho v) - \frac{\partial \sigma}{\partial x} = 0 \quad , \tag{3.34a}$$

$$\frac{\partial}{\partial t} (\tau_o q) + \frac{\partial}{\partial x} (K\theta) + q = 0 \quad , \tag{3.34b}$$

$$\frac{\partial}{\partial t} (\alpha T_o \sigma + \rho C_\sigma \theta) + \frac{\partial q}{\partial x} = 0 \quad . \tag{3.34c}$$

Applying the jump condition (3.33) to the above equations yields:

$$\| \sigma \| = -\rho V_f \, \| v \| \quad , \tag{3.35a}$$

$$\| q \| = \frac{K}{\tau_o V_f} \, \| \theta \| \quad , \tag{3.35b}$$

$$\| q \| = V_f \, \| \alpha T_o \sigma + \rho C_\sigma \theta \| \quad . \tag{3.35c}$$

The equations (3.35) which are similar to those of Chang and Cozzarolli [2.24] and Achenbach [2.29] express the differences or jumps in variables along and across the wavefront.

In a thermoelastic material, whenever both values of thermal conductivity K and thermal relaxation time τ_o are not zero, there always exist two wavefronts propagating in the body right after its boundary is suddenly hit by an external force. At the first point on the boundary (say the origin), part of the externally applied discontinuities will propagate in the medium with velocity V_1 (equation (3.22a)), and part with velocity V_2 (equation (3.22b)).

At the origin, thus, the jumps in unknowns are decomposed into:

$$\|v\| = \|v\|_1 + \|v\|_2 \quad , \tag{3.36a}$$

$$\|\sigma\| = \|\sigma\|_1 + \|\sigma\|_2 \quad , \tag{3.36b}$$

$$\|\theta\| = \|\theta\|_1 + \|\theta\|_2 \quad , \tag{3.36c}$$

$$\|q\| = \|q\|_1 + \|q\|_2 \quad , \tag{3.36d}$$

where

$\| \ \|_1$ denotes the jump across the leading wavefront,

$\| \ \|_2$ denotes the jump across the lagging wavefront.

Across the leading wavefront, the jump conditions can be directly obtained from equations (3.35) of which the wavefront speed V_f is simply replaced by V_1, then:

$$\|\sigma\|_1 = -\rho V_1 \|v\|_1 \quad , \tag{3.36e}$$

$$\|q\|_1 = \frac{K}{\tau_o V_1} \|\theta\|_1 \quad , \tag{3.36f}$$

$$\|q\|_1 = V_1 \alpha T_o \|\sigma\|_1 + V_1 \rho C_\sigma \|\theta\|_1 \quad . \tag{3.36g}$$

Similarly, across the lagging wavefront, we have:

$$\|\sigma\|_2 = -\rho V_2 \|v\|_2 \quad , \tag{3.36h}$$

$$\|q\|_2 = \frac{K}{\tau_o V_2} \|\theta\|_2 \quad , \tag{3.36i}$$

$$\|q\|_2 = V_2 \alpha T_o \|\sigma\|_2 + V_2 \rho C_\sigma \|\theta\|_2 \quad . \tag{3.36j}$$

The system of ten simultaneous equations (3.36) are composed of twelve unknowns:

$$\|v\|,\ \|v\|_1,\ \|v\|_2;\ \|\sigma\|,\ \|\sigma\|_1,\ \|\sigma\|_2;\ \|\theta\|,\ \|\theta\|_1,\ \|\theta\|_2;\ \|q\|,\ \|q\|_1,\ \|q\|_2\ .$$

These twelve unknowns can be determined if and only if two of them are given by some other conditions. The remaining unknowns are then calculated through the system (3.36). The two unknowns among the twelve unknowns are usually given by boundary conditions of the problem.

It is mentioned here that, in a quasi-linear hyperbolic system, the jump conditions are also used to numerically determine the values of unknowns in the disturbed medium.

In this thesis, the problem of wave propagation in thermoelastic conducting materials is solved along with two sets of boundary conditions given by:

(i) time-dependent velocity and a constant temperature impact:

$$\begin{cases} v(0,t) = V_o t^\delta \quad ; \quad t > 0, \ \ \delta > 0 & \text{(3.37a)} \\ \theta(0,t) = \theta_o \quad ; \quad t > 0 & \text{(3.37b)} \end{cases}$$

ii) time-dependent stress and a constant temperature impact:

$$\begin{cases} \sigma(0,t) = \sigma_o t^{\delta} \quad ; \quad t > 0 \ , \ \delta > 0 & (3.38a) \\ \theta(0,t) = \theta_o \quad ; \quad t > 0 & (3.38b) \end{cases}$$

In addition to the boundary conditions given above, the initial conditions are prescribed as:

$$v \ (x > 0, \ t = 0) = 0 \quad , \qquad (3.39a)$$

$$\sigma \ (x > 0, \ t = 0) = 0 \quad , \qquad (3.39b)$$

$$\theta \ (x > 0, \ t = 0) = 0 \quad , \qquad (3.39c)$$

$$q \ (x > 0, \ t = 0) = 0 \quad . \qquad (3.39d)$$

Along with the prescribed auxiliary conditions (3.37) (or (3.38)) and (3.39), the system of partial differential equations (3.1) which governs the wave motion in the continuous regions and the jump conditions across the wavefronts can be solved through numerical procedures.

PART B: BASIC EQUATIONS AND JUMP CONDITIONS FOR NON-CONDUCTING MATERIALS

In this part, we will consider the features of one-dimensional waves propagating in non-linear thermoelastic bodies which do not conduct heat.

The concept of non-conducting elastic solids is thermodynamically inadmissible because it is impossible to heat or cool such solids reversibly. In these solids, values of thermal conductivity K equal zero. However, in practice, values of K can never be exactly zero for a solid, because heat can only be transferred through heat conduction processes. Without heat conduction there would be no reversible path between two states of the solid which differs only in temperature.

In a limiting sense, when values of K are very small, we can assume that there is no heat conduction taking place in the body. Based on this assumption, Bland [3.5] has shown that in such a material the heat flux is no longer existent, i.e:

$$q = 0 \quad . \tag{3.40}$$

The above equation leads us to conclude that the process of thermoelastic deformation now proceeds adiabatically.

The relation between the entropy $\mathcal{S}$ and heat flux q previously given by equation (2.36b) now assumes the form:

$$\frac{\partial \mathcal{S}}{\partial t} = 0 \quad . \tag{3.41}$$

Depending on the situation of the waves propagating in the medium, we have two different cases: (i) $\mathcal{S} = \mathcal{S}(x)$, in the case of shock waves. And (ii) $\mathcal{S} = 0$ in the absence of shock waves.

On the basis of equations (3.1) and equation (3.40), the fundamental equations for a non-conductor can be expressed as:

$$\rho \frac{\partial v}{\partial t} - \frac{\partial \sigma}{\partial x} = 0 \quad , \tag{3.42a}$$

$$\frac{\partial}{\partial t} \left\{ \left(\frac{\sigma}{\mu} \right)^{n} + \alpha \theta \right\} - \frac{\partial v}{\partial x} = 0 \quad , \tag{3.42b}$$

$$\alpha T_o \frac{\partial \sigma}{\partial t} + \rho C_\sigma \frac{\partial \theta}{\partial t} = 0 \quad . \tag{3.42c}$$

The system (3.42) is now composed of three unknowns v, σ and θ and can be expressed in the form:

$$[A_1'] \underset{\sim}{U}_{2t} + [A_2'] \underset{\sim}{U}_{2x} = 0 \quad , \tag{3.43}$$

where:

$$U_{2t} = [v_t \quad \sigma_t \quad \theta_t]^T \quad , \tag{3.44a}$$

$$\underset{\sim}{U}_{2x} = [v_x \quad \sigma_x \quad \theta_x]^T \quad , \tag{3.44b}$$

$$[A_1'] = \begin{bmatrix} \rho & 0 & 0 \\ 0 & \frac{n}{\mu^n}\sigma^{n-1} & \alpha \\ 0 & \alpha T_o & \rho C_\sigma \end{bmatrix} \quad , \tag{3.44c}$$

$$[A_2'] = \begin{bmatrix} 0 & -1 & 0 \\ -1 & 0 & 0 \\ 0 & 0 & 0 \end{bmatrix} \quad . \tag{3.44d}$$

Multiplying both sides of equation (3.43) by the matrix $[A_1']^{-1}$, we have:

$$\underset{\sim}{U}_{2t} + [B_1'] \underset{\sim}{U}_{2x} = 0 \quad , \tag{3.45}$$

where matrices $[A_1']^{-1}$ and $[B_1']$ are obtained as:

$$[A_1']^{-1} = \begin{bmatrix} \frac{1}{\rho} & 0 & 0 \\ 0 & \frac{\rho C_\sigma}{\left(\beta\rho C_\sigma - \alpha^2 T_o\right)} & \frac{-\alpha}{\left(\beta\rho C_\sigma - \alpha^2 T_o\right)} \\ 0 & \frac{-\alpha T_o}{\left(\beta\rho C_\sigma - \alpha^2 T_o\right)} & \frac{\beta}{\left(\beta\rho C_\sigma - \alpha^2 T_o\right)} \end{bmatrix} , \qquad (3.46a)$$

$$[B_1'] = \begin{bmatrix} 0 & \frac{1}{\rho} & 0 \\ \frac{-\rho C_\sigma}{\left(\beta\rho C_\sigma - \alpha^2 T_o\right)} & 0 & 0 \\ \frac{\alpha T_o}{\left(\beta\rho C_\sigma - \alpha^2 T_o\right)} & 0 & 0 \end{bmatrix} . \qquad (3.46b)$$

The eigenvalues of the system (3.45) are determined similarly to those of conducting materials derived in part A. Computing the determinant of $([B_1'] - \lambda[I])$ yields:

$$\lambda \left\{ \lambda^2 - \frac{C_\sigma}{\beta\rho C_\sigma - \alpha^2 T_o} \right\} = 0 . \qquad (3.47)$$

The equation (3.47) gives:

$$\lambda_5 = 0 , \qquad (3.48a)$$

$$\lambda_6 = \sqrt{\frac{C_\sigma}{\beta\rho C_\sigma - \alpha^2 T_o}} , \qquad (3.48b)$$

$$\lambda_7 = -\sqrt{\frac{C_\sigma}{\beta\rho C_\sigma - \alpha^2 T_o}} \quad . \tag{3.48c}$$

We can directly prove that the eigenvalue λ_i (i = 6,7) are real if and only if the condition (3.20) holds.

By definition, the wave speed along the characteristic curve C_3 is expressible as:

$$V_5 = \lambda_5 = 0 \quad . \tag{3.49a}$$

Similarly, along the characteristic curve C_4^+ :

$$V_6 = \frac{dx^6}{dt} = \lambda_6 \quad , \tag{3.49b}$$

and along the characteristic curve C_4^- :

$$V_7 = \frac{dx^7}{dt} = \lambda_7 \quad . \tag{3.49c}$$

Therefore, one of the characteristic curves is straight line (parallel to the Ot-axis) and the remaining two are curvilinear (as in Figure 3.3) since characteristic speeds V_6 and V_7 are non-linear functions of the yet unknown stress σ.

It is clearly seen from equations (3.48b,c) that both V_6 and V_7 have their absolute values to be the same. Thus, we can write :

$$V_6 = -V_7 \quad . \tag{3.50}$$

Because of the absence of the coupling parameter γ_1 as previously discussed in equation (3.24) only one wavefront propagating in the medium . The jump conditions, thus, are determined much more conveniently than those in the conducting materials.

Applying the Kosinski's theorem to equation (3.42a) yields :

$$\|\sigma\| = -\rho V_6 \|v\| \quad , \tag{3.51}$$

and from (3.42c),

$$\|\sigma\| = -\frac{\rho C_\sigma}{\alpha T_o} \|\theta\| \quad . \tag{3.52}$$

It is noted that the equation (3.51) is admissible only in the absence of shock waves. If the body is disturbed by a shock, the velocity V_6 in the above equation would be replaced by a shock velocity U_s, i.e.:

$$\|\sigma\| = -\rho U_s \|v\| \quad . \tag{3.53}$$

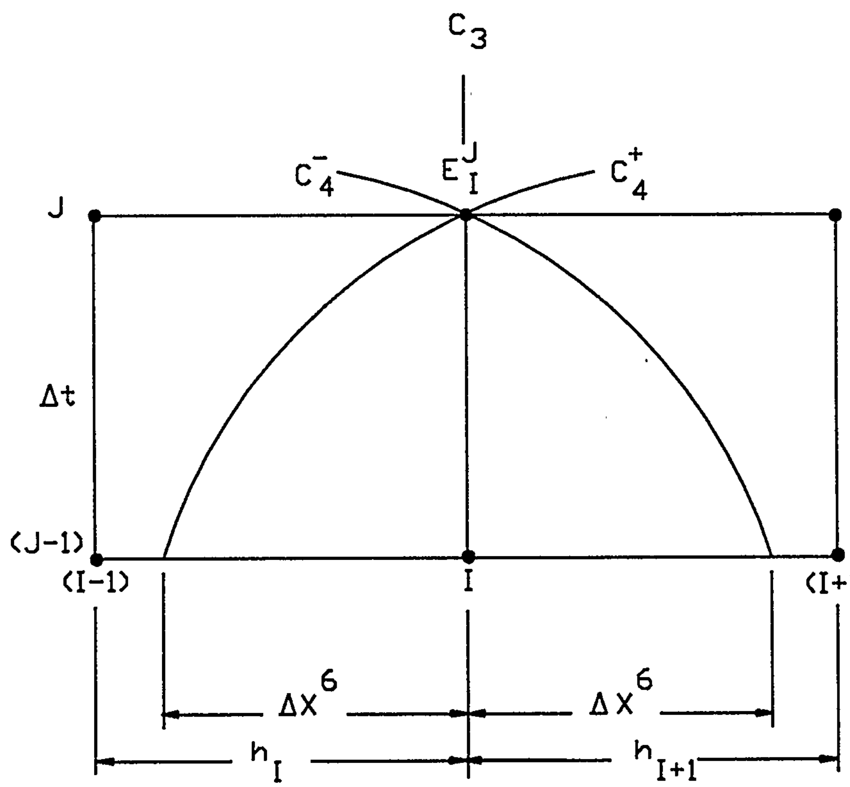

FIG. 3.3 CHARACTERISTIC CURVES PASSING THROUGH POINT E_I^J - THE CASE OF NON-CONDUCTING MATERIALS

In linear elastic materials, there is usually no shock occurring, however, in non-linear thermoelastic solids, the shock is likely to occur under certain conditions.

Most of non-linear elastic materials, stress-strain relations in an isothermal condition must have either a concave-up curve or a concave-down curve which respectively corresponds to the power n being either smaller or greater than unity.

A graphical method which is similar to the ones applied to various wave problems by Cristescu [3.6], Bland [3.5], Eringen and Suhubi [3.7], De Juhasz [3.8], Hwang and Davids [3.9], etc. will be employed here to determine whether there exists a simple wave or a shock wave propagating in the medium.

3.3 SIMPLE WAVES

The first problem to be considered is that of an elastic one-dimensional body having its stress-strain diagram as shown in Figure 3.4.

Assuming that the body is at rest in its natural state for $t < 0$ but is subjected to time-dependent stress impact on its boundary $x = 0$ for $t > 0$. Such a boundary condition is expressible as:

$$\sigma(0,t) = \sigma_o t^\delta \quad . \tag{3.54}$$

The stress is continuous and monotonically increasing along the Ot-axis. As a result, the slopes of the characteristic curves, which are the functions of the stress σ (equation (3.48b)), decline gradually. The wavelets diverge at the front as illustrated in Figure 3.5, and this type of wave is called a *simple wave* [3.10, 3.11].

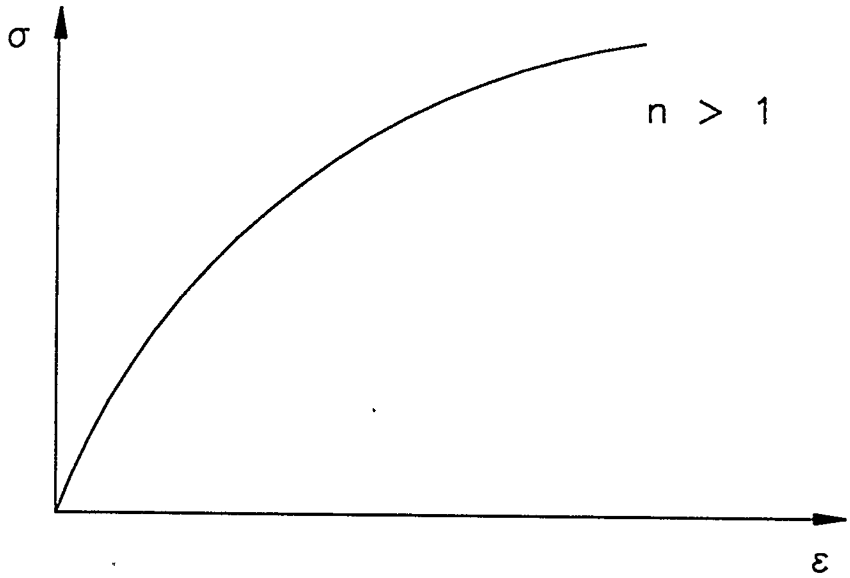

FIG. 3.4 STRESS-STRAIN DIAGRAM WITH n > 1

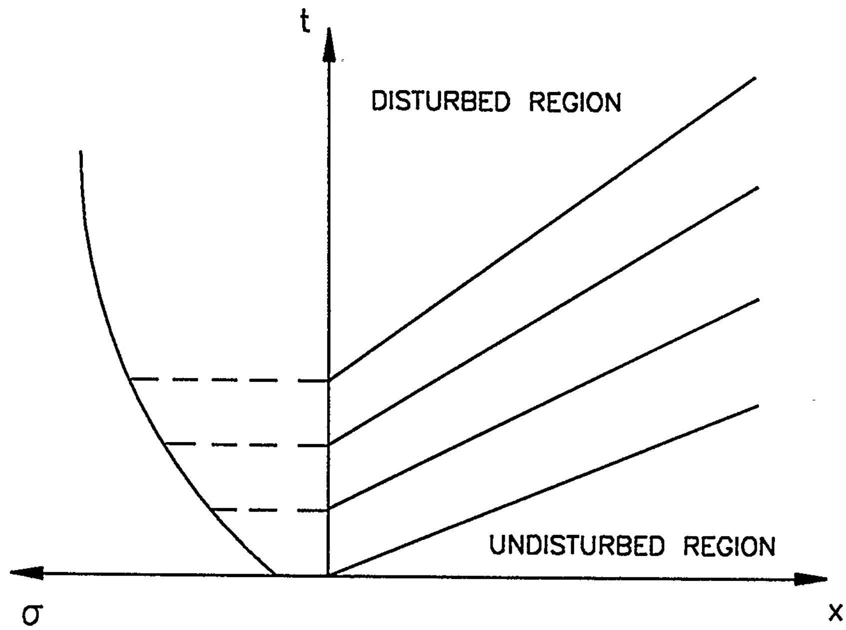

FIG. 3.5 CONFIGURATION OF A SIMPLE WAVE

In the entire simple wave region, the numerical solution presents no difficulty, the set of unknowns $\{v, \sigma, \theta\}$ can be found uniquely from the characteristic network. The wavefront must be one of the characteristic curves having a positive slope and passing through the first point on the boundary (say the origin).

3.4 SHOCK WAVES

The same boundary condition prescribed in (3.54) is applied to a material having a stress-strain diagram to be concave-up as shown in Figure 3.6. The increase of stress σ along the Ot-axis leads to the decrease of slopes of the positive characteristics and the wavelets converge at the front. The unique solution breaks down when two C_4^+ characteristics intersect as in Figure 3.7 because this implies two different values of the unknown at the same point in space-time. In that case a *shock* wave is formed and is represented by a curve in the x-t plane commencing at the first point of characteristic intersection. For convenience we may assume that the shock occurs at the origin where the waves start propagating in the medium.

It is noted that the speed of the shock U_s need not be the same as the speed of wavefront V_6 in the case of simple waves. Therefore, the path of shockfront must be independent and distinguishable completely from the characteristic curves.

3.4.1 Shock Velocity

By definition, a shock wave is a motion containing a shockfront across which the strain ε, the particle velocity v, and their derivatives are discontinuous [3.12].

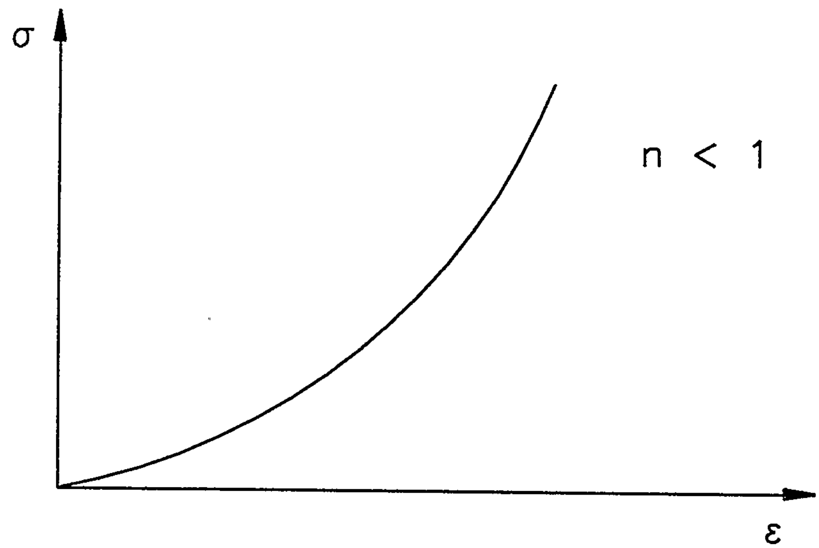

FIG. 3.6 STRESS-STRAIN DIAGRAM WITH $n < 1$

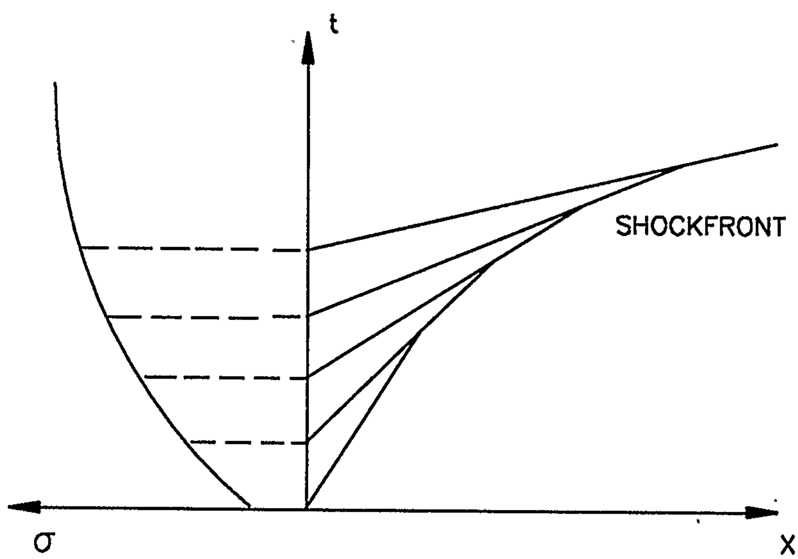

FIG. 3.7 FORMATION OF A SHOCK WAVE

If we define the discontinuity in a quantity f by:

$$\|f\| = f^{-} - f^{+} \quad , \tag{3.55}$$

where f^{-} and f^{+} are the values of f immediately behind and just in front of the shockfront.

The kinematical condition of compatibility is given by [3.12]:

$$\frac{d}{dt}\|f\| = \|\dot{f}\| + U_s \left\|\frac{\partial f}{\partial x}\right\| \quad , \tag{3.56}$$

with f = u implies that

$$U_s \|\varepsilon\| = - \|v\| \quad . \tag{3.57}$$

It is clear from this result that either $\|v\|$ or $\|\varepsilon\|$ can be taken as a measure of the amplitude of the shock.

On the basis of Kosinski's theorem, we obtain from the balance of linear momentum equation (3.42a) :

$$\|\sigma\| = - \rho\, U_s \|v\| \quad . \tag{3.58}$$

Combining (3.58) with (3.57) yields the well-known result:

$$U_s = \sqrt{\frac{1}{\rho}\frac{\|\sigma\|}{\|\varepsilon\|}} \quad , \tag{3.59}$$

for the intrinsic velocity of the shockfront.

3.4.2 Shock Amplitude Equations

Here, we shall derive the equation which governs the amplitude of a shock wave in an elastic non-conductor. If the quantity f is replaced by the strain ε and the particle velocity v, respectively ,the relation (3.56) implies that :

$$\frac{d}{dt} \|\varepsilon\| = U_s \|\varepsilon_x\| + \|\dot{\varepsilon}\| \quad , \tag{3.60}$$

and

$$\frac{d}{dt} \|v\| = U_s \|v_x\| + \|\dot{v}\| \quad . \tag{3.61}$$

Multiplying both sides of (3.60) by U_s and rearranging, we have:

$$U_s \|\dot{\varepsilon}\| = U_s \frac{d}{dt} \|\varepsilon\| - U_s^2 \|\varepsilon_x\| \quad . \tag{3.62}$$

Total differentiation of both sides of equation (3.57) gives:

$$-\frac{d}{dt} \|v\| = \|\varepsilon\| \frac{dU_s}{dt} + U_s \|\dot{\varepsilon}\| + U_s^2 \|\varepsilon_x\| \quad . \tag{3.63}$$

Furthermore, across the shockfront, the equation of motion (3.42a) yields [3.13]:

$$\|\dot{v}\| = \frac{1}{\rho} \|\sigma_x\| \quad . \tag{3.64}$$

So does the compatibility relation:

$$\|v_x\| = \|\dot{\varepsilon}\| \quad . \tag{3.65}$$

Replacing $\|\dot{v}\|$ and $\|v_x\|$ in equation (3.61) by the right-hand side of equations (3.64) and (3.65), we obtain:

$$\frac{d}{dt} \|v\| = \frac{1}{\rho} \|\sigma_x\| + U_s \|\dot{\varepsilon}\| \quad . \tag{3.66}$$

Substituting equations (3.61) and (3.66) into equation (3.63), the amplitude of the shockfront is expressed by:

$$2U_s \frac{d\|\varepsilon\|}{dt} + \|\varepsilon\| \frac{dU_s}{dt} = U_s^2 \|\varepsilon_x\| - \frac{1}{\rho} \|\sigma_x\| \quad , \tag{3.67}$$

which is similar to that of Chen [3.12] and Ting [3.14].

Thus, along the shockfront, the set of three unknowns $\{v,\sigma,\theta\}$ is determined from the three equations (3.52b), (3.58) and (3.67). In which the shock velocity U_s can be found from the formula (3.59) and the strain ε may be eliminated from the jump condition based on the constitutive relation (2.65):

$$\|\varepsilon\| = \left\|\left(\frac{\sigma}{\mu}\right)^n\right\| + \alpha\,\|\theta\| \quad . \tag{3.68}$$

In part A of this chapter, we did not mention that the shock waves could occur in the conducting materials subjected to the prescribed boundary conditions. This is because when the thermal conductivity K is taken into account, we can hardly conclude whether there exists a shock or not due to the influence of the lagging wavefront . For a non-linear thermoelastic material wherein the speeds of both wavefronts are functions in terms of the unknown stress σ, the location of the lagging wavefront as well as the jumps in unknowns across it are still an unsolved question for the investigators.

Moreover, although some predictions of linear thermoelasticity have been extended, the influence of heat-conduction on wave propagation in non-linear elastic solids is not fully understood . Because of these reasons, shock wave experiments in non-linear elastic solids are interpreted by assuming the material to be a non-conductor of heat, [3.15].

It is to be noted that when there is a shock wave involved in conducting materials, the shock amplitude equation (3.67) can also be applied for obtaining the unknowns along and across the shockfront [3.13].

For a non-conductor, the two equations (3.51,3.52) consisting of three unknowns v, σ, θ are not sufficient for solving the unknowns at the first point on the boundary (Ot-axis). To satisfy the requirement, one of the following types of boundary condition will be employed:

$$\text{(i)} \qquad v(0,t) = v_o t^{\delta} \;; \qquad t > 0 \quad , \quad \delta > 0 \quad . \tag{3.69}$$

$$\text{(ii)} \qquad \sigma(0,t) = \sigma_o t^{\delta} \;; \qquad t > 0 \quad , \quad \delta > 0 \quad . \tag{3.70}$$

Furthermore, the material is assumed to be quiescent in the beginning, the initial conditions are then written as:

$$v(x > 0, t = 0) = 0 \quad , \tag{3.71a}$$

$$\sigma(x > 0, t = 0) = 0 \quad , \tag{3.71b}$$

$$\theta(x > 0, t = 0) = 0 \quad . \tag{3.71c}$$

Together with the jump conditions, the prescribed auxiliary conditions are combined with the system of equations (3.42) to form a complete set for investigating the wave motion in a non-conductor.

CHAPTER 4
NUMERICAL METHODS FOR CONDUCTING MATERIALS

There are some well known methods available which are used to solve the system of linear as well as non-linear equations in the hyperbolic form as partly mentioned in Chapter 1.

Along with their auxiliary conditions, systems of hyperbolic equations are still the most challenging class of problems to solve. For a long time, the investigators have kept on searching for a general method or modifying the present method so that it is possible not only to obtain proper solutions but also to show clearly the jumps in unknowns at the wavefront ; especially when a problem consists of two surfaces of discontinuity or more.

Even though Lopez [4.1] and Lee et al [4.2] have achieved good results by the method of characteristics, their solutions are referred to as special cases only. The difficulty of this approximate method is increased whenever non-linear problems are considered for solutions.

To deal with the system of equations along with the auxiliary conditions given previously, in this chapter we will employ two methods, namely the characteristic method and the finite element method.

4.1 THE METHOD OF CHARACTERISTICS

So far, this method is still regarded as the most popular technique applied for treating the quasilinear hyperbolic equations. By this method, a system of partial differential equations is transformed to a system of ordinary equations along the characteristic curves. The method has been adequately developed in the monograph [4.3, 4.4, 4.5] as well as extensively applied to practical problems [4.6, 4.7, 4.8]. However, when the method is carried out, there are some different approaches which are briefly summarized as follows.

4.1.1 Diamond-Shaped Network

In the first approach, the characteristic network has a diamond shape formed by the opposite families of characteristic lines as in Figure 4.1. Field solutions for unknowns are obtained by numerical integration of the ordinary equations along their own directions. Wood and Phillips [4.9] applied this approach to the problem of wave propagation in a plastic bar. Further, Lopez [4.1], and Mengi and Turhan [3.2], as well as Lee et al [4.2] used it for solving the

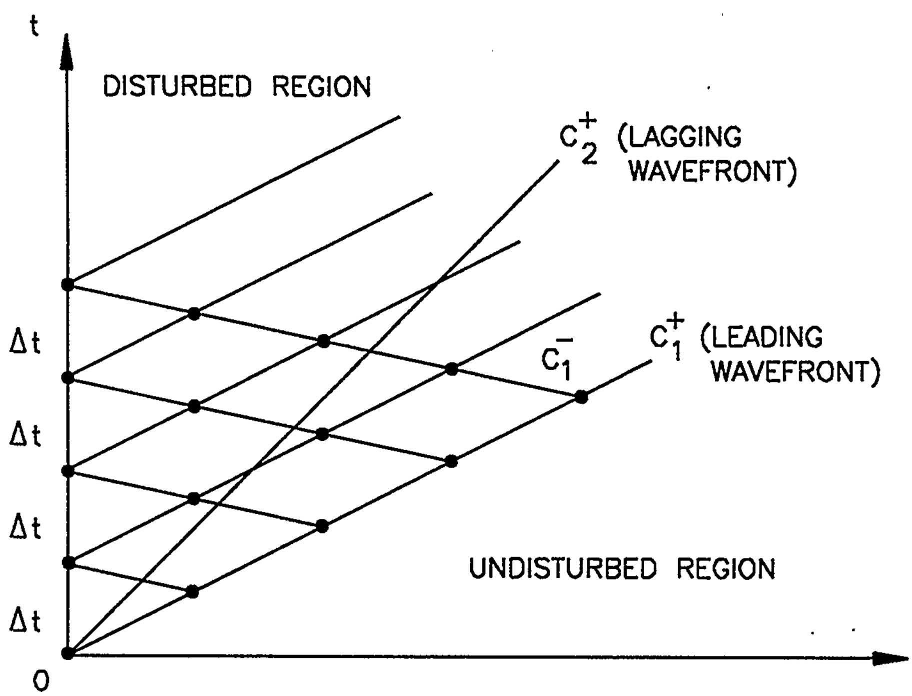

FIG. 4.1 DIAMOND-SHAPED MESHES

problems of thermomechanical waves in linear thermoelastic materials, inhomogeneous thermoelastic media and non-linear thermoviscoelastic materials, respectively.

The approach gives good features of the solutions of which not only the wavefronts are clearly located but also the jumps in unknowns along the wavefronts are properly determined. However, the satisfactory results are obtained only when characteristic curves are assumed to be straight lines leading to the uniform meshes throughout the disturbed region. The positions of grid points are then determined with no difficulty.

The technique becomes more complicated when the slopes of the characteristic curves are not constant but changing from point to point

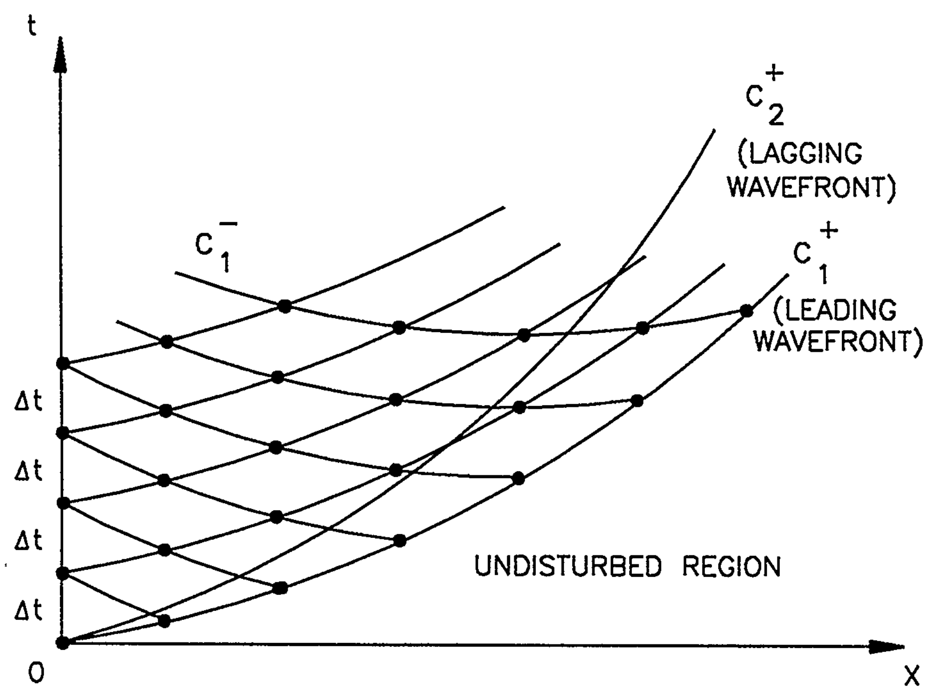

FIG. 4.2 IRREGULAR MESHES

in the medium. Non-uniform meshes, as illustrated in Figure 4.2, are formed as a result, and positions of grid points, thus, cannot be established as easily as those of diamond-shaped meshes.

4.1.2 Rectangular-Shaped Network

The second approach which was first proposed by Hartree (1953) is usually referred to as the Hartree's method [4.10] or the method of fixed time intervals. This approach has been used by numerous authors [4.8, 4.11] and recently applied by Orisamolu [4.12] to the system of equations of thermomechanical waves in inelastic solids.

Following this approach, the x-t plane is divided into uniform rectangular meshes, as in Figure 4.3, and the unknowns at each grid

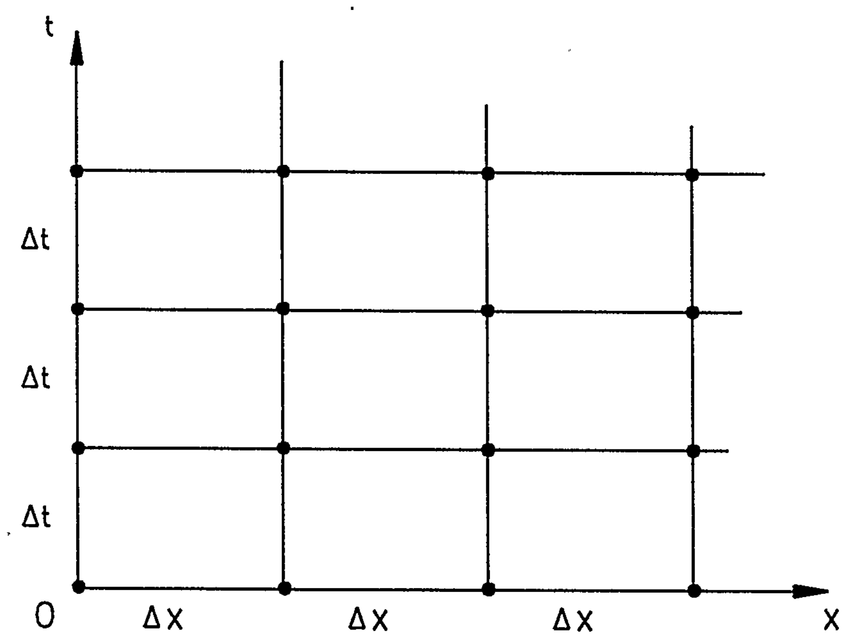

FIG. 4.3 RECTANGULAR MESHES

point are calculated by integrating the ordinary differential equations along the characteristic directions. The interpolating technique is also employed to obtain the quantities of intercepts at the feet of the characteristic curves which do not coincide with a grid point.

In contrast to the first approach, the second one can neither give an accurate position of the wavefront nor reveal any jumps across it. Nevertheless, this approach has some advantages of being (i) simple computing and programming, and (ii) applicable to several non-linear problems.

4.1.3 Combination Network

Methodically developed from the above two approaches, the third one is similar to the first in which a leading wavefront is prior determined and serves as a second boundary. The investigated region is now bounded by the Ot-axis considered as the first boundary and by the precursor front. The combination net of lines to be superimposed on the disturbed region such that one family of lines is parallel to the Ox-axis and the other family of lines is parallel to the Ot-axis. The meshes are assumed equi-spaced with time interval Δt but a non-uniform length h_I between grid points as shown in Figure 4.4.

The same as the second approach, unknowns at each grid point are obtained from the system of ordinary differential equations being integrated along the characteristic directions.

Some advantages drawn from this point of view are given as follows:

(i) Not only jumps in unknowns along and across the leading wavefront (or the shockfront) but also its location can be determined as those in the first approach.

(ii) Being applicable to either linear or non-linear hyperbolic systems.

(iii) Reducing the complicated computation as seen in the article by Lopez [4.1] without losing much accuracy of the solution.

(iv) Simple programming and high speed computation as being comparable to the other approaches.

(v) For a problem with one single wavefront, the results obtained are as accurate as being expected.

Yet, this approach is still not a fully accomplished one. For the problems of thermomechanical waves composed of thermal and

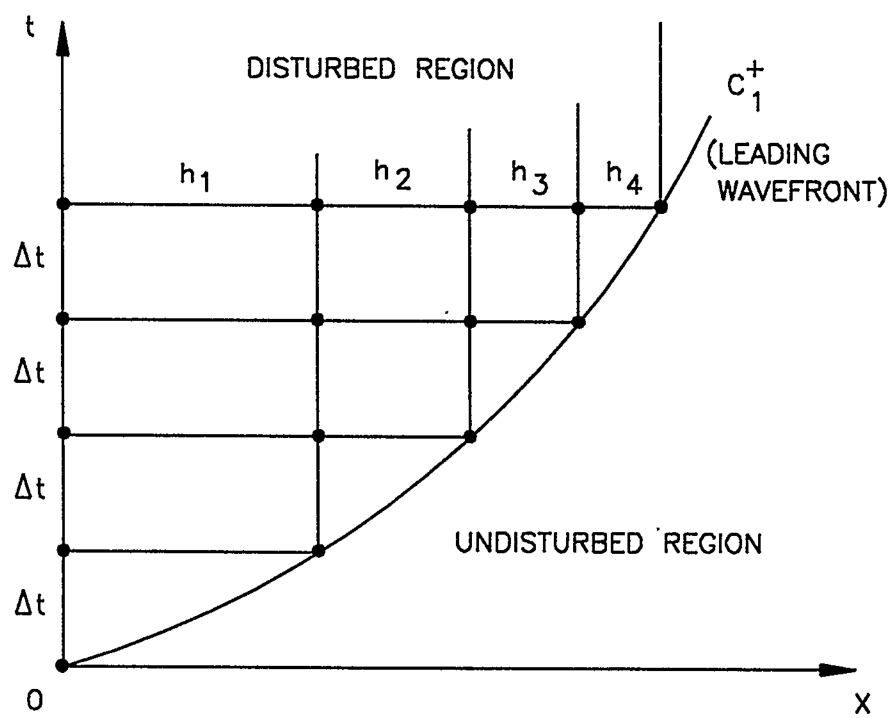

FIG. 4.4 COMBINATION MESHES

mechanical disturbances propagating simultaneously in the medium, the approach fails to locate exactly the lagging wavefront and uncertainly determines the jumps in unknowns along and across it. As a result, the oscillating solutions of those points close to the lagging wavefront cannot be controlled whenever high jumps suffered by strong discontinuity occurs there.

4.2 Numerical Computation by the Characteristic Method

Hereafter, the third approach is used to create combination meshes constrained by the two assigned boundaries for the application of the characteristic method and the finite element method.

If we denote the left eigenvectors of $[B_1]$ corresponding to the four eigenvalues λ_i by four $\underset{\sim}{\ell}^{(i)}$, respectively, where $i = 1,2,3,4$, then:

$$\underset{\sim}{\ell}^{(i)} [B_1] = \lambda_i \underset{\sim}{\ell}^{(i)} \tag{4.1}$$

Substituting the matrix $[B_1]$ given by (3.7b) into equation (4.1), eigenvectors $\underset{\sim}{\ell}^{(i)}$ are found to be:

$$\underset{\sim}{\ell}^{(i)} \begin{Bmatrix} -\rho\lambda_i \\ 1 \\ \dfrac{\rho}{\alpha T_o \gamma} (C_\sigma \gamma - \lambda_i^2) \\ \dfrac{\rho \tau_o \lambda_i}{K \alpha T_o \gamma} (C_\sigma \gamma - \lambda_i^2) \end{Bmatrix}^T , \tag{4.2}$$

where λ_i is the eigenvalue and is given by equation (3.14)

The characteristic conditions satisfied along the characteristic curves are determined as follows:

$$\underset{\sim}{\ell}^{(i)} \frac{d\underset{\sim}{U}}{dt} - \underset{\sim}{\ell}^{(i)} \underset{\sim}{B}_2 = 0 \quad , \tag{4.3}$$

or

$$\begin{Bmatrix} -\rho\lambda_i \\ 1 \\ \frac{\rho}{\alpha T_o \gamma} (C_\sigma \gamma - \lambda_i^2) \\ \frac{\rho \tau_o \lambda_i}{K\alpha T_o} (C_\sigma \gamma - \lambda_i^2) \end{Bmatrix}^T \begin{Bmatrix} v_t \\ \sigma_t \\ \theta_t \\ q_t \end{Bmatrix} - \begin{Bmatrix} -\rho\lambda_i \\ 1 \\ \frac{\rho}{\alpha T_o \gamma} (C_\sigma \gamma - \lambda_i^2) \\ \frac{\rho \tau_o \lambda_i}{K\alpha T_o} (C_\sigma \gamma - \lambda_i^2) \end{Bmatrix}^T \begin{Bmatrix} 0 \\ 0 \\ 0 \\ -\frac{q}{\tau_o} \end{Bmatrix} = 0 \; . \tag{4.4}$$

Subsequently, the system of ordinary differential equations along their own characteristic curves are expressed by:

- *along the characteristic curve* C_1^+ *with* $\lambda_1 = V_1$:

$$-\rho V_1 \frac{dv}{dt} + \frac{d\sigma}{dt} + \frac{\rho}{\alpha T_o \gamma} (C_\sigma \gamma - V_1^2) \frac{d\theta}{dt} + \frac{\rho \tau_o V_1}{K\alpha T_o \gamma} (C_\sigma \gamma - V_1^2) \frac{dq}{dt} +$$

$$\frac{\rho V_1}{K\alpha T_o} (C_\sigma \gamma - V_1^2)q = 0 \quad , \tag{4.5a}$$

- *along the characteristic curve* C_2^+ *with* $\lambda_2 = V_2$:

$$-\rho V_2 \frac{dv}{dt} + \frac{d\sigma}{dt} + \frac{\rho}{\alpha T_o \gamma} (C_\sigma \gamma - V_2^2) \frac{d\theta}{dt} + \frac{\rho \tau_o V_2}{K\alpha T_o \gamma} (C_\sigma \gamma - V_2^2) \frac{dq}{dt} +$$

$$\frac{\rho V_2}{K\alpha T_o \gamma} (C_\sigma \gamma - V_2^2) q = 0 \quad , \tag{4.5b}$$

- *along the characteristic curve* C_2^- with $\lambda_3 = -V_2$:

$$\rho V_2 \frac{dv}{dt} + \frac{d\sigma}{dt} + \frac{\rho}{\alpha T_o \gamma} (C_\sigma \gamma - V_2^2) \frac{d\theta}{dt} - \frac{\rho \tau_o V_2}{K\alpha T_o \gamma} (C_\sigma \gamma - V_2^2) \frac{dq}{dt} -$$

$$\frac{\rho V_2}{K\alpha T_o \gamma} (C_\sigma \gamma - V_2^2) q = 0 \quad , \tag{4.5c}$$

- along the characteristic curve C_1^- with $\lambda_4 = -V_1$:

$$\rho V_1 \frac{dv}{dt} + \frac{d\sigma}{dt} + \frac{\rho}{\alpha T_o \gamma} (C_\sigma \gamma - V_1^2) \frac{d\theta}{dt} - \frac{\rho \tau_o V_1}{K\alpha T_o \gamma} (C_\sigma \gamma - V_1^2) \frac{dq}{dt} -$$

$$\frac{\rho V_1}{K\alpha T_o \gamma} (C_\sigma \gamma - V_1^2) q = 0 \quad . \tag{4.5d}$$

As illustrated in Figure 4.5, the grid points being divided into three different types for the sake of computation can be categorised as follows:

- The first one is composed of those points along the precursor wavefront and denoted by A_1^1, A_2^2, ..., A_J^J. The four unknowns are explicitly found from the characteristic curve having the largest positive slope, and the jump conditions previously defined in Chapter 3.
- The second one governs the grid points along the Ot-axis and is represented by C_0^1, C_0^2,...,C_0^J. Only two unknowns instead

of four unknowns being necessarily determined due to two unknowns revealed from the given set of boundary conditions. The last one consists of any points as distinct from those above and is exhibited by E_I^J where I =1,2,..,J-1 and I ≠ 0,J . The set of ordinary differential equations (4.5) must be synchronously integrated along the characteristic directions to obtain the four unknowns at each grid point. Points which belong to this type are referred to as *interior grid points*.

4.2.1 Grid Points ALong the Leading Wavefront

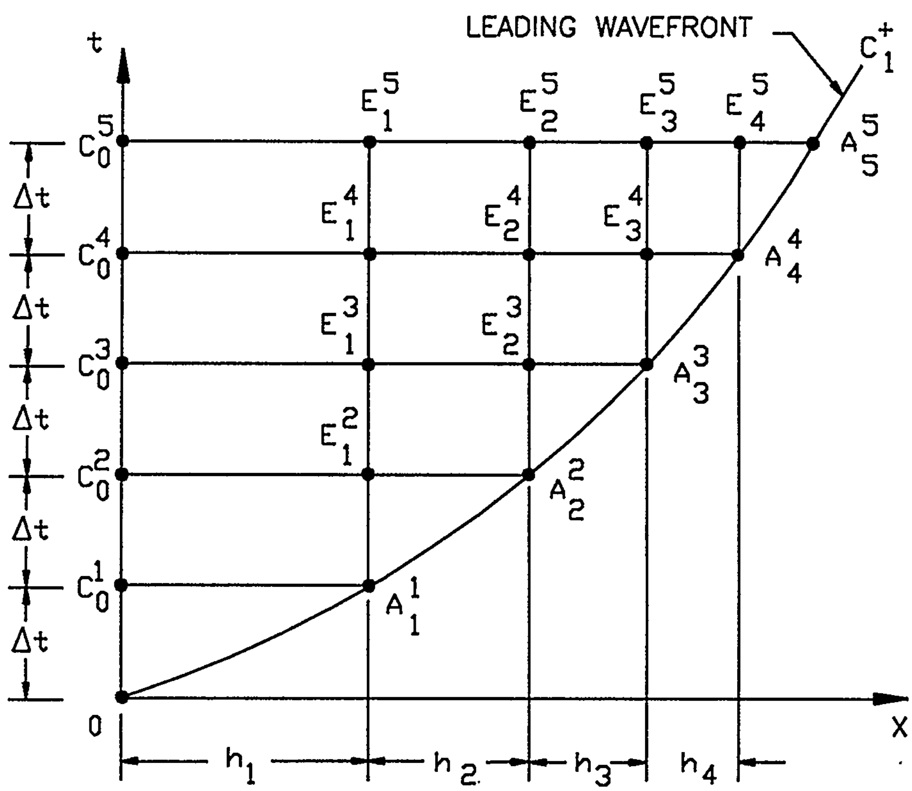

FIG. 4.5 THREE DIFFERENT TYPES OF GRID POINTS IN THE DISTURBED REGION

By the assumption of the rod being initially at rest, just in front of the leading wavefront, the medium is still in a quiet state. Without loss of any generality, we can write:

$$v^+ = \sigma^+ = \theta^+ = q^+ = 0 \quad , \tag{4.6a}$$

and

$$\|f\| = f^- - f^+ = f^- \quad , \tag{4.6b}$$

where f^- and f^+ denotes the value of f immediately behind and ahead of the leading wavefront, respectively. For convenience, the superscript $(^-)$ in equation (4.6b) may be dropped, then:

$$\|f\| = f \quad . \tag{4.7}$$

The unknowns correlated by the jump conditions (3.36) discussed in Chapter 3 are now simply expressed as:

$$\sigma = -\rho V_1 v \quad , \tag{4.8a}$$

$$q = \frac{K}{\tau_o V_1}\,\theta \quad , \tag{4.8b}$$

$$q = V_1 \alpha T_o \sigma + V_1 \rho C_\sigma \theta \quad . \tag{4.8c}$$

Together with the jump conditions (4.8), the equation (4.5a) is also taken into account to determine the unknowns. However, the direct integration of equation (4.5a) along its own characteristic direction seems to be impossible due to parameters V_1 and γ which strongly depend on the unknown stress σ. The non-linear nature of the equation immediately suggests that an iterative procedure must be employed.

It is necessary at this stage to introduce the finite difference approximation of integrals. A first-order or linear approximation is defined by the relation:

$$\int_{t_o}^{t_1} f(t)dt = f(t_o)(t_1-t_o) \quad . \tag{4.9}$$

The second-order approximation is expressed by the trapezoidal rule formula as:

$$\int_{t_o}^{t_1} f(t)dt = \frac{1}{2}\,[f(t_o) + f(t_1)]\,(t_1-t_o) \quad . \tag{4.10}$$

To illustrate the procedure, assuming that the unknowns at point A_{J-1}^{J-1} are revealed from the prior calculation, and those are being looked for at a next point A_J^J along the wavefront.

At the first iterative step, values of two parameters V_1 and γ can be obtained by setting:

$$\sigma^* = \sigma(J-1,\ J-1) \quad , \tag{4.11}$$

then

$$\gamma^{(1)} = \hat{\gamma}(\sigma^*) \quad , \tag{4.12a}$$

$$V_1^{(1)} = \hat{V}_1(\sigma^*) \quad , \tag{4.12b}$$

where $\sigma(J-1,J-1)$ denotes the stress σ at point A_{J-1}^{J-1} and the superscript (1) means the first iteration.

Substituting the defined values of γ and V_1 given by (4.12a,b) into equation (4.5a) the integrating from point A_{J-1}^{J-1} to point A_J^J, we have:

$$-\rho V_1^{(1)} \left\{ v^{(1)}(J,J) - v(J-1,J-1) \right\} + \left\{ \sigma^{(1)}(J,J) - \sigma(J-1,J-1) \right\}$$

$$+ \frac{\rho}{\alpha T_o \gamma^{(1)}} \left(C_\sigma \gamma^{(1)} - [V_1^{(1)}]^2 \right) \left\{ \theta^{(1)}(J,J) - \theta(J-1,J-1) \right\}$$

$$+ \frac{\rho \tau_o V_1^{(1)}}{K\alpha T_o \gamma^{(1)}} \left(C_\sigma \gamma^{(1)} - [V_1^{(1)}]^2 \right) \left\{ q^{(1)}(J,J) - q(J-1,J-1) \right\}$$

$$+ \frac{\rho V_1^{(1)}}{K\alpha T_o \gamma^{(1)}} \left(C_\sigma \gamma^{(1)} - [V_1^{(1)}]^2 \right) \left\{ \frac{q^{(1)}(J,J) + q(J-1,J-1)}{2} \right\} \Delta t = 0 \ , \tag{4.13}$$

which leads to:

$$-\rho V_1^{(1)} v^{(1)}(J,J) + \sigma^{(1)}(J,J) + \frac{\rho}{\alpha T_o \gamma^{(1)}} \left(C_\sigma \gamma^{(1)} - [V_1^{(1)}]^2 \right) \theta^{(1)}(J,J)$$

$$+ \frac{\rho V_1^{(1)}}{K\alpha T_o \gamma^{(1)}} \left(C_\sigma \gamma^{(1)} - [V_1^{(1)}]^2 \right) \left(\tau_o + \frac{\Delta t}{2} \right) q^{(1)} (J,J) = C1 \quad , \tag{4.14}$$

where

$$C1 = -\rho V_1^{(1)} v(J-1,J-1) + \sigma(J-1,J-1)$$

$$+ \frac{\rho}{\alpha T_o \gamma^{(1)}} \left(C_\sigma \gamma^{(1)} - [V_1^{(1)}]^2 \right) \theta(J-1,J-1) + \frac{\rho V_1^{(1)}}{K\alpha T_o \gamma^{(1)}}$$

$$\times \left(C_\sigma \gamma^{(1)} - [V_1^{(1)}]^2 \right) \left(\tau_o - \frac{\Delta t}{2} \right) q(J-1,J-1) \quad . \tag{4.15}$$

The jump conditions (4.8) applied to point A_J^J give:

$$\sigma^{(1)}(J,J) = -\rho V_1^{(1)} \; v^{(1)}(J,J) \quad , \qquad (4.16a)$$

$$q^{(1)}(J,J) = \frac{K}{\tau_o V_1^{(1)}} \, \theta^{(1)}(J,J) \quad , \qquad (4.16b)$$

$$q^{(1)}(J,J) = V_1^{(1)} \; \alpha T_o \sigma^{(1)}(J,J) + V_1^{(1)} \rho C_\sigma \theta^{(1)}(J,J) \quad . \qquad (4.16c)$$

The system of equations (4.14) and (4.16), consisting of four unknowns, namely $v^{(1)}(J,J)$, $\sigma^{(1)}(J,J)$, $\theta^{(1)}(J,J)$, and $q^{(1)}(J,J)$, and $q^{(1)}(J,J)$ can be solved by an elimination technique.

Next iterations are also proceeded in a similar manner. After the first one, however, the value of σ^* expressed by (4.11) is replaced as:

$$\sigma^* = \frac{1}{2} \left\{ \sigma(J-1,J-1) + \sigma^{(k-1)}(J,J) \right\} \quad , \qquad (4.17)$$

where $k = 2,3,\ldots,N$.

It is reminded that the unknowns at the origin (say) being the first point suffered by the force impact and separating the waves into two types of disturbances propagating in the medium cannot be similarly found by this procedure but by the other way as discussed in Chapter 3.

The length h_J between two points A_{J-1}^{J-1} and A_J^J denoting the distance which the leading wavefront is moving in a small time interval Δt is approximately computed by:

$$h_J \approx V_1^{(k)} \, \Delta t \quad , \qquad (4.18)$$

where $V_1^{(k)}$ is the converged value of the wavefront speed V_1 at the kth iteration.

Also, it should be mentioned that the spatial increment h_I ($I = 1,2,3,\ldots,J$), of course, is not necessarily the same.

4.2.2 Grid Points Along the Ot-Axis

Treatment of the unknowns at these points is primarily based on the given boundary conditions and the two characteristic curves having the negative slopes as shown in Figure 4.6.

In the case of the boundary grid points, there are only two characteristic equations involved since there are only two characteristic curves C_1^- and C_2^- that pass through the point C_o^J ($J= 1,2,\ldots,N$) and lie within the solution domain. The positive characteristic curves C_1^+ and C_2^+ pass through the same point but lie outside the solution domain. Therefore, the equations along these curves are temporarily neglected under the circumstances.

In the characteristic equations (4.5c,d), the presence of three unknowns parameters γ, V_1 and V_2 which are functions of stress σ, causes a great deal of difficulty in the integrations. To make the numerical computation become simpler, the iterative technique formerly applied to those points along the leading wavefront is employed here.

Assuming that the values of parameters are given by:

$$V_1^{(1)} = \hat{V}_1(\sigma^*) \quad , \tag{4.19a}$$

$$V_2^{(1)} = \hat{V}_2(\sigma^*) \quad , \tag{4.19b}$$

$$\gamma_{H_1}^{(1)} = \gamma_{G_1}^{(1)} = \hat{\gamma}(\sigma^*) \quad , \tag{4.19c}$$

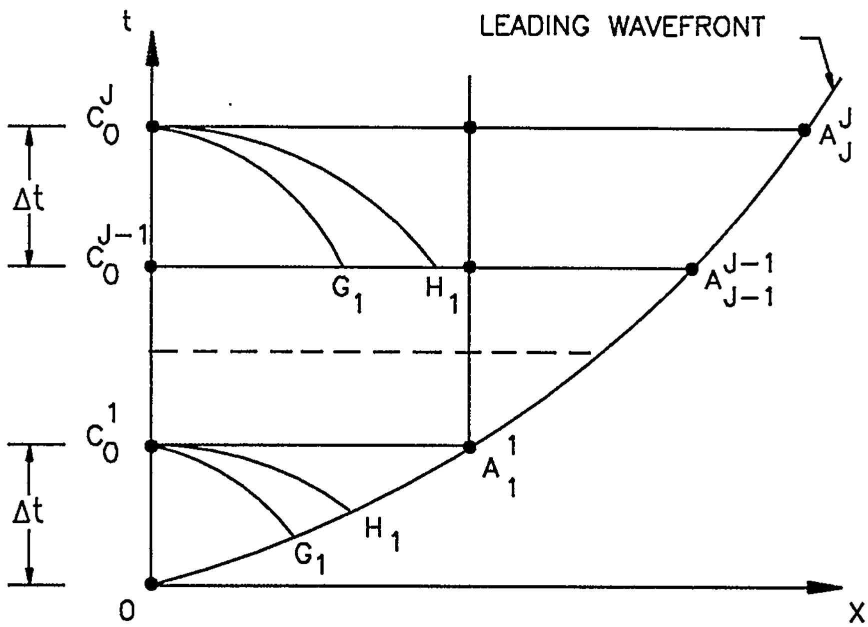

FIG. 4.6 CHARACTERISTIC CURVES PASSING THROUGH BOUNDARY GRID POINTS - THE CASE OF CONDUCTING MATERIALS

where

$$\sigma^* = \sigma(0,J-1) \quad . \tag{4.20}$$

Also, assuming that the characteristic curves having the negative slopes $-V_1^{(1)}$ and $-V_2^{(2)}$ pass through the point C_0^J and intersect the horizontal line drawn from the point C_0^{J-1} at H_1 and G_1, respectively. The intermediate unknowns at these two points are found by either linear or quadratic interpolation whichever is suitable .

Integrating the equation (4.5c) and (4.5d) along the characteristic curves $C_0^J H_1$ and $C_0^J G_1$, respectively, and taking into account the prescribed boundary conditions, we have the two following cases:

<u>Case (i): $v(0,t)$ and $\theta(0,t)$ prescribed:</u>

– *along* $C_0^J H_1$:

$$\sigma^{(1)}(0,J) - \frac{\rho V_1^{(1)}}{K\alpha T_o \gamma_{H_1}^{(1)}} \left(C_\sigma \gamma_{H_1}^{(1)} - [V_1^{(1)}]^2\right) \left(\tau_o + \frac{\Delta t}{2}\right) q^{(1)}(0,J) = C2 \quad , \tag{4.21a}$$

– *along* $C_0^J G_1$:

$$\sigma^{(1)}(0,J) - \frac{\rho V_2^{(1)}}{K\alpha T_o \gamma_{G_1}^{(1)}} \left(C_\sigma \gamma_{G_1}^{(1)} - [V_2^{(1)}]^2\right) \left(\tau_o + \frac{\Delta t}{2}\right) q^{(1)}(0,J) = C3 \quad , \tag{4.21b}$$

where C2 and C3 are constant and given by:

$$C2 = -\rho V_1^{(1)} \left\{v(0,J) - v_{H_1}^{(1)}\right\} + \sigma_{H_1}^{(1)} - \frac{\rho}{\alpha T_o \gamma_{H_1}^{(1)}} \left(C_\sigma \gamma_{H_1}^{(1)} - [V_1^{(1)}]^2\right)$$

$$\times \left\{\theta(0,J) - \theta_{H_1}^{(1)}\right\} - \frac{\rho V_1^{(1)}}{K\alpha T_o \gamma_{H_1}^{(1)}} \left(C_\sigma \gamma_{H_1}^{(1)} - [V_1^{(1)}]^2\right) \left(\tau_o - \frac{\Delta t}{2}\right) q_{H_1}^{(1)} \quad , \tag{4.21c}$$

$$C3 = -\rho V_2^{(1)} \left\{v(0,J) - v_{G_1}^{(1)}\right\} + \sigma_{G_1}^{(1)} - \frac{\rho}{\alpha T_o \gamma_{G_1}^{(1)}} \left(C_\sigma \gamma_{G_1}^{(1)} - [V_2^{(1)}]^2\right)$$

$$\times \left\{\theta(0,J) - \theta_{G_1}^{(1)}\right\} - \frac{\rho V_2^{(1)}}{K\alpha T_o \gamma_{G_1}^{(1)}} \left\{C_\sigma \gamma_{G_1}^{(1)} - [V_2^{(1)}]^2\right\} \left(\tau_o - \frac{\Delta t}{2}\right) q_{G_1}^{(1)} \quad . \tag{4.21d}$$

The two equations (4.21a) and (4.21b) contain two unknowns $\sigma^{(1)}(0,J)$ and $q^{(1)}(0,J)$ which are determined by the elimination method.

<u>Case (ii): $\sigma(0,t)$ and $\theta(0,t)$ prescribed</u>:

– *along* $C_0^J H_1$:

$$\rho V_1^{(1)}\, v^{(1)}(0,J) - \frac{\rho V_1^{(1)}}{K\alpha T_o \gamma_{H_1}^{(1)}} \left(C_\sigma \gamma_{H_1}^{(1)} - [V_1^{(1)}]^2\right) \left(\tau_o + \frac{\Delta t}{2}\right) q^{(1)}(0,J) = C4 \ , \tag{4.22a}$$

– *along* $C_0^J G_1$:

$$\rho V_2^{(1)} v^{(1)}(0,J) - \frac{\rho V_2^{(1)}}{K\alpha T_o \gamma_{G_1}^{(1)}} \left(C_\sigma \gamma_{G_1}^{(1)} - [V_2^{(1)}]^2\right) \left(\tau_o + \frac{\Delta t}{2}\right) q^{(1)}(0,J) = C5 \ , \tag{4.22b}$$

where C4 and C5 are defined by:

$$C4 = \rho V_1^{(1)} v_{H_1}^{(1)} - \left\{\sigma(0,J) - \sigma_{H_1}^{(1)}\right\} - \frac{\rho}{\alpha T_o \gamma_{H_1}^{(1)}} \left(C_\sigma \gamma_{H_1}^{(1)} - [V_1^{(1)}]^2\right)$$

$$\times \left\{\theta(0,J) - \theta_{H_1}^{(1)}\right\} - \frac{\rho V_1^{(1)}}{K\alpha T_o \gamma_{H_1}^{(1)}} \left(C_\sigma \gamma_{H_1}^{(1)} - [V_1^{(1)}]^2\right) \left(\tau_o - \frac{\Delta t}{2}\right) q_{H_1}^{(1)} \ , \tag{4.22c}$$

$$C5 = \rho V_2^{(1)} v_{G_1}^{(1)} - \left\{\sigma(0,J) - \sigma_{G_1}^{(1)}\right\} - \frac{\rho}{\alpha T_o \gamma_{G_1}^{(1)}} \left(C_\sigma \gamma_{G_1}^{(1)} - [V_2^{(1)}]^2\right)$$

$$\times \left\{\theta(0,J) - \theta_{G_1}^{(1)}\right\} - \frac{\rho V_2^{(1)}}{K\alpha T_o \gamma_{G_1}^{(1)}} \left(C_\sigma \gamma_{G_1}^{(1)} - [V_2^{(1)}]^2\right) \left(\tau_o - \frac{\Delta t}{2}\right) q_{G_1}^{(1)} \ . \tag{4.22d}$$

The two unknowns $v^{(1)}(0,J)$ and $q^{(1)}(0,J)$ in equations (4.22a,b) are then obtained by the elimination method, as before.

The next iteration is performed similar to the first one except that the stress σ^* previously defined by (4.20) is changed to :

$$\sigma^*_{H_1} = \frac{1}{2}\left\{\sigma^{(1)}(0,J) + \sigma^{(1)}_{H_1}\right\} \quad , \tag{4.23a}$$

$$\sigma^*_{G_1} = \frac{1}{2}\left\{\sigma^{(1)}(0,J) + \sigma^{(1)}_{G_1}\right\} \quad . \tag{4.23b}$$

From which values of parameters being in terms of the stress σ are expressible as :

$$V^{(2)}_1 = \hat{V}_1\ (\sigma^*_{H_1}) \quad , \tag{4.24a}$$

$$V^{(2)}_1 = \hat{V}_2\ (\sigma^*_{G_1}) \quad , \tag{4.24b}$$

$$\gamma^{(2)}_{H_1} = \hat{\gamma}_1\ (\sigma^*_{H_1}) \quad , \tag{4.24c}$$

$$\gamma^{(2)}_{G_1} = \hat{\gamma}_2\ (\sigma^*_{G_1}) \quad . \tag{4.24d}$$

At point C^1_0 , the procedure for determining the values of unknowns is the same as that applied to other points along the Ot-axis. However, in this case, two points H_1 and G_1 are now the intersections of the characteristic curves C^-_1 and C^-_2 passing through C^1_0 and the leading wavefront, respectively. The term $\frac{\Delta t}{2}$ in equations (4.21) and (4.22) is then replaced by $\left(\frac{\Delta t - t_{H_1}}{2}\right)$ and $\left(\frac{\Delta t - t_{G_1}}{2}\right)$, where t_{H_1} and t_{G_1} are the time coordinates of H_1 and G_1. The values of t_{H_1} and t_{G_1} are found as:

$$t_{H_1} = \frac{\Delta t V^{(1)}_1(\sigma^*)}{[V_f + V^{(1)}_1(\sigma^*)]} \quad , \tag{4.25a}$$

$$t_{G_1} = \frac{\Delta t\ V_2^{(1)}(\sigma^*)}{[V_f + V_2^{(1)}(\sigma^*)]} \quad , \tag{4.25b}$$

where V_f is the speed of the leading wavefront and is computed from the origin to point A_1^1 .

4.2.3 Interior Grid Points

With the purpose of determining the unknowns at these grid points, four characteristic equations (4.5) are taken into account and numerically integrated along their own characteristic directions. A typical interior grid point, E_I^J, is illustrated in Figure 4.7 wherein I_1, J_1, G_1 and H_1 are the feet of the characteristic curves C_1^+, C_2^+, C_2^- and C_1^-, respectively. The solution at point E_I^J is to be computed with the knowledge of the solutions at points E_{I-1}^{J-1}, E_I^{J-1} and E_{I+1}^{J-1}.

The procedure performed here is similar to that applied to the grid points along the boundaries. At the first iteration, we may assume that the parameters existing in the set of ordinary differential equations (4.5) are in the following form:

$$V_1^{(1)} = \hat{V}_1(\sigma^*) \quad , \tag{4.26a}$$

$$V_2^{(1)} = \hat{V}_2(\sigma^*) \quad , \tag{4.26b}$$

$$\gamma_{I_1}^{(1)} = \gamma_{H_1}^{(1)} = \hat{\gamma}_1(\sigma^*) \quad , \tag{4.26c}$$

$$\gamma_{J_1}^{(1)} = \gamma_{G_1}^{(1)} = \hat{\gamma}_2(\sigma^*) \quad , \tag{4.26d}$$

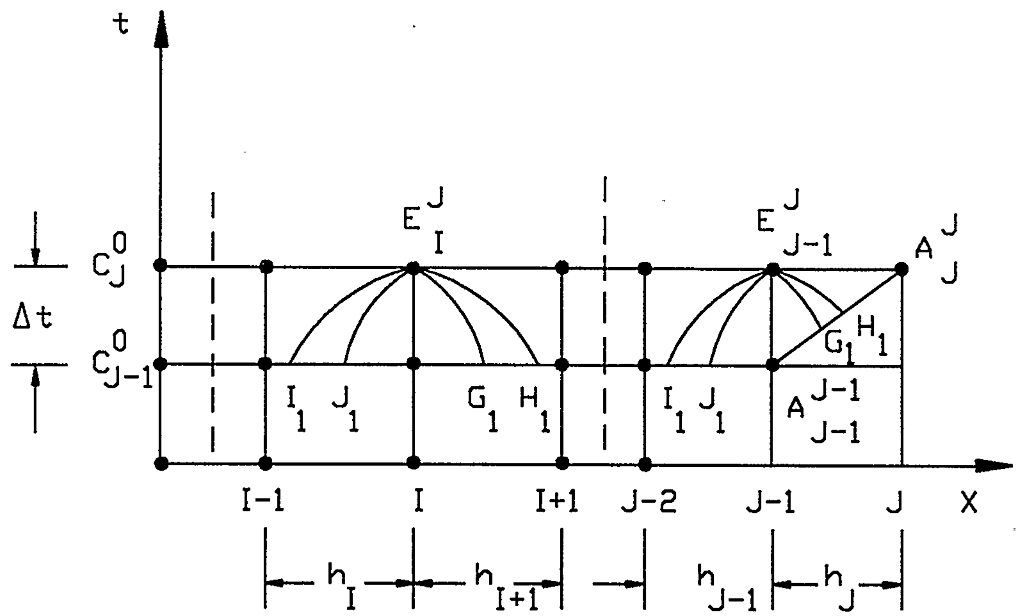

FIG. 4.7 CHARACTERISTIC CURVES PASSING THROUGH INTERIOR GRID POINTS - THE CASE OF CONDUCTING MATERIALS

in which, σ^* is defined as:

$$\sigma^* = \sigma(I,J-1) \quad . \tag{4.27}$$

After the positions of the points I_1, J_1, G_1 and H_1 are approximately found by a geometric method, intermediate unknowns at these points are simply determined by the technique of interpolation among the points at level (J-1).

The four differential equations (4.5) can now be integrated along $E_I^J I_1$, $E_I^J J_1$, $E_I^J G_1$ and $E_I^J H_1$ using the trapezoidal integration rule given by equation (4.10) with the priorly calculated intermediate unknowns.

- *Along the characteristic curve* $E_I^J I_1$:

$$- \rho V_1^{(1)} v^{(1)}(I,J) + \sigma^{(1)}(I,J) + \frac{\rho}{\alpha T_o \gamma_{I_1}^{(1)}} \left(C_\sigma \gamma_{I_1}^{(1)} - [V_1^{(1)}]^2 \right) \theta^{(1)}(I,J) +$$

$$\frac{\rho V_1^{(1)}}{K\alpha T_o \gamma_{I_1}^{(1)}} \left(C_\sigma \gamma_1^{(1)} - [V_1^{(1)}]^2 \right) \left(\tau_o + \frac{\Delta t}{2} \right) q^{(1)}(I,J) = C6 \quad , \tag{4.28a}$$

- *along the characteristic curve* $E_I^J J_1$:

$$- \rho V_2^{(1)} v^{(1)}(I,J) + \sigma^{(1)}(I,J) + \frac{\rho}{\alpha T_o \gamma_{J_1}^{(1)}} \left(C_\sigma \gamma_{J_1}^{(1)} - [V_2^{(1)}]^2 \right) \theta^{(1)}(I,J) +$$

$$\frac{\rho V_2^{(1)}}{K\alpha T_o \gamma_{J_1}^{(1)}} \left(C_\sigma \gamma_{J_1}^{(1)} - [V_2^{(1)}]^2 \right) \left(\tau_o + \frac{\Delta t}{2} \right) q^{(1)}(I,J) = C7 \quad , \tag{4.28b}$$

- *along the characteristic curve* $E_I^J G_1$:

$$\rho V_2^{(1)} \, v^{(1)}(I,J) + \sigma^{(1)}(I,J) + \frac{\rho}{\alpha T_o \gamma_{J_1}^{(1)}} \left(C_\sigma \gamma_{J_1}^{(1)} - [V_2^{(1)}]^2 \right) \theta^{(1)}(I,J)$$

$$- \frac{\rho V_2^{(1)}}{K\alpha T_o \gamma_{J_1}^{(1)}} \left(C_\sigma \gamma_{J_1}^{(1)} - [V_2^{(1)}]^2 \right) \left(\tau_o + \frac{\Delta t}{2} \right) q^{(1)}(I,J) = C8 \quad , \tag{4.28c}$$

- *along the characteristic curve* $E_I^J H_1$:

$$\rho V_1^{(1)} \, v^{(1)}(I,J) + \sigma^{(1)}(I,J) + \frac{\rho}{\alpha T_o \gamma_{I_1}^{(1)}} \left(C_\sigma \gamma_{I_1}^{(1)} - [V_1^{(1)}]^2 \right) \theta^{(1)}(I,J)$$

$$- \frac{\rho V_1^{(1)}}{K\alpha T_o \gamma_{I_1}^{(1)}} \left(C_\sigma \gamma_{I_1}^{(1)} - [V_1^{(1)}]^2 \right) \left(\tau_o + \frac{\Delta t}{2} \right) q^{(1)}(I,J) = C9 \quad , \tag{4.28d}$$

where:

$$C6 = -\rho V_1^{(1)} v_{I_1}^{(1)} + \sigma_{I_1}^{(1)} + \frac{\rho}{\alpha T_o \gamma_{I_1}^{(1)}} \left(C_\sigma \gamma_{I_1}^{(1)} - [V_1^{(1)}]^2 \right) \theta_{I_1}^{(1)}$$

$$+ \frac{\rho V_1^{(1)}}{K\alpha T_o \gamma_{I_1}^{(1)}} \left(C_\sigma \gamma_{I_1}^{(1)} - [V_1^{(1)}]^2 \right) \left(\tau_o - \frac{\Delta t}{2} \right) q_{I_1}^{(1)} \quad , \qquad (4.29a)$$

$$C7 = -\rho V_2^{(1)} v_{J_1}^{(1)} + G_{J_1}^{(1)} + \frac{\rho}{\alpha T_o \gamma_{J_1}^{(1)}} \left(C_\sigma \gamma_{J_1}^{(1)} - [V_2^{(1)}]^2 \right) \theta_{J_1}^{(1)}$$

$$+ \frac{\rho V_2^{(1)}}{K\alpha T_o \gamma_{J_1}^{(1)}} \left(C_\sigma \gamma_{J_1}^{(1)} - [V_2^{(1)}]^2 \right) \left(\tau_o - \frac{\Delta t}{2} \right) q_{J_1}^{(1)} \quad , \qquad (4.29b)$$

$$C8 = \rho V_2^{(1)} v_{G_1}^{(1)} + \sigma_{G_1}^{(1)} + \frac{\rho}{\alpha T_o \gamma_{J_1}^{(1)}} \left(C_\sigma \gamma_{J_1}^{(1)} - [V_2^{(1)}]^2 \right) \theta_{G_1}^{(1)} -$$

$$+ \frac{\rho V_2^{(1)}}{K\alpha T_o \gamma_{J_1}^{(1)}} \left(C_\sigma \gamma_{J_1}^{(1)} - [V_2^{(1)}]^2 \right) \left(\tau_o - \frac{\Delta t}{2} \right) q_{G_1}^{(1)} \quad , \qquad (4.29c)$$

$$C9 = \rho V_1^{(1)} v_{H_1}^{(1)} + \sigma_{H_1}^{(1)} + \frac{\rho}{\alpha T_o \gamma_{I_1}^{(1)}} \left(C_\sigma \gamma_{I_1}^{(1)} - [V_1^{(1)}]^2 \right) \theta_{H_1}^{(1)} \quad -$$

$$\frac{\rho V_1^{(1)}}{K\alpha T_o \gamma_{I_1}^{(1)}} \left(C_\sigma \gamma_{I_1}^{(1)} - [V_1^{(1)}]^2 \right) \left(\tau_o - \frac{\Delta t}{2} \right) q_{H_1}^{(1)} \quad . \qquad (4.29d)$$

The set of four simultaneous equations (4.28) consisting of four unknowns $v^{(1)}(I,J)$, $\sigma^{(1)}(I,J)$, $\theta^{(1)}(I,J)$ and $q^{(1)}(I,J)$ is a linear system and can be solved by the method of Gauss elimination.

Further iteration can be performed similarly to the first one,

one, but the new values of stress σ^* are now defined as:

$$\sigma^*_{I_1} = \frac{1}{2}\left\{\left(\frac{\sigma^{(k-1)}(I,J) + \sigma^{(k-1)}_{I_1}}{2}\right) + \left(\frac{\sigma^{(k-1)}(I,J) + \sigma^{(k-1)}_{H_1}}{2}\right)\right\} \quad , \tag{4.30a}$$

$$\sigma^*_{J_1} = \frac{1}{2}\left\{\left(\frac{\sigma^{(k-1)}(I,J) + \sigma^{(k-1)}_{J_1}}{2}\right) + \left(\frac{\sigma^{(k-1)}(I,J) + \sigma^{(k-1)}_{G_1}}{2}\right)\right\} \quad . \tag{4.30b}$$

The parameters are then given by:

$$V^{(k)}_1 = \hat{V}_1\ (\sigma^*_{I_1}) \quad , \tag{4.31a}$$

$$V^{(k)}_2 = \hat{V}_2\ (\sigma^*_{J_1}) \quad , \tag{4.31b}$$

$$\gamma^{(k)}_{H_1} = \gamma^{(k)}_{I_1} = \hat{\gamma}_1\ (\sigma^*_{I_1}) \quad , \tag{4.31c}$$

$$\gamma^{(k)}_{G_1} = \gamma^{(k)}_{J_1} = \hat{\gamma}_2\ (\sigma^*_{J_1}) \quad . \tag{4.31d}$$

However, to compute the unknowns at point E^J_{J-1} , the term $\frac{\Delta t}{2}$ in equations (4.28c,4.29c) and (4.28d,4.29d) must be replaced by $\left(\frac{\Delta t - t_{G_1}}{2}\right)$ and $\left(\frac{\Delta t - t_{H_1}}{2}\right)$ respectively, where t_{G_1} and t_{H_1} are determined from the equations (4.25a,4.25b) in which V_f is now the speed of the leading wavefront computed from point A^{J-1}_{J-1} to point A^J_J as shown in Fig.4.7.

The above procedures for computing the unknowns in the disturbed region which consists of three different types of grid points as discussed can be generally summarized in the flow diagrams as shown in Figures 4.8,4.9 and 4.10.

4.3 FINITE ELEMENT METHOD

Recently the rapid evolution of the finite element method is noteworthy. The use of finite elements is an alternative approach to that of finite differences and its considerable advantages and relatively simple logic make it ideally suited for digital computation. In contrast to the finite difference schemes in which the domain of interest is replaced by a set of *discrete points*, in the finite element schemes the domain is divided into subdomains commonly referred to as *finite elements*. The finite element method employs piecewise continuous polynomials to interpolate between node points whereas the finite difference method can be presented using Taylor series in a rather straightforward manner.

The application of finite element method is very vast and successful in various branches. In the field of wave propagation, however, it has not yielded satisfactory solutions yet. Therefore, a refinement of the method is still within the investigations.

In the treatment of hyperbolic system of PDEs logically derived for a wave phenomenon, there are considerable difficulties involved especially in the presence of jump discontinuities. These difficulties require the modification of finite element techniques to achieve acceptable convergence properties.

By using the finite element method Li et al [4.13] have solved the problem of coupled dynamical thermoelasticity in a long hollow

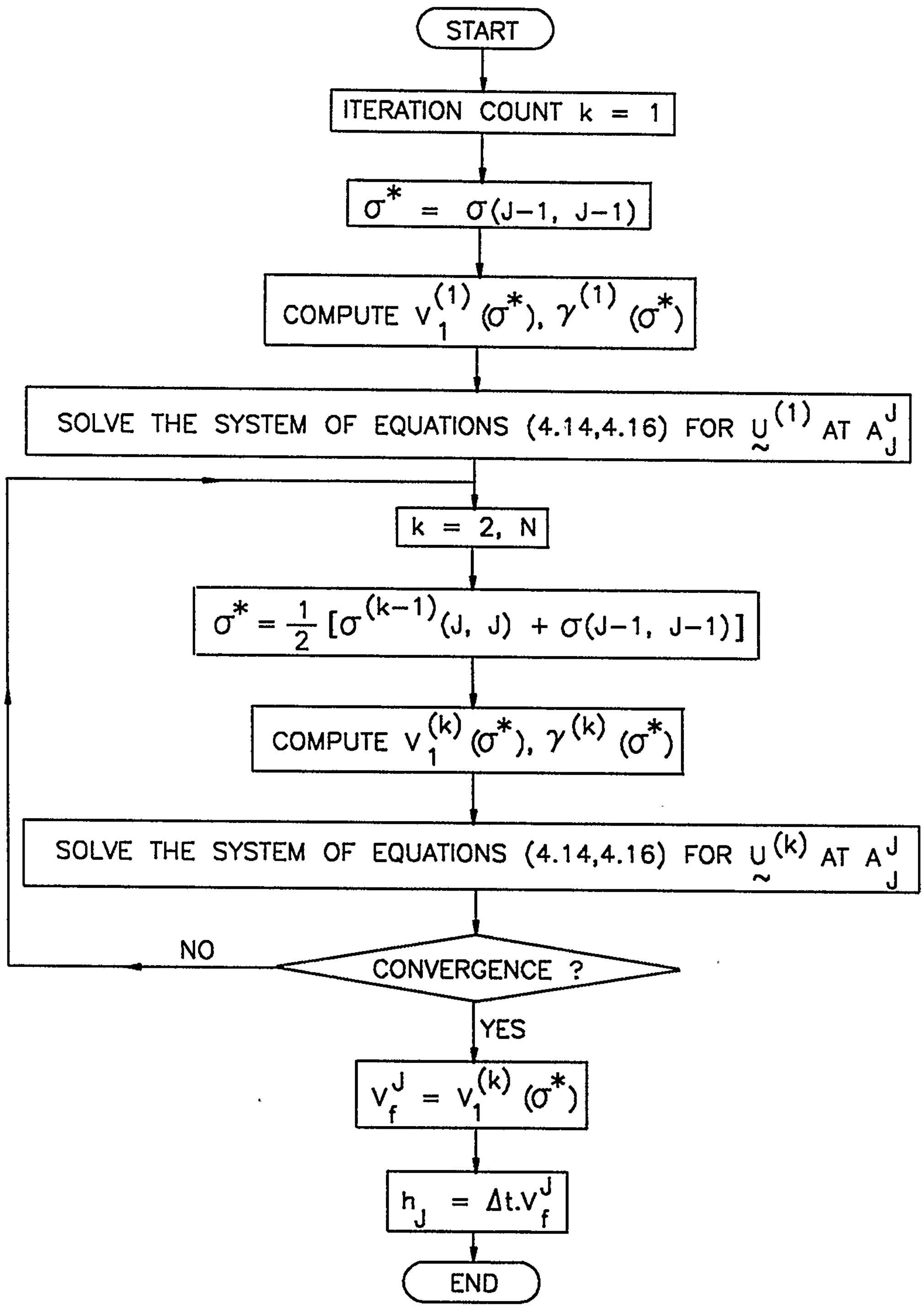

FIG. 4.8 A FLOW DIAGRAM FOR COMPUTING UNKNOWNS AT POINT A_J^J ALONG THE LEADING WAVEFRONT

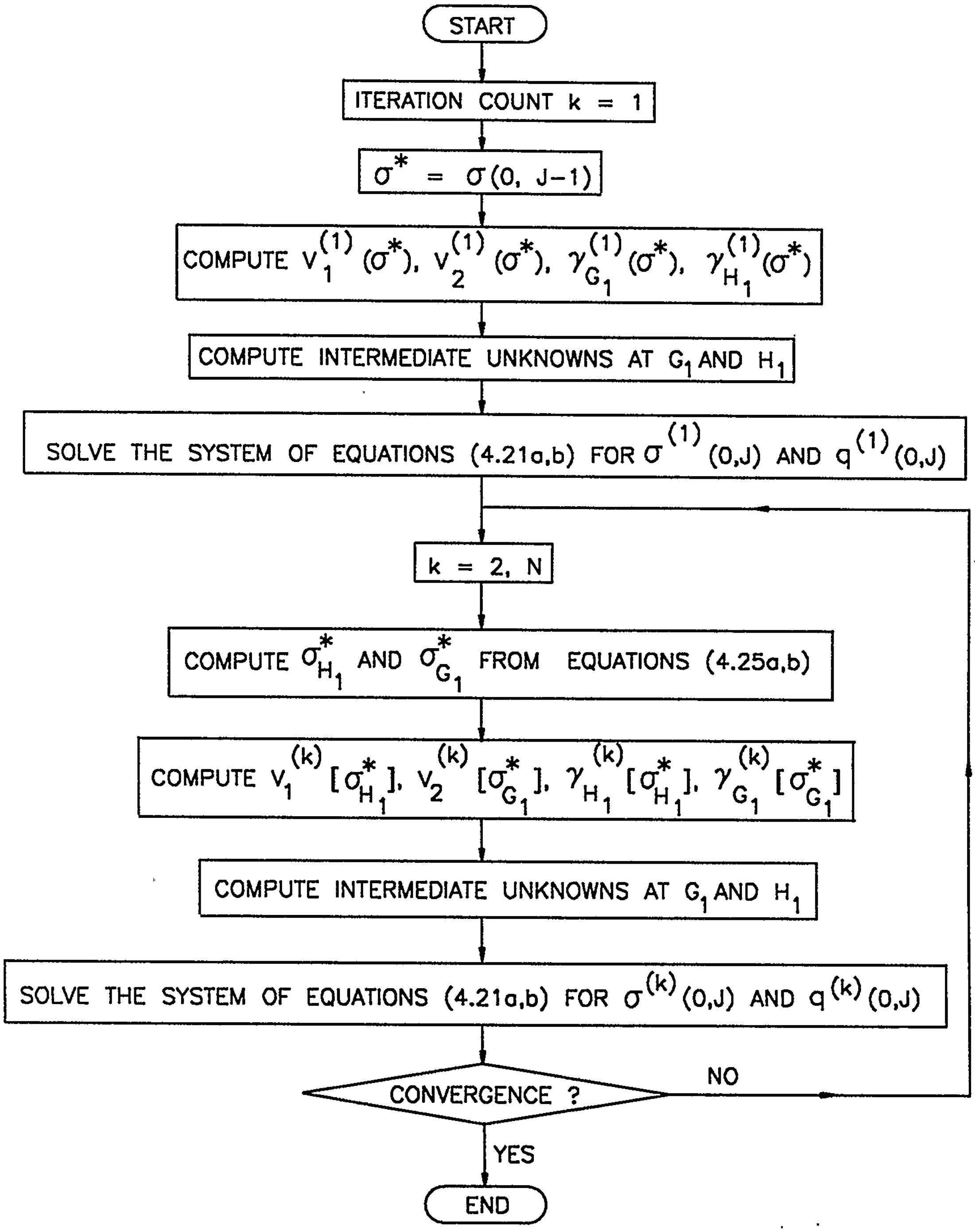

FIG. 4.9 A FLOW DIAGRAM FOR COMPUTING UNKNOWNS AT POINT C_0^J ALONG THE 0t-AXIS WITH $v(0,t)$ AND $\theta(0,t)$ PRESCRIBED

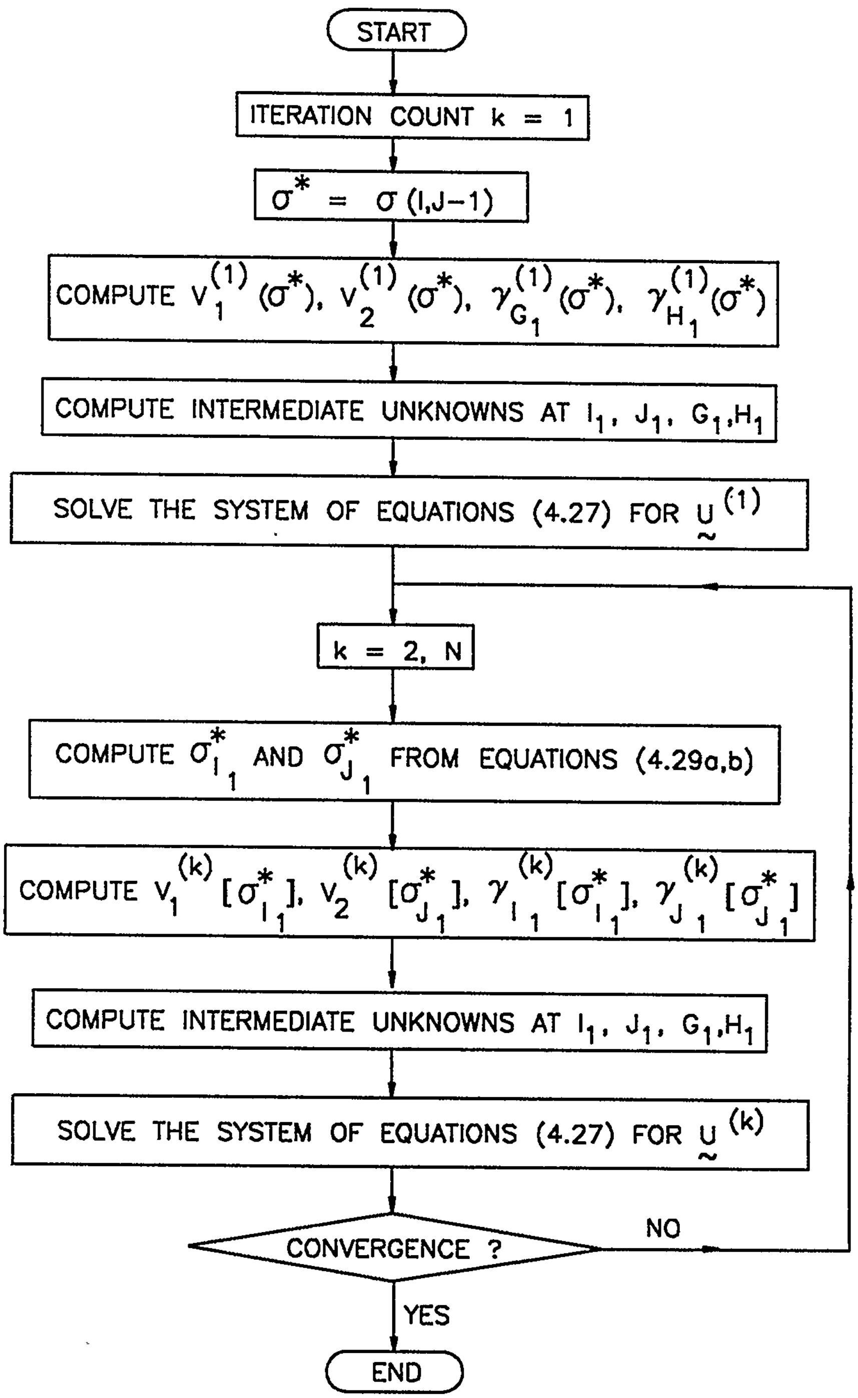

FIG. 4.10 A FLOW DIAGRAM FOR COMPUTING UNKNOWNS AT AN INTERIOR GRID POINT E_I^J

cylinder. Fost et al [4.14] combined it with the Lax-Wendroff method for analyzing the non-linear wave phenomena in hyper-elastic bodies. Prevost and Tao [4.15] employed the method along with the predictor and corrector method to investigate the transient phenomena in thermoelastic solids including the second sound effect. Besides, many published papers [4.16,4.17] relating to the area of fluid mechanics are also found in the similar manner.

In this section, a new approach of the finite element method is introduced for suitably treating strong discontinuities at the fronts. This approach is a synthesis of the method of characteristics, the finite difference method and the finite element method having the functions which are briefly stated as follows.

(i) The method of characteristics is used to determine the second boundary formed by the leading wavefront as well as the jump in unknowns along and across it.

(ii) The finite difference method is implied for solving the unknowns at those points along the Ot-axis (first boundary) and at the points next to the leading wavefront.

(iii) The finite element method being the main purpose of this part, is employed to obtain the solutions of unknowns at interior grid points in the disturbed region .

For the sake of analysis, the system of basic equations of a one-dimensional non-linear thermoelastic material is rewritten from the equations (2.72a,b,c,d) as:

$$\rho \frac{\partial v}{\partial t} - \frac{\partial \sigma}{\partial x} = 0 \qquad , \qquad (4.32a)$$

$$\frac{\partial}{\partial t}\left\{\left(\frac{\sigma}{\mu}\right)^n + \alpha\theta\right\} - \frac{\partial\theta}{\partial x} = 0 \quad , \tag{4.32b}$$

$$\tau_o \frac{\partial q}{\partial t} + q + K\frac{\partial\theta}{\partial x} = 0 \quad , \tag{4.32c}$$

$$\alpha T_o \frac{\partial\sigma}{\partial t} + \rho C_\sigma \frac{\partial\theta}{\partial t} + \frac{\partial q}{\partial x} = 0 \quad . \tag{4.32d}$$

4.3.1 Interior Grid Points

According to the Galerkin finite element method, functions of dependent variables can be expressed in finite element notations as:

$$v(x,t) \cong \hat{v}(x,t) = \sum_{i=1}^{N} V(t)\ \phi_i(x) \quad , \tag{4.33a}$$

$$\sigma(x,t) \cong \hat{\sigma}(x,t) = \sum_{i=1}^{N} S(t)\ \phi_i(x) \quad , \tag{4.33b}$$

$$\theta(x,t) \cong \hat{\theta}(x,t) = \sum_{i=1}^{N} \Delta(t)\ \phi_i(x) \quad , \tag{4.33c}$$

$$q(x,t) \cong \hat{q}(x,t) = \sum_{i=1}^{N} Q(t)\ \phi_i(x) \quad . \tag{4.33d}$$

In addition to the above approximation, the power term σ^n in equation (4.32b) is given by [Cf.4.18,4.19]:

$$\sigma^n(x,t) \cong \hat{\sigma}^n(x,t) = \sum_{i=1}^{N} S^n(t)\ \phi_i(x) \quad , \tag{4.33e}$$

where $\phi_i(x)$ is usually called the shape function or trial function which has a linear form as illustrated in Figure 4.11 and is defined as follows:

$$\phi_1^e(x) = 1 - \frac{x}{h_I} \quad , \qquad (4.34a)$$

$$\phi_2^e(x) = \frac{x}{h_I} \quad , \qquad (4.34b)$$

$$0 \le x \le h_I \quad ,$$

where h_I is the length of the element consisting of two nodes (I-1) and I. Values of h_I's as previously mentioned in the method of characteristics (section 4.2) need not be constant.

Substituting equation (4.33) into the system (4.32), we have:

$$R_1(x,t) = \rho \frac{\partial \hat{v}}{\partial t} - \frac{\partial \hat{\sigma}}{\partial x} \quad , \qquad (4.35a)$$

$$R_2(x,t) = \frac{\partial}{\partial t}\left(\frac{\hat{\sigma}}{\mu}\right)^n + \alpha \frac{\partial \hat{\theta}}{\partial t} - \frac{\partial \hat{v}}{\partial x} \quad , \qquad (4.35b)$$

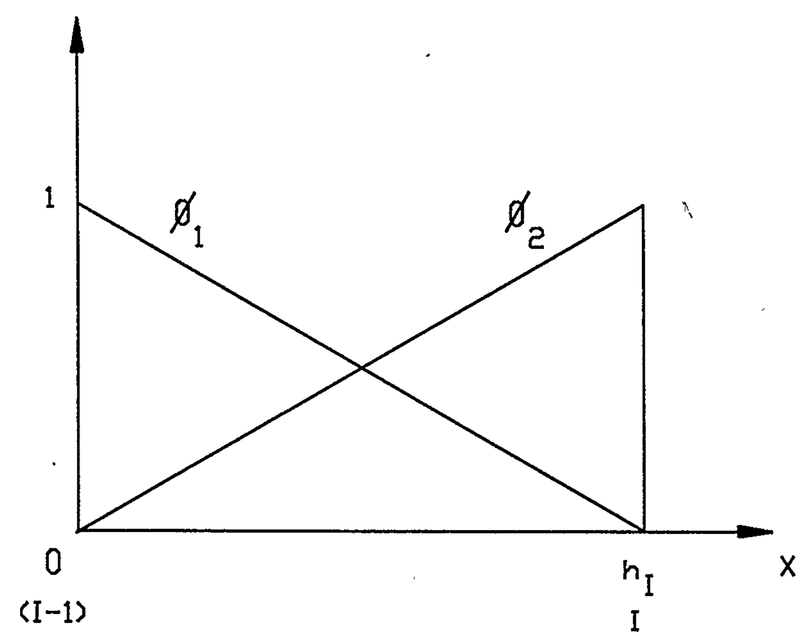

FIG. 4.11 LINEAR BASIC FUNCTION OF THE FINITE ELEMENT METHOD

$$R_3(x,t) = \tau_o \frac{\partial \hat{q}}{\partial t} + K \frac{\partial \hat{\theta}}{\partial x} + \hat{q} \quad , \tag{4.35c}$$

$$R_4(x,t) = \alpha T_o \frac{\partial \hat{\sigma}}{\partial t} + \rho C_\sigma \frac{\partial \hat{\theta}}{\partial t} + \frac{\partial \hat{q}}{\partial x} \quad . \tag{4.35d}$$

In which $R_i(x,t)$, $(i = 1,2,3,4)$ are referred to as the residual errors and made orthogonal to each of the N basic functions appearing in equations (4.33).

The set of $(4 \times N)$ equations in $(4 \times N)$ unknowns is generally represented by:

$$\int R_i(x,t)\, w_j(x)\, dx = 0 \quad , \tag{4.36}$$

$$i = 1,2,3,4 \quad \text{and} \quad j = 1,2$$

where $w_j(x)$ denotes the test function [4.20]. One of the forms of test functions introduced in this thesis is given by [4.21]:

$$w_1(x) = \phi_1(1-\xi_1) + \xi_1 \left\{ 2(2-3\xi_2) - 6(1-2\xi_2) \frac{x}{h_I} \right\} \quad , \tag{4.37a}$$

$$w_2(x) = (1-\xi_1)\, \phi_2 \quad , \tag{4.37b}$$

$$\text{for } 0 \le x \le h_I$$

The two parameters ξ_1 and ξ_2 called *damping factors* help to reduce the oscillations occurring during the numerical computation. When ξ_1 equals zero, the equation (4.36) is reduced to:

$$\int R_i(x,t)\, \phi_j(x)\, dx = 0 \quad , \tag{4.38}$$

$$\text{where } i = 1,2,3,4 \quad \text{and} \quad j = 1,2$$

The equation (4.38) is familiarly realized as the *conventional Galerkin formulation* whereas the equations (4.36) are considered as the *generalized Galerkin formulation.*

Indeed, the generalized Galerkin finite elements are distinguished from the classical Galerkin finite elements by the fact that they allow the test functions to differ from the trial functions which are used to represent the actual numerical solution. The theoretical background of the generalized Galerkin method is extensively developed in the literature [4.20, 4.21, 4.22] and widely applied to the fluid dynamic problems [4.23, 4.24, 4.25] so far.

Taking derivatives of equation (4.33a) with respect to t, and equation (4.33b) with respect to x, we have:

$$\frac{\partial \hat{v}}{\partial t} = \sum_{i=1}^{N_j} \left\{\frac{dV(t)}{dt}\right\} \phi_i(x) \quad , \tag{4.39a}$$

$$\frac{\partial \hat{\sigma}}{\partial x} = \sum_{i=1}^{N_j} S(t) \left\{\frac{d\phi_i(x)}{dx}\right\} \quad . \tag{4.39b}$$

Substituting equations (4.39a,b) into (4.35a) yields:

$$R_1(x,t) = \rho \sum_{i=1}^{N_J} \left\{\frac{dV(t)}{dt}\right\} \phi_i(x) - \sum_{i=1}^{N_J} S(t) \left\{\frac{d\phi_i(x)}{dx}\right\} \quad . \tag{4.40}$$

Substituting the expressions of $R_1(x,t)$ and $w_j(x)$ given by equations (4.35) and (4.37), respectively, into equation (4.36a), then integrating, a general equation can be written as:

$$\rho[K_1] \frac{d\underset{\sim}{V}}{dt} - [K_2] \underset{\sim}{S}(t) = 0 \quad , \tag{4.41}$$

where $[K_1]$ and $[K_2]$ denote the mass and stiffness matrices of the equation of motion (4.32a), respectively, and are defined by:

$$[K_1] = \sum_{i=1}^{N_J} [K_1]_i \quad , \tag{4.42a}$$

$$[K_2] = \sum_{i=1}^{N_J} [K_2]_i \quad , \tag{4.42b}$$

in which:

$$[K_1]_i = \int_0^{h_I} \begin{Bmatrix} W_1(x) \\ W_2(x) \end{Bmatrix} \begin{bmatrix} \phi_1(x) & \phi_2(x) \end{bmatrix} dx \quad , \tag{4.43a}$$

$$[K_2]_i = \int_0^{h_I} \begin{Bmatrix} W_1(x) \\ W_2(x) \end{Bmatrix} \begin{bmatrix} \dfrac{d\phi_1(x)}{dx} & \dfrac{d\phi_2(x)}{dx} \end{bmatrix} dx \quad . \tag{4.43b}$$

By the same token, other general equations can be expressed as:

$$-[K_2]\underset{\sim}{V}(t) + \frac{n}{\mu^n} \underset{\sim}{S}^{n-1}[K_1] \frac{d\underset{\sim}{S}}{dt} + \alpha[K_1] \frac{d\underset{\sim}{\Delta}}{dt} = 0 \quad , \tag{4.44a}$$

corresponding with equation (4.32b).

$$\tau_o[K_1] \frac{d\underset{\sim}{Q}}{dt} + [K_1]\underset{\sim}{Q}(t) + K[K_2]\underset{\sim}{\Delta}(t) = 0 \quad , \tag{4.44b}$$

corresponding with equation (4.32c).

$$\alpha T_o[K_1] \frac{d\underset{\sim}{S}}{dt} + [K_2]\underset{\sim}{Q}(t) + \rho C_\sigma [K_1] \underset{\sim}{\Delta}(t) = 0 \quad , \tag{4.44c}$$

corresponding with equation (4.32d).

The system of general equations consisting of (4.41) and (4.44) and corresponding with the system (4.32) is totally formulated by:

$$[M_1] \frac{d\underset{\sim}{U}_1}{dt} + [C_1] \underset{\sim}{U}_1 = 0 \quad , \tag{4.45}$$

where:

$$\underset{(4\times N_J)}{\underset{\sim}{U}_1} = \left\{ \underset{N_J}{\{V\}} \quad \underset{N_J}{\{S\}} \quad \underset{N_J}{(Q)} \quad \underset{N_J}{\{\Delta\}} \right\}^T \quad , \tag{4.46a}$$

$$\underset{(4N_J\times 4N_J)}{[M_1]} = \begin{bmatrix} \rho[K_1] & [0] & [0] & [0] \\ [0] & \frac{n}{\mu^n} S^{n-1} [K_1] & [0] & \alpha[K_1] \\ [0] & [0] & \tau_o[K_1] & [0] \\ [0] & \alpha T_o[K_1] & [0] & \rho C_\sigma[K_1] \end{bmatrix} \quad , \tag{4.46b}$$

$$\underset{(4N_J\times 4N_J)}{[C_1]} = \begin{bmatrix} [0] & -[K_2] & [0] & [0] \\ -[K_2] & [0] & [0] & [0] \\ [0] & [0] & [K_1] & K[K_2] \\ [0] & [0] & [K_2] & [0] \end{bmatrix} \quad . \tag{4.46c}$$

Applying the general implicit method [4.13, 4.26] to equation (4.45), the following two-point recurrence scheme yields:

$$[M_1] \left(\frac{\underset{\sim}{U}_1^J - \underset{\sim}{U}_1^{J-1}}{\Delta t} \right) + [C_1] \left\{ \xi_2 \underset{\sim}{U}_1^J + (1-\xi_2) \underset{\sim}{U}_1^{J-1} \right\} = 0 \quad , \tag{4.47a}$$

or

$$\frac{1}{\Delta t}[M_1]\underset{\sim}{U}_1^J + \xi_2[C_1]\underset{\sim}{U}_1^J = \frac{1}{\Delta t}[M_1]\underset{\sim}{U}_1^{J-1} - (1-\xi_2)[C_1]\underset{\sim}{U}_1^{J-1} \quad , \qquad (4.47b)$$

where N_J denotes the number of elements considered at the level J.

It should be noted that values of N_J are not constant but changing from time to time. Comparing with other approaches [4.14, 4.27] wherein N_J is assumed to be constant throughout the numerical calculation, this one gives faster computation due to smaller sizes of matrices $[M_1]$ and $[C_1]$.

As illustrated in Figure 4.5, at the interior grid points represented by E_I^J $(I = 1,2,\ldots,J-1)$, the unknowns are obtained by solving the system of simultaneous equations (4.47b).

4.3.2 Grid Points Along the Ot-Axis and Next to the Leading Wavefront

The unknowns at these points can be treated by the help of finite difference method.

(i) At a point denoted by C_0^J along the Ot-axis together with the assumption of $v(0,t)$ and $\theta(0,t)$ prescribed the remaining two unknowns are found from the forward finite difference scheme [4.28, 4.29] applied to equations (4.32b,c):

$$\sigma^{(1)}(0,J) = \sigma(0,J-1) + \left(\frac{\mu^n}{n}\right)\frac{\left\{\frac{\Delta t}{h_1}\left[v(1,J-1)-v(0,J-1)\right]-\alpha\left[\theta(0,J)-(\theta(0,J-1)\right]\right\}}{\left[\frac{\sigma(0,J)\ +\ \sigma(0,J-1)}{2}\right]^{n-1}} \quad , \qquad (4.48a)$$

$$q^{(1)}(0,J) = \frac{1}{\left[\frac{\tau_o}{\Delta t} + 0.5\right]} \left\{\left(\frac{\tau_o}{\Delta t} - 0.5\right) q(0,J-1) - \frac{K}{h_1}\left[\theta(1,J-1) - \theta(0,J-1)\right]\right\} \quad . \qquad (4.48b)$$

The values of stress σ and heat flux q given by (4.48) are considered as the first approximation. Next iterations will be performed after the unknowns at the interior grid points are obtained. The backward finite difference scheme is applied to equations (4.32a) and (4.32d) which yield:

$$\sigma^{(k)}(0,J) = \sigma^{(k-1)}(1,J) - \frac{h_1}{\Delta t}\rho\left\{v(0,J) - v(0,J-1)\right\} \quad , \qquad (4.49a)$$

$$q^{(k)}(0,J) = q^{(k-1)}(1,J) + \frac{h_1}{\Delta t}\left\{\rho C_\sigma\left[\theta(0,J) - \theta(0,J-1)\right] + \alpha T_o\left[\sigma^{(k-1)}(0,J) - \sigma(0,J-1)\right]\right\} \quad . \qquad (4.49b)$$

(ii) At those points next to the leading wavefront such as E_{J-1}^{J}, the unknowns are also determined by the finite difference method. The reason why we employ this method here is to eliminate the difficulty caused by the discontinuous elements due to the feature of combination meshes as shown in Figure 4.5.

Applying the backward finite difference scheme to the system (4.32), we have:

$$\rho v^{(1)}(J-1,J) = \rho v(J-1,J-1) + \frac{\Delta t}{h_{J-1}}\left\{\sigma(J-1,J-1) - \sigma(J-2,J-1)\right\} \quad , \qquad (4.50a)$$

$$\frac{n}{\mu^n}\left[\frac{\sigma^{(1)}(J-1,J)+\sigma(J-1,J-1)}{2}\right]^{n-1}\sigma^{(1)}(J,J-1)+\alpha\theta^{(1)}(J-1,J)=$$

$$\frac{n}{\mu^n}\left[\frac{\sigma^{(1)}(J-1,J)+\sigma(J-1,J-1)}{2}\right]^{n-1}\sigma(J-1,J-1)+\alpha\theta(J-1,J-1)+$$

$$\frac{\Delta t}{h_{J-1}}\left\{v(J-1,J-1)-v(J-2,J-1)\right\}\quad,\qquad(4.50b)$$

$$\left(\tau_o+\frac{\Delta t}{2}\right)q^{(1)}(J-1,J)=\left(\tau_o-\frac{\Delta t}{2}\right)q(J-1,J-1)-\frac{K}{h_{J-1}}\left\{\theta(J-1,J-1)-\theta(J-2,J-1)\right\}\quad,\qquad(4.50c)$$

$$\alpha T_o\sigma^{(1)}(J-1,J)+\rho C_\sigma\theta^{(1)}(J-1,J)=\alpha T_o\sigma(J-1,J-1)+\rho C_\sigma\theta(J-1,J-1)+$$

$$\frac{\Delta t}{h_{J-1}}\left\{q(J-1,J-1)-q(J-2,J-1)\right\}\quad.\qquad(4.50d)$$

The system (4.50) consisting of four unknowns $v^{(1)}(J-1,J)$, $\sigma^{(1)}(J-1,J)$, $\theta^{(1)}(J-1,J)$ and $q^{(1)}(J-1,J)$ can be solved by Gauss elimination method together with an iterative technique.

Next approximations of the unknowns can be computed by the centered finite difference scheme. The unknowns, at this stage, are obtained from the following system of equations:

$$\rho v^{(k)}(J-1,J)=\rho v(J-1,J-1)+\frac{\Delta t}{(h_{J-1}+h_J)}\left\{\sigma(J,J)-\sigma^{(k-1)}(J-2,J)\right\}\quad,$$

(4.51a)

$$\frac{n}{\mu^n}\left[\frac{\sigma^{(k)}(J-1,J)+\sigma(J-1,J-1)}{2}\right]^{n-1}\sigma^{(k)}(J-1,J)+\alpha\theta^{(k)}(J-1,J)=$$

$$\frac{n}{\mu^n}\left[\frac{\sigma^{(k)}(J-1,J)+\sigma(J-1,J-1)}{2}\right]^{n-1}\sigma(J-1,J-1)+\alpha\theta(J-1,J-1)+$$

$$\frac{\Delta t}{(h_{J-1}+h_J)}\left\{v(J,J)-v^{(k-1)}(J-2,J)\right\}\quad, \tag{4.51b}$$

$$\left(\tau_o+\frac{\Delta t}{2}\right)q^{(k)}(J-1,J)=\left(\tau_o-\frac{\Delta t}{2}\right)q(J-1,J-1)-\frac{K}{(h_{J-1}+h_J)}\left\{\theta(J,J)-\right.$$

$$\left.\theta^{(k-1)}(J-2,J)\right\}\quad, \tag{4.51c}$$

$$\alpha T_o\sigma^{(k)}(J-1,J)+\rho C_\sigma\theta^{(k)}(J-1,J)=\alpha T_o\sigma(J-1,J-1)+\rho C_\sigma\theta(J-1,J-1)-$$

$$\frac{\Delta t}{(h_{J-1}+h_J)}\left\{q(J,J)-q^{(k-1)}(J-2,J)\right\}\quad. \tag{4.51d}$$

4.3.3 Grid Points Along the Leading Wavefront

Determination of the locations of points forming the leading wavefront as well as the jumps in unknowns is similar to the one performed by the method of characteristics. Thus, a repeated procedure is not necessary here.

The process of defining unknowns in the disturbed region by the finite element method discussed above can be partially outlined in the following flow diagram (Figure 4.12).

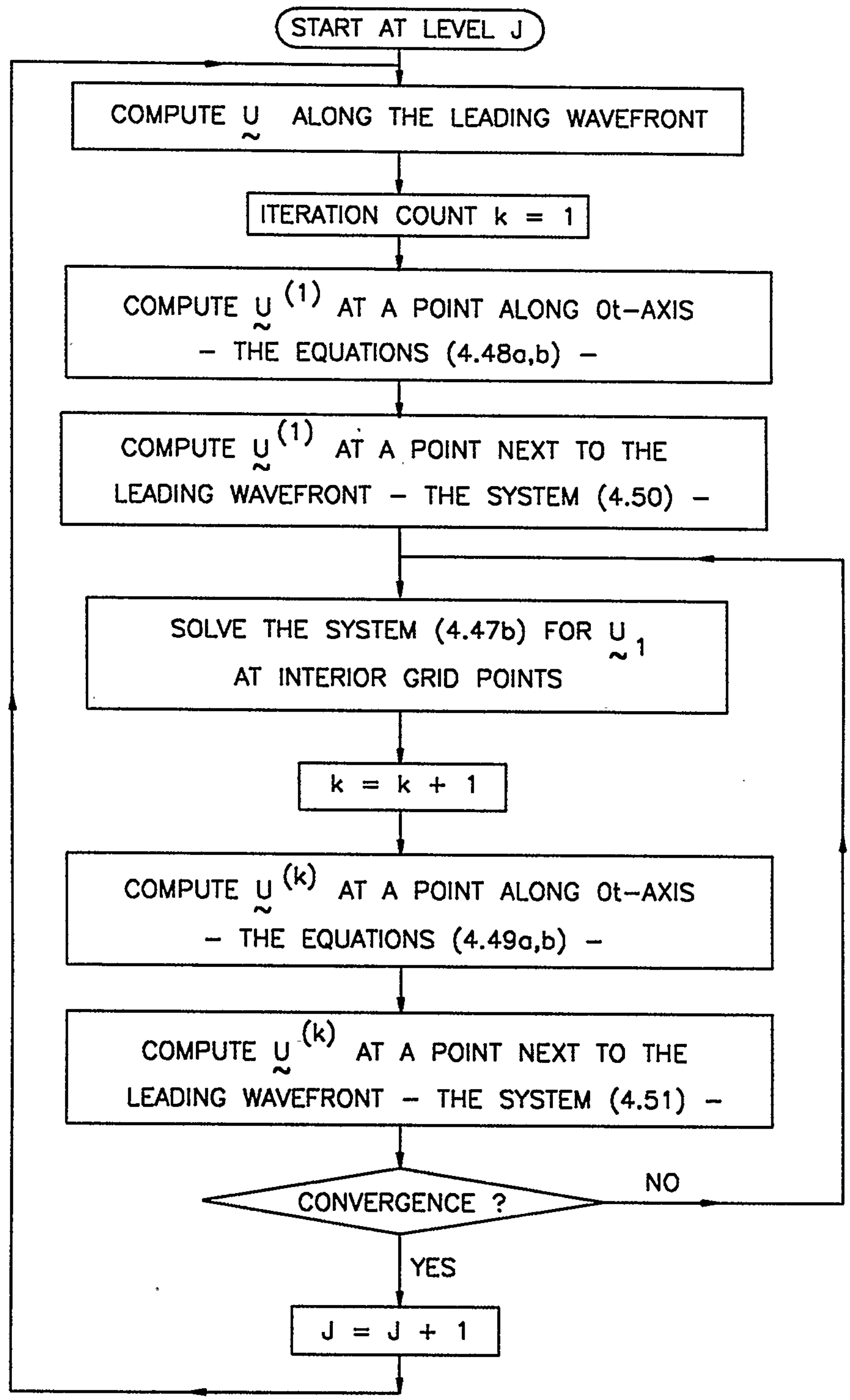

FIG. 4.12 A FLOW DIAGRAM FOR THE NUMERICAL COMPUTATION BASED ON THE FINITE ELEMENT METHOD

CHAPTER 5
NUMERICAL METHOD FOR NON-CONDUCTING MATERIALS

In this chapter, numerical procedures are developed for seeking the solutions of waves propagating in non-conductors through the system of equations along with its auxiliary conditions discussed in Chapter 3.

Three methods will be presented here, namely the characteristic method, the finite element method and the similarity method. The concepts of the first two methods are introduced and discussed in detail in Chapter 4 for the quasi-linear hyperbolic equations expressing the wave motion in conductors. The last method, which is widely applied to various problems in science and engineering, consists in searching for a solution which is invariant under a group of transformations.

Considering a semi-infinite thermally elastic non-conducting medium that is initially at rest and has a uniform temperature, for a one-dimensional case, the fundamental equations are recalled from Chapter 3:

$$\rho \frac{\partial v}{\partial t} - \frac{\partial \sigma}{\partial x} = 0 \quad , \tag{5.1a}$$

$$\frac{\partial}{\partial t}\left\{\left(\frac{\sigma}{\mu}\right)^n + \alpha\theta\right\} - \frac{\partial \theta}{\partial x} = 0 \quad , \tag{5.1b}$$

$$\alpha T_o \frac{\partial \sigma}{\partial t} + \rho C_\sigma \frac{\partial \theta}{\partial t} = 0 \quad . \tag{5.1c}$$

5.1 THE METHOD OF CHARACTERISTICS

After the transformation, the system of equations (5.1) can be written in a general form as follows:

$$\underset{\sim}{U}_{2t} + [B_1'] \, \underset{\sim}{U}_{2x} = 0 \quad . \tag{5.2}$$

where $\underset{\sim}{U}_{2t}$, $\underset{\sim}{U}_{2x}$ and $[B_1']$ are given by (3.44a), (3.44b) and (3.46b), respectively. The eigenvalues of equation (5.2) have been found to be:

$$C_3: \quad \lambda_5 = 0 \quad , \tag{5.3a}$$

$$C_4^+: \quad \lambda_6 = \sqrt{\frac{C_\sigma}{\beta\rho C_\sigma - \alpha^2 T_o}} \quad , \tag{5.3b}$$

$$C_4^-: \quad \lambda_7 = \sqrt{\frac{C_\sigma}{\beta\rho C_\sigma - \alpha^2 T_o}} \quad , \tag{5.3c}$$

where β is defined by equation (3.8a).

The left eigenvectors associated with the matrix $[B_1']$ are given by:

$$\underset{\sim}{\ell}^{(5)} = \begin{Bmatrix} 0 \\ 1 \\ \dfrac{\rho C_\sigma}{\alpha T_o} \end{Bmatrix}^T ; \quad \text{corresponding to } \lambda_5 = 0 \quad , \tag{5.4a}$$

$$\underset{\sim}{\ell}^{(6)} = \begin{Bmatrix} -\rho\lambda_6 \\ 1 \\ 0 \end{Bmatrix}^T ; \quad \text{corresponding to } \lambda_6 = \frac{dx^6}{dt} \quad , \tag{5.4b}$$

$$\underset{\sim}{\ell}^{(7)} = \begin{Bmatrix} -\rho\lambda_7 \\ 1 \\ 0 \end{Bmatrix}^T \quad ; \quad \text{corresponding to } \lambda_7 = -\lambda_6 = -\frac{dx^6}{dt} \quad . \tag{5.4c}$$

The equation along the characteristic C_3 with $\lambda_5 = 0$ is:

$$\frac{d\sigma}{dt} + \rho \frac{C_\sigma}{\alpha T_o} \frac{d\theta}{dt} = 0 \quad . \tag{5.5a}$$

Equation (5.5a) is merely a restatement of equation (5.1c) along C_3. Similarly, the characteristic equations along C_4^+ and C_4^- are, respectively:

$$-\rho\lambda_6 \frac{dv}{dt} + \frac{d\sigma}{dt} = 0 \quad , \tag{5.5b}$$

$$\rho\lambda_6 \frac{dv}{dt} + \frac{d\sigma}{dt} = 0 \quad . \tag{5.5c}$$

As in the case of conducting materials (Chapter 4), the combination meshes are distributed in the disturbed region bounded by the Ot-axis and the wavefront . The unknowns at grid points which are categorized into three types are then determined in a similar manner.

5.1.1 Grid Points Along the Front Path

As mentioned in part B of Chapter 3, the wave path may be traced by either the wavefront as one of the characteristic curves or by the shockfront mainly developed from the Rankine-Hugoniot conditions. There are two cases that must be considered :

(i) Case 1: Simple Waves

In this case, the wavefront is determined from the characteristic curve having a positive slope and passing through the first point along the boundary. As the medium is quiescent at the initial state, the jump conditions across the front are written as:

$$\sigma = -\rho V_f v \quad , \tag{5.6a}$$

$$\sigma = -\frac{\rho C_\sigma}{\alpha T_o}\,\theta \quad , \tag{5.6b}$$

where V_f denotes the velocity of the wavefront and is defined by:

$$V_f = V_6 = \sqrt{\frac{C_\sigma}{\beta\rho C_\sigma - \alpha^2 T_o}} \quad . \tag{5.7}$$

It is obvious that the value V_6 is a function of a yet unknown stress σ. To eliminate the difficulty caused by the non-linear term β at this juncture, the iterative method which is aforementioned in Chapter 4 is employed. Let:

$$\sigma^* = \sigma(J-1,J-1) \quad , \tag{5.8}$$

where $\sigma(J-1,J-1)$ is the computed stress at the grid point A_{J-1}^{J-1} along the wavefront. The value of V_6 is then given by:

$$V_f^{(1)} = V_6^{(1)} = \hat{V}_6\,(\sigma^*) \quad . \tag{5.9}$$

Integrating characteristic equation (5.5b) from point A_{J-1}^{J-1} to point A_J^J, we have:

$$-\rho V_f^{(1)}\, v^{(1)}(J,J) + \sigma^{(1)}(J,J) = -\rho V_f^{(1)}\, v(J-1,J-1) + \sigma(J-1,J-1) \quad . \tag{5.10a}$$

At point A_J^J, the jump conditions (5.6) imply that:

$$\sigma^{(1)}(J,J) = -\rho V_f^{(1)} v^{(1)}(J,J) \quad , \tag{5.10b}$$

$$\sigma^{(1)}(J,J) = \frac{-\rho C_\sigma}{\alpha T_o} \theta^{(1)}(J,J) \quad . \tag{5.10c}$$

The above system (5.10) consisting of three unknowns $v^{(1)}(J,J)$, $\sigma^{(1)}(J,J)$ and $\theta^{(1)}(J,J)$ is solvable by an elimination method.

By the same token, next iterations are carried out, however, the stress σ^* is now defined by:

$$\sigma^* = \frac{1}{2}\left\{\sigma(J-1,J-1) + \sigma^{(k-1)}(J,J)\right\} \quad , \tag{5.11}$$

$$\text{where } k \geq 2 \quad .$$

The distance which the wavefront is travelling in a time interval Δt is also determined as:

$$h_J = \Delta t \; V_f^{(k)} \quad . \tag{5.12}$$

It is noted that the distances $h_1, h_2, \ldots, h_J$ are not necessarily to be the same.

(ii) Case 2: Shock Waves

The problem becomes more complicated when there are shock waves involved. In reality, the shock wave is not a discontinuity at all but a narrow zone, a few mean free paths in thickness through which the variables change continuously, even though very steeply. However, seeking the smooth solution of the problem containing shocks is still an important point for investigations. By employing *ad hoc* procedures, many workers [5.1-5.4] neglected the existence of shock and smeared out the solutions at the shockfronts.

With the aid of artificial dissipative terms first introduced by von Neumann and Richtmyer [5.5], the shock is treated not as a discontinuity but as a confined region across which the dependent variables vary rapidly but continuously. The successful calculations by this method was reported by Brode [5.6] who considered the determination of blast waves and explosions in the presence of cylindrical and spherical symmetry. Even so, this technique may lead to the inaccurate results since the viscosity term tends to smear the entire solution. The stability solutions can also be obtained by the two-step finite difference schemes [5.7] automatically treating the shocks, whenever and wherever they may occur, without necessity of the tedious application of the jump conditions at each time step of the solution process.

Bailey and Chen [5.8] have recently suggested "a shock fitting" method that keeps track of the location of the shock. By this method, they not only acquired the solution variables along the front but also defined the location of the shockfront of the disturbance propagating in a non-linear elastic material.

Analogously, the shock fitting method will be employed in this chapter to determine the salient features at the front.

It is recalled that the amplitude of the shock derived in Chapter 3 is expressible as:

$$2U_s \frac{d\varepsilon}{dt} + \varepsilon \frac{dU_s}{dt} = U_s^2 \frac{\partial \varepsilon}{dx} - \frac{1}{\rho} \frac{\partial \sigma}{\partial x} \quad , \qquad (5.13)$$

where

$$U_s = \sqrt{\frac{1}{\rho}\frac{\sigma}{\varepsilon}} \quad . \tag{5.14}$$

The brackets "$\|\quad\|$" in equations (3.59) and (3.67) are dropped in equations (5.14) and (5.13) respectively, due to the medium assumed to be initially at rest.

Referring to Figure 5.1, the finite difference method is applied to equation (5.13) yields :

$$2U_s^J \left\{\frac{\varepsilon(J,J) - \varepsilon(J-1,J-1)}{\Delta t}\right\} + \varepsilon(J,J)\left\{\frac{U_s^J - U_s^{J-1}}{\Delta t}\right\} =$$

$$(U_s^J)^2 \left\{\frac{\varepsilon(J-1,J-1) - \varepsilon(J-2,J-1)}{h_{J-1}}\right\} - \frac{1}{\rho}\left\{\frac{\sigma(J-1,J-1) - \sigma(J-2,J-1)}{h_{J-1}}\right\} \quad . \tag{5.15}$$

Across the shockfront, the jump conditions imply that:

$$v = -\frac{1}{\rho U_s}\sigma \quad , \tag{5.16a}$$

$$\theta = -\frac{\alpha T_o}{\rho C_\sigma}\sigma \quad , \tag{5.16b}$$

$$\varepsilon = \left(\frac{\sigma}{\mu}\right)^n + \alpha\theta \quad . \tag{5.16c}$$

Substituting equation (5.16b) into (5.16c), we have:

$$\varepsilon = \left(\frac{\sigma}{\mu}\right)^n - \frac{\alpha^2 T_o}{\rho C_\sigma}\sigma \quad . \tag{5.17}$$

Eliminating the strain ε in equation (5.15) by the right-hand side of equation (5.17), the stress at the point A_J^J is defined by:

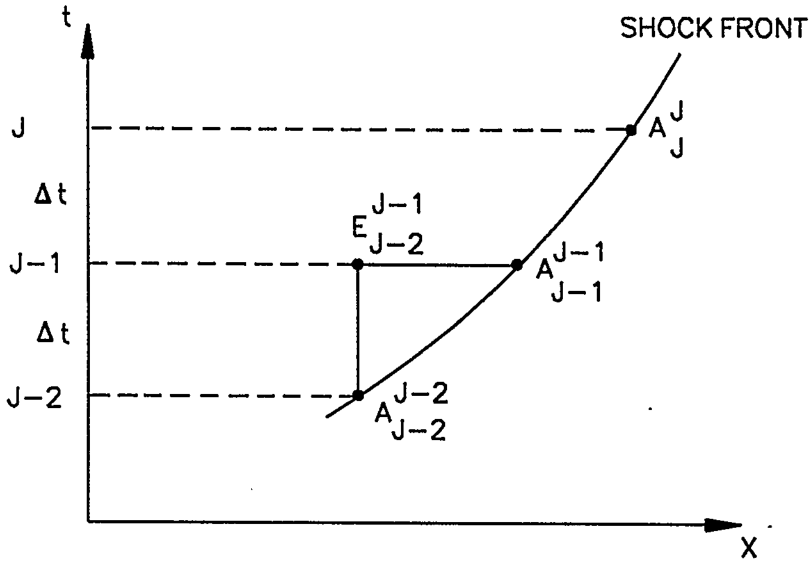

FIG. 5.1 TREATMENT OF POINTS ALONG THE SHOCKFRONT

$$\sigma(J,J) = \frac{Z1 + Z2 + Z3}{\left\{1 - \frac{\rho C_\sigma}{\alpha^2 T_o \mu^n} [\sigma(J,J)]^{n-1}\right\}} \quad , \tag{5.18}$$

or

$$\sigma(J,J) = \hat{\sigma}(Z1,\ Z2,\ Z3,\ \sigma) \quad , \tag{5.19}$$

where

$$Z1 = \frac{1}{3U_s^J - U_s^{J-1}} \left\{1 - \frac{\rho C_\sigma}{\alpha^2 T_o \mu^n} \Big[\sigma(J\text{-}1,J\text{-}1)\Big]^{n-1}\right\} \left\{2U_s^J + \frac{\Delta t}{h_{J-1}} (U_s^J)^2\right\} \times \sigma(J\text{-}1,J\text{-}1) \quad , \tag{5.20a}$$

$$Z2 = \frac{-(U_s^J)^2\ \Delta t}{h_{J-1}\left(3U_s^J - U_s^{J-1}\right)} \left\{1 - \frac{\rho C_\sigma}{\alpha^2 T_o \mu^n} \Big[\sigma(J\text{-}1,J\text{-}2)\Big]^{n-1}\right\} \sigma(J\text{-}2,J\text{-}1) \quad , \tag{5.20b}$$

$$Z3 = \frac{\Delta t C_\sigma}{h_{J-1}\left(3U_s^J - U_s^{J-1}\right)} \left\{\frac{\sigma(J-1,J-1) - \sigma(J-2,J-1)}{\alpha^2 T_o}\right\} \quad , \qquad (5.20c)$$

and U_s^J denoting the speed of shockfront at point A_J^J is given as:

$$U_s^J = \left\{ \frac{\sigma(J,J)}{\rho\left\{\left[\frac{\sigma(J,J)}{\mu}\right]^n - \frac{\alpha^2 T_o}{\rho C_\sigma}\sigma(J,J)\right\}} \right\}^{1/2} \quad , \qquad (5.21)$$

or

$$U_s^J = \hat{U}_s\ (\sigma(J,J)) \quad . \qquad (5.22)$$

The speeds of shockfront at other points are also found in the similar manner.

The first iteration is done by setting:

$$\sigma^* = \sigma(J-1,J-1) \quad . \qquad (5.23)$$

The values of U_s^J and $\sigma(J,J)$ are respectively estimated as:

$$\overset{(1)}{U_s^J} = \hat{U}_s\ (\sigma^*) \quad , \qquad (5.24)$$

$$\sigma^{(1)}(J,J) = \hat{\sigma}\ (Z1^{(1)},\ Z2^{(1)},\ Z3^{(1)},\ \sigma^*) \quad . \qquad (5.25)$$

in which $Z1^{(1)}$, $Z2^{(1)}$, $Z3^{(1)}$ are determined from equations (5.21).

Next iterations are analogously performed. However, the stress σ^* is assumed to be:

$$\sigma^* = \sigma^{(k-1)}(J,J) \qquad (5.26)$$

with $k \geq 2$.

The distance between two points A_{J-1}^{J-1} and A_J^J is approximately computed as:

$$h_J = \Delta t \; \overset{(k)}{U_s^J} \quad . \tag{5.27}$$

5.1.2 Grid Points Along the Ot-Axis

With the help of iterative methods, let:

$$\sigma^* = \sigma(0,J-1) \quad . \tag{5.28}$$

The wave speed V_6 is evaluated by:

$$V_6^{(1)} = \hat{V}_6(\sigma^*) \quad . \tag{5.29}$$

Integrating the characteristic equation (5.5c) along the path $C_0^J G_1$, where G_1 is the intersection of the curve C_4^- and the horizontal line passing through the point C_0^{J-1} (as in Figure 5.2):

$$\rho V_6^{(1)} v^{(1)}(0,J) + \sigma^{(1)}(0,J) = \rho V_6^{(1)} \; v_{G_1}^{(1)} + \sigma_{G_1}^{(1)} \quad , \tag{5.30}$$

in which the values of $v_{G_1}^{(1)}$ and $\sigma_{G_1}^{(1)}$ are determined by the interpolating technique.

Together with the prescribed boundary condition, the equation (5.30) consisting of two unknowns $v^{(1)}(0,J)$ and $\sigma^{(1)}(0,J)$ can be solved without any difficulty.

The procedure is repeated until the values of unknowns to be converged. It is noted that from the second iteration, the stress σ^* is assumed to be:

$$\sigma^* = \frac{1}{2}\left\{\sigma^{(k-1)}(0,J) + \sigma_{G_1}^{(k-1)}\right\} \quad . \tag{5.31}$$

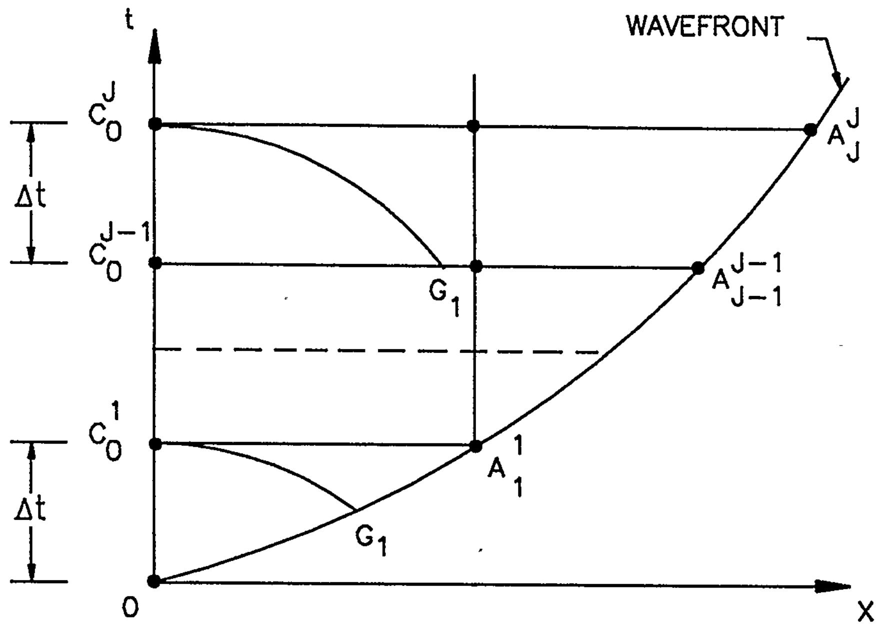

FIG. 5.2 CHARACTERISTIC CURVES PASSING THROUGH THE BOUNDARY GRID POINTS - THE CASE OF NON-CONDUCTING MATERIALS

The temperature θ is determined by:

$$\theta(0,J) = -\frac{\alpha T_o}{\rho C_\sigma}\,\sigma^{(k)}(0,J) \quad . \tag{5.32}$$

5.1.3 Interior Grid Points

The unknowns at each interior grid point can be determined by integrating each of the characteristic equation (5.5) along its own direction.

As usual, we set:

$$\sigma^* = \sigma(I,J-1) \quad , \tag{5.33}$$

$$V_6^{(1)} = \hat{V}_6\,(\sigma^*) \quad . \tag{5.34}$$

As illustrated in Figure 5.3, I_1 and J_1 are the feet of the characteristic curves C_4^+ and C_4^- respectively. Values of immediate unknowns v and σ at points I_1 and J_1 are computed by either linear or quadratic interpolation based on the known values of the variables which are prior calculated at the level (J-1).

Integration of equation (5.56) along $E_I^J I_1$ leads to :

$$-\rho V_6^{(1)}\, v^{(1)}\,(I,J) + \sigma^{(1)}(I,J) = -\rho V_6^{(1)}\, v_{I_1}^{(1)} + \sigma_{I_1}^{(1)} \;, \tag{5.35a}$$

and integration of equation (5.5c) along $E_I^J J_1$ gives :

$$\rho V_6^{(1)}\, v^{(1)}\,(I,J) + \sigma^{(1)}(I,J) = \rho V_6^{(1)}\, v_{J_1} + \sigma_{J_1}^{(1)} \;. \tag{5.35b}$$

After the unknowns $v^{(1)}(I,J)$ and $\sigma^{(1)}(I,J)$ included in equations (5.35) are obtained, next steps of the computation can be processed by assuming that:

$$\sigma^* = \frac{1}{2}\left\{\sigma^{(k-1)}(I,J) + \sigma_{I_1}^{(k-1)}\right\} \tag{5.36}$$

The unknown θ is determined from the characteristic equation (5.5a) integrated along the characteristic line C_3 which is parallel to the Ot-axis. The result is obtained as:

$$\theta^{(k)}(I,J) = -\frac{\alpha T_o}{\rho C_\sigma}\,\sigma^{(k)}(I,J) \quad . \tag{5.37}$$

It should be noted that the algorithm of the characteristic

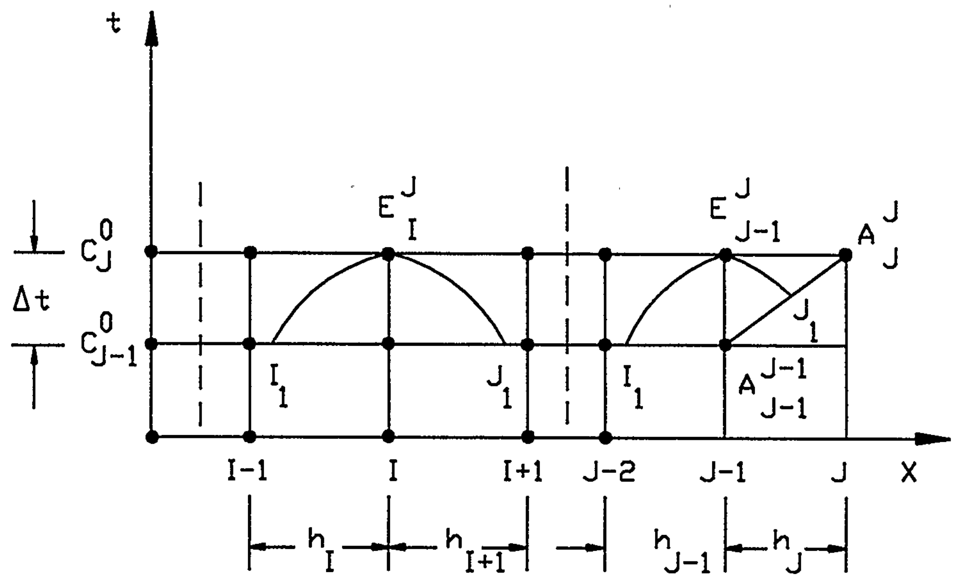

FIG. 5.3 CHARACTERISTIC CURVES PASSING THROUGH INTERIOR GRID POINTS - THE CASE OF NON-CONDUCTING MATERIALS

method developed above yields smooth solutions for the case of simple waves or weak shock waves only. When there is a strong shock involved in the problem, the solutions of unknowns at the points adjacent to the shockfront are unstable due to the explicit application of this method. To improve the numerical results, a finite difference scheme is applied to such points .

At the point E_{J-1}^J, the unknowns are determined by the following system of equations obtained from the basic equations (5.1):

$$\rho v(J-1,J) = \frac{\Delta t}{h_{J-1}+h_J} \{\sigma(J,J) - \sigma(J-2,J)\} + \rho v(J-1,J-1) \quad , \tag{5.38a}$$

$$\frac{n}{\mu^n}\left[\frac{\sigma(J-1,J)+\sigma(J-1,J-1)}{2}\right]^{n-1}[\sigma(J-1,J)]+\alpha\theta(J-1,J)=$$

$$\frac{n}{\mu^n}\left[\frac{\sigma(J-1,J)+\sigma(J-1,J-1)}{2}\right]^{n-1}[\sigma(J-1,J-1)]+\alpha\theta(J-1,J-1)+$$

$$\frac{\Delta t}{h_{J-1}+h_J}\{v(J,J)-v(J-2,J)\}\quad, \tag{5.38b}$$

$$\alpha T_o\,\sigma(J-1,J)+\rho C_\sigma\,\theta(J-1,J)=\alpha T_o\sigma(J-1,J-1)+\rho C_\sigma\theta(J-1,J-1)\quad. \tag{5.38c}$$

The above system composed of three unknowns $v(J-1,J)$, $\sigma(J-1,J)$ and $\theta(J-1,J)$ can be solved by an iterative method.

5.2 THE FINITE ELEMENT METHOD

Based on the analysis of finite element method discussed in detail in Chapter 4, the results are now summarized in the following.

5.2.1 Interior Grid Points

Applying the generalized Galerkin method to the system of equations (5.1) yields:

$$[M_2]\frac{d\underset{\sim}{U}_3}{dt}+[C_2]\underset{\sim}{U}_3=0\quad, \tag{5.39}$$

where:

$$\underset{(3N_J)}{\underset{\sim}{U}_3}=\left\{\underset{(N_J)}{\{V\}}\quad\underset{(N_J)}{\{S\}}\quad\underset{(N_J)}{\{\Delta\}}\right\}^T\quad, \tag{5.40a}$$

$$\underset{(3N_J \times 3N_J)}{[M_2]} = \begin{bmatrix} \rho[K_1] & [0] & [0] \\ [0] & \frac{n}{\mu^n} S^{n-1}[K_1] & \alpha[K_1] \\ [0] & \alpha T_o[K_1] & \rho C_\sigma[K_1] \end{bmatrix} , \qquad (5.40b)$$

$$\underset{(3N_J \times 3N_J)}{[C_2]} = \begin{bmatrix} [0] & -[K_2] & [0] \\ -[K_2] & [0] & [0] \\ [0] & [0] & [0] \end{bmatrix} . \qquad (5.40c)$$

Under the implicit finite difference scheme, equation (5.39) is expressible as:

$$\frac{1}{\Delta t} [M_2] \underset{\sim}{U}_3^J + \xi_2 [C_2] \underset{\sim}{U}_3^J = \frac{1}{\Delta t} [M_2] \underset{\sim}{U}_3^{J-1} - (1-\xi_2) [C_2] \underset{\sim}{U}_3^{J-1} . \qquad (5.41)$$

5.2.2 Grid Points Along the Ot-Axis and Next to the Front Path

With the help of the finite difference method the unknowns at those points can be treated as follows:

(i) <u>Grid Points Along the Ot-Axis</u>

Assuming that the boundary of the medium is subjected to the time-dependent velocity impact. Values of the stress σ and the temperature θ are computed by:

- *the predictor step*: wherein the forward finite difference scheme is employed, the equations (5.1b,c) are respectively expressible as:

$$\frac{n}{\mu^n}\left[\frac{\sigma^{(1)}(0,J) + \sigma(0,J-1)}{2}\right]^{n-1}\left[\sigma^{(1)}(0,J)\right] + \alpha\theta^{(1)}(0,J) =$$

$$\frac{\Delta t}{h_1}\{v(1,J-1) - v(0,J-1)\} + \frac{n}{\mu^n}\left[\frac{\sigma^{(1)}(0,J) + \sigma(0,J-1)}{2}\right]^{n-1}\sigma(0,J-1)$$

$$+ \alpha\theta(0J-1) \quad , \tag{5.42a}$$

$$\alpha T_o\, \sigma^{(1)}(0,J) + \rho C_\sigma \theta^{(1)}(0,J) = \alpha T_o\, \sigma(0,J-1) + \rho C_\sigma \theta(0,J-1) \quad . \tag{5.42b}$$

The two unknowns $\sigma^{(1)}(0,J)$ and $\theta^{(1)}(0,J)$ contained in the above equations can be obtained by simultanuos solution of the two equations.

– *the corrector step:* using the backward finite difference scheme, equation (5.1a) is written as:

$$\rho\left\{\frac{v(0,J) - v(0,J-1)}{\Delta t}\right\} - \left\{\frac{\sigma^{(k)}(0,J) - \sigma^{(k-1)}(1-J)}{h_1}\right\} = 0 \tag{5.43}$$

which yields:

$$\sigma^{(k)}(0,J) = \rho\,\frac{h_1}{\Delta t}\{v(0,J) - v(0,J-1)\} + \sigma^{(k-1)}(1,J) \quad . \tag{5.44a}$$

Similarly, the equation (5.1c) implies that:

$$\theta^{(k)}(0,J) = \theta(0,J-1) - \frac{\alpha T_o}{\rho C_\sigma}\left\{\sigma^{(k)}(0,J) - \sigma(0,J-1)\right\} \quad , \tag{5.44b}$$

where $k \geq 2$.

(ii) <u>Grid Points Next to the Front Path</u>

By the same procedure, as above, the computation of unknowns at these points are also divided into two steps:

- *the predictor step:* the backward finite difference scheme is applied to the system (5.1) yields:

$$v^{(1)}(J-1,J) = v(J-1,J-1) + \frac{\Delta t}{\rho h_{J-1}} \{\sigma(J-1,J-1) - \sigma(J-2,J-1)\} \quad , \tag{5.45a}$$

$$\frac{n}{\mu^n}\left[\frac{\sigma^{(1)}(J-1,J) + \sigma(J-1,J-1)}{2}\right]^{n-1}\left[\sigma^{(1)}(J-1,J)\right] + \alpha\theta^{(1)}(J-1,J) =$$

$$\frac{n}{\mu^n}\left[\frac{\sigma^{(1)}(J-1,J) + \sigma(J-1,J-1)}{2}\right]^{n-1}\left[\sigma(J-1,J-1)\right] + \alpha\theta(J-1,J-1)$$

$$+ \frac{\Delta t}{h_{J-1}} \{v(J-1,J-1) - v(J-2,J-1)\} \quad , \tag{5.45b}$$

$$\alpha T_o\sigma^{(1)}(J-1,J) + \rho C_\sigma\theta^{(1)}(J-1,J) = \alpha T_o\sigma(J-1,J-1) + \rho C_\sigma\theta(J-1,J-1) \quad , \tag{5.45c}$$

from which the three unknowns $v^{(1)}(J-1,J)$, $\sigma^{(1)}(J-1,J)$ and $\theta^{(1)}(J-1,J)$ are determined.

- *the corrector step:* with the aid of the centered finite difference scheme, we have:

$$v^{(k)}(J-1,J) = v(J-1,J-1) + \frac{\Delta t}{\rho(h_{J-1}+h_J)}\left\{\sigma(J,J) - \sigma^{(k-1)}(J-2,J)\right\} \quad , \tag{5.46a}$$

$$\frac{n}{\mu^n}\left[\frac{\sigma^{(k)}(J-1,J) + \sigma(J-1,J-1)}{2}\right]^{n-1}\left[\sigma^{(k)}(J-1,J)\right] + \alpha\theta^{(k)}(J-1,J) =$$

$$\frac{n}{\mu^n}\left[\frac{\sigma^{(k)}(J-1,J) + \sigma(J-1,J-1)}{2}\right]^{n-1}[\sigma(J-1,J-1)] + \alpha\theta(J-1,J-1) +$$

$$\frac{\Delta t}{(h_{J-1}+h_J)}\left\{v(J,J) - \sigma^{(k-1)}(J-2,J)\right\} \quad , \tag{5.46b}$$

$$\alpha T_o\sigma^{(k)}(J-1,J) + \rho C_\sigma\theta^{(k)}(J-1,J) = \alpha T_o\sigma(J-1,J-1) + \rho C_\sigma\theta(J-1,J-1) \quad . \tag{5.46c}$$

5.2.3 Grid Points ALong the Front Path

The front path (wavefront or shockfront) as well as the unknowns along and across it are determined similarly to the case of the characteristic method which is previously analyzed in this chapter.

5.3 THE SIMILARITY METHOD

In recent times, the theory of similarity has been extensively developed in the literature [5.9-5.12]. The mathematical interpretation of the term *similarity* is a transformation of variables, so carried out, that a reduction in the number of independent variables is achieved. A similarity transformation will reduce a partial differential equation in two independent variables and the associated auxiliary conditions, to an ordinary differential equation and appropriate boundary conditions.

The application of the similarity method has been widely extended in various fields such as fluid mechanics, heat transfer, wave propagation, etc. Generally, the method of similarity analysis can be divided into three main categories [5.13]:

(i) Direct method

(ii) Dimensional analysis

(iii) Group theoretic technique.

As a part of this thesis, we do not go through all the above categories but merely employ the *group theoretic technique* to solve the system (5.1). In addition, the theory of this technique is also omitted here since it is beyond the scope of this chapter.

One of the first to use the group theory for obtaining a similarity representation is probably Birkhoff [5.14]. The work was further extended by Moran and Gaggioli [5.15] who developed a systematic formalism which takes into account the auxiliary conditions as a part of the analysis. Moreover, Moran and Marshek [5.16] have extended the analysis for a dimensional matrix by making use of the matrix of exponent of the parameters of a group of transformations. Under the transformation, a given set of governing equations along with their auxiliary conditions are invariant in form.

Following the theory of Moran and his co-workers, Frydrychowicz and Singh extend it to the problems of wave motion in a non-linear elastic rod [1.9] and in a non-linear viscoelastic rod [5.17]. Both are subjected to time dependent velocity impact.

In this section, the analogous technique based on the work of Frydrychowicz and Singh is employed to solve the system (5.1) representing the propagation of disturbances in a non-conductor. Along with the governing equations, the auxiliary conditions are given as follows:

- *Boundary condition*:

$$v(x = 0, t) = V_o t^{\delta} \; ; \quad t > 0 \quad . \tag{5.47a}$$

- *Initial conditions:*

$$v(x, t = 0) = 0 \quad , \tag{5.47b}$$

$$\sigma(x, t = 0) = 0 \quad , \tag{5.47c}$$

$$\theta(x, t = 0) = 0 \quad . \tag{5.47d}$$

5.3.1 Construction of the Group of Transformations

In order that the given system of equations (5.1) together with the auxiliary conditions (5.47) are invariant under a group, a 12-parameter group of transformations is constructed as follows :

$$G_{12}^{A} = \left\{ \begin{array}{l} S_9^A = \left\{ \begin{array}{llll} \bar{x} = A_x x \;, & \bar{t} = A_t t \;; & & \textit{Independent variables} \\ \bar{\rho} = A_\rho \rho \;, & \bar{\mu} = A_\mu \mu \;, & \bar{n} = A_n n & \\ \bar{C}_\sigma = A_{C_\sigma} \;, & \bar{\alpha} = A_\alpha \alpha \;, & \bar{T}_o = A_{T_o} T_o \;, & \\ \bar{V}_o = A_{V_o} V_o \;; & & & \textit{Physical parameters} \end{array} \right. \\ \bar{v} = A_v v \;, \\ \bar{\sigma} = A_\sigma \sigma \;, \qquad\qquad\qquad \textit{Dependent variables} \\ \bar{\theta} = A_\theta \theta \;. \end{array} \right. \tag{5.48}$$

where A_x, A_t, A_ρ, A_μ, A_n, A_{C_σ}, A_α, A_{T_o}, A_{V_o}, A_v, A_σ and A_θ are twelve nondimensional parameters introduced to characterize the eight parameter dimensional group of transformations.

The group G_{12}^{A} may be expanded by including the following transformations defined by:

$$\overline{\frac{\partial v}{\partial t}} = \frac{\partial \bar{v}}{\partial \bar{t}} = A_t^{-1} A_v \frac{\partial v}{\partial t} \quad , \qquad (5.49a)$$

$$\overline{\frac{\partial v}{\partial x}} = \frac{\partial \bar{v}}{\partial \bar{x}} = A_x^{-1} A_v \frac{\partial v}{\partial x} \quad , \qquad (5.49b)$$

$$\overline{\frac{\partial \sigma}{\partial t}} = \frac{\partial \bar{\sigma}}{\partial \bar{t}} = A_t^{-1} A_\sigma \frac{\partial \sigma}{\partial t} \quad , \qquad (5.49c)$$

$$\overline{\frac{\partial \sigma}{\partial x}} = \frac{\partial \bar{\sigma}}{\partial \bar{x}} = A_x^{-1} A_\sigma \frac{\partial \sigma}{\partial x} \quad , \qquad (5.49d)$$

$$\overline{\frac{\partial \theta}{\partial t}} = \frac{\partial \bar{\theta}}{\partial \bar{t}} = A_t^{-1} A_\theta \frac{\partial \theta}{\partial t} \quad , \qquad (5.49e)$$

$$\overline{\frac{\partial}{\partial t} \left(\frac{\sigma}{\mu} \right)^{n}} = \frac{\partial}{\partial \bar{t}} \left(\frac{\bar{\sigma}}{\bar{\mu}} \right)^{\bar{n}} = A_t^{-1} \left(\frac{A_\sigma}{A_\mu} \right)^{A_n n} \frac{\partial}{\partial t} \left(\frac{\sigma}{\mu} \right)^{n} \quad . \qquad (5.49f)$$

Substituting the transformations (5.49) into the system of equations (5.1), respectively, yields:

$$A_x^{-1} A_\sigma \left(\frac{\partial \sigma}{\partial x} \right) = A_\rho A_t^{-1} A_v \left(\rho \frac{\partial v}{\partial t} \right) \quad , \qquad (5.50a)$$

$$A_x^{-1} A_v \left(\frac{\partial v}{\partial x} \right) = A_t^{-1} \left(\frac{A_\sigma}{A_\mu} \right)^{A_n n} \frac{\partial}{\partial t} \left(\frac{\sigma}{\mu} \right)^{n} + A_t^{-1} A_\alpha A_\theta \frac{\partial}{\partial t} (\alpha\theta) \quad , \qquad (5.50b)$$

$$A_\alpha A_{T_o} A_t^{-1} A_\sigma \left(\alpha T_o \frac{\partial \sigma}{\partial t}\right) + A_\rho A_{C_\sigma} A_t^{-1} A_\theta \left(\rho C_\sigma \frac{\partial \theta}{\partial t}\right) = 0 \quad . \qquad (5.50c)$$

Under the group of transformations G_{12}^A, the invariance of the system (5.1) implies that:

From (5.50a):
$$A_x^{-1} A_\sigma = A_\rho A_t^{-1} A_v \quad , \qquad (5.51a)$$

From (5.50b):
$$A_x^{-1} A_v = A_t^{-1} \left(\frac{A_\sigma}{A_\mu}\right)^{A_n n} = A_t^{-1} A_\alpha A_\theta \quad , \qquad (5.51b)$$

$$A_n = 1 \quad , \qquad (5.51c)$$

From (5.50c):
$$A_\alpha A_{T_o} A_t^{-1} A_\sigma = A_\rho A_{C_\sigma} A_t^{-1} A_\theta \quad . \qquad (5.51d)$$

The relations of the nondimensional parameters can then be established as:

$$A_v = A_x^{-\left(\frac{1+n}{n-1}\right)} \quad A_t^{\left(\frac{1+n}{n-1}\right)} \quad A_\rho^{-\frac{n}{n-1}} \quad A_\mu^{\frac{n}{n-1}} \quad , \qquad (5.52a)$$

$$A_\sigma = A_x^{-\frac{2}{n-1}} \quad A_t^{\frac{2}{n-1}} \quad A_\rho^{-\frac{1}{n-1}} \quad A_\mu^{\frac{n}{n-1}} \quad , \qquad (5.52b)$$

$$A_\theta = A_x^{-\frac{2n}{n-1}} \quad A_t^{\frac{2n}{n-1}} \quad A_\rho^{-\frac{n}{n-1}} \quad A_\mu^{\frac{n}{n-1}} \quad A_\alpha^{-1} \quad , \qquad (5.52c)$$

$$A_{C_\sigma} = A_x^2 \quad A_t^{-2} \quad A_\alpha^2 \quad A_{T_o} \quad . \qquad (5.52d)$$

By the same token, the boundary condition (5.57a) leads to:

$$A_{V_o} = A_x^{-\left(\frac{1+n}{n-1}\right)} \; A_t^{\frac{1+n}{n-1} - \delta} \; A_\rho^{-\frac{n}{n-1}} \; A_\mu^{\frac{n}{n-1}} \quad . \tag{5.52e}$$

As a result, the expressions (5.52) form a system of five equations among the twelve parameters. It is obvious that at the most six of the parameters can be considered to be independent. Therefore, the six-parameter group of transformations G_6^A is assumed in the form:

$$G_6^A = \begin{cases} S_6^A = \begin{cases} \bar{x} = A_x x \quad , \quad \bar{t} = A_t t \quad ; \quad \textit{Independent variables} \\ \bar{\rho} = A_\rho \rho \quad , \quad \bar{\mu} = A_\mu \mu \quad , \quad \bar{\alpha} = A_\alpha \alpha \\ \bar{T}_o = A_{T_o} T_o \quad , \qquad \textit{Physical parameters} \\ \bar{C}_\sigma = A_x^2 \; A_t^{-2} \; A_\alpha^2 \; A_{T_o} \; C_\sigma \quad , \\ \bar{V}_o = A_x^{-\left(\frac{1+n}{n-1}\right)} \; A_t^{\frac{1+n}{n-1} - \delta} \; A_\rho^{-\frac{n}{n-1}} \; A_\mu^{\frac{n}{n-1}} \; V_o \quad ; \end{cases} \\ \bar{v} = A_x^{-\left(\frac{1+n}{n-1}\right)} \; A_t^{\frac{1+n}{n-1}} \; A_\rho^{-\frac{n}{n-1}} \; A_\mu^{\frac{n}{n-1}} \; v \quad , \\ \bar{\sigma} = A_x^{-\frac{2}{n-1}} \; A_t^{\frac{2}{n-1}} \; A_\rho^{-\frac{1}{n-1}} \; A_\mu^{\frac{n}{n-1}} \; \sigma \quad , \\ \bar{\theta} = A_x^{-\frac{2n}{n-1}} \; A_t^{\frac{2n}{n-1}} \; A_\rho^{-\frac{n}{n-1}} \; A_\mu^{\frac{n}{n-1}} \; A_\alpha^{-1} \; \theta \quad , \\ \qquad \textit{Dependent variables} \end{cases} \tag{5.53}$$

where S_6^A denotes a six-parameter subgroup of G_6^A.

The dimensional matrices corresponding to the dimensional group of transformations G_6^A are expressed by:

$$[A] = \begin{bmatrix} -\left(\frac{1+n}{n-1}\right) & \left(\frac{1+n}{n-1}\right) & -\frac{n}{n-1} & \frac{n}{n-1} & 0 & 0 \\ -\frac{2}{n-1} & \frac{2}{n-1} & -\frac{1}{n-1} & \frac{n}{n-1} & 0 & 0 \\ -\frac{2n}{n-1} & \frac{2n}{n-1} & -\frac{n}{n-1} & \frac{n}{n-1} & -1 & 0 \end{bmatrix} , \tag{5.54a}$$

$$[B] = \begin{bmatrix} 1 & 0 & 0 & 0 & 0 & 0 \\ 0 & 1 & 0 & 0 & 0 & 0 \end{bmatrix} , \tag{5.54b}$$

$$[C] = \begin{bmatrix} 0 & 0 & 1 & 0 & 0 & 0 \\ 0 & 0 & 0 & 1 & 0 & 0 \\ 0 & 0 & 0 & 0 & 1 & 0 \\ 0 & 0 & 0 & 0 & 0 & 1 \\ 2 & -2 & 0 & 0 & 2 & 1 \\ -\left(\frac{1+n}{n-1}\right) & \left(\frac{1+n}{n-1} - \delta\right) & -\frac{n}{n-1} & \frac{n}{n-1} & 0 & 0 \end{bmatrix} . \tag{5.54c}$$

Augmenting matrix [B] with matrix [C], the matrix [BC] is represented by:

$$[BC] = \begin{bmatrix} 1 & 0 & 0 & 0 & 0 & 0 \\ 0 & 1 & 0 & 0 & 0 & 0 \\ 0 & 0 & 1 & 0 & 0 & 0 \\ 0 & 0 & 0 & 1 & 0 & 0 \\ 0 & 0 & 0 & 0 & 1 & 0 \\ 0 & 0 & 0 & 0 & 0 & 1 \\ 2 & -2 & 0 & 0 & 2 & 1 \\ -\left(\frac{1+n}{n-1}\right) & \left(\frac{1+n}{n-1} - \delta\right) & -\frac{n}{n-1} & \frac{n}{n-1} & 0 & 0 \end{bmatrix} . \tag{5.55}$$

Obviously, the supplemented matrix [BC] has the rank $r_{BC} = 6$, moreover, the number of independent parameters of group G_6^A is also the same. According to Moren and Marshek [5.16], a similarity transformation exists if, and only if the rank r_C of matrix [C] is smaller than the rank r_{BC} of matrix [BC], i.e.:

$$r_C < r_{BC} \quad . \tag{5.56}$$

Since [C] is the square matrix (6x6), the condition of $r_C < 6$ is satisfied only when:

$$\det [C] = 0 \quad , \tag{5.57}$$

which leads to the restriction:

$$\delta = 0 \quad . \tag{5.58}$$

5.3.2 Independent Absolute Invariants of Group G_6^A

Based on the theorem 3 of reference [5.16], the set of independent absolute invariants of G_6^A has $[m_1 + m_2 + p - r_{BC}] = [3 + 2 + 6 - 6] = 5$ elements, where m_1 is a number of *dependent variables*, m_2 of *independent variables*, and p of *physical parameters*.

The similarity variable is expressible as [5.18]:

$$\eta = x(t)^{\Gamma_{12}} \quad (\rho)^{\gamma_{11}} \quad (\mu)^{\gamma_{12}} \quad (\alpha)^{\gamma_{13}} \quad (T_o)^{\gamma_{14}} \quad (V_o)^{\gamma_{15}} \tag{5.59}$$

where Γ_{12} and γ_{1j}, j = 1,2,3,4,5 are the linearly independent solutions of the following system of equations:

$$\Gamma_{12}\begin{bmatrix}0\\1\\0\\0\\0\\0\end{bmatrix} + \gamma_{11}\begin{bmatrix}0\\0\\1\\0\\0\\0\end{bmatrix} + \gamma_{12}\begin{bmatrix}0\\0\\0\\1\\0\\0\end{bmatrix} + \gamma_{13}\begin{bmatrix}0\\0\\0\\0\\1\\0\end{bmatrix} + \gamma_{14}\begin{bmatrix}0\\0\\0\\0\\0\\1\end{bmatrix} + \gamma_{15}\begin{bmatrix}-\left(\frac{1+n}{n-1}\right)\\ \frac{1+n}{n-1}\\ -\frac{n}{n-1}\\ \frac{n}{n-1}\\ 0\\ 0\end{bmatrix} = -\begin{bmatrix}1\\0\\0\\0\\0\\0\end{bmatrix} \tag{5.60}$$

Solving the above system (5.60) yields:

$$\Gamma_{12} = -1 \quad , \tag{5.61a}$$

$$\gamma_{11} = \frac{n}{n+1} \quad , \tag{5.61b}$$

$$\gamma_{12} = -\frac{n}{n+1} \quad , \tag{5.61c}$$

$$\gamma_{13} = 0 \quad , \tag{5.61d}$$

$$\gamma_{14} = 0 \quad , \tag{5.61e}$$

$$\gamma_{15} = \frac{n-1}{n+1} \quad . \tag{5.61f}$$

Substituting equations (5.61) into equation (5.59), we obtain:

$$\eta = \frac{x}{t} \left(\frac{\rho}{\mu}\right)^{\frac{n}{n+1}} (V_o)^{\frac{n-1}{n+1}} \quad . \tag{5.62}$$

Other independent absolute invariants which are related to the dependent variables v, σ and θ are also expressible in the following forms:

$$F_1(\eta) = v(t)^{\Lambda_{12}} (\rho)^{\lambda_{11}} (\mu)^{\lambda_{12}} (\alpha)^{\lambda_{13}} (T_o)^{\lambda_{14}} (V_o)^{\lambda_{15}} , \tag{5.63}$$

$$F_2(\eta) = \sigma(t)^{\Lambda_{22}} (\rho)^{\lambda_{21}} (\mu)^{\lambda_{22}} (\alpha)^{\lambda_{23}} (T_o)^{\lambda_{24}} (V_o)^{\lambda_{25}} , \tag{5.64}$$

$$F_3(\eta) = \theta(t)^{\Lambda_{32}} (\rho)^{\lambda_{31}} (\mu)^{\lambda_{32}} (\alpha)^{\lambda_{33}} (T_o)^{\lambda_{34}} (V_o)^{\lambda_{35}} , \tag{5.65}$$

where those parameters Λ_{i2} and λ_{ij} (i = 1,2,3, and j = 1,2,3,4,5) provide linearly independent solutions to:

$$\Lambda_{i2}\begin{bmatrix}0\\1\\0\\0\\0\\0\end{bmatrix} + \lambda_{i1}\begin{bmatrix}0\\0\\1\\0\\0\\0\end{bmatrix} + \lambda_{i2}\begin{bmatrix}0\\0\\0\\1\\0\\0\end{bmatrix} + \lambda_{i3}\begin{bmatrix}0\\0\\0\\0\\1\\0\end{bmatrix} + \lambda_{i4}\begin{bmatrix}0\\0\\0\\0\\0\\1\end{bmatrix} + \lambda_{i5}\begin{bmatrix}-\left(\frac{1+n}{n-1}\right)\\ \frac{1+n}{n-1}\\ -\frac{n}{n-1}\\ \frac{n}{n-1}\\ 0\\ 0\end{bmatrix} = -\begin{bmatrix}a_{i1}\\a_{i2}\\a_{i3}\\a_{i4}\\a_{i5}\\a_{i6}\end{bmatrix},$$

(5.66)

with i = 1 corresponding to:

$$\left\{a_{11}\ a_{12}\ a_{13}\ a_{14}\ a_{15}\ a_{16}\right\}^T = \left\{-\left(\frac{1+n}{n-1}\right)\ \frac{1+n}{n-1}\ -\frac{n}{n-1}\ \frac{n}{n-1}\ 0\ 0\right\}^T .$$

(5.67)

Substituting (5.67) into the right-hand column of the system (5.66) and solving for the unknowns, we obtain from equation (5.63):

$$F_1(\eta) = v\, V_o^{-1} \quad , \tag{5.68a}$$

or

$$v(x,t) = V_o F_1(\eta) \quad . \tag{5.68b}$$

Analogously, i = 2,3, respectively, corresponding to:

$$\left\{a_{21}\ a_{22}\ a_{23}\ a_{24}\ a_{25}\ a_{26}\right\}^T = \left\{-\frac{2}{n-1}\ \frac{2}{n-1}\ -\frac{1}{n-1}\ \frac{n}{n-1}\ 0\ 0\right\}^T ,$$

(5.69)

$$\left\{a_{31}\ a_{32}\ a_{33}\ a_{34}\ a_{35}\ a_{36}\right\}^T = \left\{-\frac{2n}{n-1}\ \frac{2n}{n-1}\ -\frac{n}{n-1}\ \frac{n}{n-1}\ -1\ 0\right\}^T . \tag{5.70}$$

Substituting (5.69) in the system (5.66) and solving for the unknowns, the invariant $F_2(\eta)$ assumes the form:

$$F_2(\eta) = \sigma(\rho)^{-\frac{1}{n+1}} (\mu)^{-\frac{n}{n+1}} (V_o)^{-\frac{2}{n+1}} , \tag{5.71a}$$

or

$$\sigma(x,t) = (\mu^n \rho V_o^2)^{\frac{1}{n+1}} F_2(\eta) . \tag{5.71b}$$

Solving the system (5.66) with the last column expressed by (5.70), the unknowns are determined and substituted into equation (5.65) to obtain:

$$F_3(\eta) = \theta \left(\frac{\rho V_o^2}{\mu}\right)^{-\frac{n}{n-1}} \alpha , \tag{5.72a}$$

or

$$\theta(x,t) = \frac{1}{\alpha}\left(\frac{\rho V_o^2}{\mu}\right)^{\frac{n}{n+1}} F_3(\eta) . \tag{5.72b}$$

It should be noted that the rank of matrix [C] ($r_C = 5$) is smaller than the number of physical parameters ($p = 6$), hence, the last absolute invariant Z_o determined solely from the physical variables [5.17] is given by:

$$Z_o = C_\sigma(\rho)^{\delta_{61}} (\mu)^{\delta_{62}} (\alpha)^{\delta_{63}} (T_o)^{\delta_{64}} (V_o)^{\delta_{65}} , \tag{5.73}$$

where δ_{6j} ($j = 1,2,3,4,5$) is the solution of the following system:

$$\delta_{61}\begin{bmatrix}0\\0\\1\\0\\0\\0\end{bmatrix} + \delta_{62}\begin{bmatrix}0\\0\\0\\1\\0\\0\end{bmatrix} + \delta_{63}\begin{bmatrix}0\\0\\0\\0\\1\\0\end{bmatrix} + \delta_{64}\begin{bmatrix}0\\0\\0\\0\\0\\1\end{bmatrix} + \delta_{65}\begin{bmatrix}-\left(\frac{1+n}{n-1}\right)\\ \left(\frac{1+n}{n-1}\right)\\ -\frac{n}{n-1}\\ \frac{n}{n-1}\\ 0\\ 0\end{bmatrix} = -\begin{bmatrix}2\\-2\\0\\0\\2\\1\end{bmatrix} \quad . \tag{5.74}$$

Solving the system (5.74) for the unknowns, then substituting into equation (5.73) leads to:

$$Z_o = C_\sigma \left(\frac{\rho}{\mu}\right)^{\frac{2n}{n+1}} \alpha^{-2}\, T_o^{-1}\, V_o^{2\left(\frac{n-1}{n+1}\right)} \quad . \tag{5.75}$$

In summary, the set of five independent absolute invariants of group G_6^A composed of η, $F_1(\eta)$, $F_2(\eta)$, $F_3(\eta)$ and Z_o is written as:

$$\eta = L_1 \frac{x}{t} \quad , \tag{5.76a}$$

$$Z_o = L_2 C_\sigma \quad , \tag{5.76b}$$

$$v(x,t) = V_o F_1(\eta) \quad , \tag{5.76c}$$

$$\sigma(x,t) = L_3 F_2(\eta) \quad , \tag{5.76d}$$

$$\theta(x,t) = L_4 F_3(\eta) \quad , \tag{5.76e}$$

where:

$$L_1 = \left(\frac{\rho}{\mu}\right)^{\frac{n}{n+1}} (V_o)^{\frac{n-1}{n+1}} \quad , \tag{5.76f}$$

$$L_2 = \left(\frac{\rho}{\mu}\right)^{\frac{2n}{n+1}} \alpha^{-2} T_o^{-1} \; V_o^{2\left(\frac{n-1}{n+1}\right)} \quad , \tag{5.76g}$$

$$L_3 = \left(\mu^n \rho V_o^2\right)^{\frac{1}{n+1}} \quad , \tag{5.76h}$$

$$L_4 = \left(\frac{\rho V_o^2}{\mu}\right)^{\frac{n}{n+1}} \alpha^{-1} \quad . \tag{5.76i}$$

5.3.3 Similarity Representation for Basic Equations

Making use of the similarity transformations (5.76), the system of equations (5.1) and auxiliary conditions (5.47) can be reduced to an ordinary boundary value problem. Partial derivatives appearing in the system (5.1) can be expressed in terms of similarity transformations (5.76) as:

$$\frac{\partial v}{\partial t} = -\frac{1}{t}\,\eta V_o F_1'(\eta) \quad , \tag{5.77a}$$

$$\frac{\partial \sigma}{\partial x} = \frac{1}{t}\, L_1 L_3 F_2'(\eta) \quad , \tag{5.77b}$$

$$\frac{\partial v}{\partial x} = \frac{1}{t}\, V_o L_1 F_1'(\eta) \quad , \tag{5.77c}$$

$$\frac{\partial\theta}{\partial t} = -\frac{1}{t}\,\eta L_4 F_3'(\eta) \quad . \tag{5.77e}$$

Substituting (5.77a,b) into (5.1a) leads to:

$$\rho\left\{-\frac{1}{t}\,\eta V_o F_1'(\eta)\right\} - \frac{1}{t}\,L_1 L_3 F_2'(\eta) = 0 \quad . \tag{5.78}$$

Since:

$$L_1 L_3 = \left\{\left(\frac{\rho}{\mu}\right)^{\frac{n}{n+1}} V_o^{\frac{n-1}{n+1}}\right\}\left\{\left(\mu^n \rho V_o^2\right)^{\frac{1}{n+1}}\right\} = \rho V_o \quad . \tag{5.79}$$

Introducing (5.79) in (5.78) and simplifying, the equation of motion (5.1a) is then written in terms of similarity transformations as:

$$\eta F_1'(\eta) + F_2'(\eta) = 0 \quad . \tag{5.80}$$

The constitutive law (5.1b) and the conservation of energy equation (5.1c), taking into account (5.77), are respectively expressible as :

$$F_1'(\eta) = -\eta\left\{n\left[F_2(\eta)\right]^{n-1} F_2'(\eta) + F_3'(\eta)\right\} \quad , \tag{5.81}$$

and

$$F_2'(\eta) + Z_o F_3'(\eta) = 0 \quad . \tag{5.82}$$

The equations (5.80) and (5.82) yield:

$$F_1'(\eta) = -\frac{1}{\eta}\,F_2'(\eta) \quad , \tag{5.83}$$

$$F_3'(\eta) = -\frac{1}{Z_o}\,F_2'(\eta) \quad . \tag{5.84}$$

Substituting equations (5.83) and (5.84) into equation (5.81), we obtain:

$$\left[\eta^2 \left\{n \left[F_2(\eta)\right]^{n-1} - \frac{1}{Z_o}\right\} - 1\right] F_2'(\eta) = 0 \quad , \qquad (5.85)$$

which leads to a question being that of either:

$$\eta^2 \left\{n \left[F_2(\eta)\right]^{n-1} - \frac{1}{Z_o}\right\} - 1 = 0 \quad , \qquad (5.86)$$

or

$$F_2'(\eta) = 0 \quad . \qquad (5.87)$$

5.3.4 Similarity Analysis of the Wavefront

The application of similarity transformation to the analysis of the location of the front in the transformed space is well developed in the articles [5.17, 5.18, 5.19]. It is reminded that depending upon the type of materials as well as the type of boundary conditions used, there may exist either the simple wavefront or the shock wavefront as previously discussed in Chapter 3.

However, the zero value of δ being constrained by the condition of the invariant group implies that waves propagating in the elastic non-conducting materials must be simple waves. This is because when the boundary of the medium is subjected to constant velocity impact, the energy produced is held constant throughout the disturbed region due to the absence of heat flux q. Therefore, the stress σ is also unchanged along the boundary. The wavelets, which have the velocities representing functions in terms of stress σ, construct a family of parallel lines in the x-t plane. And by definition, the simple waves are formed as a special case.

The simple wavefront or the wavefront simply called, has the speed given by (equation (5.3b)):

$$V_f = \frac{dX_w}{dt} = \sqrt{\frac{C_\sigma}{\beta\rho C_\sigma - \alpha^2 T_o}} \quad , \tag{5.88}$$

where X_w is the location of wavefront in x-t plane. Along the wavefront, the equation (5.76a) implies that:

$$X_w = \frac{t}{L_1}\,\eta_w \quad , \tag{5.89}$$

which yields:

$$\frac{dX_w}{dt} = \frac{1}{L_1}\,\eta_w \quad . \tag{5.90}$$

Substituting equation (5.90) into equation (5.88) and taking into account equations (5.76), the location of the wavefront is written in terms of similarity transformations as:

$$\eta_w = \left\{ \frac{1}{n\left[F_2(\eta_w)\right]^{n-1} - \frac{1}{Z_o}} \right\} \quad . \tag{5.91}$$

It is obvious that the equation (5.91) is only a special form of (5.86) when $\eta = \eta_w$. Furthermore, $\eta < \eta_w$ leads to:

$$\frac{1}{\eta\left[F_2(\eta)\right]^{n-1} - \frac{1}{Z_o}} < \frac{1}{\eta\left[F_2(\eta_w)\right]^{n-1} - \frac{1}{Z_o}}$$

or

$$\left[F_2(\eta_w)\right]^{n-1} < \left[F_2(\eta)\right]^{n-1} \quad . \tag{5.92}$$

By mathematical analysis, the condition (5.86) does not hold when $\eta = 0$. Moreover, along with the inequality (5.92), the condition (5.86) seems to be invalid with $n = 1$. In terms of physical meaning, the inequality (5.92) leads to the energy changing from point to point in the disturbed region. This situation is not acceptable in the case of an elastic non-conductor subjected to a constant velocity impact since the energy is supposed to be unalternated through the course of wave propagating.

Based on the above arguments, we can conclude that the condition (5.86) is inadmissible to fulfill the requirement of equation (5.85). As a result, the equation (5.87) is logically considered as a necessary and sufficient condition for the equation (5.85).

5.4.4 Similarity and Jump Conditions

Assuming that the initial conditions prescribe a quiescent state ahead of the front, the jump conditions are recalled as:

$$\sigma = -V_f \, \rho v \quad , \tag{5.93}$$

$$\sigma = -\frac{\rho C_\sigma}{\alpha T_o} \theta \quad . \tag{5.94}$$

Applying the similarity transformations (5.76) to equations (5.93) and (5.94), respectively, yield:

$$F_2(\eta_w) = -\left\{ \frac{1}{n\left[F_2(\eta_w)\right]^{n-1} - Z_o} \right\}^{1/2} F_1(\eta_w) \quad , \tag{5.95}$$

and

$$F_2(\eta_w) + Z_o F_3(\eta_w) = 0 \quad . \tag{5.96}$$

Under the necessary and sufficient condition $F_2'(\eta) = 0$ (equation (5.87)), the relations (5.83) and (5.84) imply that:

$$F_1'(\eta) = 0 \quad , \tag{5.97}$$

$$F_3'(\eta) = 0 \quad . \tag{5.98}$$

From which we obtain:

$$F_1(\eta) = C10 \quad , \tag{5.99a}$$

$$F_2(\eta) = C11 \quad , \tag{5.99b}$$

$$F_3(\eta) = C12 \quad . \tag{5.99c}$$

where C10, C11, C12 are constants.

The boundary condition (5.47a) can also be transformed to the similarity space as :

$$F_1(0) = 1 \quad . \tag{5.100}$$

The combination of (5.100) with (5.99a) yields:

$$F_1(\eta) = 1 \quad . \tag{5.101a}$$

$$F_1(\eta = \eta_w) = 1 \quad . \tag{5.101b}$$

Substituting the value of $F_1(\eta_w)$ into equation (5.93) gives:

$$F_2(\eta_w) = -\left\{ \frac{1}{n\left[F_2(\eta_w)\right]^{n-1} - \frac{1}{Z_o}} \right\}^{1/2} . \qquad (5.102a)$$

Along with (5.99b), equation (5.102a) can be written as:

$$F_2(\eta) = -\left\{ \frac{1}{n\left[F_2(\eta)\right]^{n-1} - \frac{1}{Z_o}} \right\}^{1/2} . \qquad (5.102b)$$

Analogously, equation (5.96) leads to:

$$F_3(\eta_w) = -\frac{1}{Z_o} F_2 (\eta_w) \quad , \qquad (5.103a)$$

and implies that:

$$F_3(\eta) = -\frac{1}{Z_o} F_2 (\eta) \quad . \qquad (5.103b)$$

since $F_3(\eta)$ is constant throughout the interval $[0,\eta_w]$. The value of $F_2(\eta)$ can be determined by performing the iterative method or by approximating the calculation as follows:

$$\eta\left[F_2(\eta)\right]^{n-1} - \frac{1}{Z_o} \approx n \left[F_2(\eta)\right]^{n-1} . \qquad (5.104)$$

Since Z_o depends on parameters V_o, n, material constant μ, ρ, C_σ, α and reference temperature T_o, the equation (5.75) reveals that the value Z_o is very large as compared with the unity.

Substituting the equivalent term (5.104) into equation (5.102b) gives:

$$F_2(\eta) \cong \left(\frac{1}{n} \right)^{\frac{1}{n+1}} \quad . \tag{5.105}$$

From equation (5.103b), we obtain:

$$F_3(\eta) \cong -\frac{1}{Z_o} \left(\frac{1}{n} \right)^{\frac{1}{n+1}} \quad . \tag{5.106}$$

The location of the wavefront is, thus, determined by substituting the approximate term (5.104) into equation (5.91). The formula of η_w is then written in a simple form as:

$$\eta_w \cong \left(\frac{1}{n} \right)^{\frac{1}{n+1}} \quad . \tag{5.107}$$

The above analysis of similarity representation leads us to conclude that:

(i) The results are obtained quickly without any great deal of calculation involved.

(ii) The results are as reliable as those obtained by the characteristic method and the finite element method.

(iii) The location of the front can be instantly determined whenever the power "n" is given.

(iv) The features of the wave propagating in the medium can be seen more clearly than when they are examined by the other methods.

However, there are also some disadvantages:

(i) This method requires a long interpretation and argument.

(ii) The boundary conditions are restricted to fulfill the requirement of the invariant transformations.

CHAPTER 6
NUMERICAL SIMULATIONS

6.1 SOME REMARKS OF NUMERICAL SIMULATIONS

6.1.1 Stability Condition

Not only is the characteristic method but also the finite element method required to satisfy the conditions of consistency, stability and convergence. In general, a convergence solution which leads to the true solution of the partial differential equation is usually linked by:

$$convergence = consistency + stability \quad . \tag{6.1}$$

Thus, in addition to the consistency, the stability is also an important factor that has a strong effect on the numerical solution, as Richtmyer and Morton [6.1] stated that *stability is the necessary and sufficient condition for convergence.*

In equation (6.1), each element on the right-hand side also has a different function. The consistency implies that the truncation errors approach zero when the meshes formed in the disturbed region are refined, and the stability controls the oscillation caused by strong discontinuities at the fronts.

Rigorous stability analysis of the above properties is not available for non-linear problems. However, from the linearized forms of hyperbolic systems, stability and convergence have been proven provided the slope of any characteristic curve nowhere exceeds a value of $\frac{\Delta x}{\Delta t}$. Thus, the stability criterion is written as:

$$\max |\lambda_i| < \frac{\Delta x}{\Delta t} \quad , \tag{6.2}$$

where Δx and Δt respectively denote the spatial increment and time interval being kept constant in both. The inequality (6.2) is well-known as the Courant-Friedrichs-Lewy condition or CFL condition as it is usually called. The condition can be extended to the non-linear hyperbolic system given in this thesis such that:

$$\max |\lambda_i \ (E_I^J)| < \frac{\min \ (h_I, \ h_{I+1})}{\Delta t} \quad . \tag{6.3}$$

As previously mentioned, h_I and h_{I+1} are the meshed lengths on both sides of node I. The term max $|\lambda_i(E_I^J)|$ stands for the numerically largest eigenvalue of the matrix $[B_1]$ (or $[B_1']$) computed at point E_I^J.

The CFL number, ν_c, is then defined by:

$$\nu_c = \max |\lambda_i \ (E_I^J)| \ \frac{\Delta t}{\min \ (h_I, \ h_{I+1})} \leq 1 \quad . \tag{6.4}$$

By the new approach of combination meshes, the CFL condition is definitely satisfied in the case of simple waves since the meshed lengths h_I's are determined from the wavefront speed which has the greatest value in the family of wavelets. However, when the shock is involved in the problem, the condition fails due to the minimum speed of the wavefront. Such an occurrence can be treated by adding an intermediate step as shown in Figure 6.1. The procedures of calculating the unknowns at those intermediate grid points are similar to the ones performed at the main grid points.

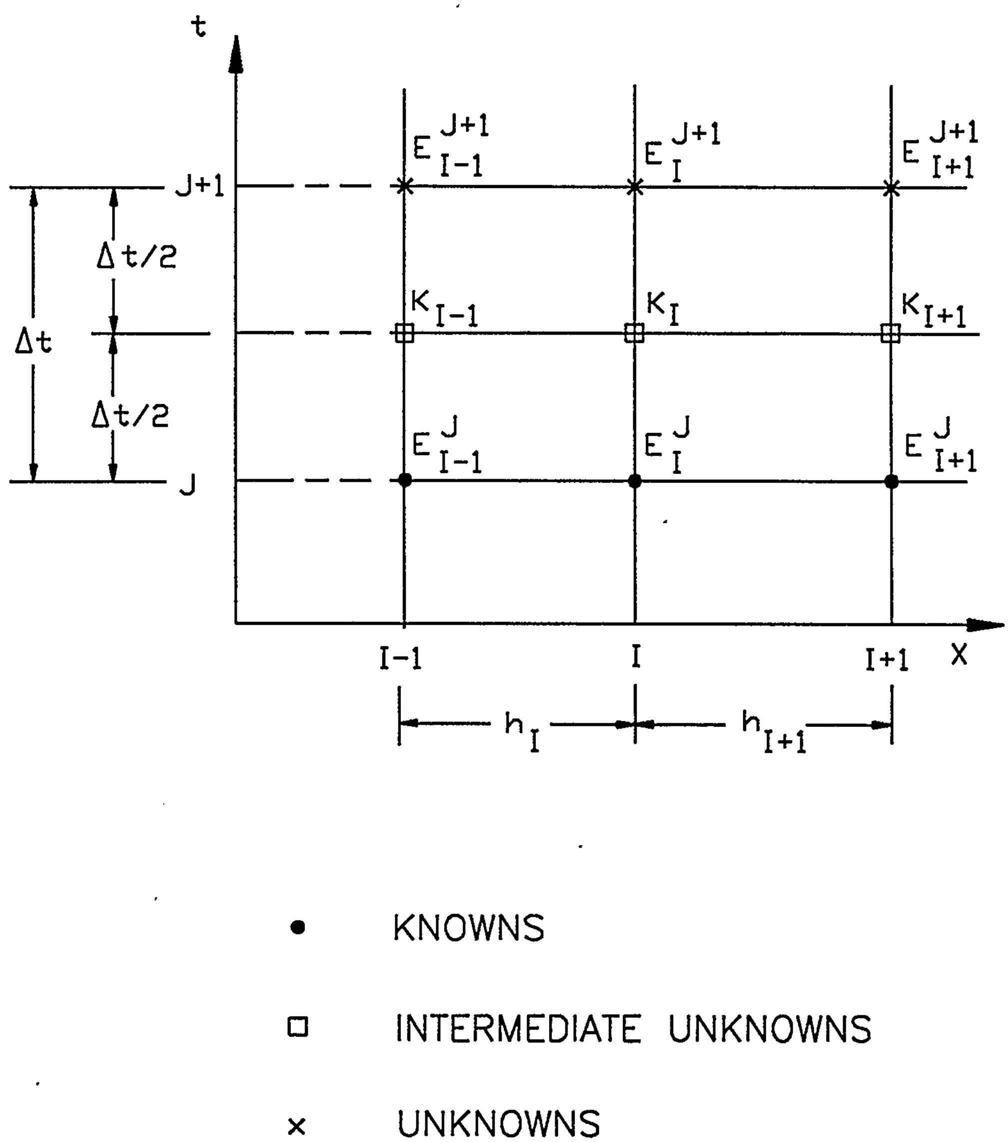

FIG. 6.1 INTERMEDIATE GRID POINTS

6.1.2 Computer Implementation

Four computer programs are coded in the Fortran 77 language and are classified as follows:

(i) Two programs are based on the characteristic method. One is used to treat the waves in conducting materials and the other is applied to deal with the waves in non-conducting materials.

(ii) The last two programs are based on the finite element method and have the same purposes as those above.

Because of the large size of matrices included in the program of finite element methods, the CYB 860 (or Nov/ve) system is employed for faster computation whereas the program of the characteristic method can be executed on the Sun Unix system since the unknowns in the disturbed region are explicitly computed at each grid point. The time intervals Δt used for the investigation of wave motion in conductors and non-conductors are 10^{-13} and 10^{-7} second, respectively.

The details of the programs are very complicated. Therefore, we only present simplified flow diagrams of the main computer programs instead of going over all steps of computation. The features of each diagram can be briefly explained as follows:

(i) As illustrated in Figure 6.2, the procedure is used for both methods. By the method of characteristics, the unknowns at the first point on the boundary and the next two points along the wavefront are determined. The distance which the wavefront is travelling in a time interval Δt is also estimated.

(ii) In Figure 6.3, the procedure shows how the values of unknowns are computed at each grid point by the characteristic method. Since the method attempts to obtain the solutions from point to point, the CPU time required for running this program is much less than the one needed by the program based on the finite element method.

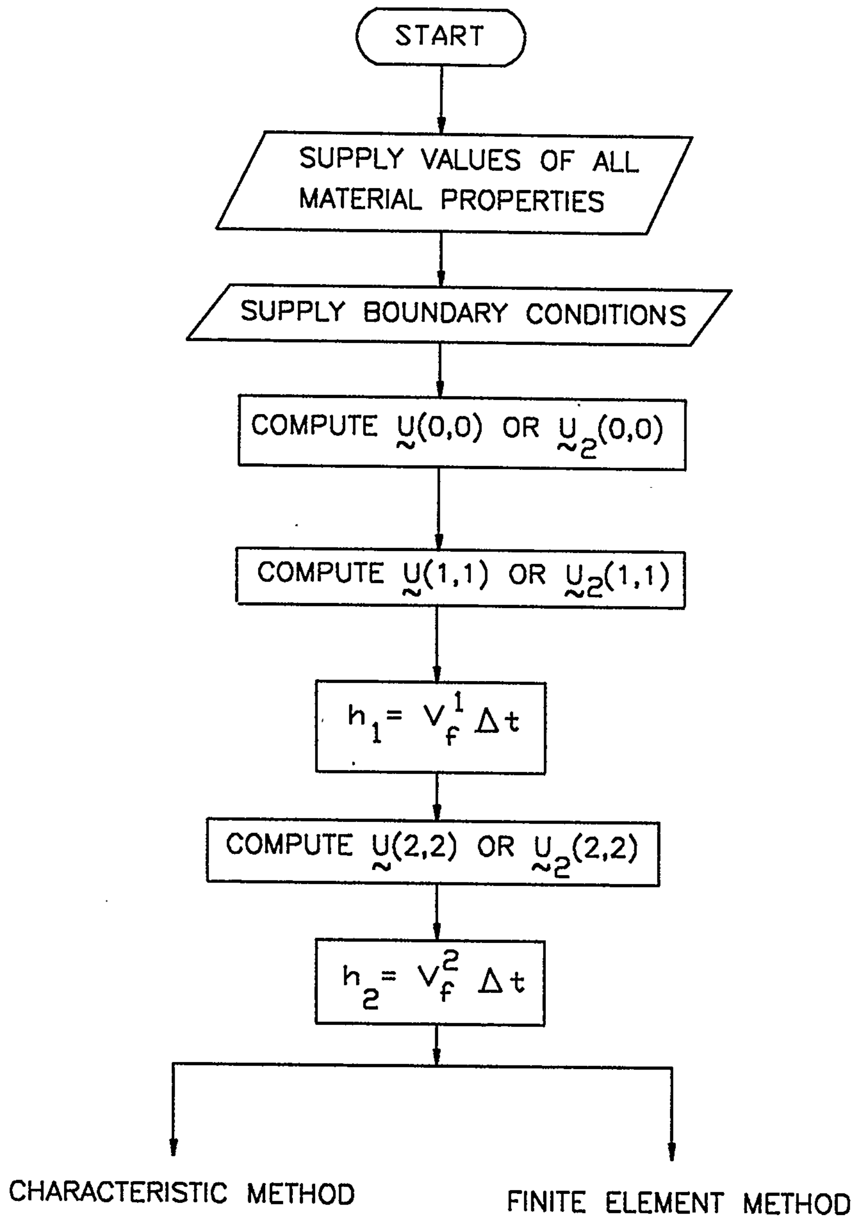

FIG. 6.2 FLOW DIAGRAM OF THE CHARACTERISTIC AND FINITE ELEMENT SCHEMES AT THE FIRST STEP OF COMPUTATION

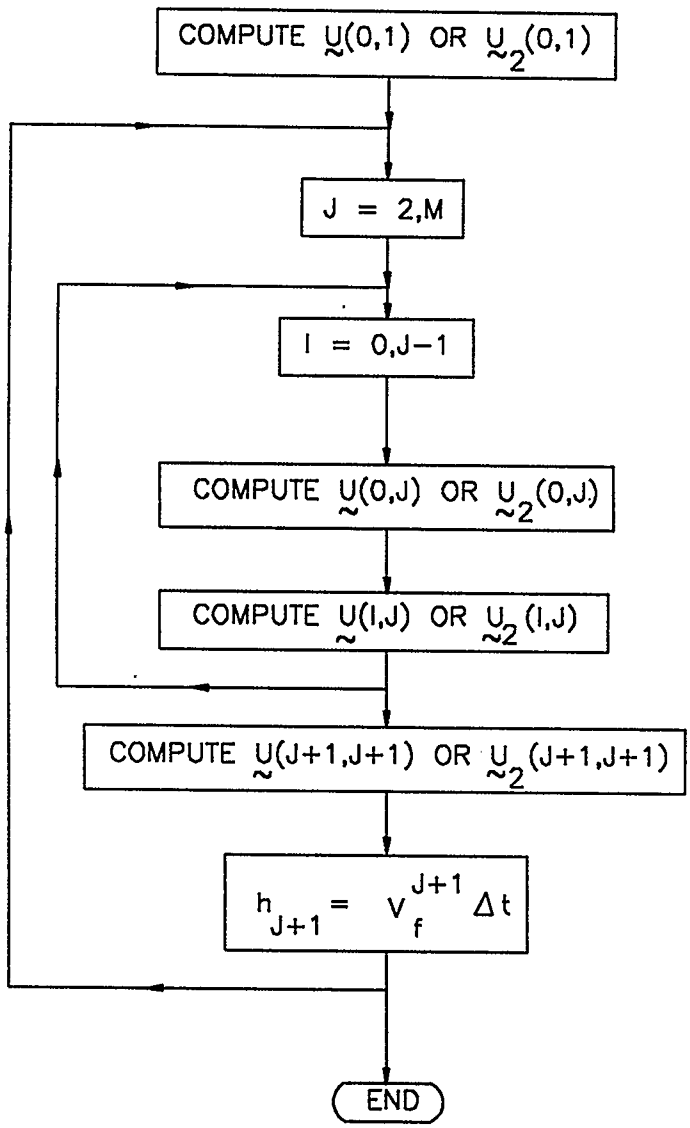

FIG. 6.3 FLOW DIAGRAM OF THE CHARACTERISTIC SCHEME

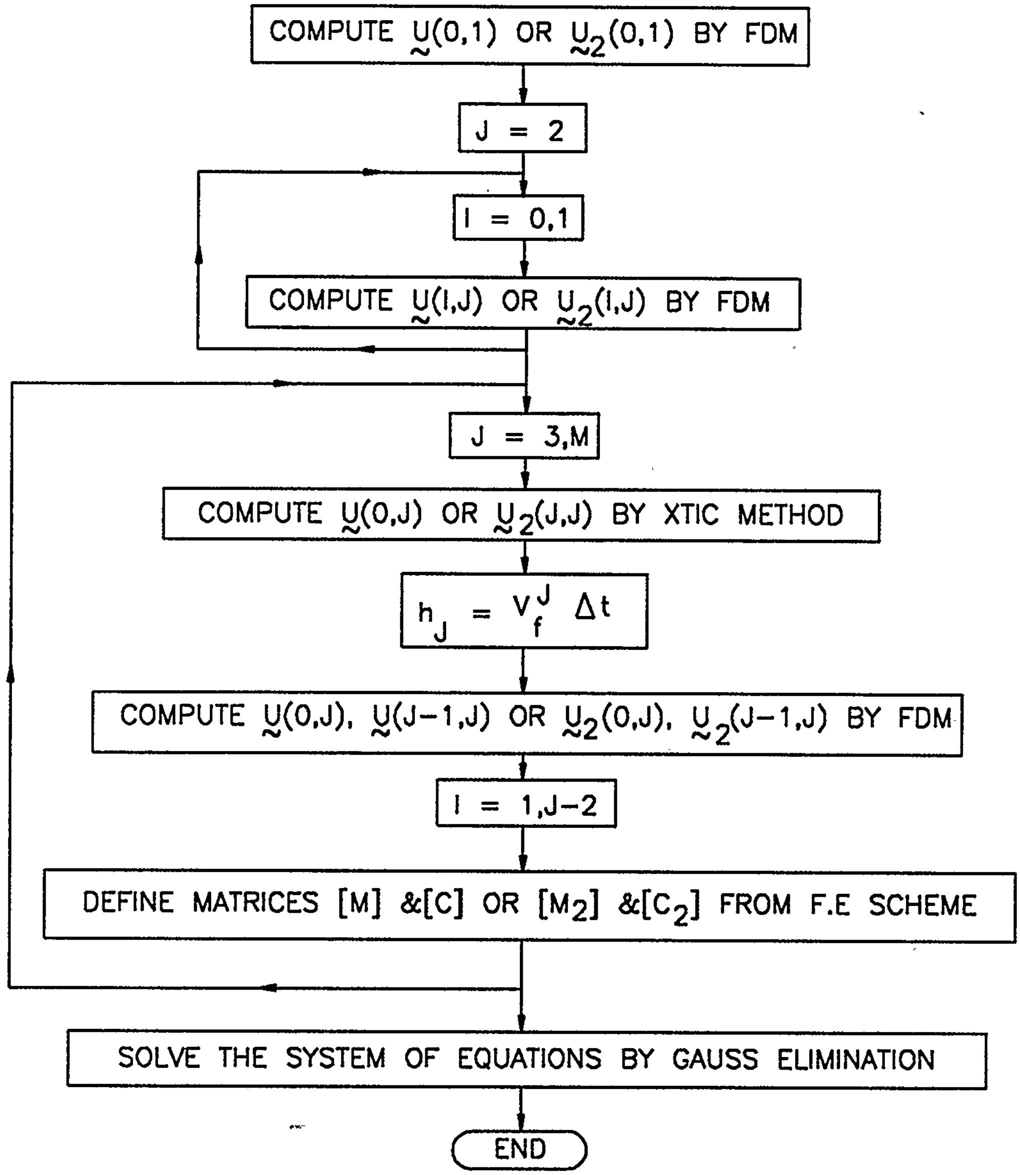

FIG. 6.4 FLOW DIAGRAM OF THE FINITE ELEMENT SCHEME

(iii) Extra caution should be taken into account when the finite element programs are written. As shown in Figure 6.4, the unknowns at points along the wavefront are obtained by the characteristic method. At the points along the Ot-axis as well as the ones next to the wavefront, a finite difference scheme can be employed to determine the unknowns. Finally, the finite element method is applied for solving the unknowns at interior grid points - the simultaneous equations formed by the implicit scheme can then be solved by Gauss elimination method.

6.2 BOUNDARY CONDITIONS

Two types of time-dependent inputs applied to the ends of the semi infinite thin rods are expressed as follows:

(i) Step Input :

Stress impact: $$\sigma(0,t) = \sigma_o H(t) \quad , \tag{6.5a}$$

Velocity impact: $$v(0,t) = V_o H(t) \quad , \tag{6.5b}$$

Temperature impact: $$\theta(0,t) = \theta_o H(t) \quad , \tag{6.5c}$$

where H(t) is referred to as the Heaviside unit step function and defined by:

$$H(t) = \begin{cases} 0 \;\; ; \;\; t < 0 \;\; , \\ 1 \;\; ; \;\; t > 0 \;\; . \end{cases} \tag{6.6}$$

(ii) Time-Dependent Input :

The time-dependent inputs in stress and velocity are given as:

$$\sigma(0,t) = \sigma_o T_o(t) \quad , \tag{6.7a}$$

$$v(0,t) = V_o T_o(t) \quad , \tag{6.7b}$$

where the function $T_o(t)$ has a form :

$$T_o(t) = \begin{cases} 0 & ; \ t < 0 \ , \\ t^{\delta} & ; \ t > 0 \ \text{and} \ \delta > 0 \ . \end{cases} \tag{6.8}$$

6.3 DATA OF THERMOELASTIC MATERIAL PROPERTIES

By notation, the tensile stress is assumed to be positive. In addition, the material properties used in the numerical computation are taken from many sources and listed in Tables 6.1 and 6.2.

Except those marked by asterisks, the rest of the data is based on tables from Sucec [6.2] and White [6.3]. Other data are also recorded as follows: (*) is basically computed and taken from the sources surveyed by Bell [1.8]. (**) is calculated from the formula (2.42) in which we assumed that $C_v \approx C_\sigma$ and the velocity of sound $V_s = \left(\frac{E}{\rho}\right)^{\frac{1}{2}}$ where E is the Young's modulus. (***) is adopted from Timosenko and Gere's table [6.4]. (****) and (*****) are extracted from the hand book by Bolz and Tuve [6.5] and the paper by Weir [6.6], respectively.

6.4 RESULT REPRESENTATION

The results obtained from the numerical computation are presented in Figures 6.5 - 6.31d. The prescribed boundary conditions (6.5a,b,c) and (6.7a,b) are also given in the titles of the Figures.

TABLE 6.1 PROPERTIES OF THREE DIFFERENT CONDUCTING MATERIALS:

STEEL, CAST IRON AND COPPER AT ROOM TEMPERATURE ($20^{\circ}C$)

Materials	(*) n	(*) μ(GPa)	ρ(kg/m^3)	K(W/m$^{\circ}$K)	C_{σ}(J/kg$^{\circ}$K)	(**) τ_o(sec)	(***) α($^{\circ}$K^{-1})
Steel	1.012	176.6	7801	43	473	1.4×10^{-12}	$12\text{x}10^{-6}$
Cast Iron	1.2074	18.1	7272	52	420	3.83×10^{-12}	10×10^{-6}
Copper	1.047	78.35	8954	386	383.1	2.7×10^{-11}	16.6×10^{-6}
Copper I	1.0	(***) 110	-"-	-"-	-"-	-"-	-"-
Copper II	1.0	(***) 120	-"-	-"-	-"-	-"-	-"-

TABLE 6.2 PROPERTIES OF TWO DIFFERENT NON-CONDUCTING MATERIALS: RUBBER AND LEATHER AT ROOM TEMPERATURE ($20^{\circ}C$)

Material	(*) n	(*) μ(GPa)	$\rho(kg/m^3)$	$K(W/m^{\circ}K)$	$C_{\sigma}(J/kg^{\circ}K)$	$\alpha(^{\circ}K^{-1})$
Rubber	1.6	0.978057×10^{-3}	1170	0.16	2000	(***) 130×10^{-6}
Leather	0.7545	12.6	860	(****) 0.1675	(****) 1503.72	(*****) 22×10^{-6}

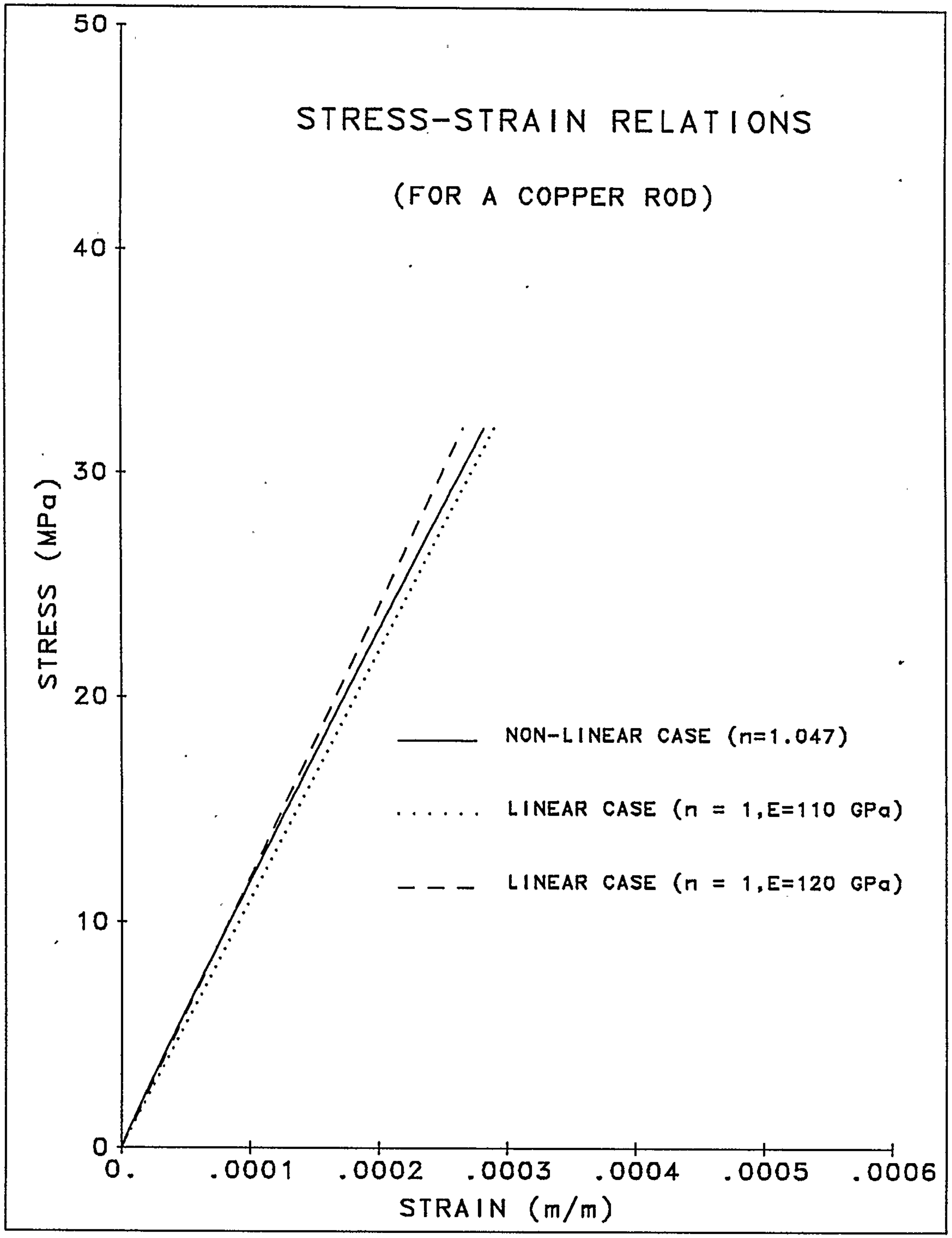

FIG. 6.5 STRESS-STRAIN DIAGRAM OF A COPPER ROD AT ROOM TEMPERATURE

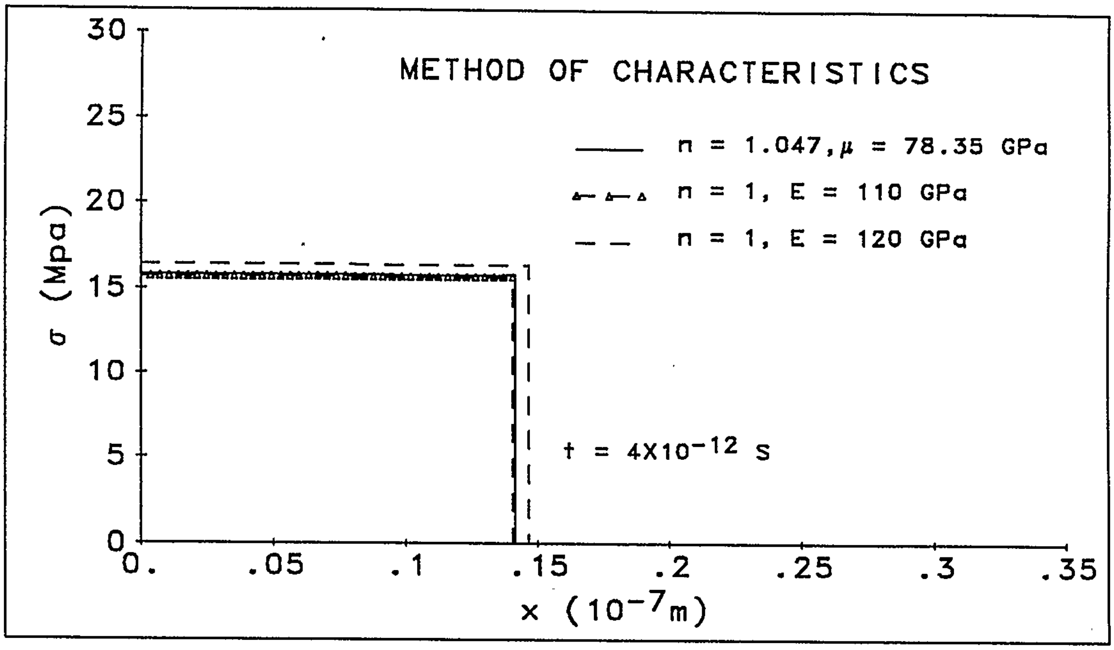

FIG. 6.6a STRESS RESPONSE OF THREE TYPES OF COPPER RODS TO $v(0,t) = -0.5$ m/s AND $\theta(0,t) = 0$. (BY THE XTIC METHOD)

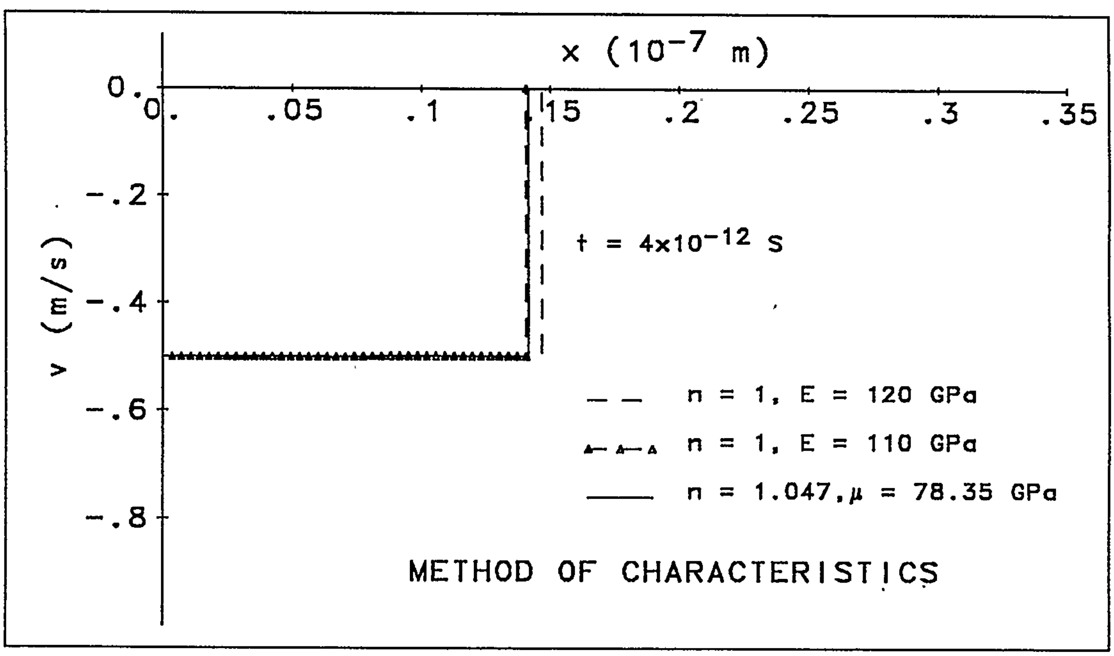

FIG. 6.6b VELOCITY RESPONSE OF THREE TYPES OF COPPER RODS TO $v(0,t) = -0.5$ m/s AND $\theta(0,t) = 0$. (BY THE XTIC METHOD)

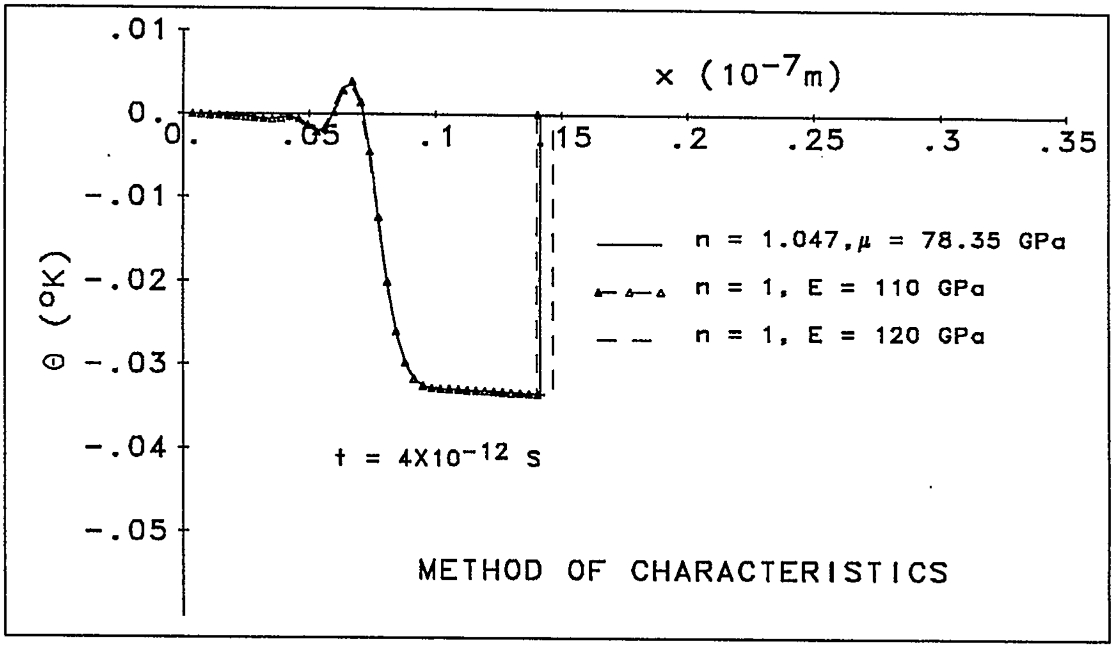

FIG. 6.6c TEMPERATURE RESPONSE OF THREE TYPES OF COPPER RODS TO $v(0,t) = -0.5$ m/s AND $\theta(0,t) = 0$. (BY THE XTIC METHOD)

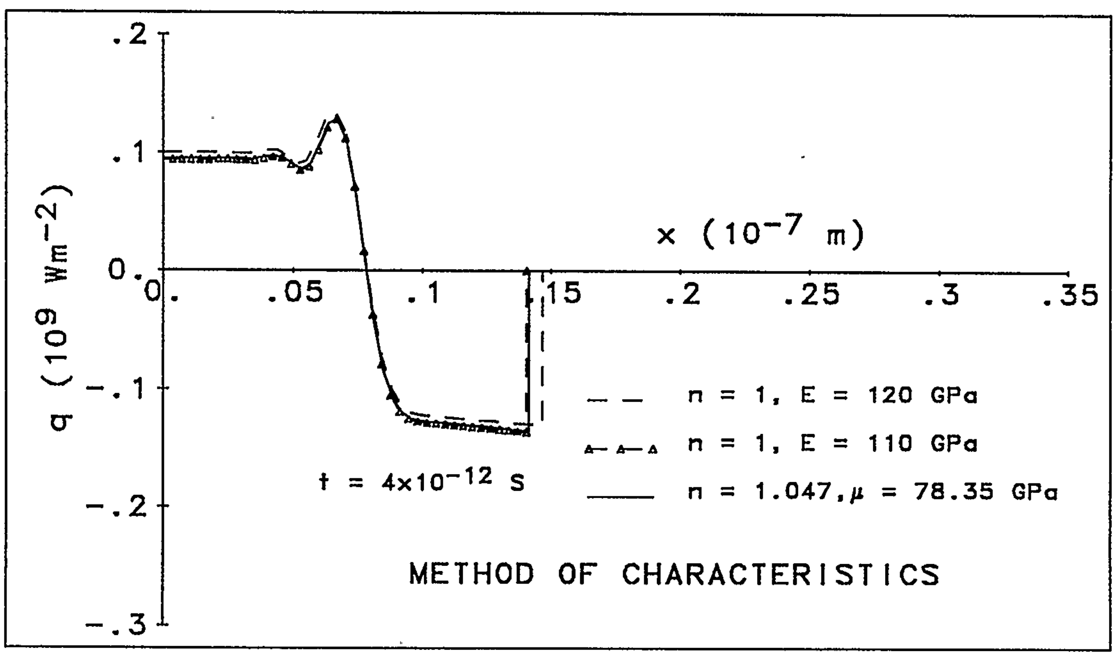

FIG. 6.6d HEAT FLUX RESPONSE OF THREE TYPES OF COPPER RODS TO $v(0,t) = -0.5$ m/s AND $\theta(0,t) = 0$. (BY THE XTIC METHOD)

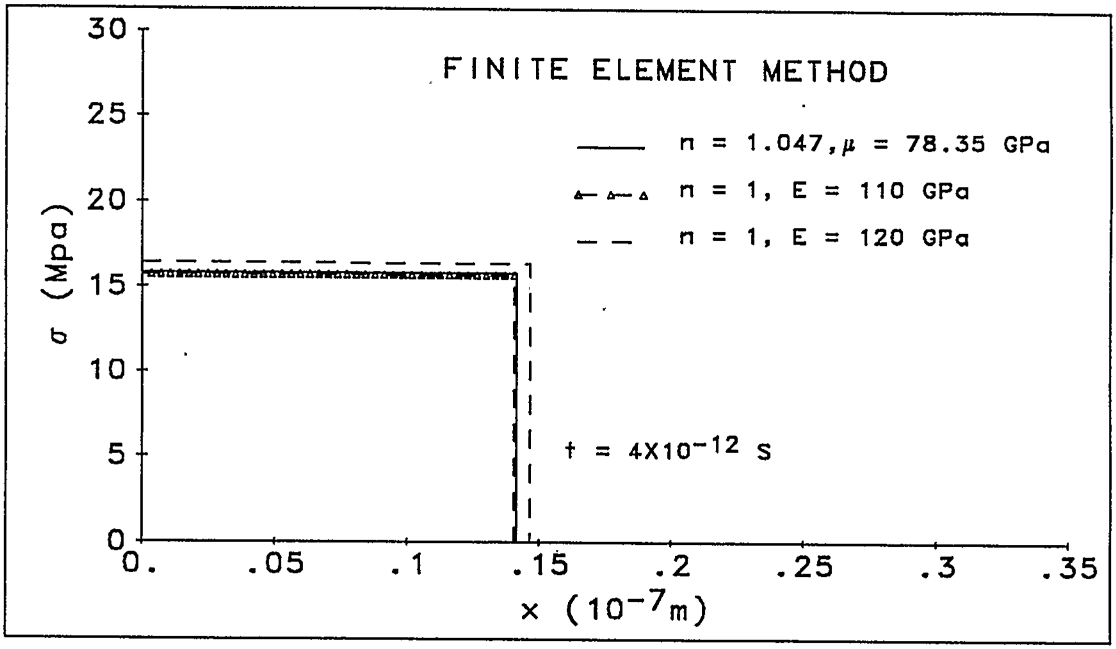

FIG. 6.7a STRESS RESPONSE OF THREE TYPES OF COPPER RODS TO $v(0,t) = -0.5$ m/s AND $\theta(0,t) = 0$. (BY THE F.E METHOD)

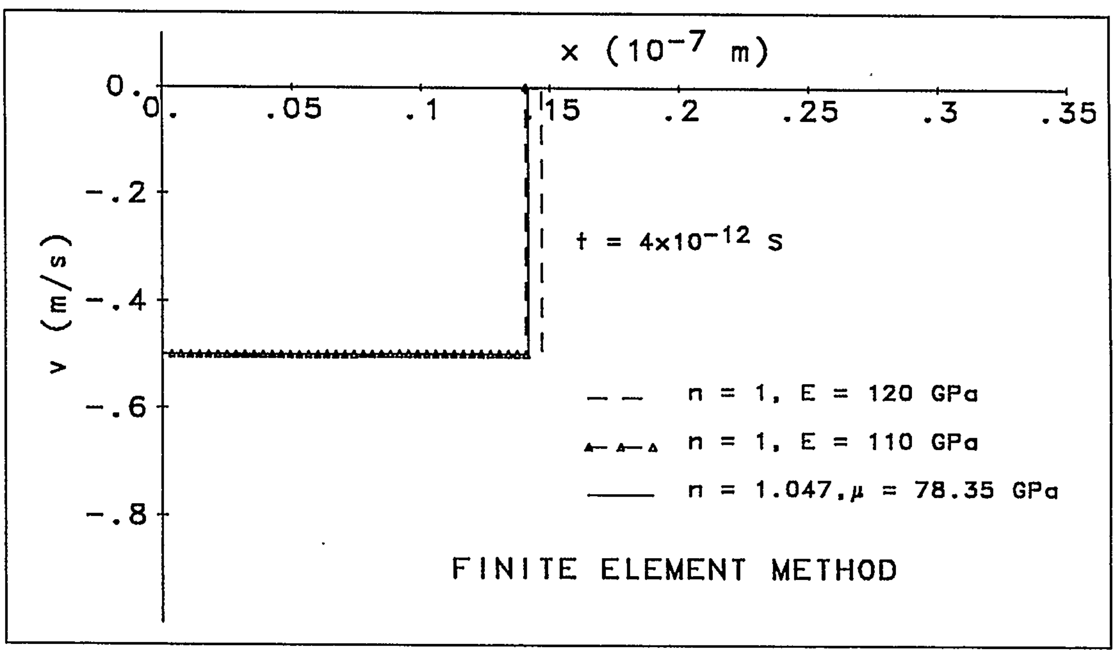

FIG. 6.7b VELOCITY RESPONSE OF THREE TYPES OF COPPER RODS TO $v(0,t) = -0.5$ m/s AND $\theta(0,t) = 0$. (BY THE F.E METHOD)

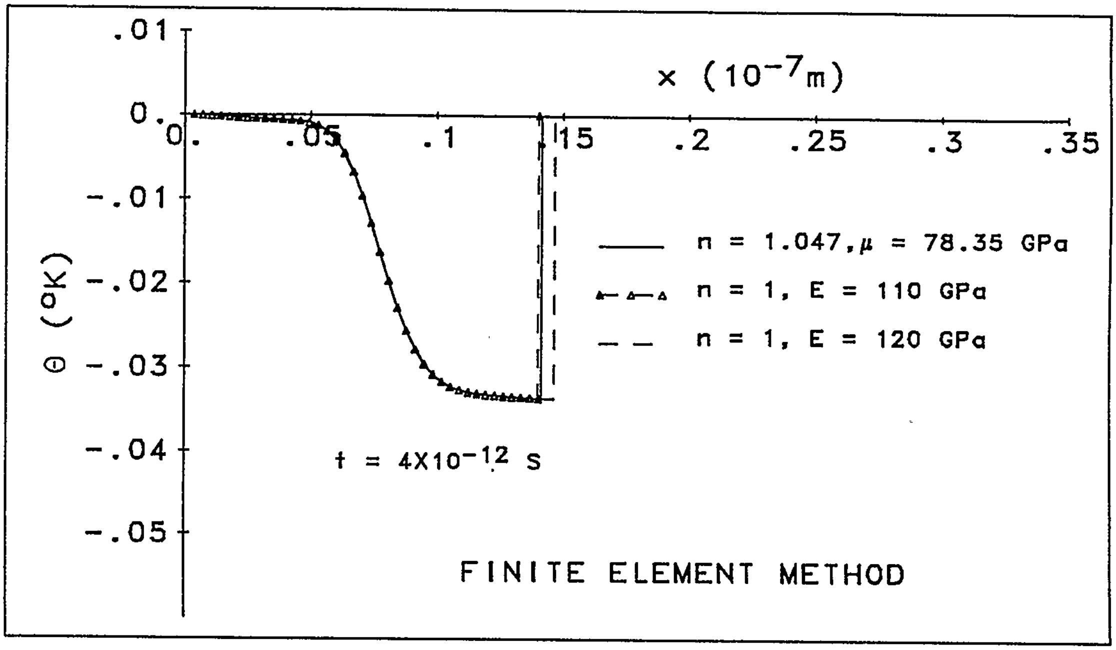

FIG. 6.7c TEMPERATURE RESPONSE OF THREE TYPES OF COPPER RODS TO $v(0,t) = -0.5$ m/s AND $\theta(0,t) = 0$. (BY THE F.E METHOD)

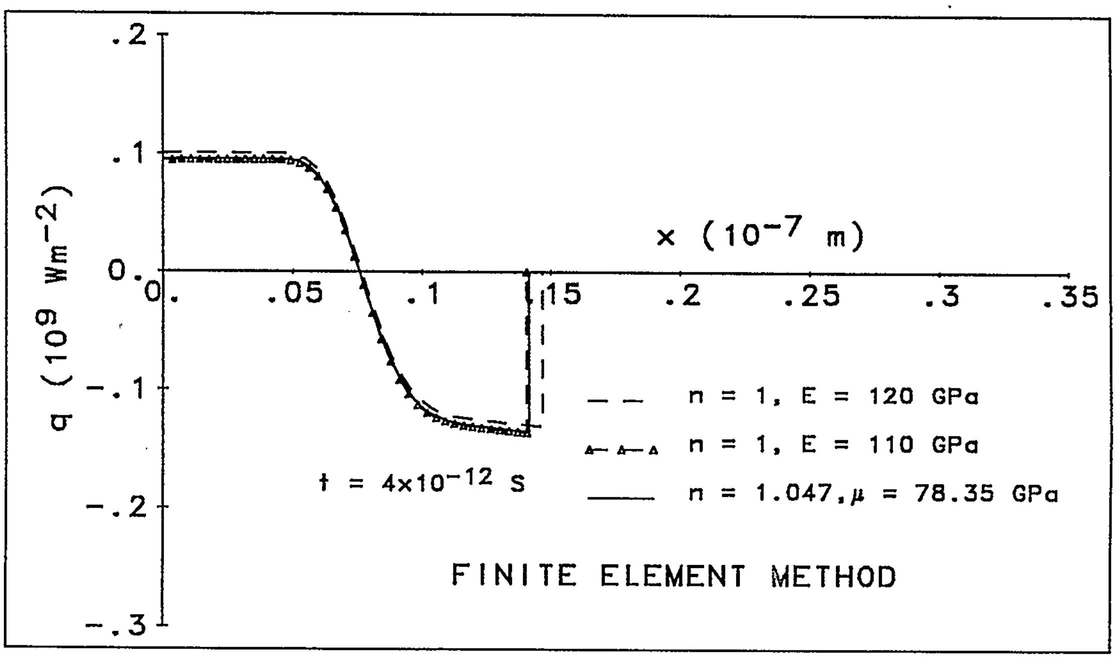

FIG. 6.7d HEAT FLUX RESPONSE OF THREE TYPES OF COPPER RODS TO $v(0,t) = -0.5$ m/s AND $\theta(0,t) = 0$. (BY THE F.E METHOD)

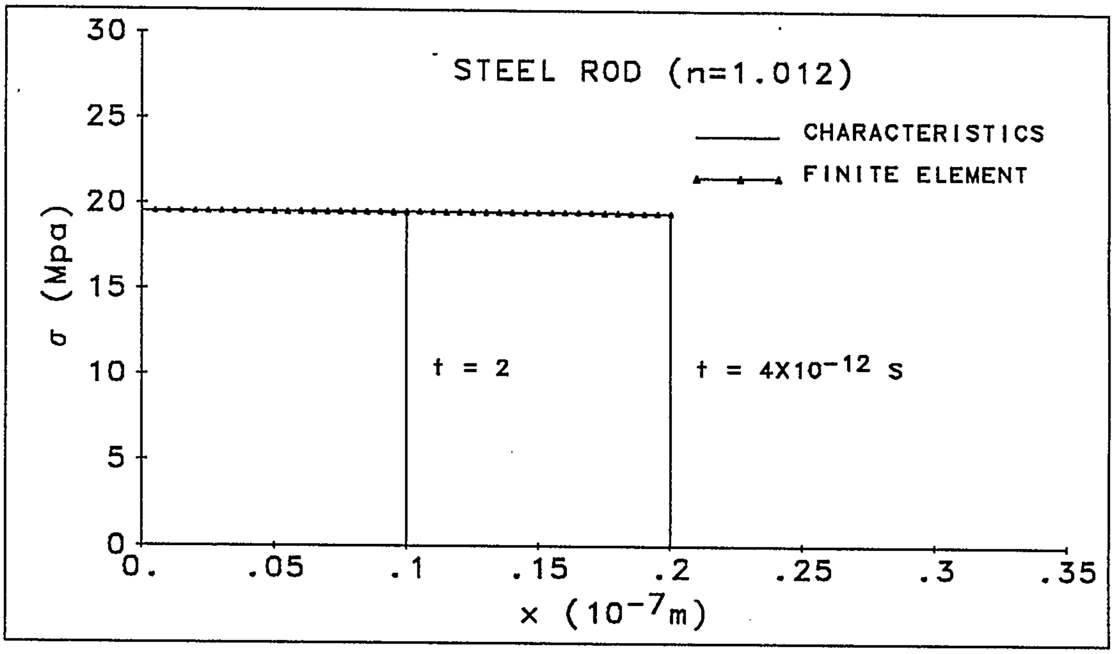

FIG. 6.8a STRESS RESPONSE OF A STEEL ROD (n = 1.012) TO $v(0,t) = -0.5$ m/s AND $\theta(0,t) = 0$.

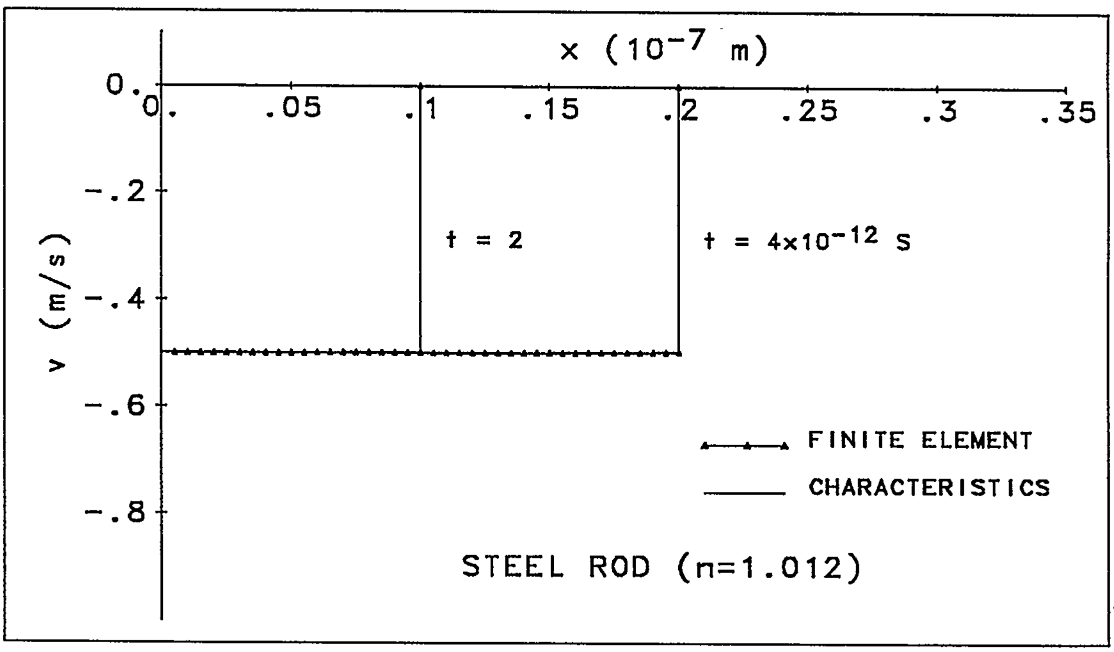

FIG. 6.8b VELOCITY RESPONSE OF A STEEL ROD (n = 1.012) TO $v(0,t) = -0.5$ m/s AND $\theta(0,t) = 0$.

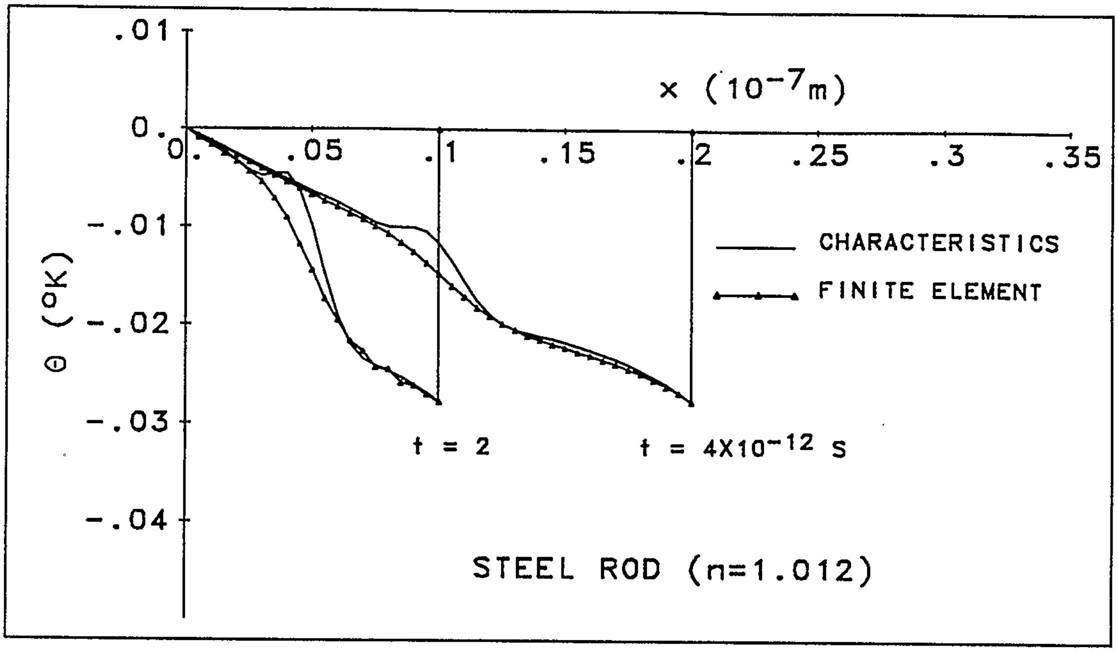

FIG. 6.8c TEMPERATURE RESPONSE OF A STEEL ROD (n = 1.012) TO $v(0,t) = -0.5$ m/s AND $\theta(0,t) = 0$.

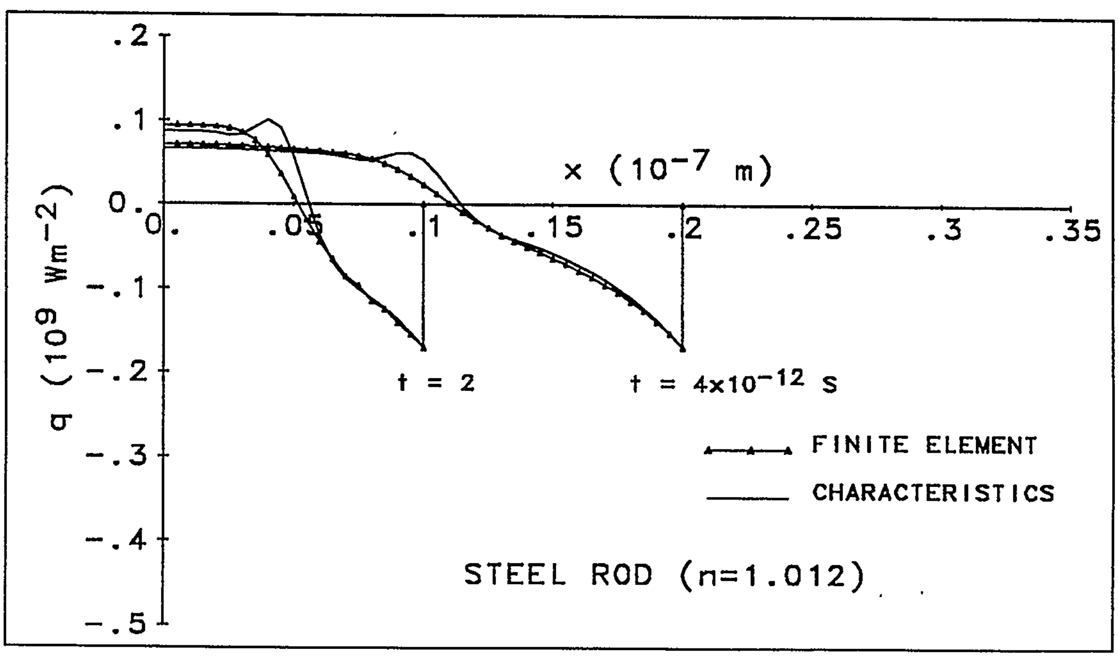

FIG. 6.8d HEAT FLUX RESPONSE OF A STEEL ROD (n = 1.012) TO $v(0,t) = -0.5$ m/s AND $\theta(0,t) = 0$.

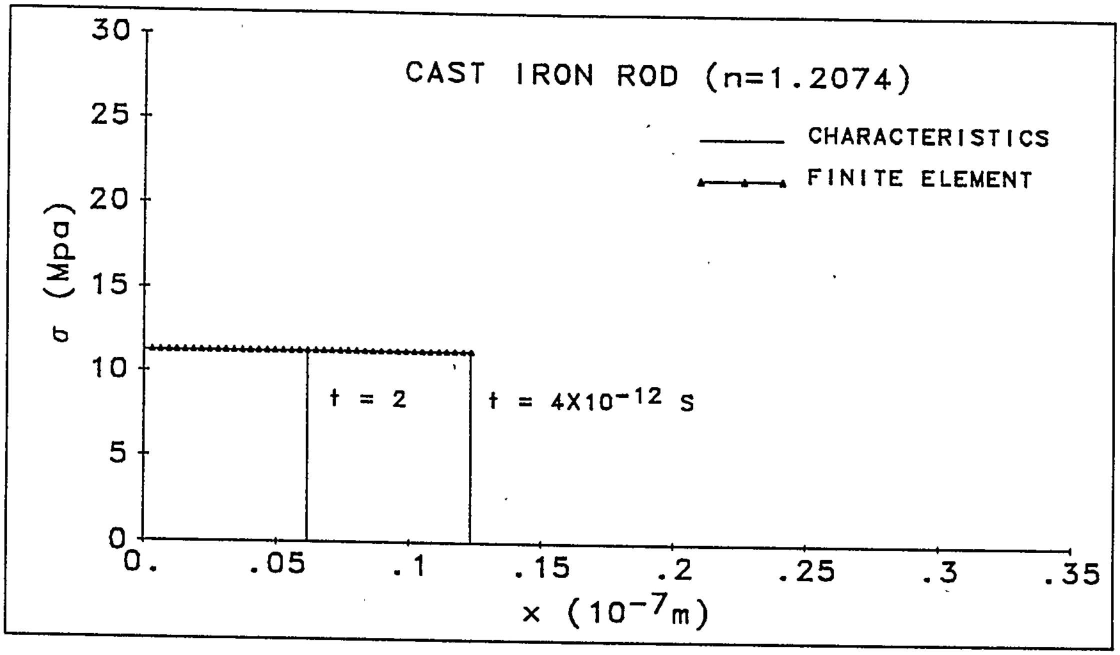

FIG. 6.9a STRESS RESPONSE OF A CAST IRON ROD (n = 1.2074) TO $v(0,t) = -0.5$ m/s AND $\theta(0,t) = 0$.

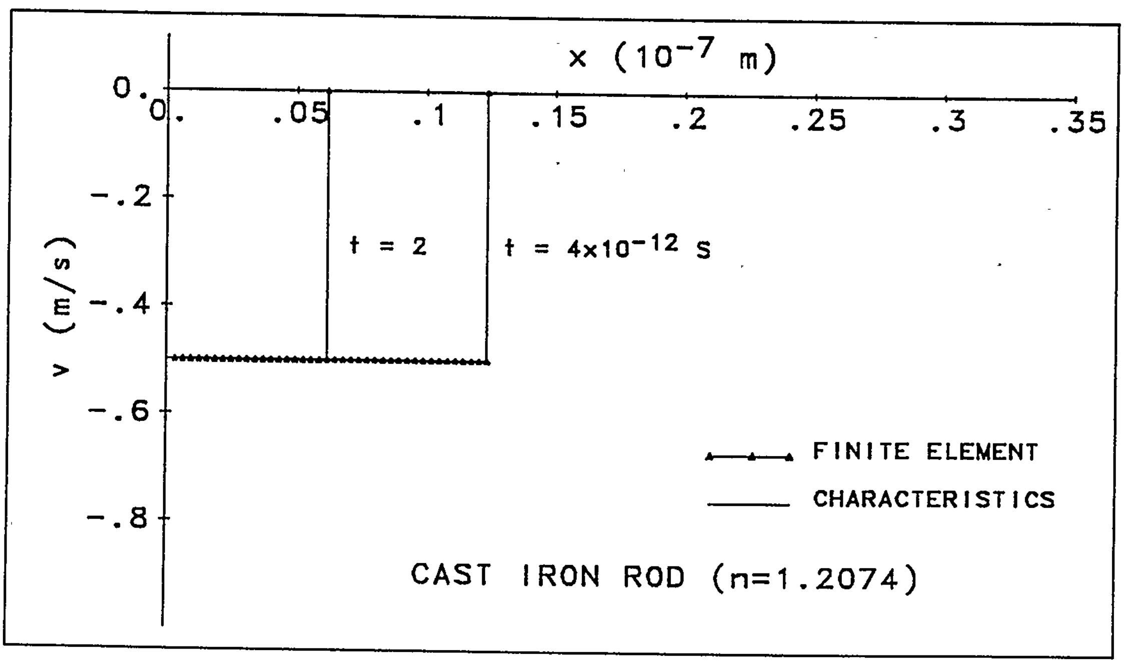

FIG. 6.9b VELOCITY RESPONSE OF A CAST IRON ROD (n = 1.2074) TO $v(0,t) = -0.5$ m/s AND $\theta(0,t) = 0$.

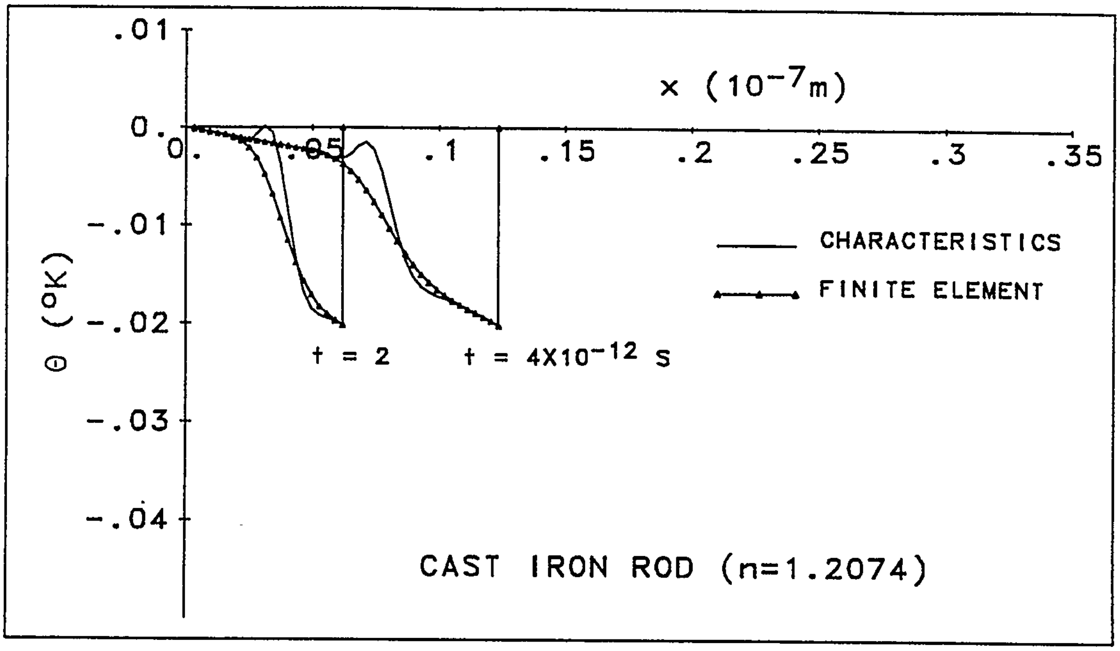

FIG. 6.9c TEMPERATURE RESPONSE OF A CAST IRON ROD (n = 1.2074) TO $v(0,t) = -0.5$ m/s AND $\theta(0,t) = 0$.

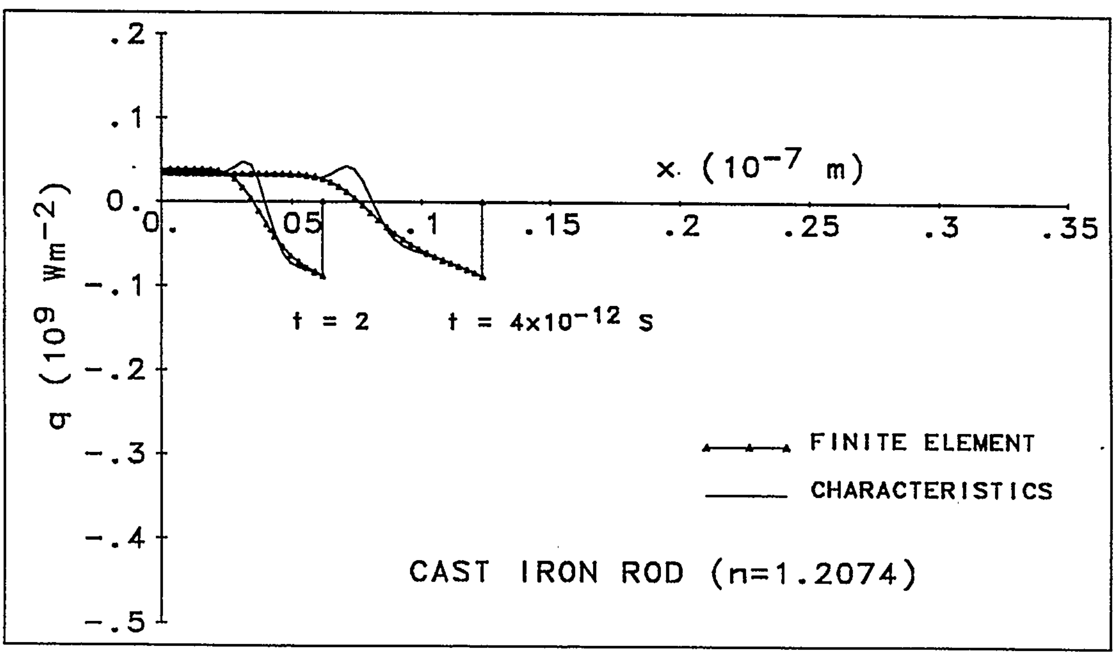

FIG. 6.9d HEAT FLUX RESPONSE OF A CAST IRON ROD (n = 1.2074) TO $v(0,t) = -0.5$ m/s AND $\theta(0,t) = 0$.

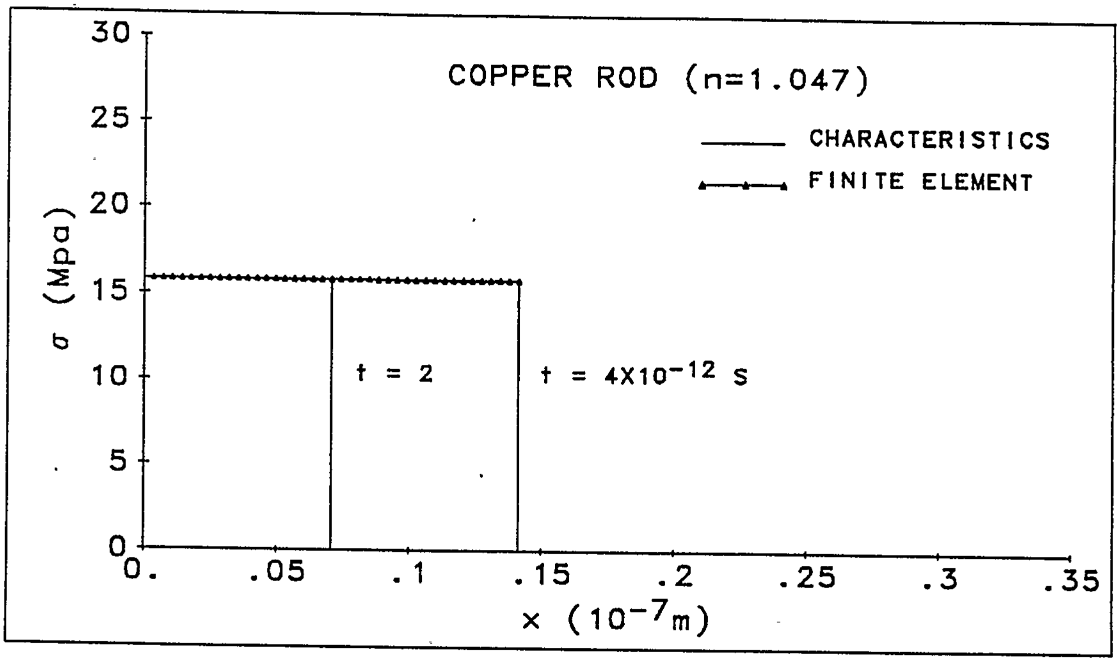

FIG. 6.10a STRESS RESPONSE OF A COPPER ROD (n = 1.047) TO $v(0,t) = -0.5$ m/s AND $\theta(0,t) = 0$.

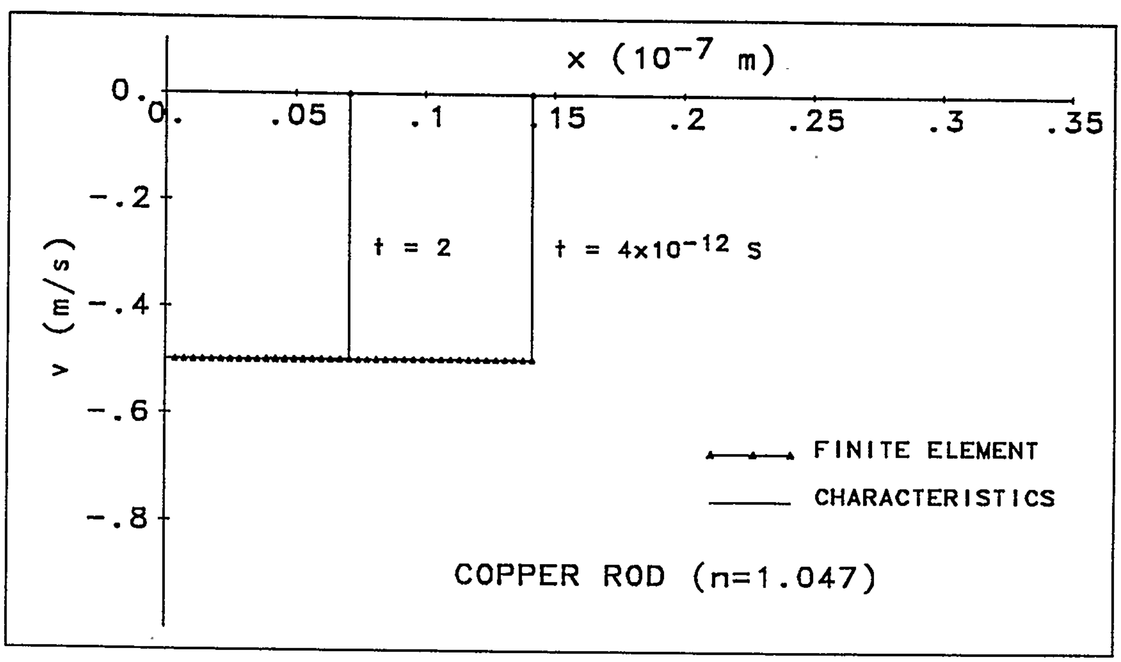

FIG. 6.10b VELOCITY RESPONSE OF A COPPER ROD (n = 1.047) TO $v(0,t) = -0.5$ m/s AND $\theta(0,t) = 0$.

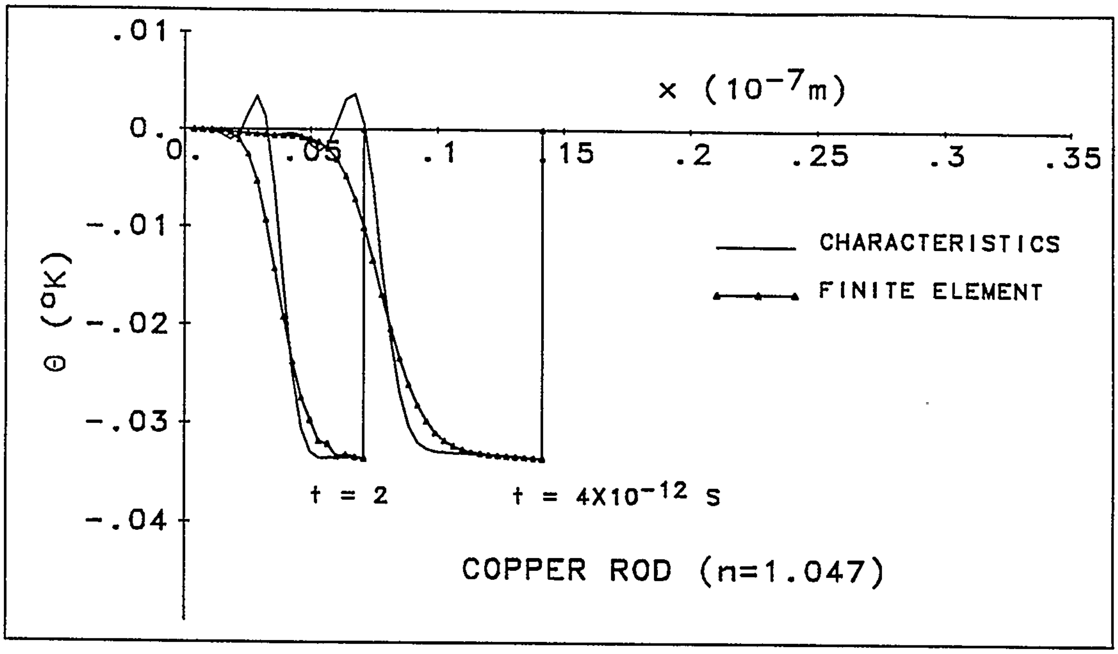

FIG. 6.10c TEMPERATURE RESPONSE OF A COPPER ROD (n = 1.047) TO $v(0,t) = -0.5$ m/s AND $\theta(0,t) = 0$.

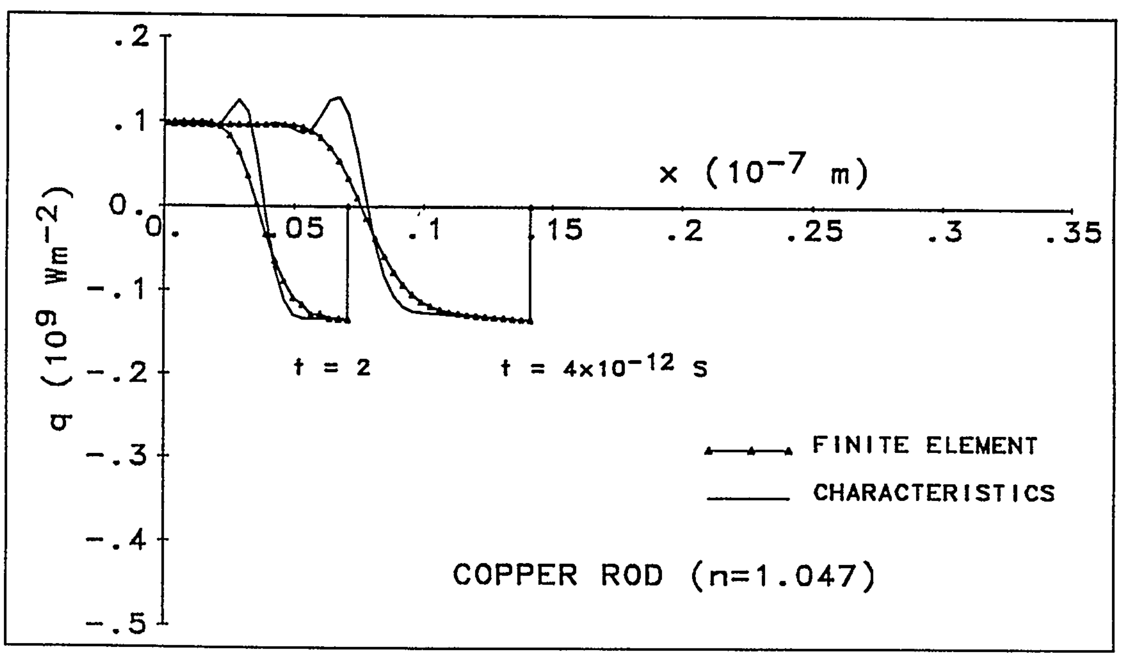

FIG. 6.10d HEAT FLUX RESPONSE OF A COPPER ROD (n = 1.047) TO $v(0,t) = -0.5$ m/s AND $\theta(0,t) = 0$.

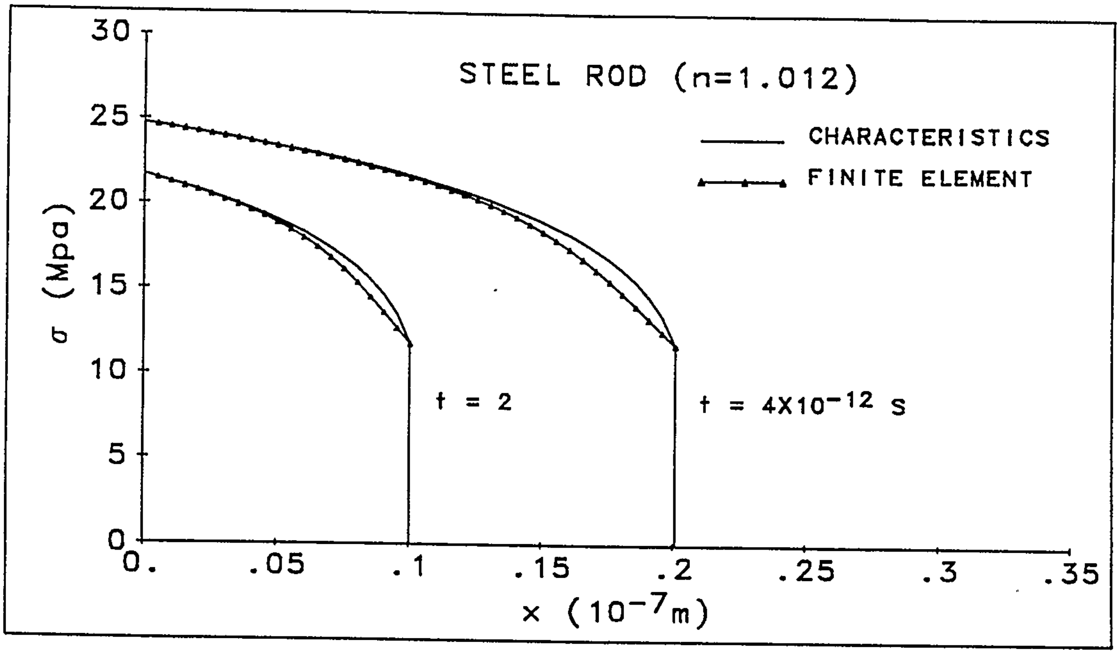

FIG. 6.11a STRESS RESPONSE OF A STEEL ROD (n = 1.012) TO $v(0,t) = - 120 \times t^{0.2}$ m/s AND $\theta(0,t) = 0$.

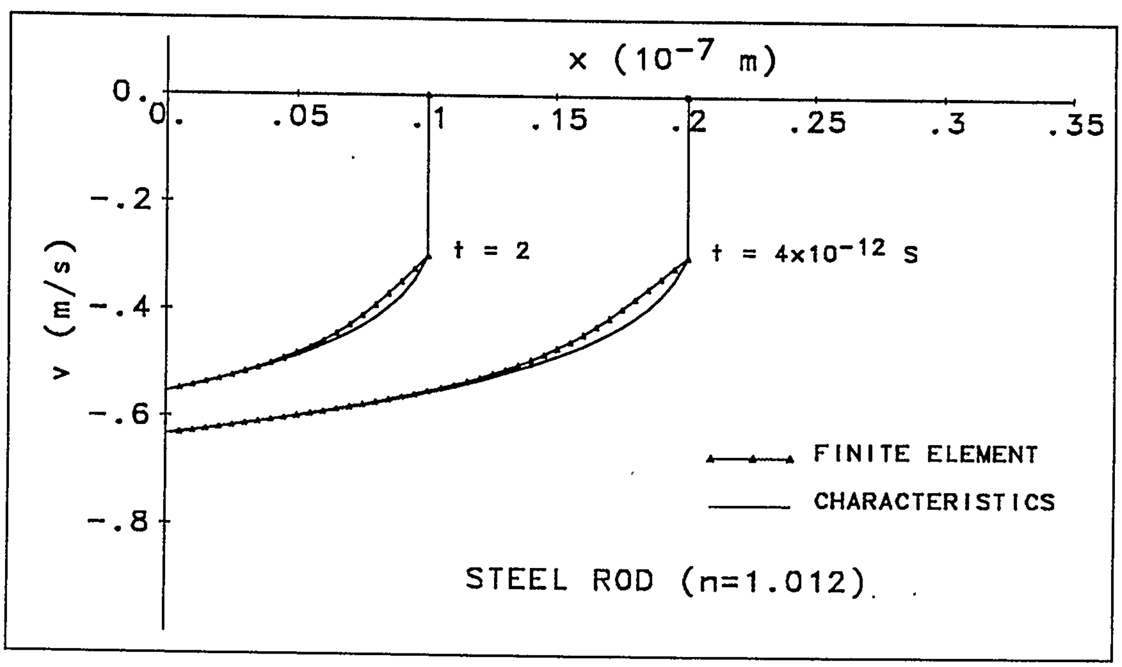

FIG. 6.11b VELOCITY RESPONSE OF A STEEL ROD (n = 1.012) TO $v(0,t) = - 120 \times t^{0.2}$ m/s AND $\theta(0,t) = 0$.

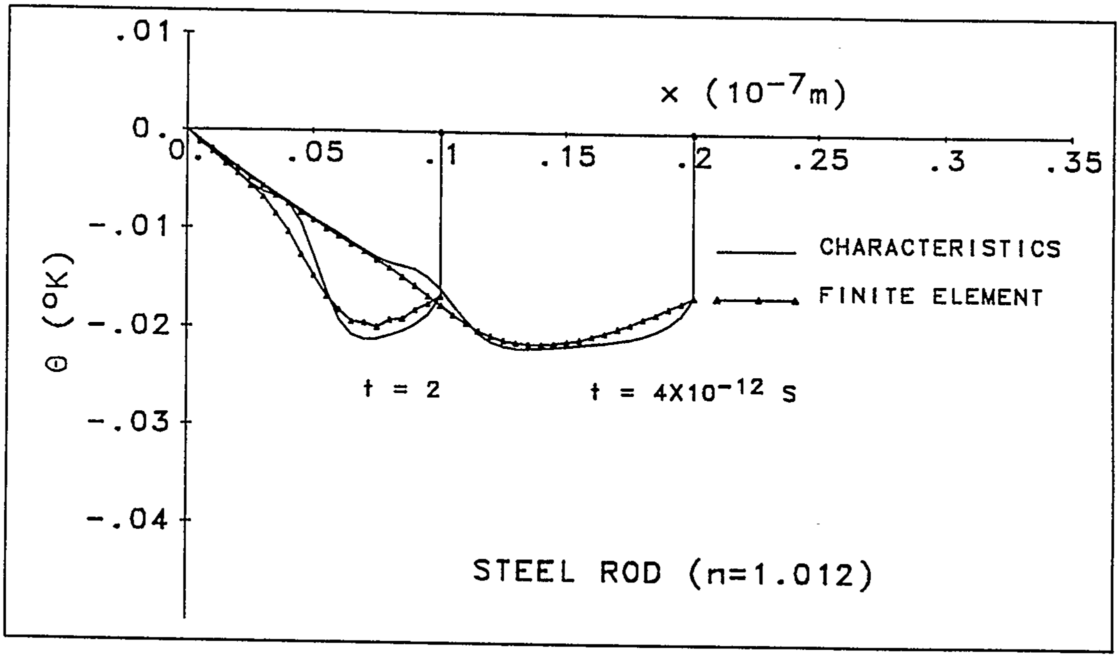

FIG. 6.11c TEMPERATURE RESPONSE OF A STEEL ROD (n = 1.012) TO $v(0,t) = - 120 \times t^{0.2}$ m/s AND $\theta(0,t) = 0$.

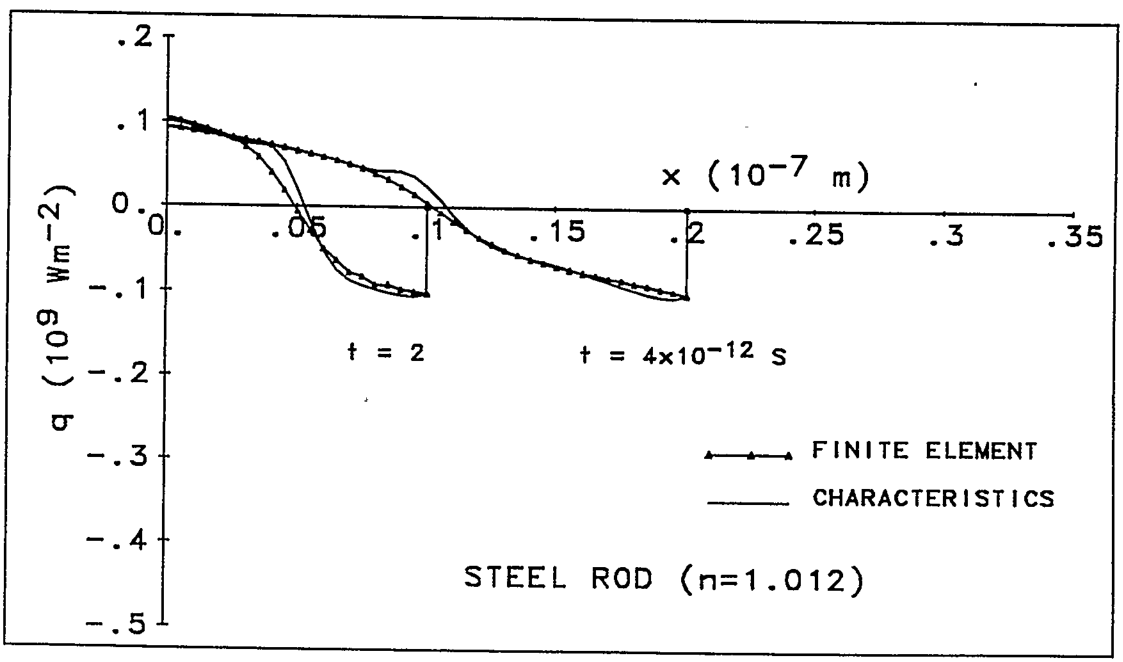

FIG. 6.11d HEAT FLUX RESPONSE OF A STEEL ROD (n = 1.012) TO $v(0,t) = - 120 \times t^{0.2}$ m/s AND $\theta(0,t) = 0$.

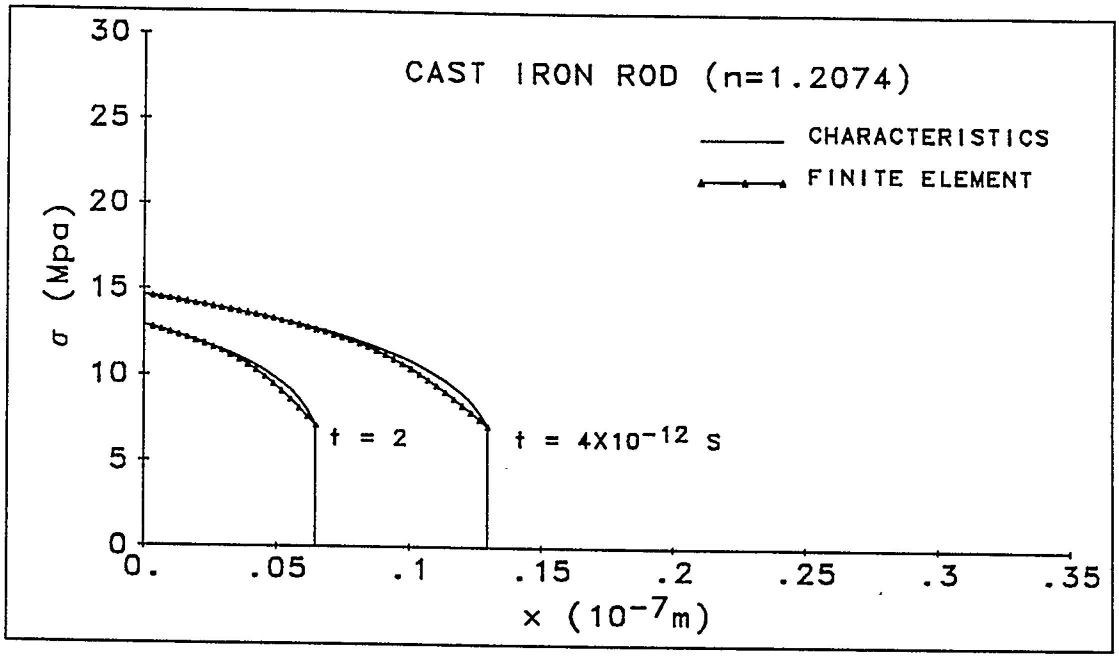

FIG. 6.12a STRESS RESPONSE OF A CAST IRON ROD (n = 1.2074) TO $v(0,t) = -120 \times t^{0.2}$ m/s AND $\theta(0,t) = 0$.

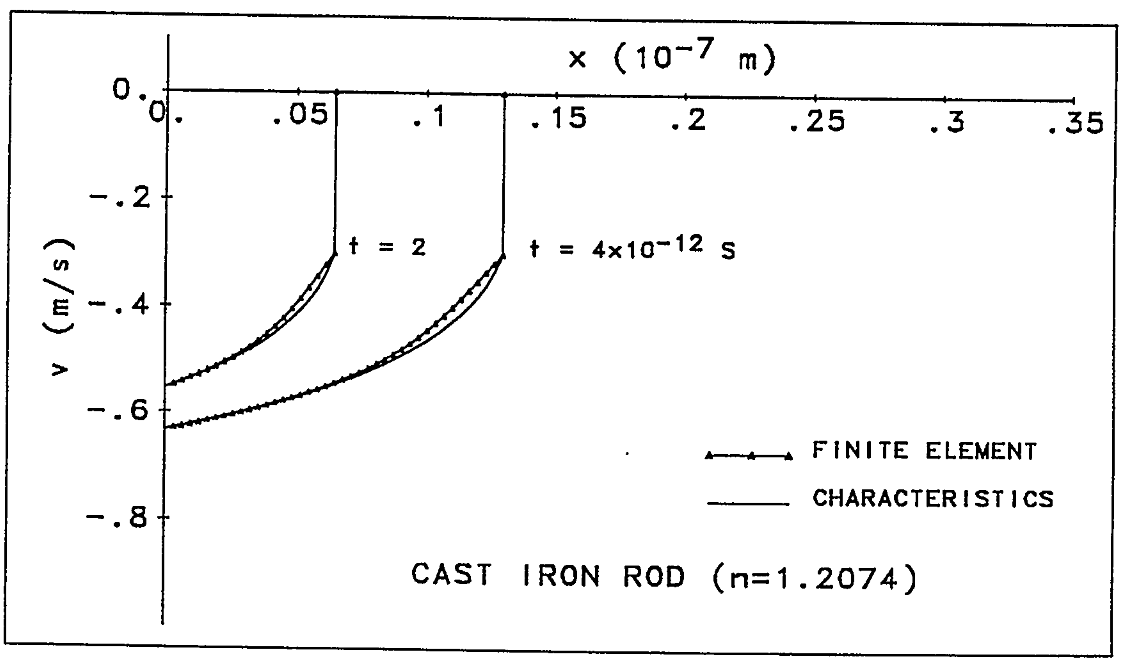

FIG. 6.12b VELOCITY RESPONSE OF A CAST IRON ROD (n = 1.2074) TO $v(0,t) = -120 \times t^{0.2}$ m/s AND $\theta(0,t) = 0$.

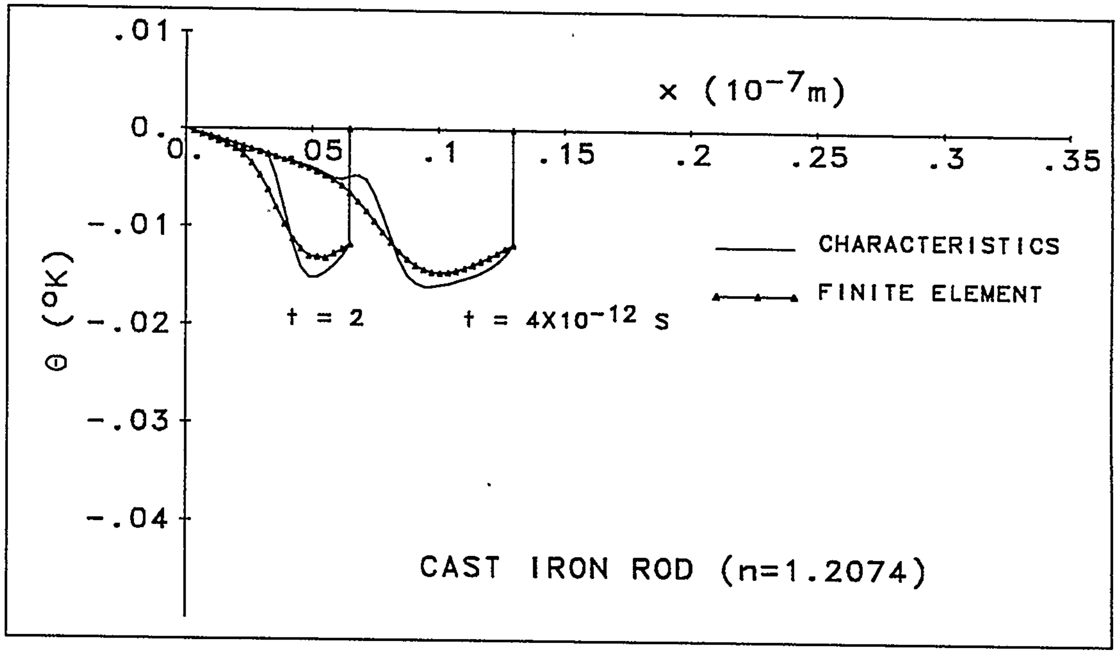

FIG. 6.12c TEMPERATURE RESPONSE OF A CAST IRON ROD (n = 1.2074) TO $v(0,t) = -120 \times t^{0.2}$ m/s AND $\theta(0,t) = 0$.

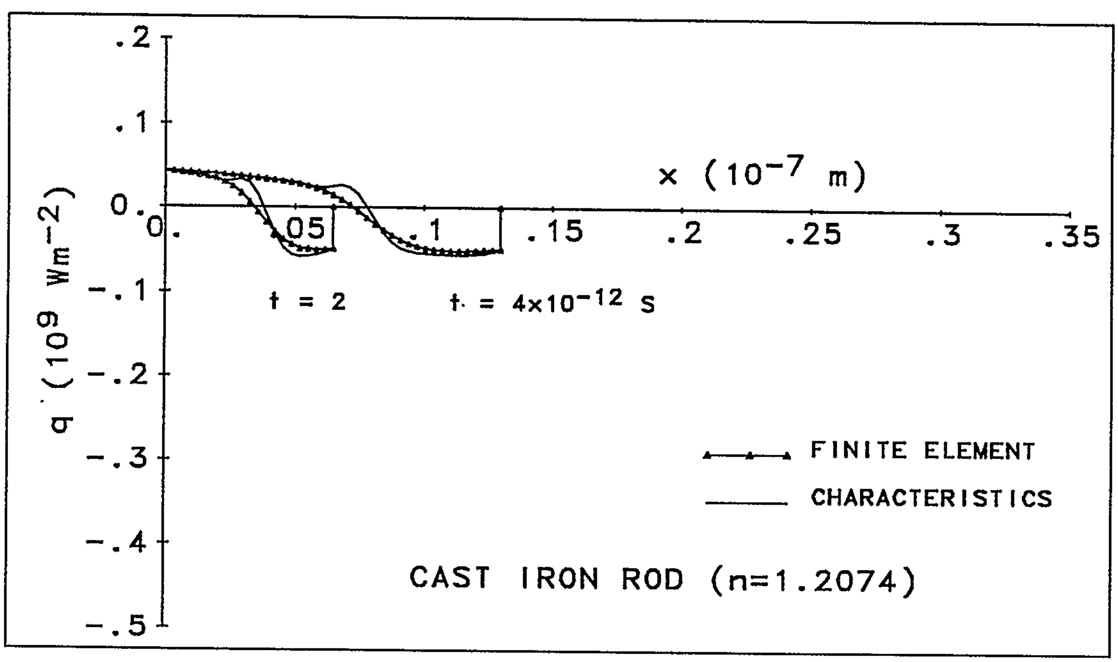

FIG. 6.12d HEAT FLUX RESPONSE OF A CAST IRON ROD (n = 1.2074) TO $v(0,t) = -120 \times t^{0.2}$ m/s AND $\theta(0,t) = 0$.

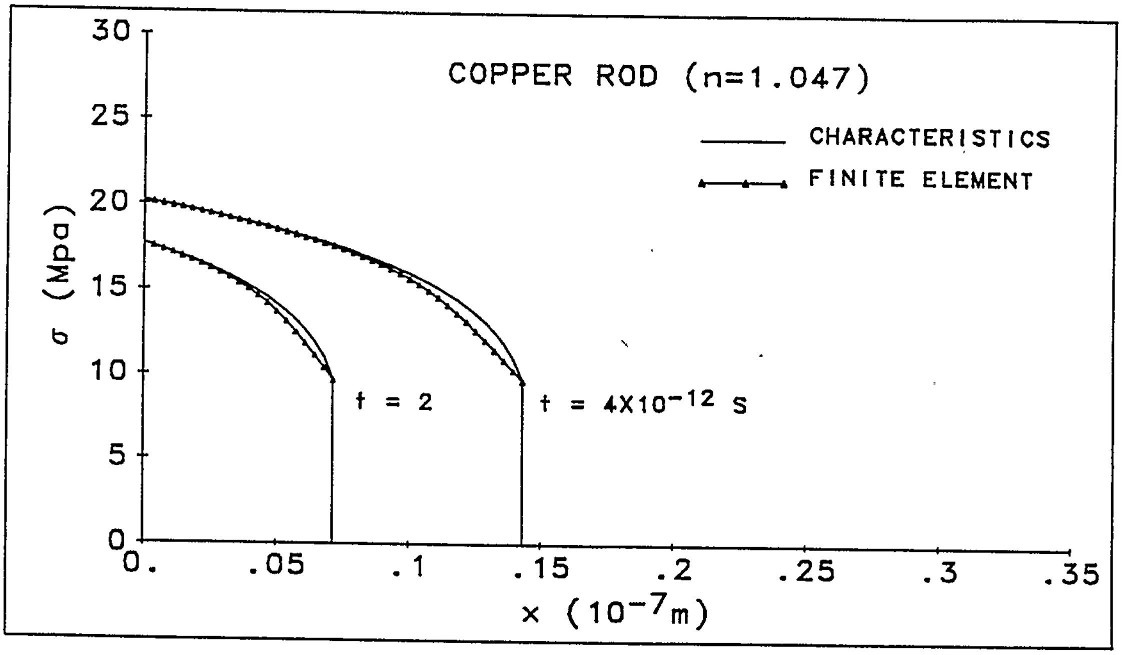

FIG. 6.13a STRESS RESPONSE OF A COPPER ROD (n = 1.047) TO $v(0,t) = -120 \times t^{0.2}$ m/s AND $\theta(0,t) = 0$.

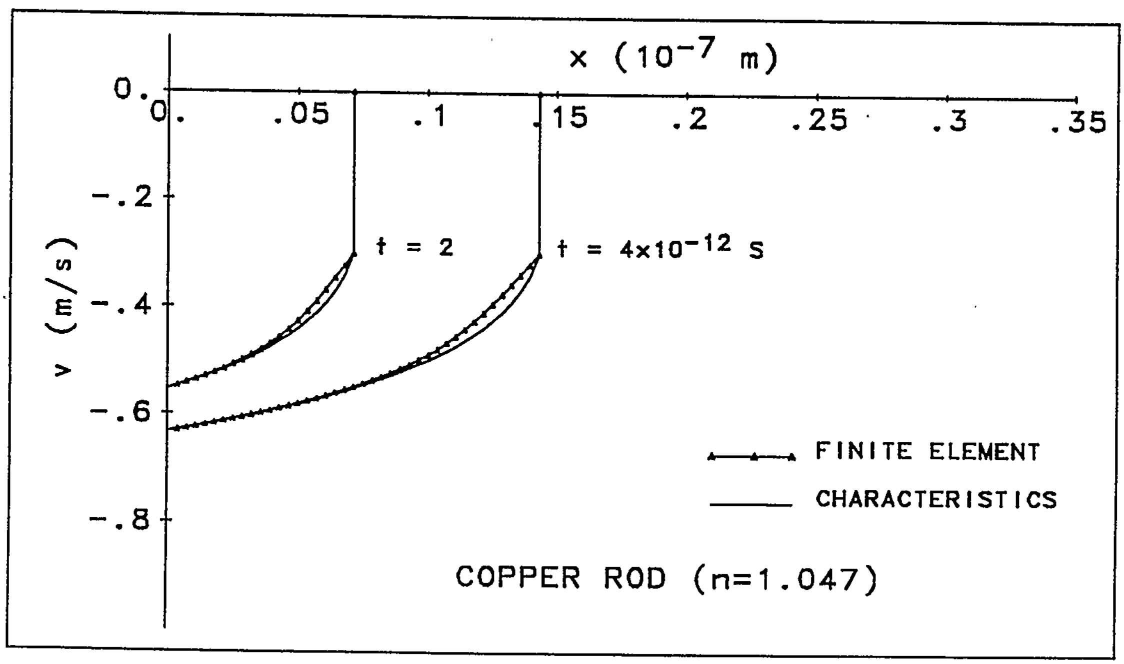

FIG. 6.13b VELOCITY RESPONSE OF A COPPER ROD (n = 1.047) TO $v(0,t) = -120 \times t^{0.2}$ m/s AND $\theta(0,t) = 0$.

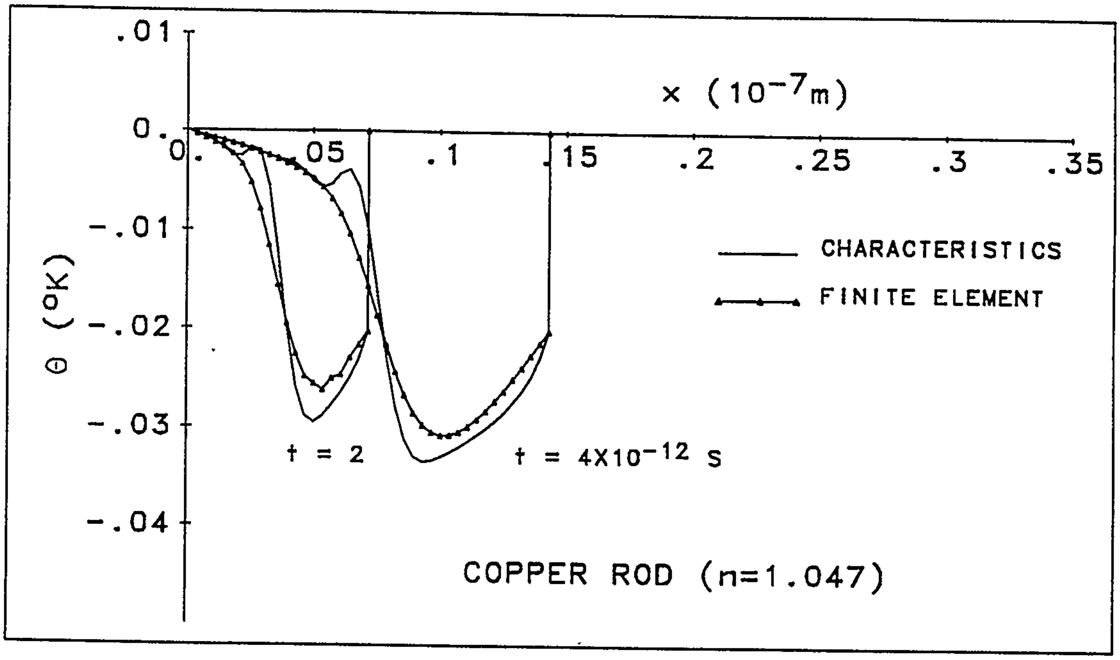

FIG. 6.13c TEMPERATURE RESPONSE OF A COPPER ROD (n = 1.047) TO $v(0,t) = -120 \times t^{0.2}$ m/s AND $\theta(0,t) = 0$.

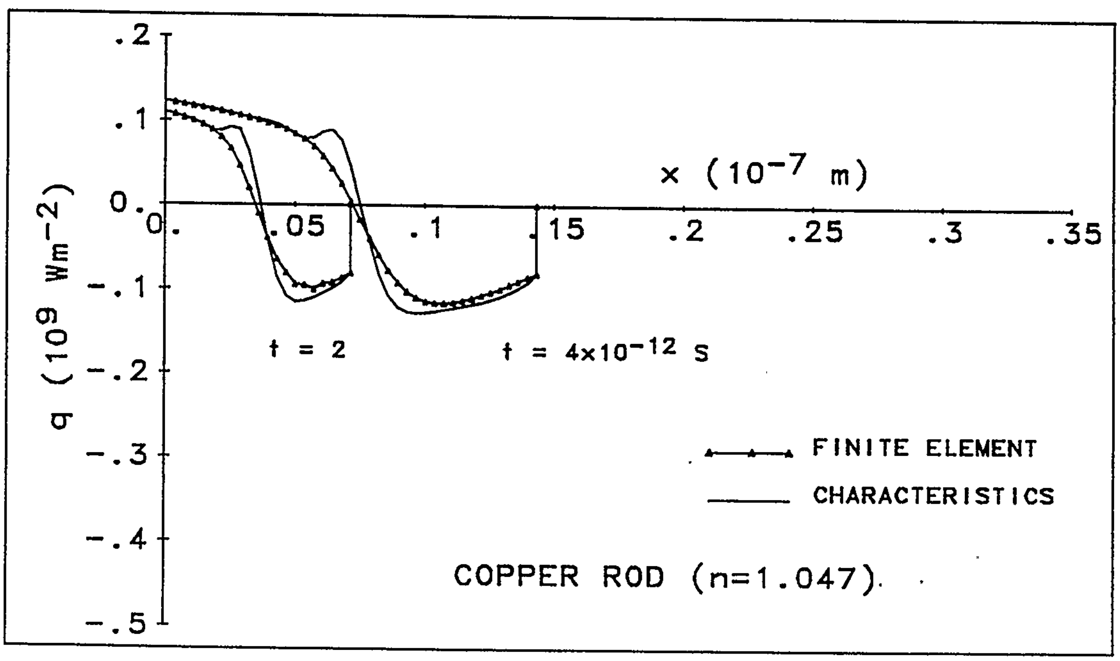

FIG. 6.13d HEAT FLUX RESPONSE OF A COPPER ROD (n = 1.047) TO $v(0,t) = -120 \times t^{0.2}$ m/s AND $\theta(0,t) = 0$.

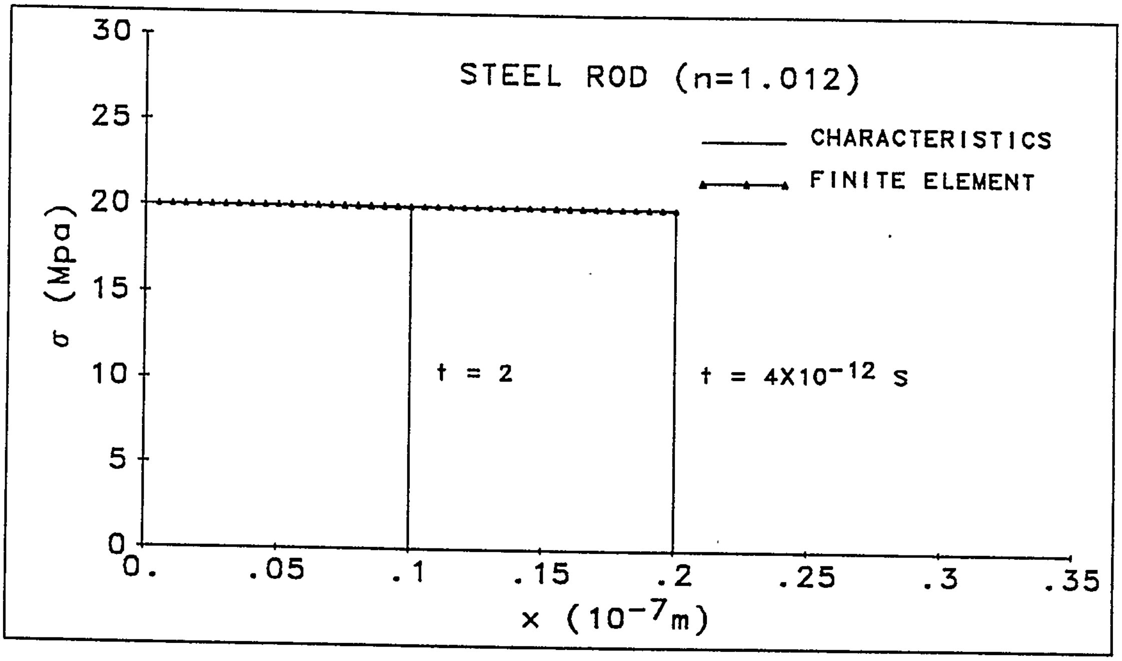

FIG. 6.14a STRESS RESPONSE OF A STEEL ROD (n = 1.012) TO $\sigma(0,t) = 20$ MPa AND $\theta(0,t) = 0$.

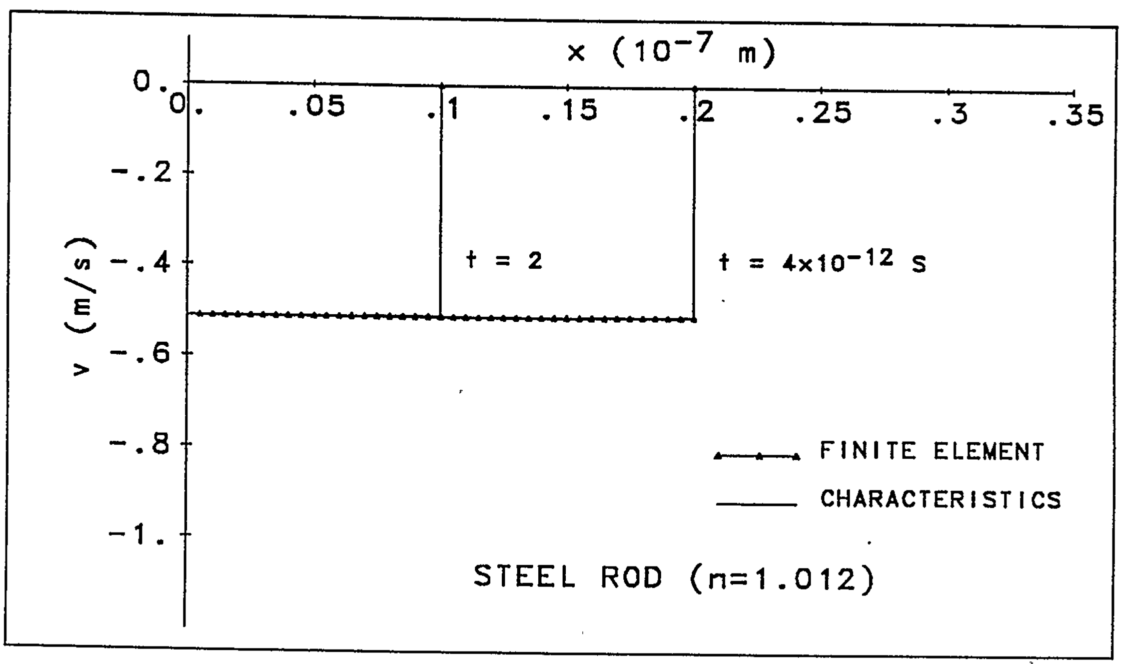

FIG. 6.14b VELOCITY RESPONSE OF A STEEL ROD (n = 1.012) TO $\sigma(0,t) = 20$ MPa AND $\theta(0,t) = 0$.

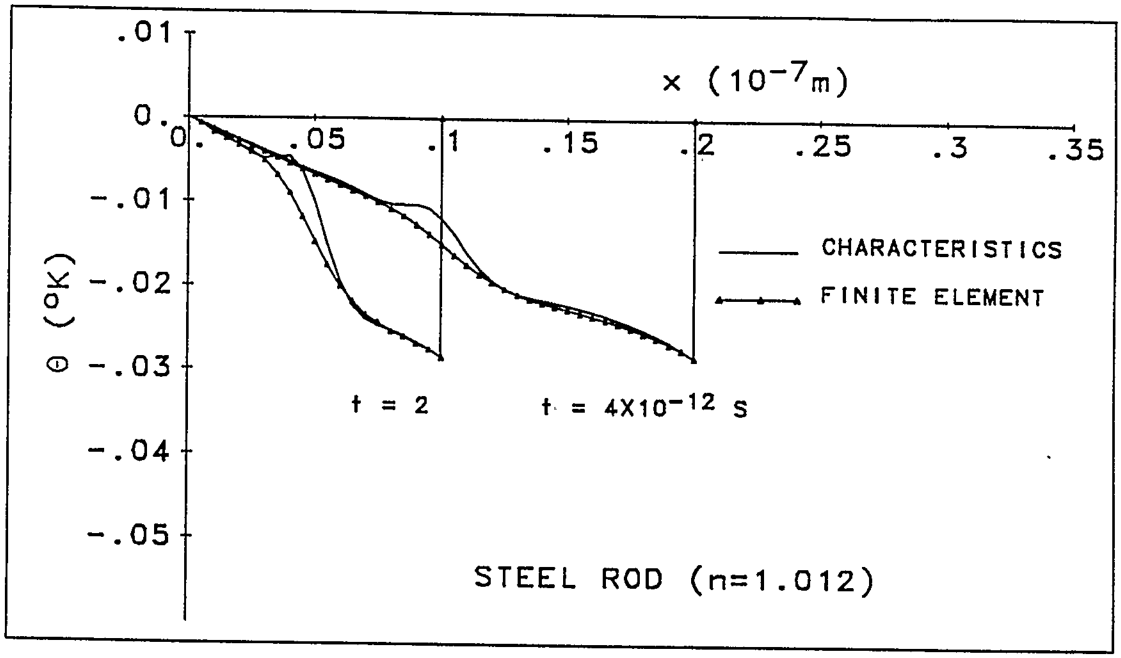

FIG. 6.14c TEMPERATURE RESPONSE OF A STEEL ROD (n = 1.012) TO $\sigma(0,t)$ = 20 MPa AND $\theta(0,t) = 0$.

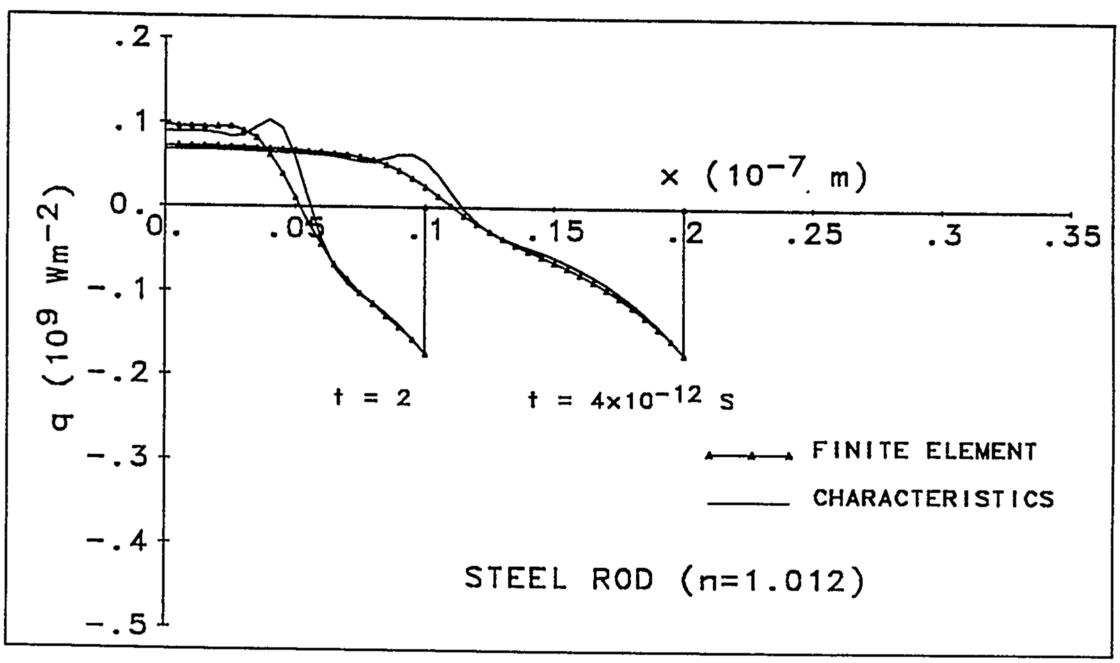

FIG. 6.14d HEAT FLUX RESPONSE OF A STEEL ROD (n = 1.012) TO $\sigma(0,t)$ = 20 MPa AND $\theta(0,t) = 0$.

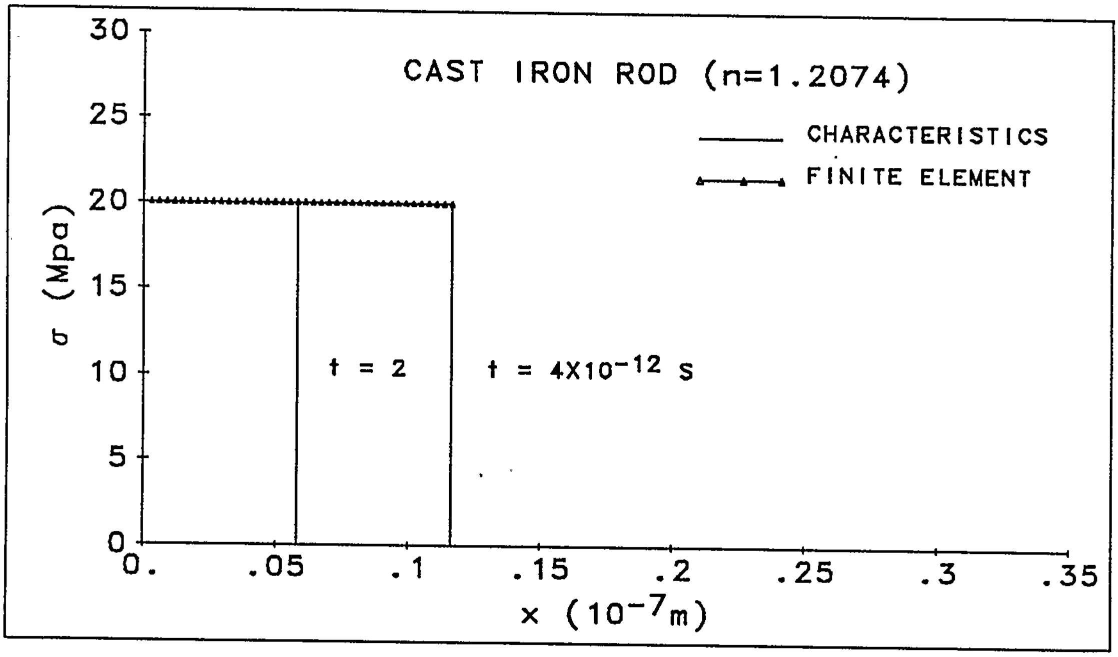

FIG. 6.15a STRESS RESPONSE OF A CAST IRON ROD (n = 1.2074) TO $\sigma(0,t)$ = 20 MPa AND $\theta(0,t)$ = 0.

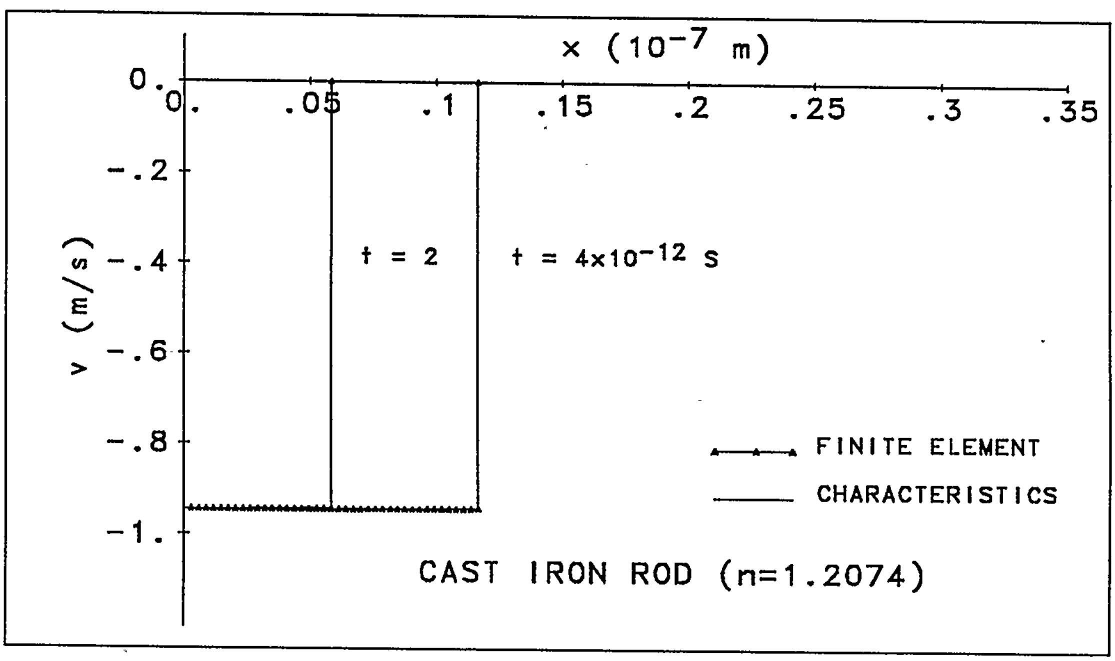

FIG. 6.15b VELOCITY RESPONSE OF A CAST IRON ROD (n = 1.2074) TO $\sigma(0,t)$ = 20 MPa AND $\theta(0,t)$ = 0.

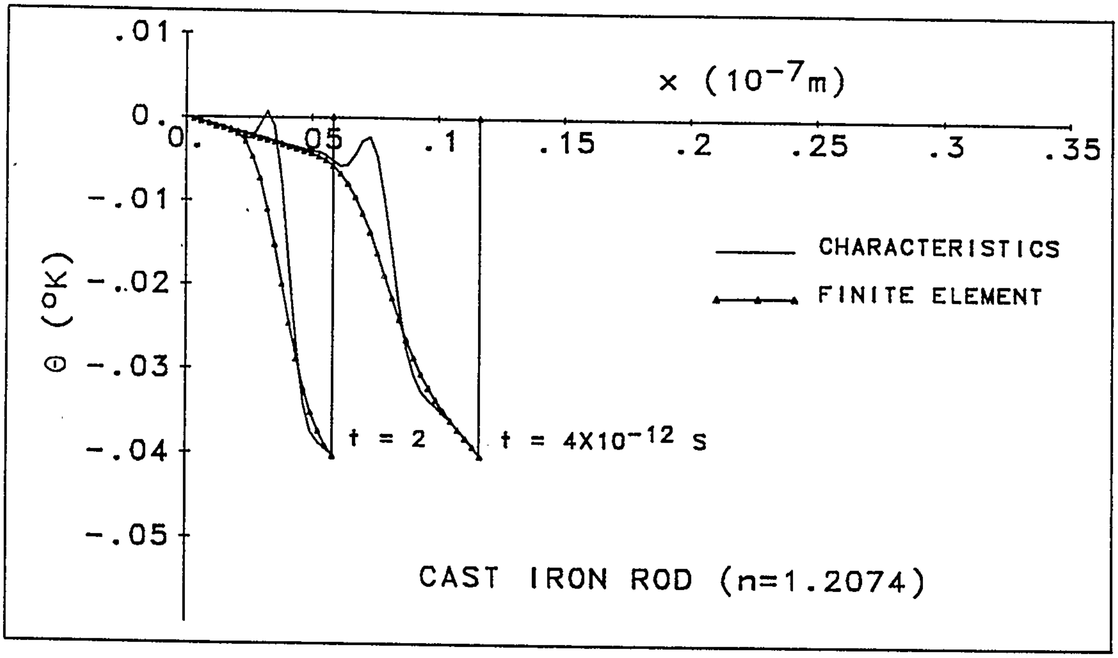

FIG. 6.15c TEMPERATURE RESPONSE OF A CAST IRON ROD (n = 1.2074) TO $\sigma(0,t)$ = 20 MPa AND $\theta(0,t)$ = 0.

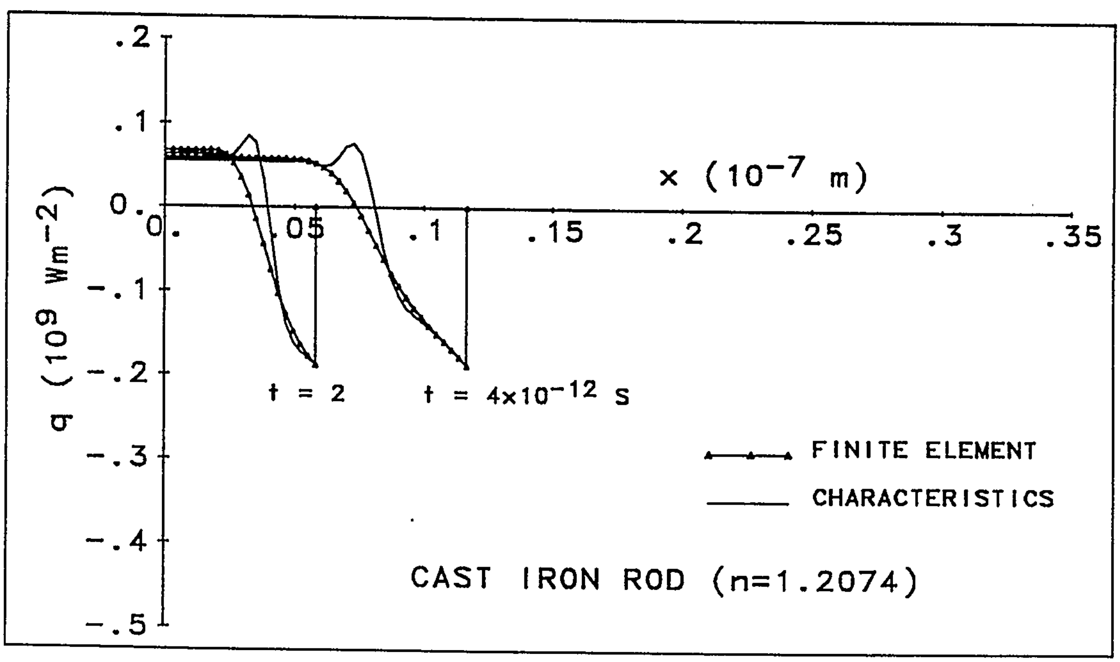

FIG. 6.15d HEAT FLUX RESPONSE OF A CAST IRON ROD (n = 1.2074) TO $\sigma(0,t)$ = 20 MPa AND $\theta(0,t)$ = 0.

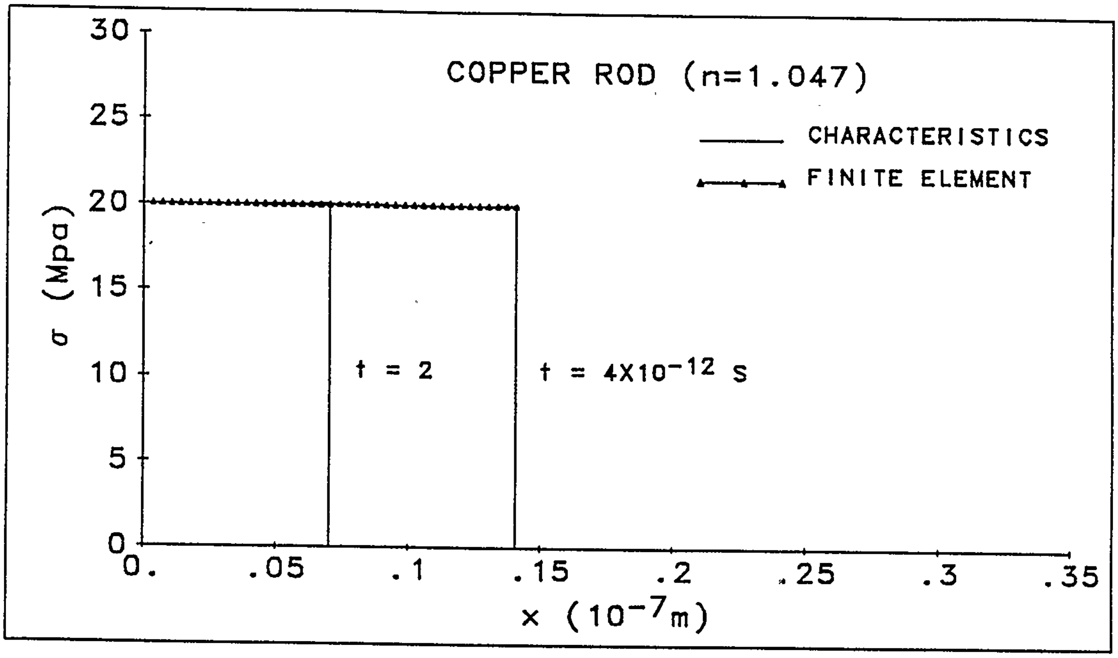

FIG. 6.16a STRESS RESPONSE OF A COPPER ROD (n = 1.047) TO $\sigma(0,t)$ = 20 MPa AND $\theta(0,t)$ = 0.

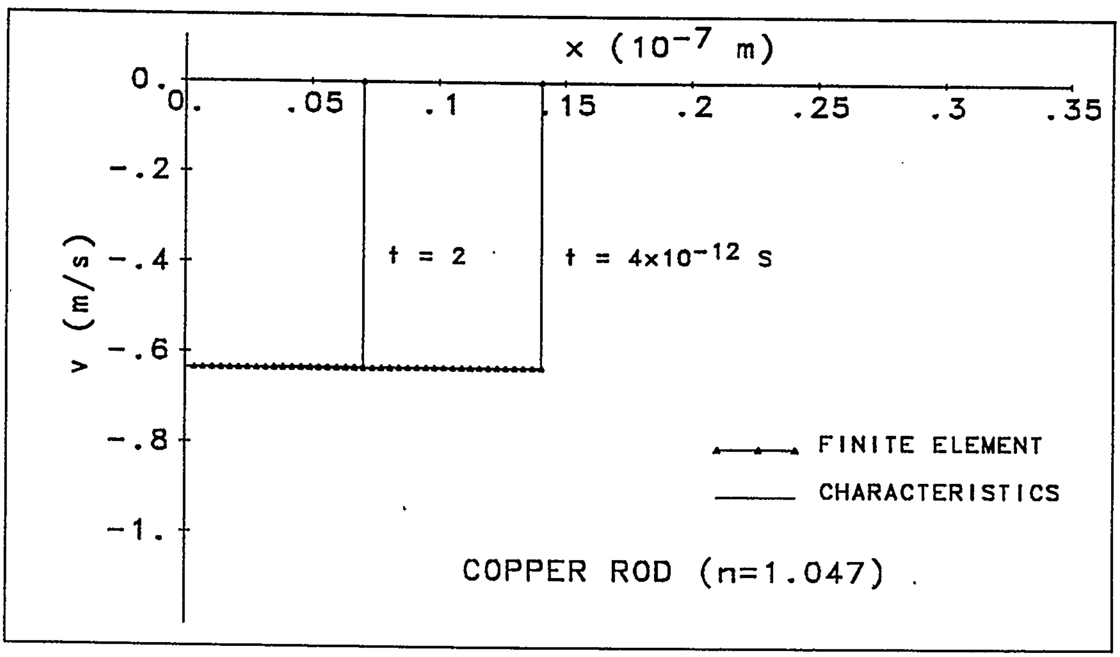

FIG. 6.16b VELOCITY RESPONSE OF A COPPER ROD (n = 1.047) TO $\sigma(0,t)$ = 20 MPa AND $\theta(0,t)$ = 0.

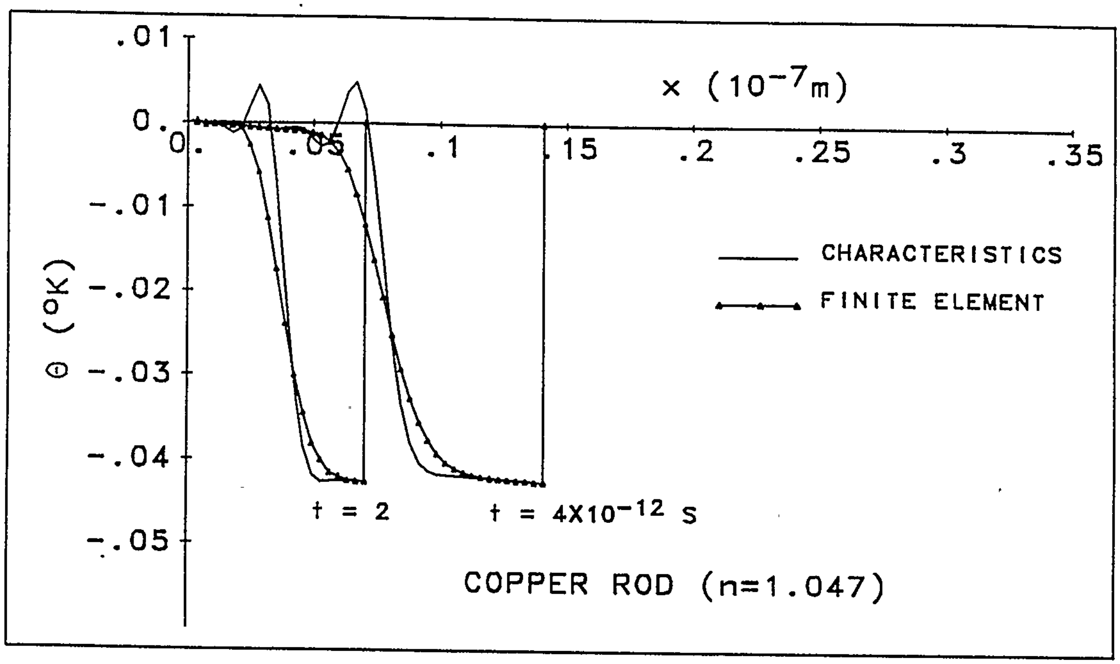

FIG. 6.16c TEMPERATURE RESPONSE OF A COPPER ROD (n = 1.047) TO $\sigma(0,t)$ = 20 MPa AND $\theta(0,t)$ = 0.

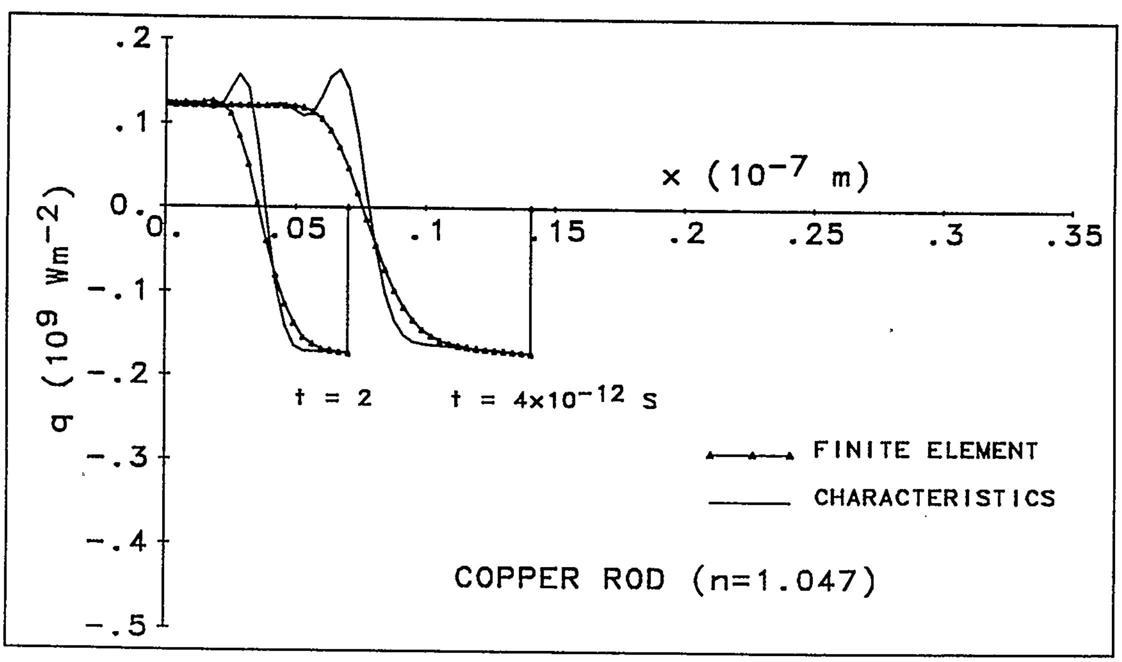

FIG. 6.16d HEAT FLUX RESPONSE OF A COPPER ROD (n = 1.047) TO $\sigma(0,t)$ = 20 MPa AND $\theta(0,t)$ = 0.

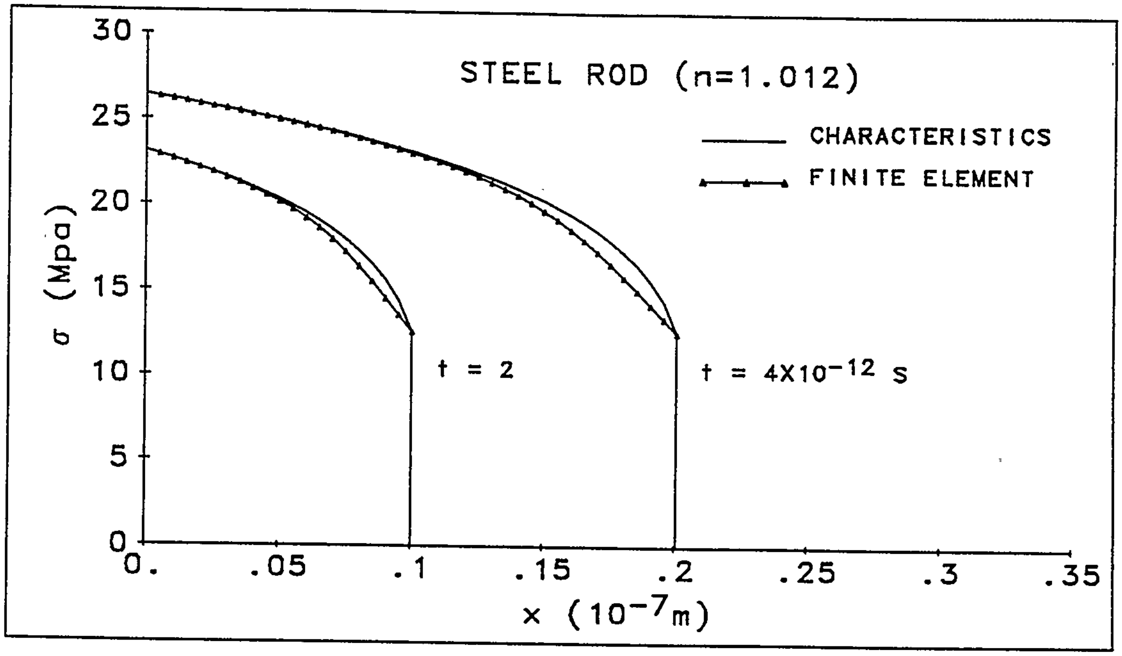

FIG. 6.17a STRESS RESPONSE OF A STEEL ROD (n = 1.012) TO

$\sigma(0,t) = 5 \times t^{0.2}$ GPa AND $\theta(0,t) = 0$.

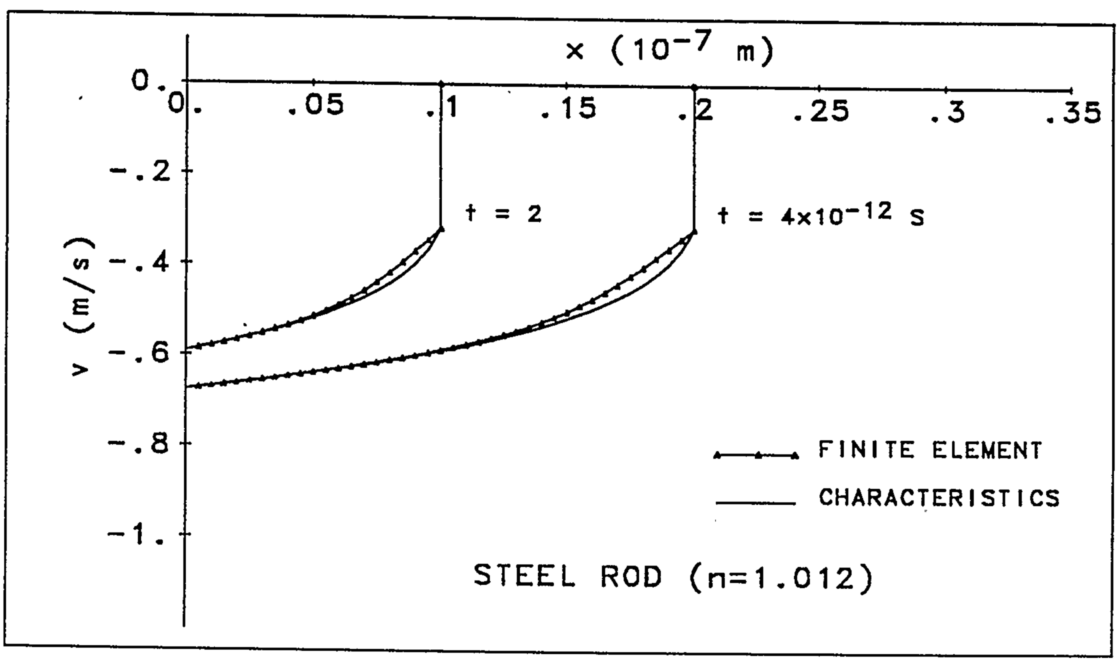

FIG. 6.17b VELOCITY RESPONSE OF A STEEL ROD (n = 1.012) TO

$\sigma(0,t) = 5 \times t^{0.2}$ GPa AND $\theta(0,t) = 0$.

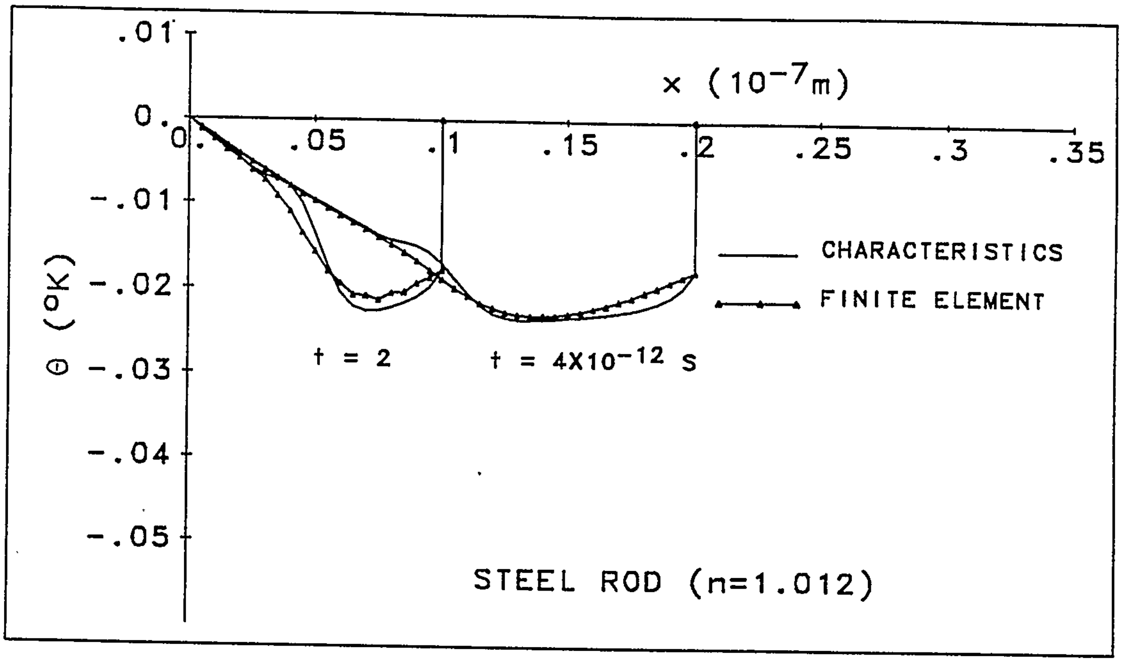

FIG. 6.17c TEMPERATURE RESPONSE OF A STEEL ROD (n = 1.012) TO $\sigma(0,t) = 5 \times t^{0.2}$ GPa AND $\theta(0,t) = 0$.

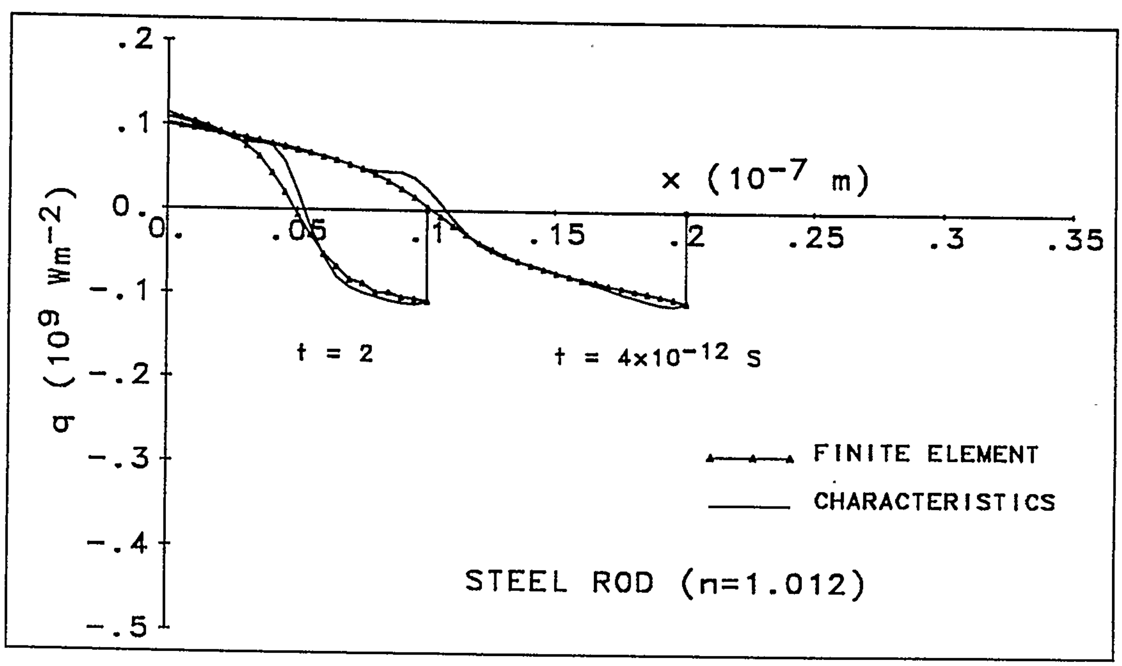

FIG. 6.17d HEAT FLUX RESPONSE OF A STEEL ROD (n = 1.012) TO $\sigma(0,t) = 5 \times t^{0.2}$ GPa AND $\theta(0,t) = 0$.

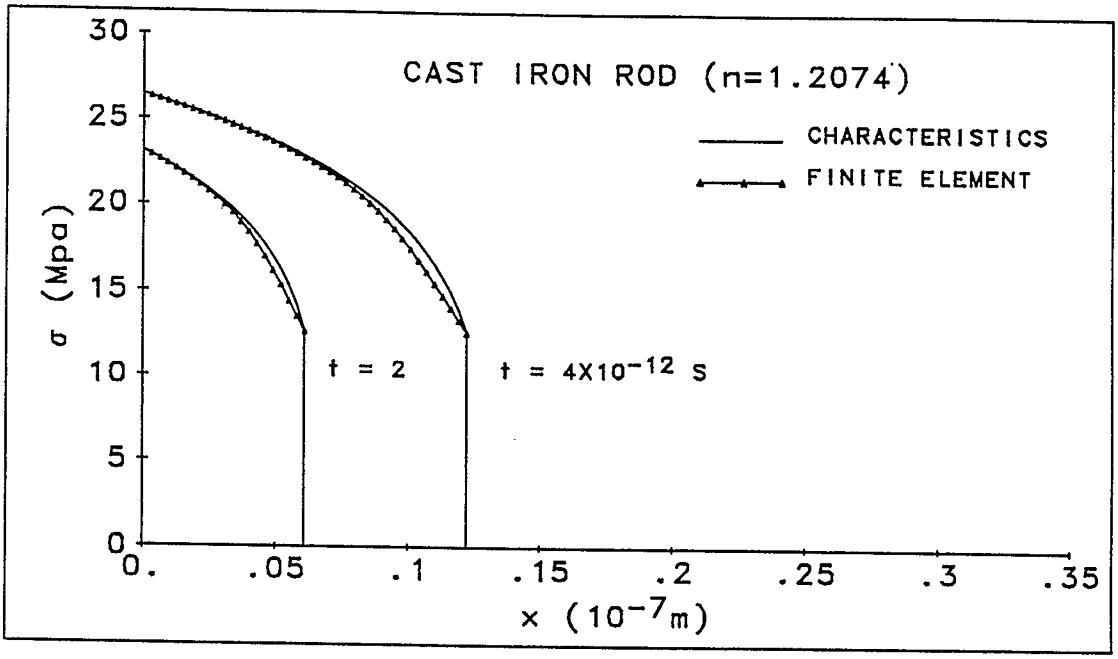

FIG. 6.18a STRESS RESPONSE OF A CAST IRON ROD (n = 1.2074) TO $\sigma(0,t) = 5 \times t^{0.2}$ GPa AND $\theta(0,t) = 0$.

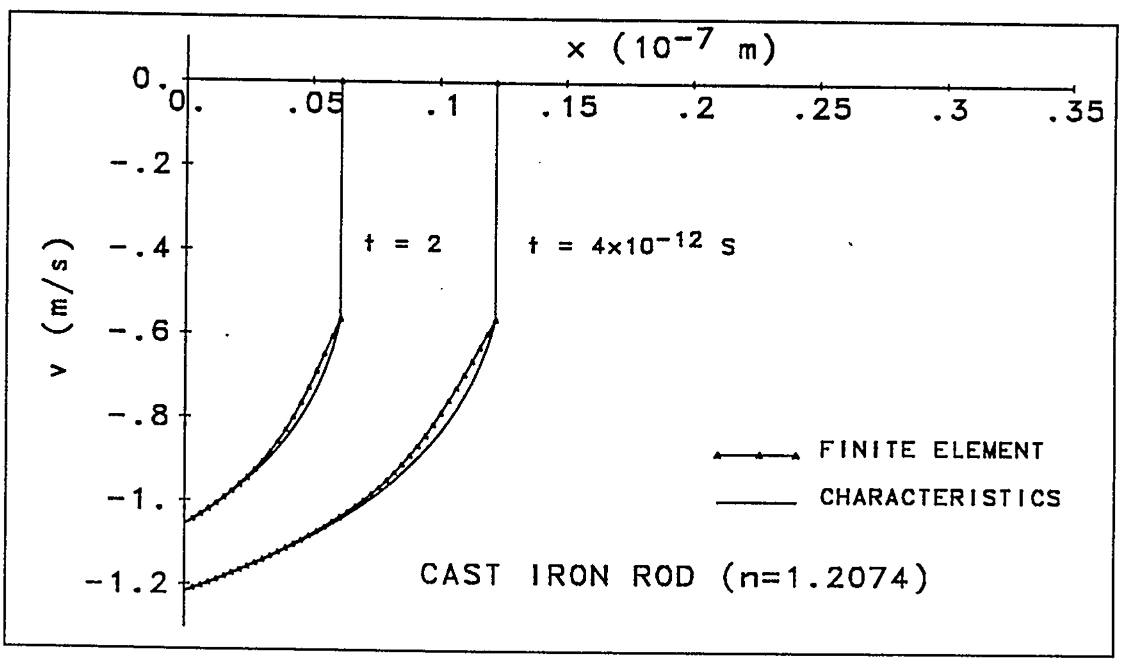

FIG. 6.18b VELOCITY RESPONSE OF A CAST IRON ROD (n = 1.2074) TO $\sigma(0,t) = 5 \times t^{0.2}$ GPa AND $\theta(0,t) = 0$.

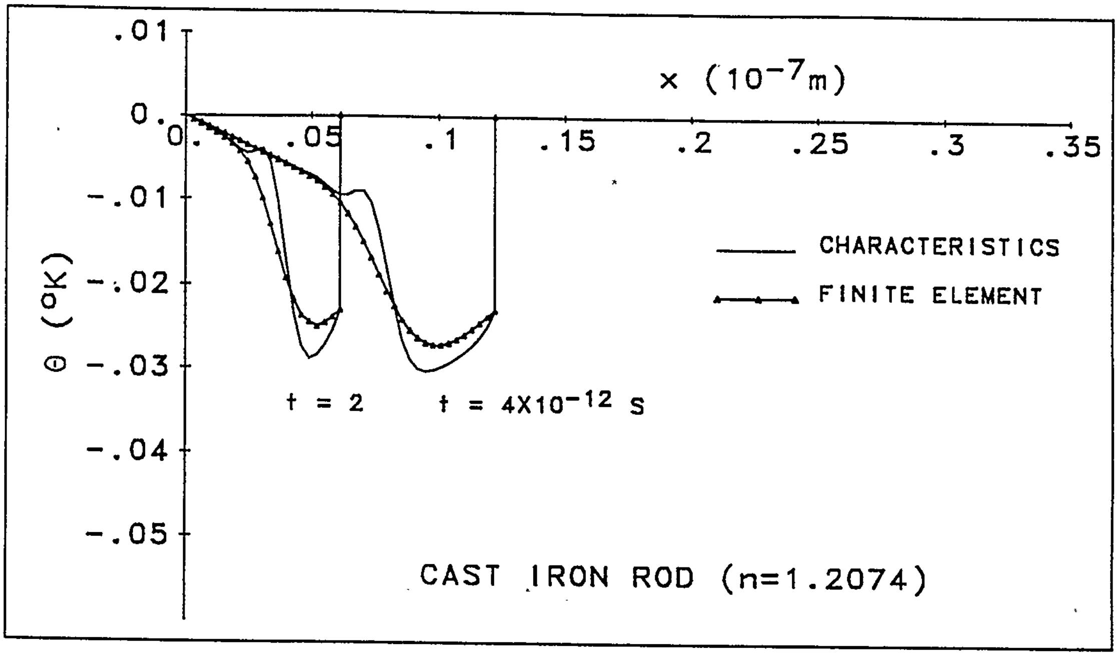

FIG. 6.18c TEMPERATURE RESPONSE OF A CAST IRON ROD (n = 1.2074) TO $\sigma(0,t) = 5 \times t^{0.2}$ GPa AND $\theta(0,t) = 0$.

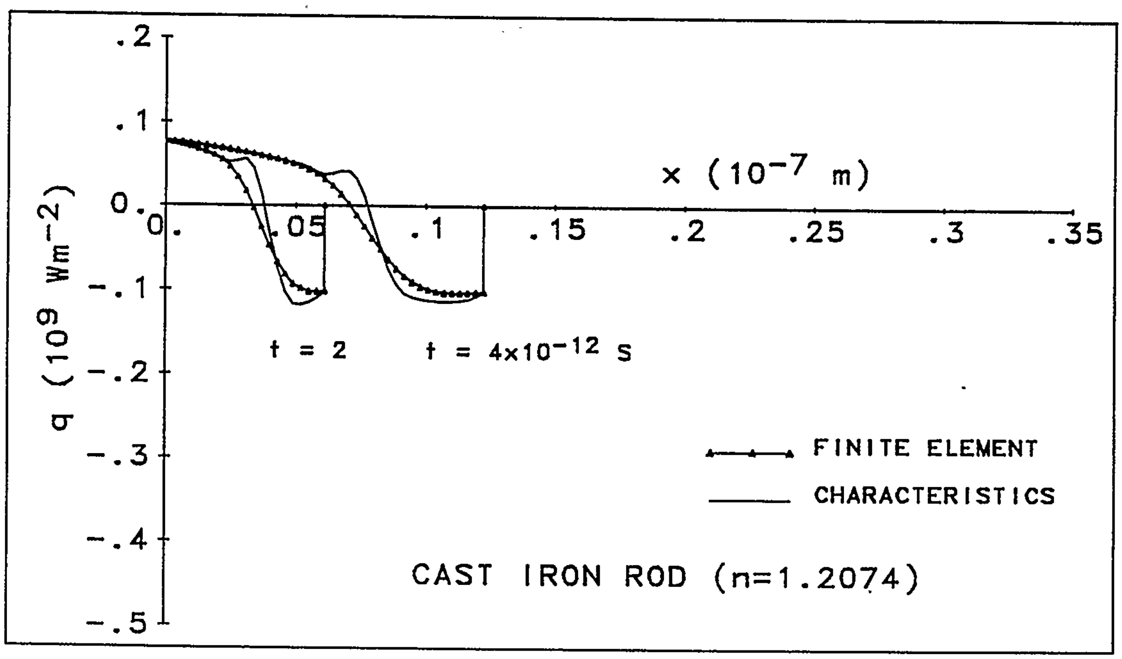

FIG. 6.18d HEAT FLUX RESPONSE OF A CAST IRON ROD (n = 1.2074) TO $\sigma(0,t) = 5 \times t^{0.2}$ GPa AND $\theta(0,t) = 0$.

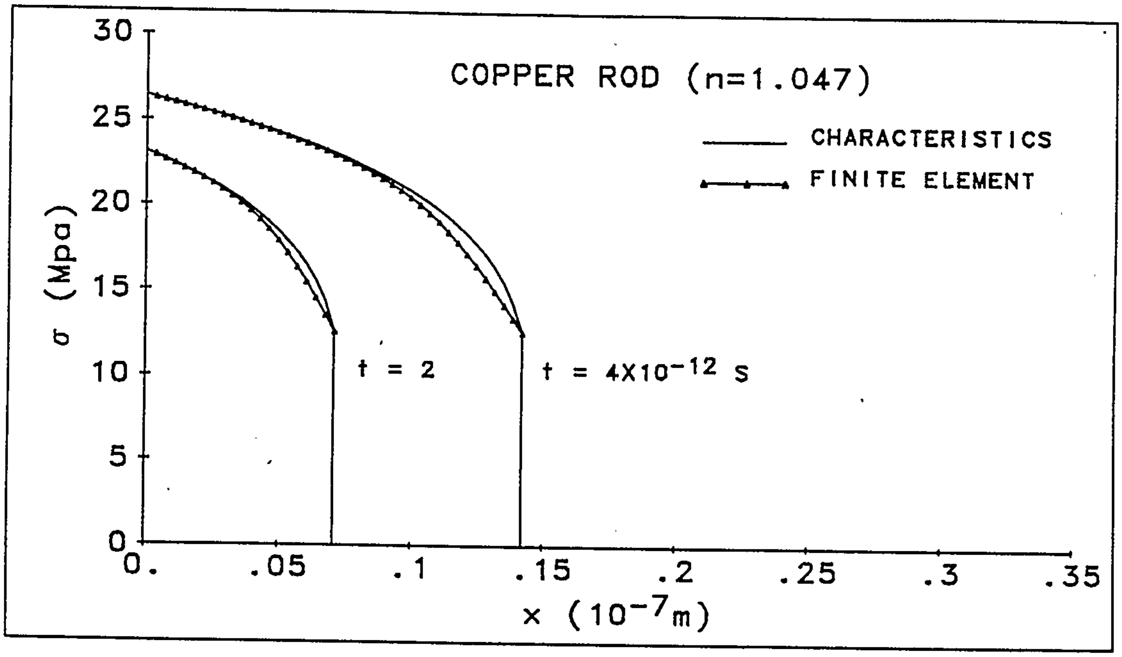

FIG. 6.19a STRESS RESPONSE OF A COPPER ROD (n = 1.047) TO $\sigma(0,t) = 5 \times t^{0.2}$ GPa AND $\theta(0,t) = 0$.

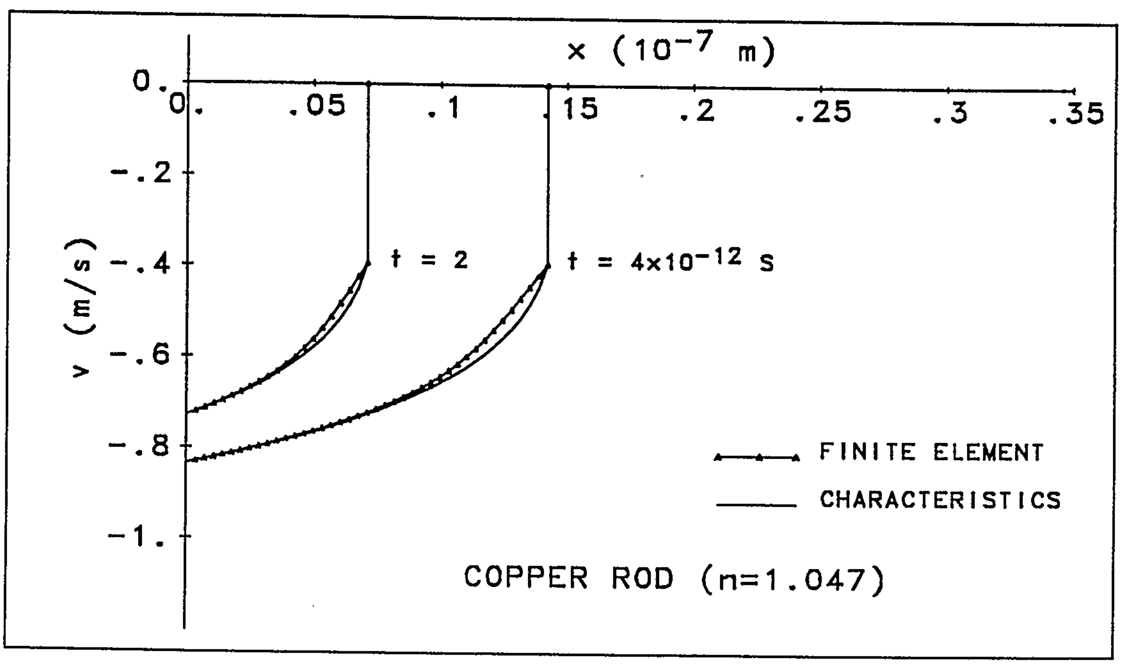

FIG. 6.19b VELOCITY RESPONSE OF A COPPER ROD (n = 1.047) TO $\sigma(0,t) = 5 \times t^{0.2}$ GPa AND $\theta(0,t) = 0$.

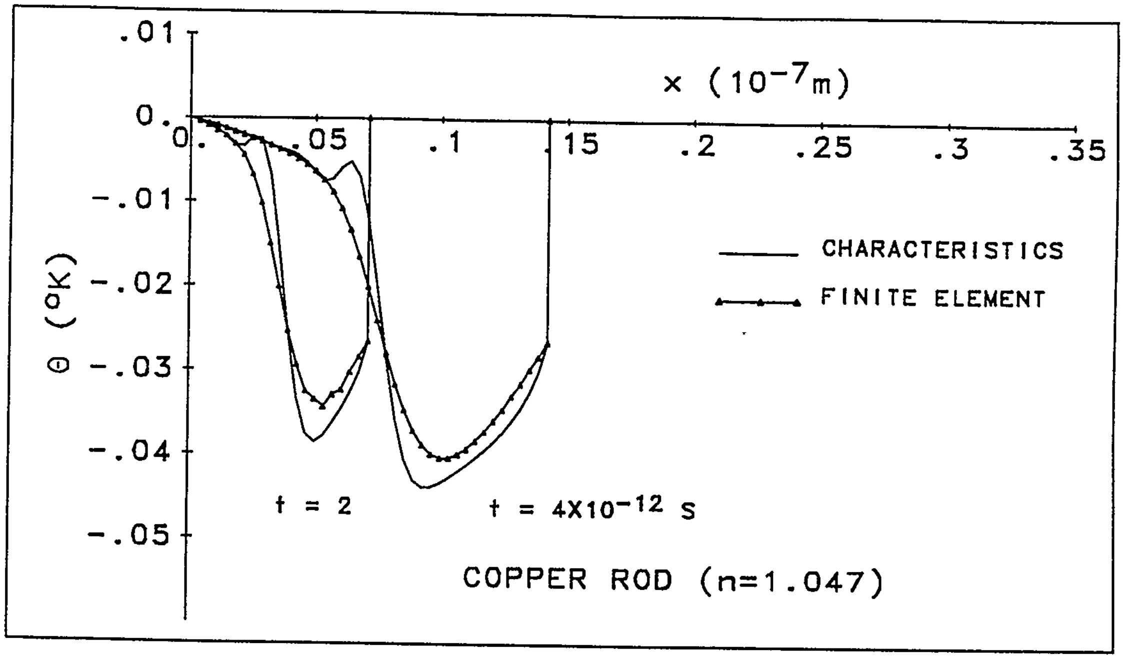

FIG. 6.19c TEMPERATURE RESPONSE OF A COPPER ROD (n = 1.047) TO $\sigma(0,t) = 5 \times t^{0.2}$ GPa AND $\theta(0,t) = 0$.

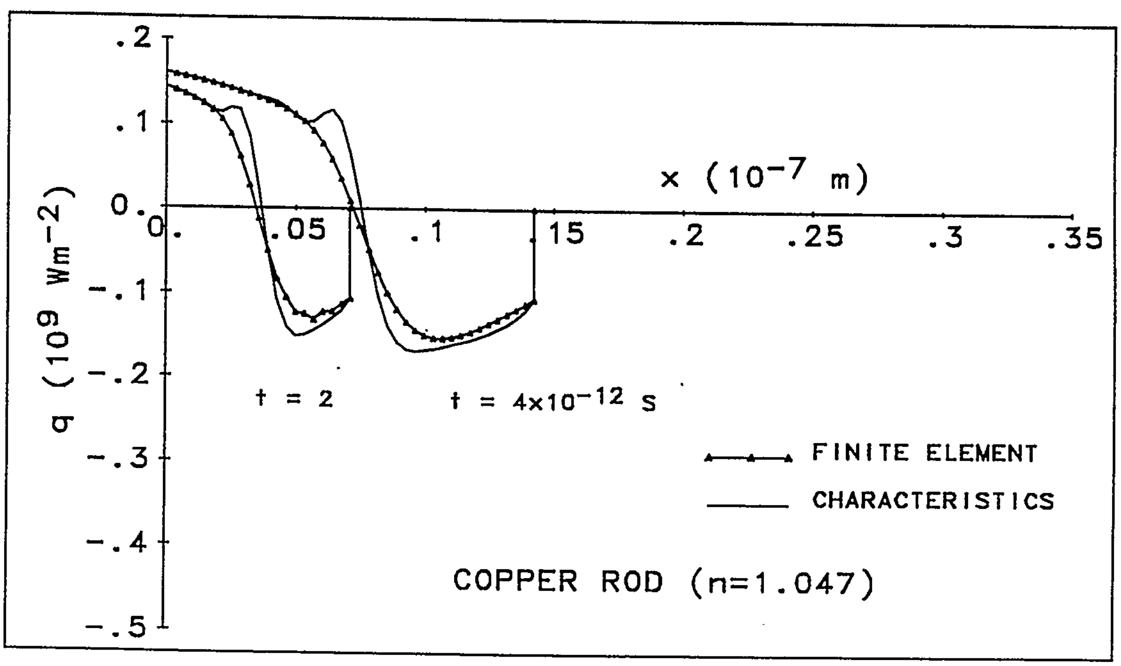

FIG. 6.19d HEAT FLUX RESPONSE OF A COPPER ROD (n = 1.047) TO $\sigma(0,t) = 5 \times t^{0.2}$ GPa AND $\theta(0,t) = 0$.

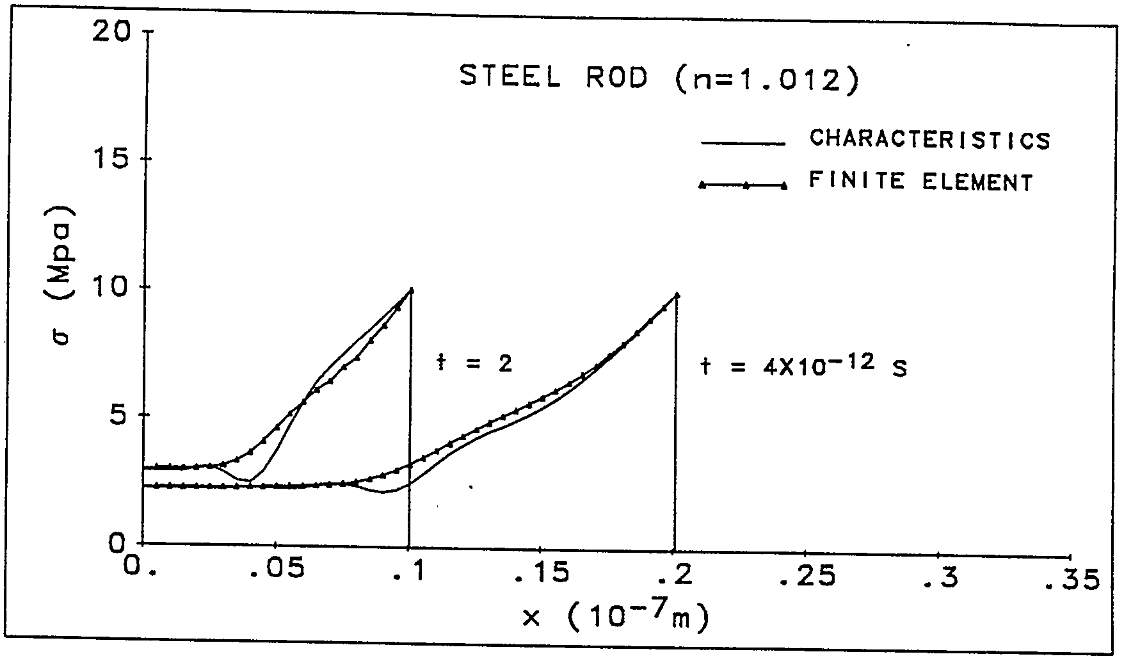

FIG. 6.20a STRESS RESPONSE OF A STEEL ROD (n = 1.012) TO $v(0,t) = 0$ AND $\theta(0,t) = -5\ ^{o}K$

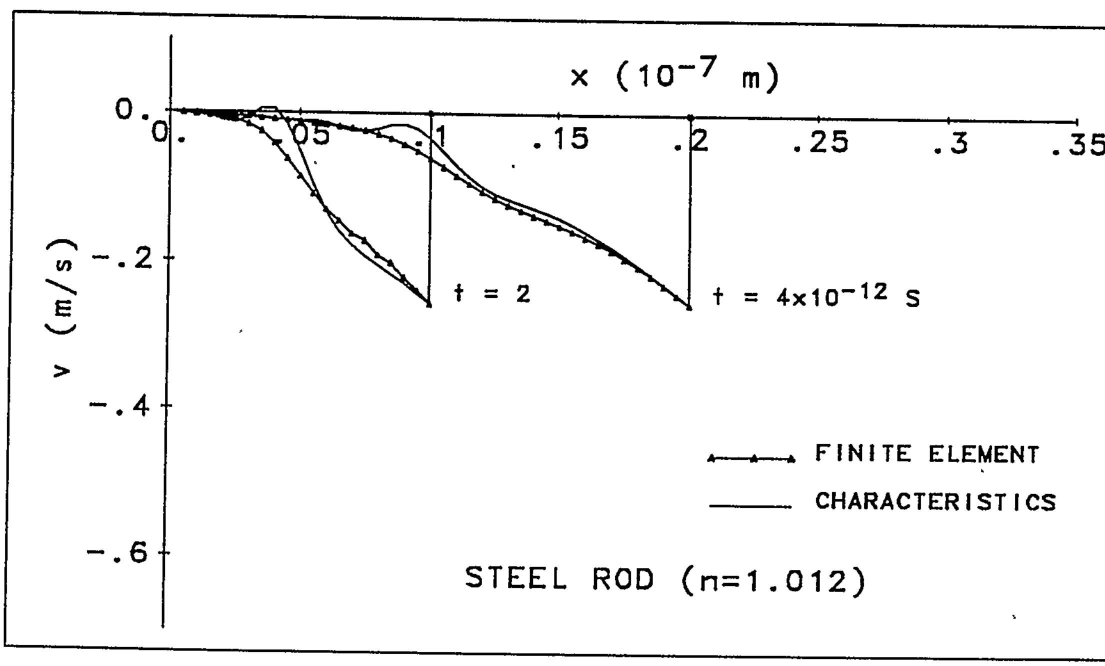

FIG. 6.20b VELOCITY RESPONSE OF A STEEL ROD (n = 1.012) TO $v(0,t) = 0$ AND $\theta(0,t) = -5\ ^{o}K$

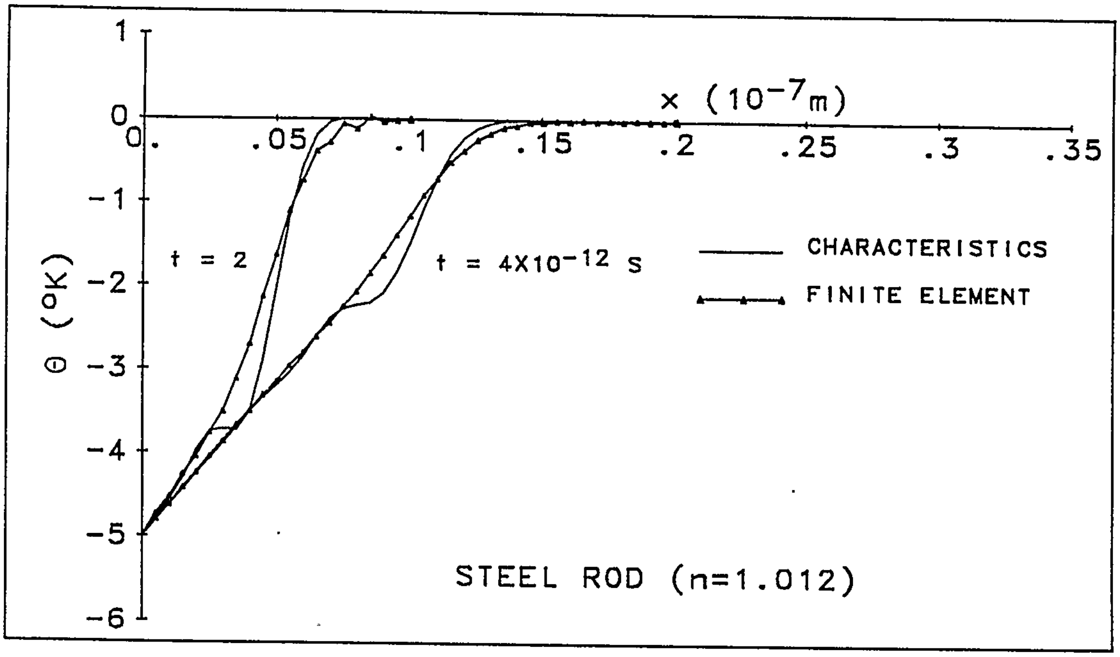

FIG. 6.20c TEMPERATURE RESPONSE OF A STEEL ROD (n = 1.012) TO $v(0,t) = 0$ AND $\theta(0,t) = -5\ ^{o}K$

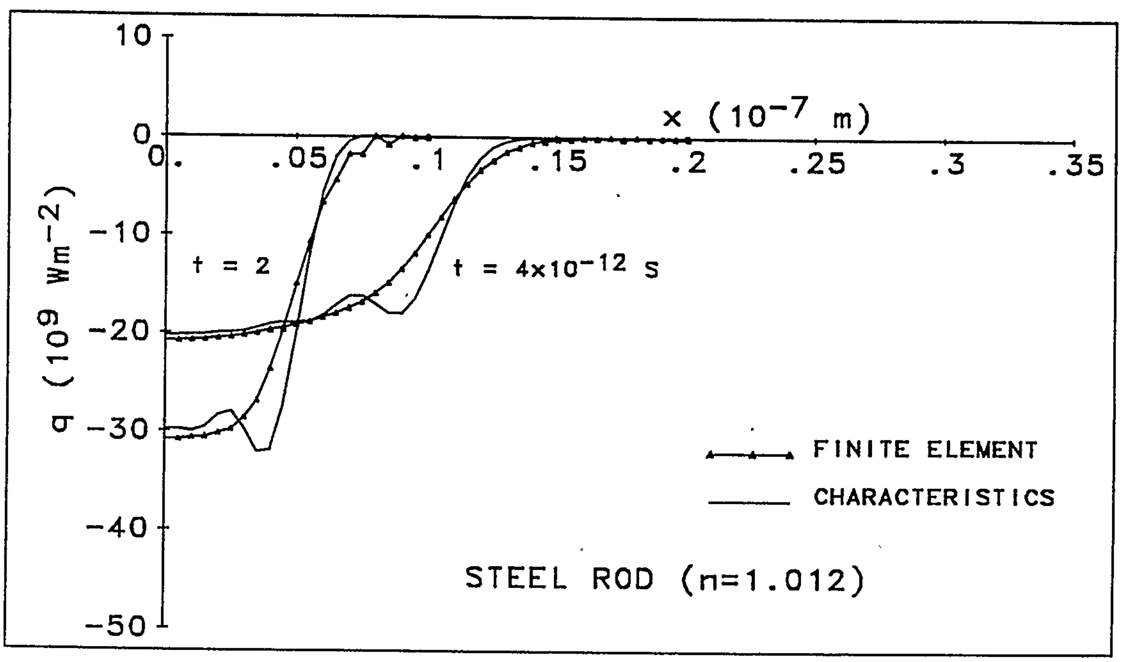

FIG. 6.20d HEAT FLUX RESPONSE OF A STEEL ROD (n = 1.012) TO $v(0,t) = 0$ AND $\theta(0,t) = -5\ ^{o}K$

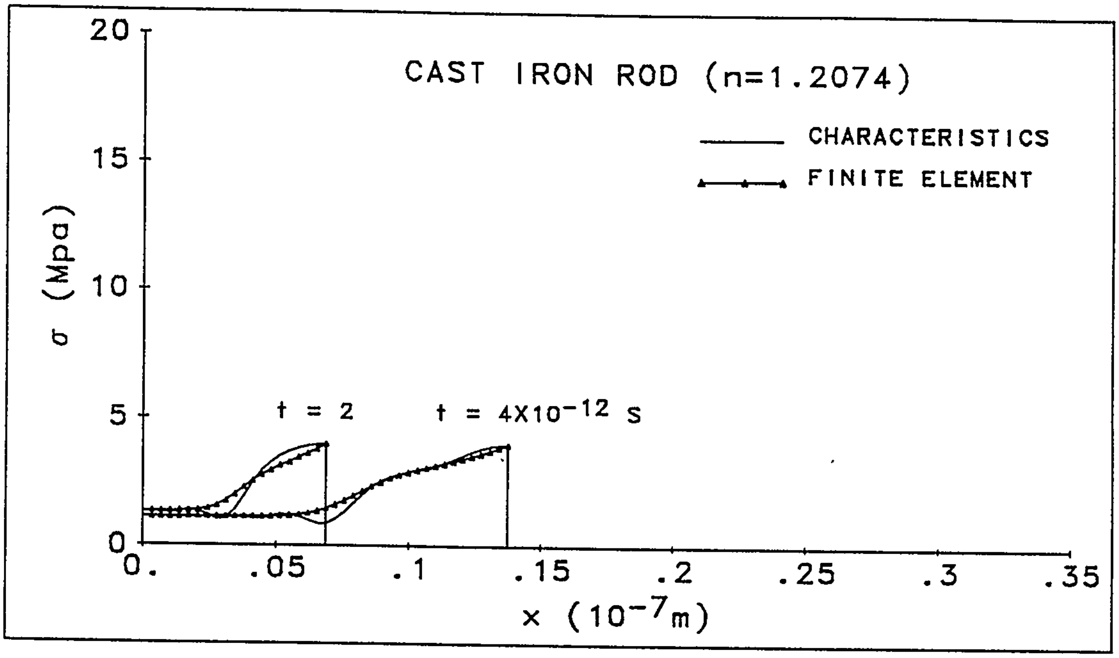

FIG. 6.21a STRESS RESPONSE OF A CAST IRON ROD (n = 1.2074) TO $v(0,t) = 0$ AND $\theta(0,t) = -5\ ^{o}K$

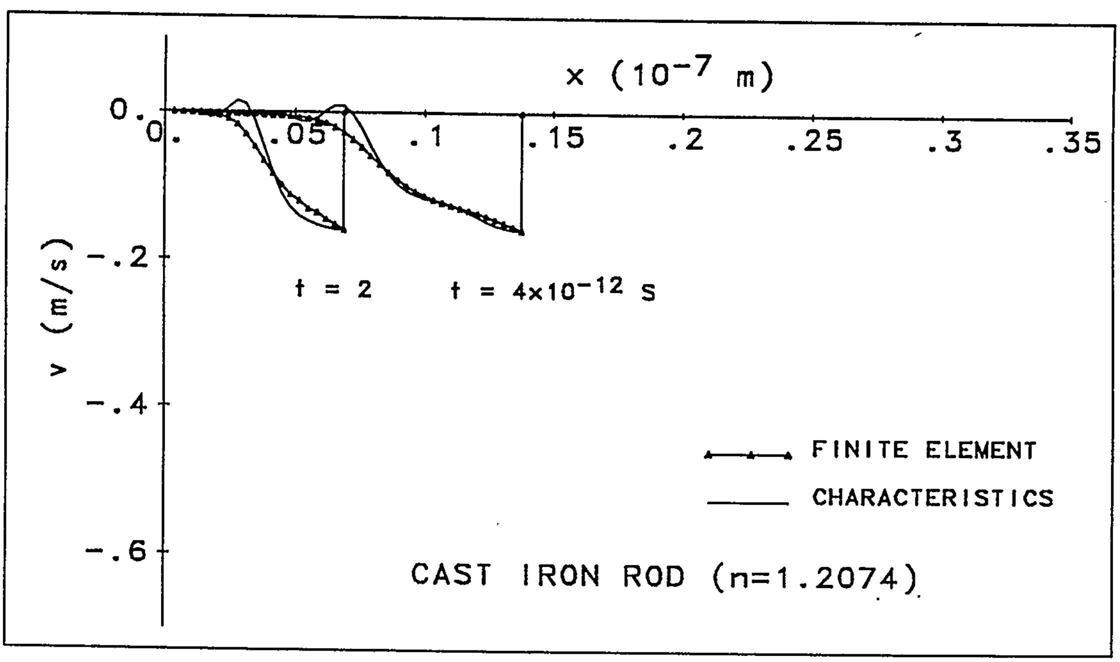

FIG. 6.21b VELOCITY RESPONSE OF A CAST IRON ROD (n = 1.2074) TO $v(0,t) = 0$ AND $\theta(0,t) = -5\ ^{o}K$

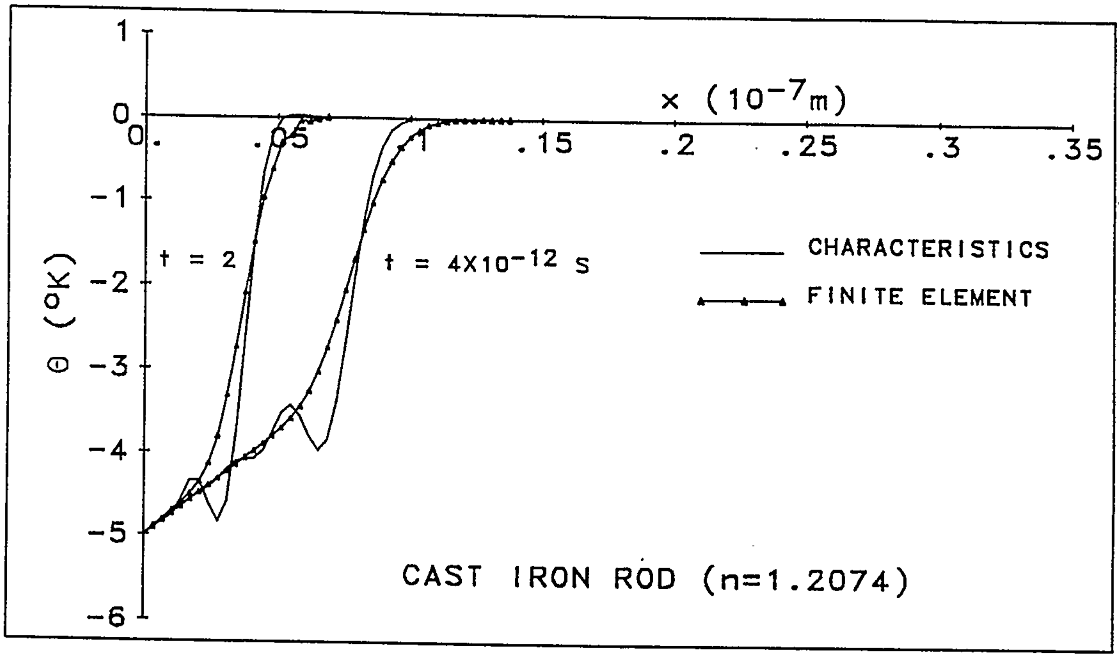

FIG. 6.21c TEMPERATURE RESPONSE OF A CAST IRON ROD (n = 1.2074) TO $v(0,t) = 0$ AND $\theta(0,t) = -5\ ^{o}K$

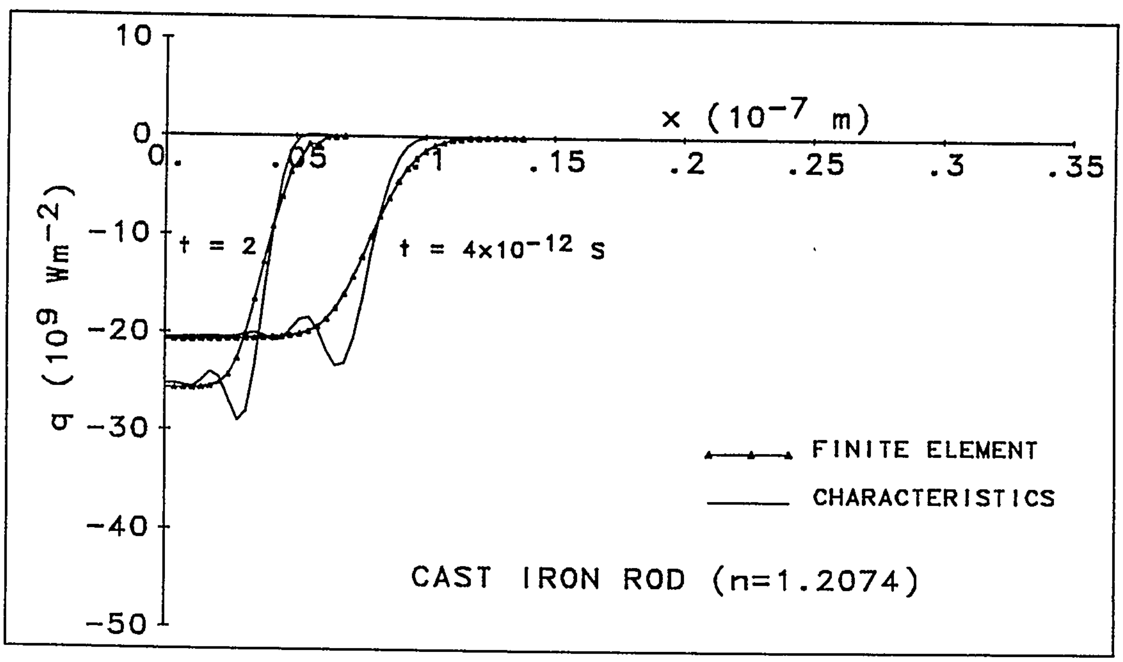

FIG. 6.21d HEAT FLUX RESPONSE OF A CAST IRON ROD (n = 1.2074) TO $v(0,t) = 0$ AND $\theta(0,t) = -5\ ^{o}K$

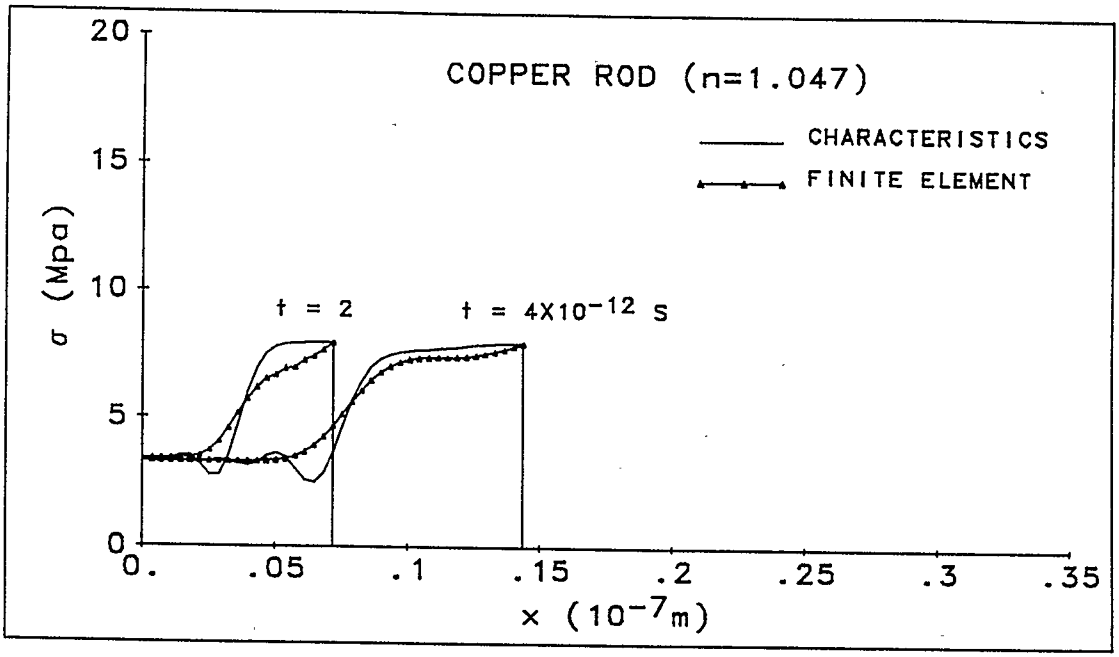

FIG. 6.22a STRESS RESPONSE OF A COPPER ROD (n = 1.047) TO

$v(0,t) = 0$ AND $\theta(0,t) = -5\ ^{o}K$

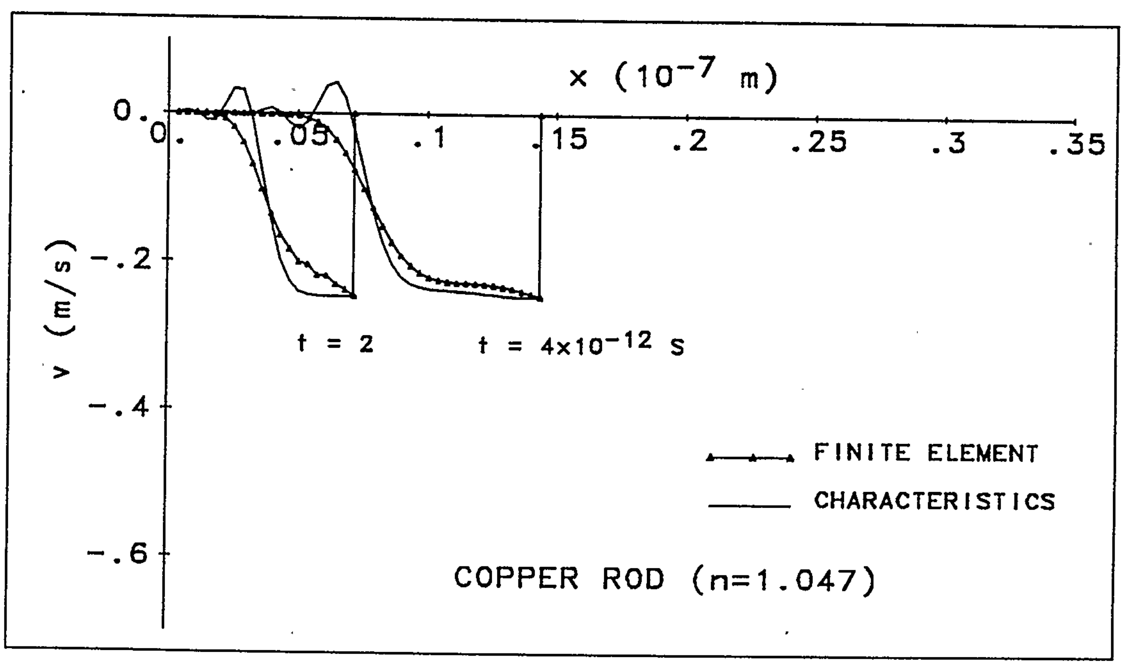

FIG. 6.22b VELOCITY RESPONSE OF A COPPER ROD (n = 1.047) TO

$v(0,t) = 0$ AND $\theta(0,t) = -5\ ^{o}K$

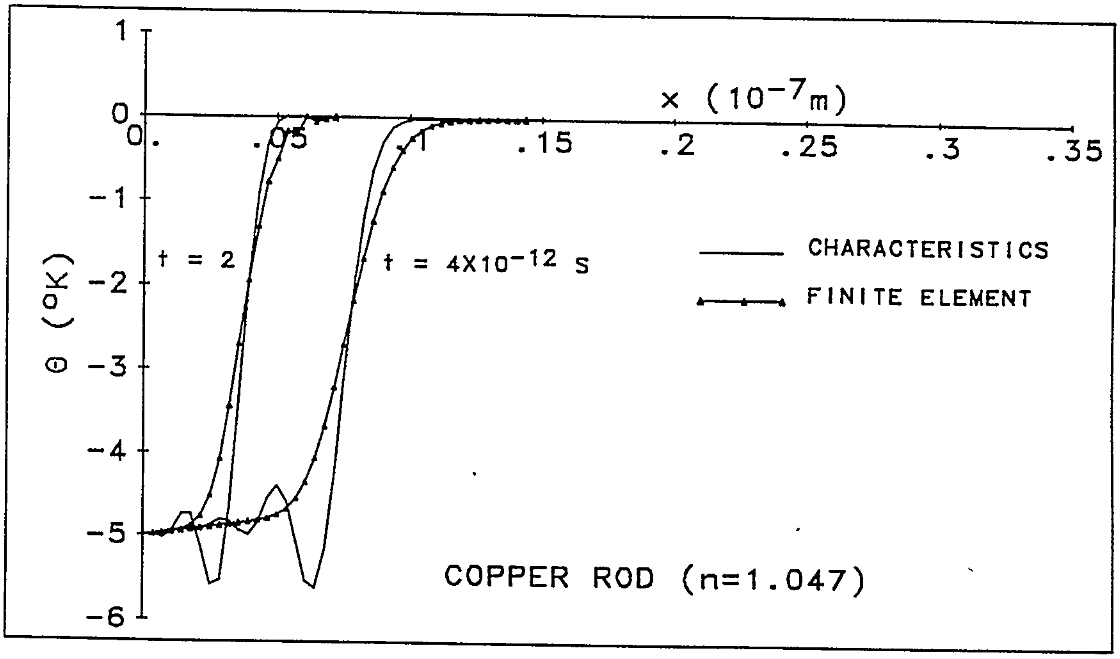

FIG. 6.21c TEMPERATURE RESPONSE OF A COPPER ROD (n = 1.047) TO $v(0,t) = 0$ AND $\theta(0,t) = -5\ ^{o}K$

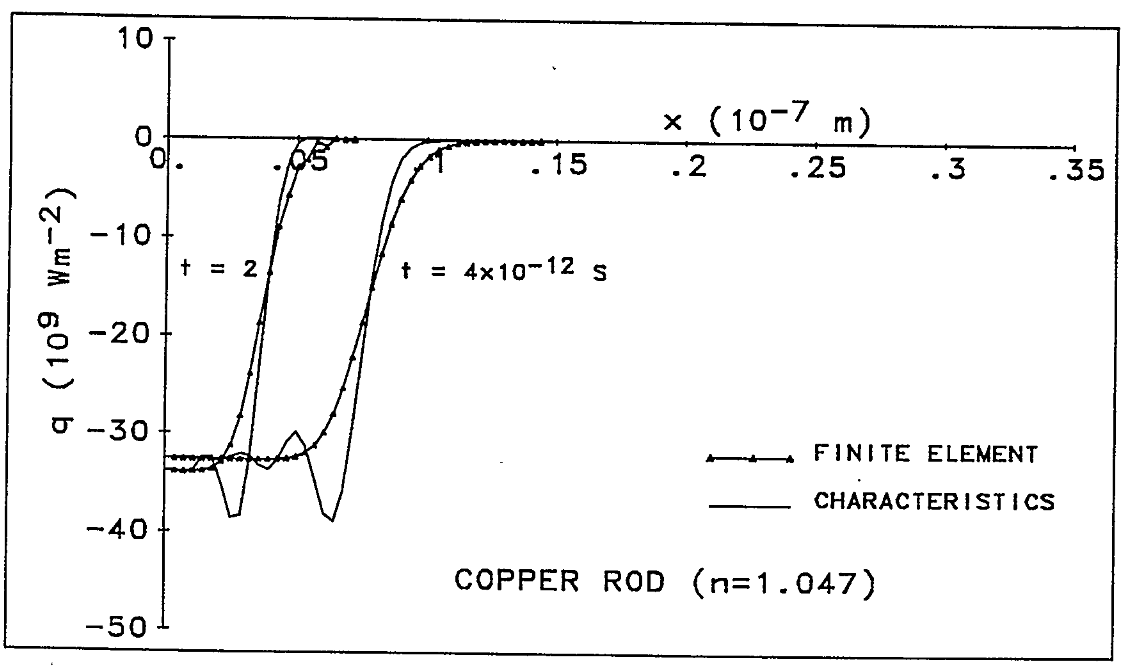

FIG. 6.22d HEAT FLUX RESPONSE OF A COPPER ROD (n = 1.047) TO $v(0,t) = 0$ AND $\theta(0,t) = -5\ ^{o}K$

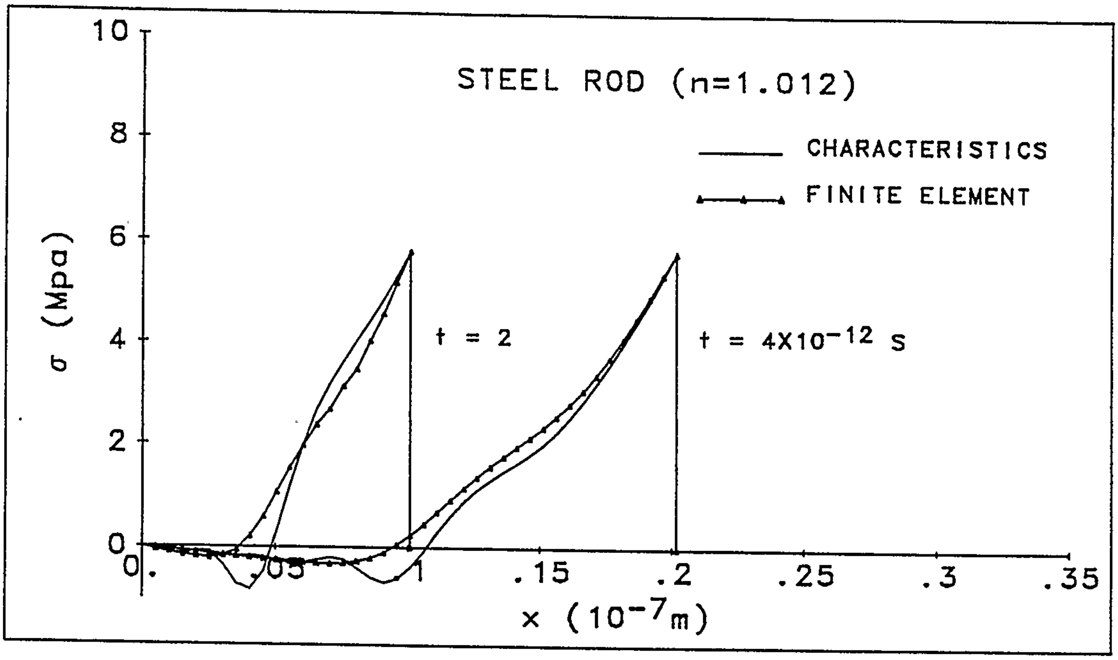

FIG. 6.23a STRESS RESPONSE OF A STEEL ROD (n = 1.012) TO

$\sigma(0,t) = 1$ Pa AND $\theta(0,t) = -5\ ^{o}K$

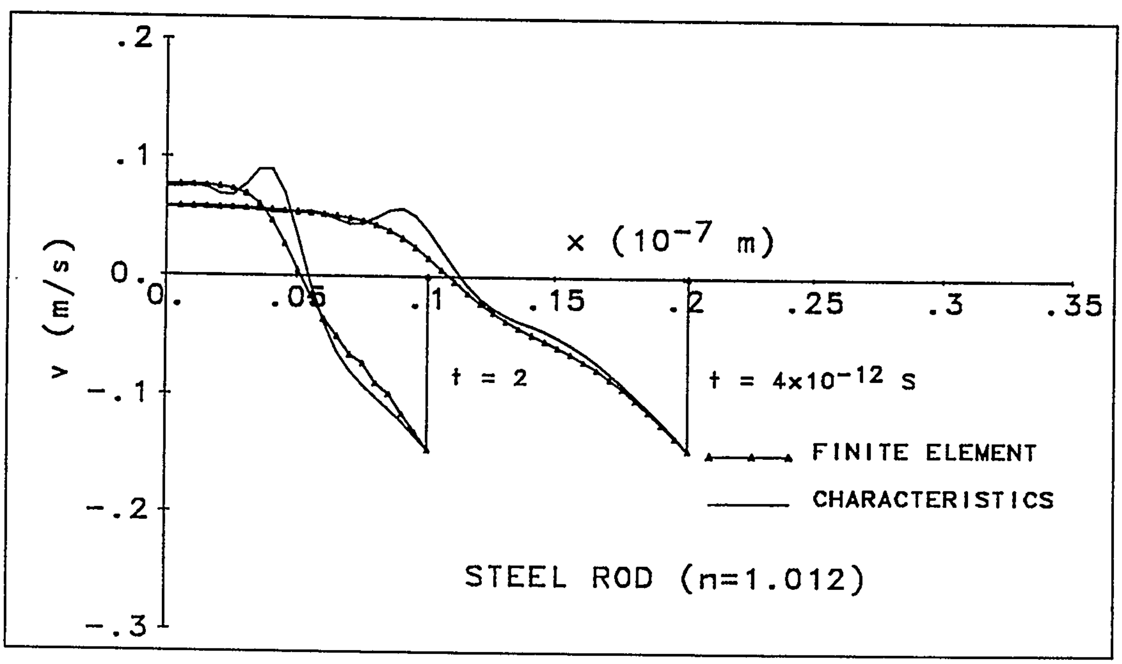

FIG. 6.23b VELOCITY RESPONSE OF A STEEL ROD (n = 1.012) TO

$\sigma(0,t) = 1$ Pa AND $\theta(0,t) = -5\ ^{o}K$

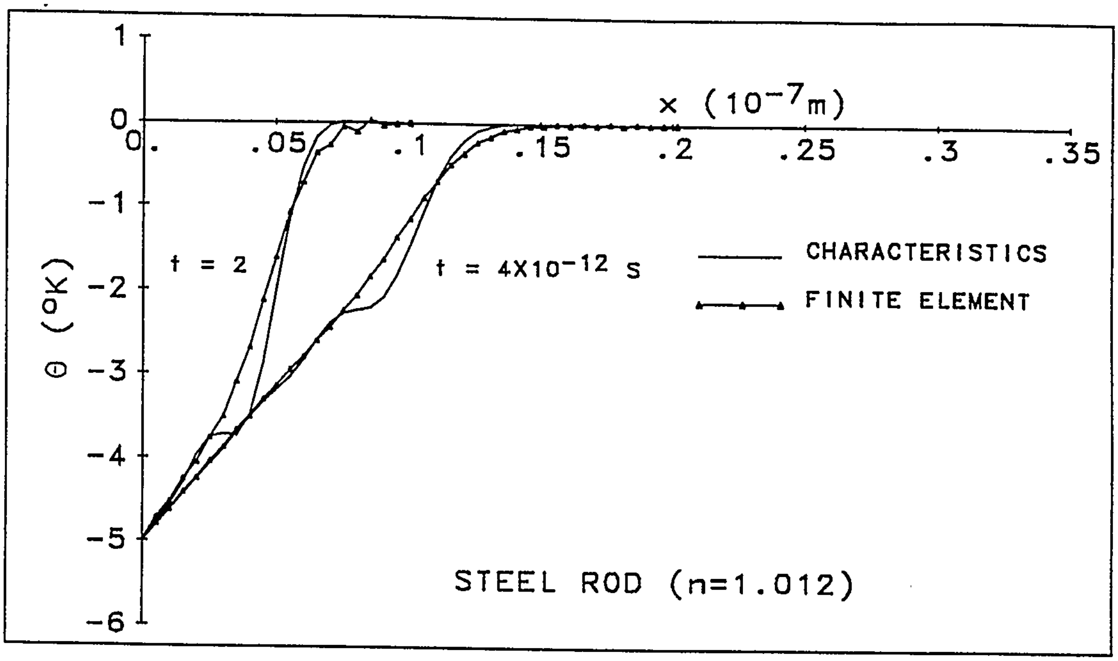

FIG. 6.23c TEMPERATURE RESPONSE OF A STEEL ROD (n = 1.012) TO $\sigma(0,t)$ = 1 Pa AND $\theta(0,t)$ = - 5 °K

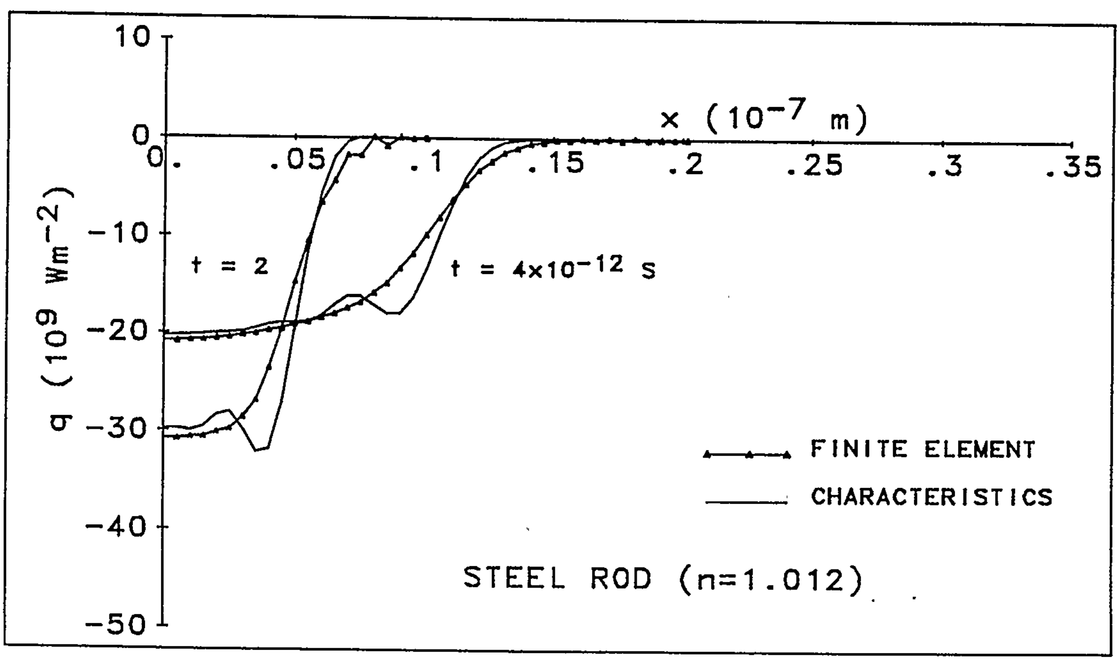

FIG. 6.23d HEAT FLUX RESPONSE OF A STEEL ROD (n = 1.012) TO $\sigma(0,t)$ = 1 Pa AND $\theta(0,t)$ = - 5 °K

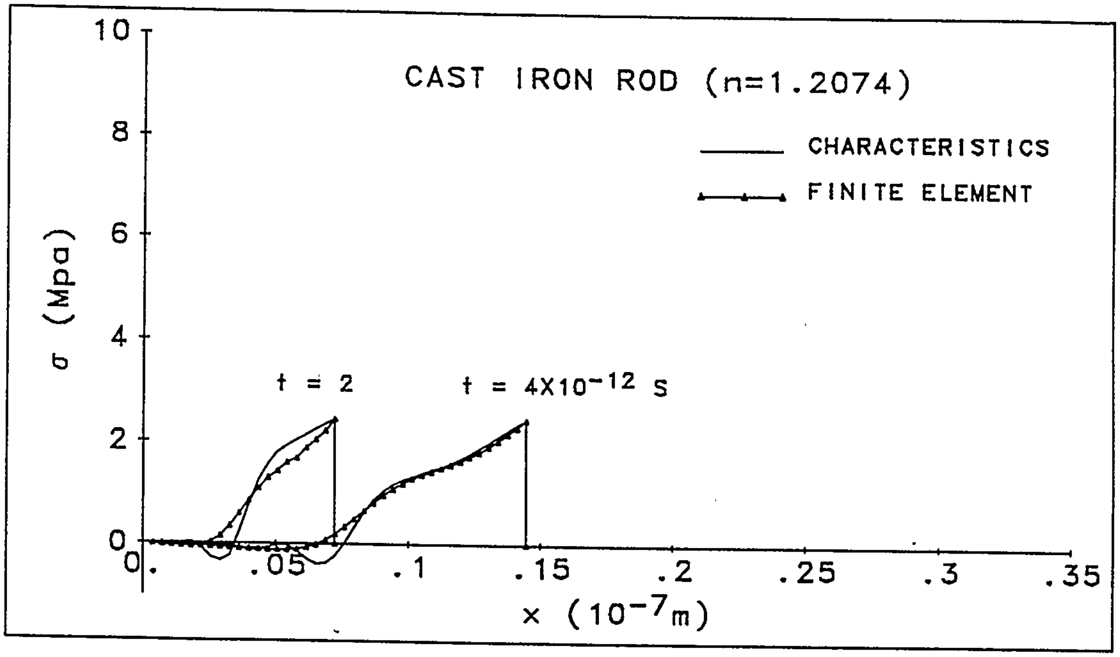

FIG. 6.24a STRESS RESPONSE OF A CAST IRON ROD (n = 1.2074) TO $\sigma(0,t)$ = 1 Pa AND $\theta(0,t)$ = - 5 ^{o}K

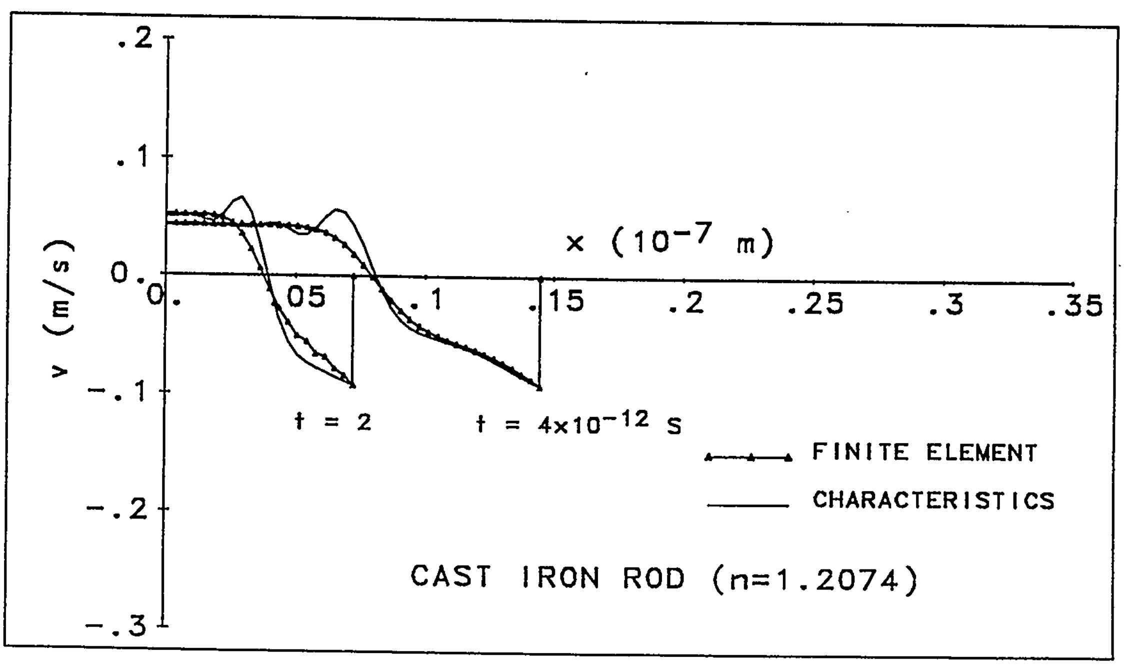

FIG. 6.24b VELOCITY RESPONSE OF A CAST IRON ROD (n = 1.2074) TO $\sigma(0,t)$ = 1 Pa AND $\theta(0,t)$ = - 5 ^{o}K

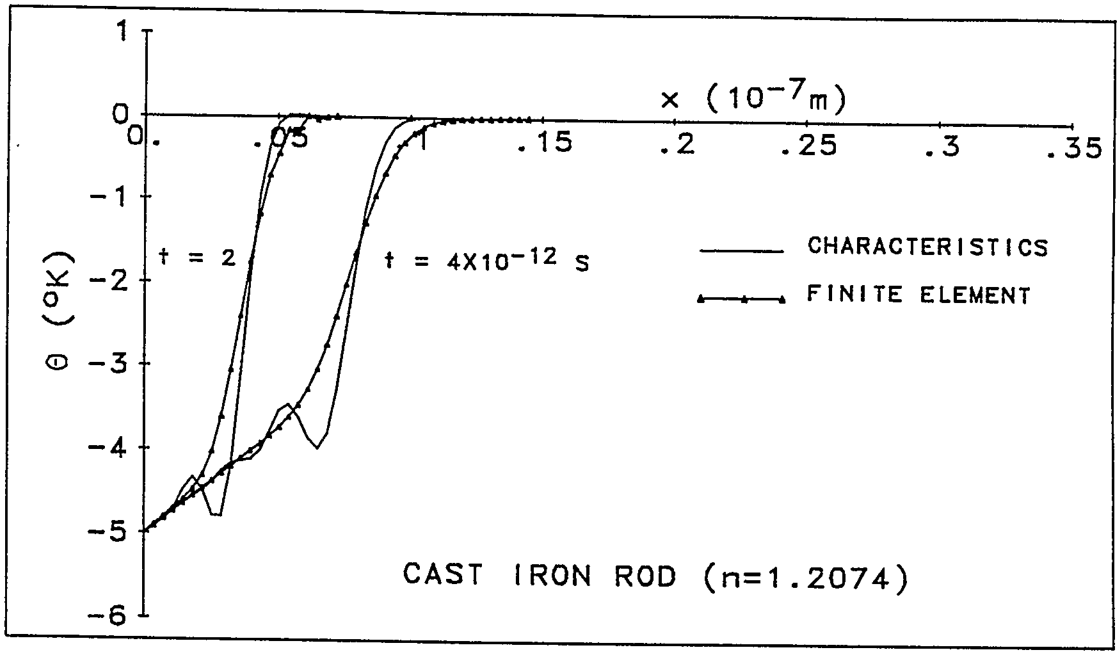

FIG. 6.24c TEMPERATURE RESPONSE OF A CAST IRON ROD (n = 1.2074) TO $\sigma(0,t) = 1$ Pa AND $\theta(0,t) = -5$ °K

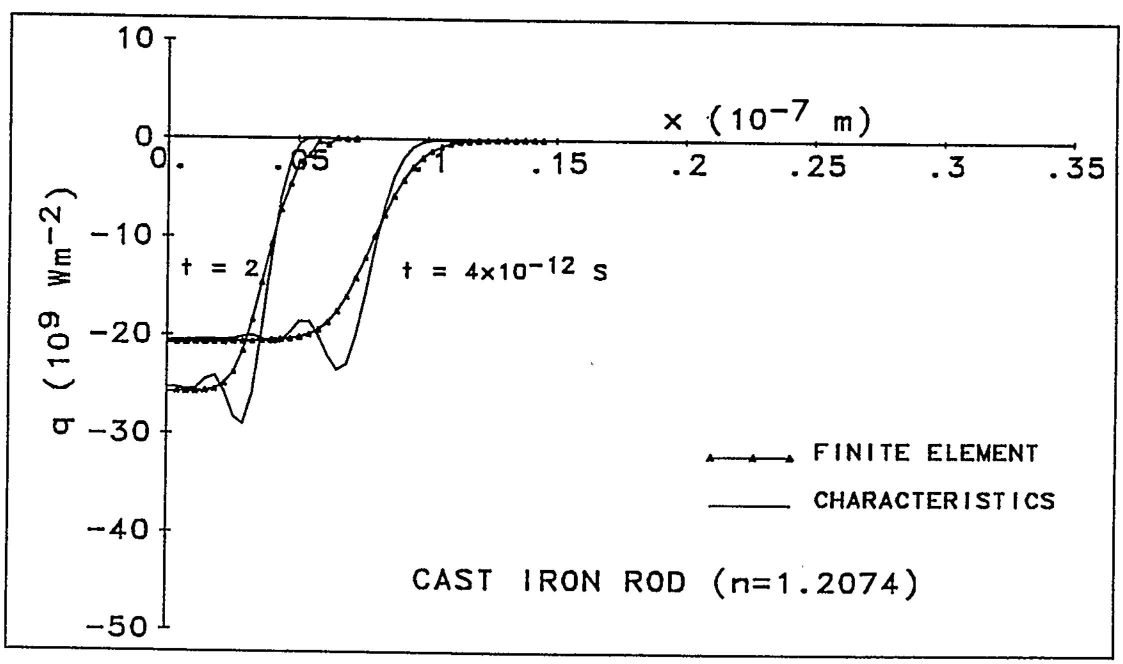

FIG. 6.24d HEAT FLUX RESPONSE OF A CAST IRON ROD (n = 1.2074) TO $\sigma(0,t) = 1$ Pa AND $\theta(0,t) = -5$ °K

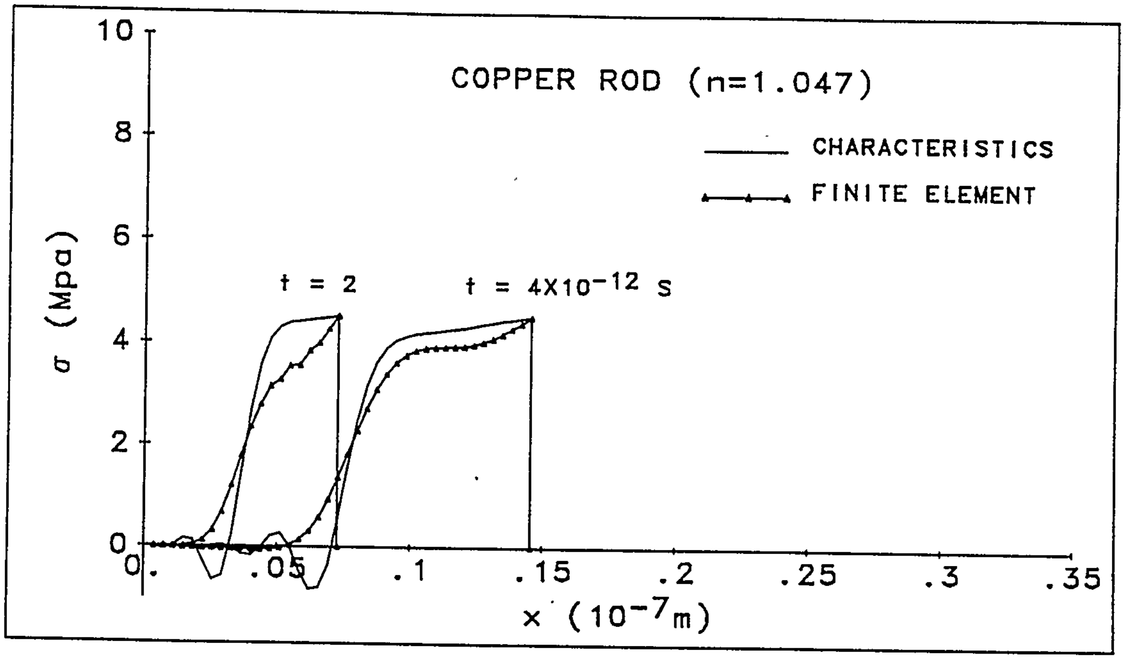

FIG. 6.25a STRESS RESPONSE OF A COPPER ROD (n = 1.047) TO $\sigma(0,t) = 1$ Pa AND $\theta(0,t) = -5\ ^{o}K$

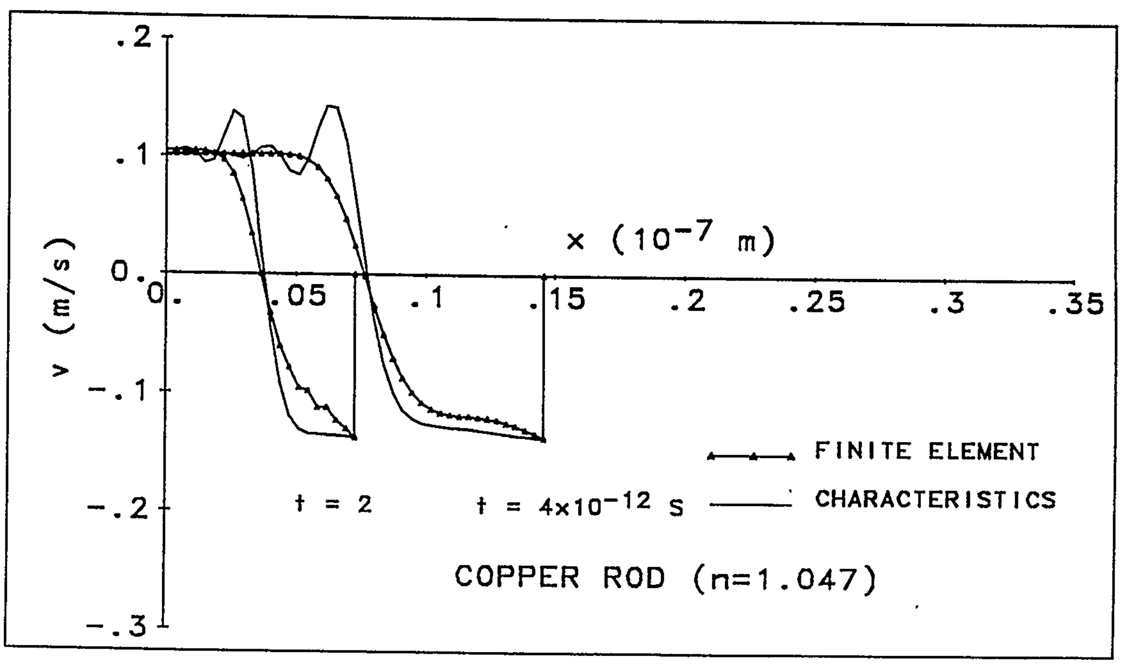

FIG. 6.25b VELOCITY RESPONSE OF A COPPER ROD (n = 1.047) TO $\sigma(0,t) = 1$ Pa AND $\theta(0,t) = -5\ ^{o}K$

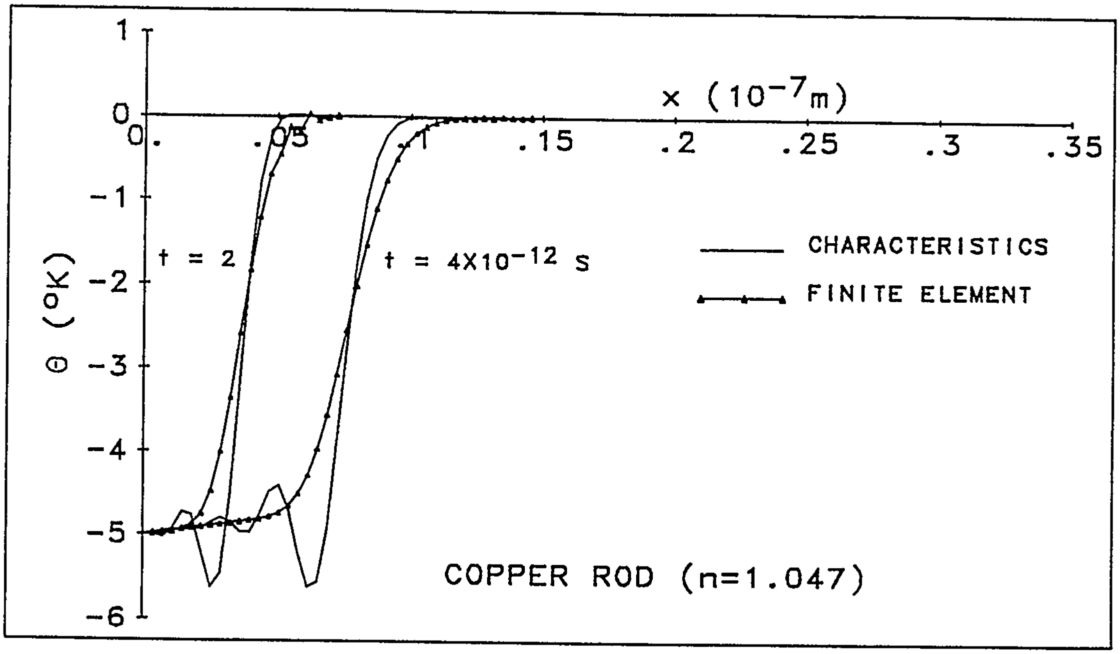

FIG. 6.25c TEMPERATURE RESPONSE OF A COPPER ROD (n = 1.047) TO $\sigma(0,t)$ = 1 Pa AND $\theta(0,t)$ = − 5 °K

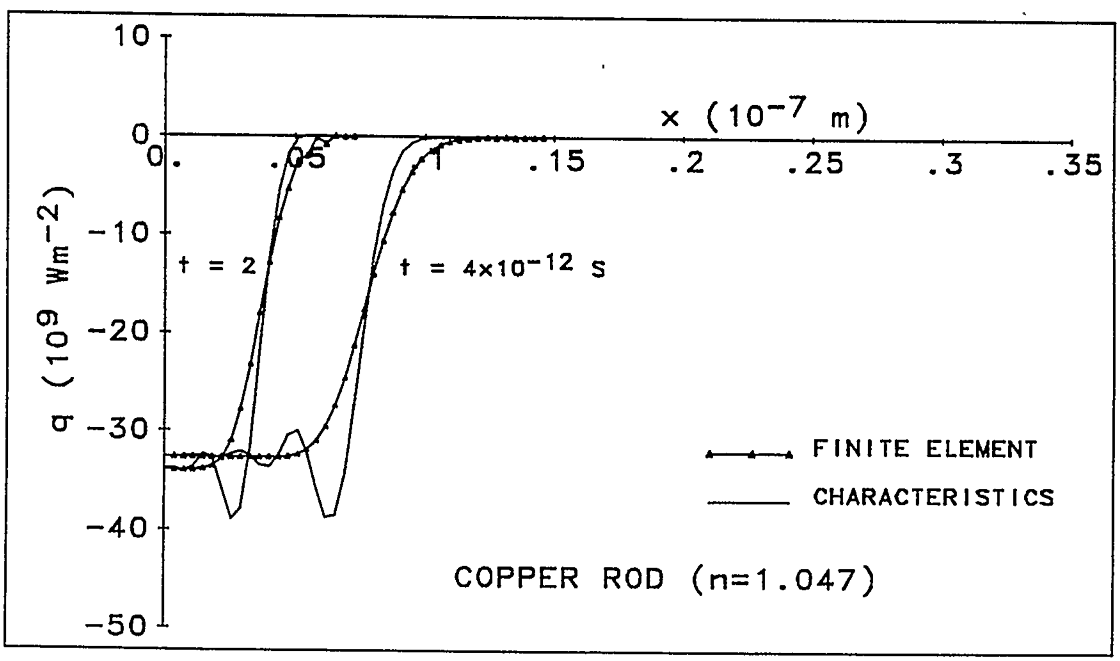

FIG. 6.25d HEAT FLUX RESPONSE OF A COPPER ROD (n = 1.047) TO $\sigma(0,t)$ = 1 Pa AND $\theta(0,t)$ = − 5 °K

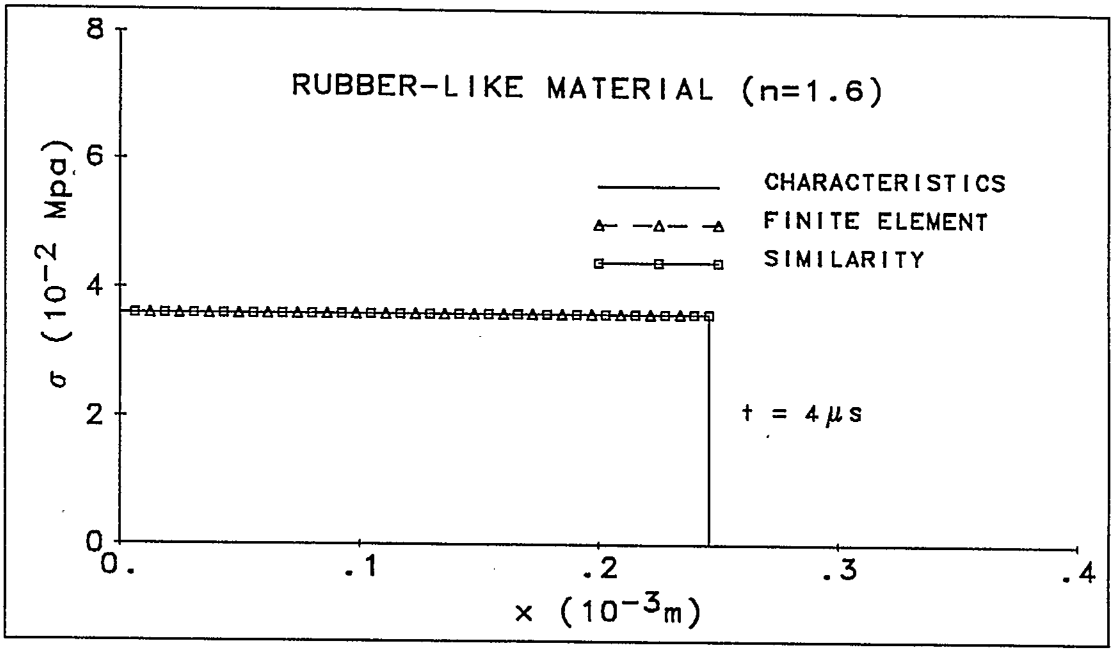

FIG. 6.26a STRESS RESPONSE OF A STRING OF A RUBBER-LIKE MATERIAL (n = 1.6) TO v(0,t) = - 0.5 m/s

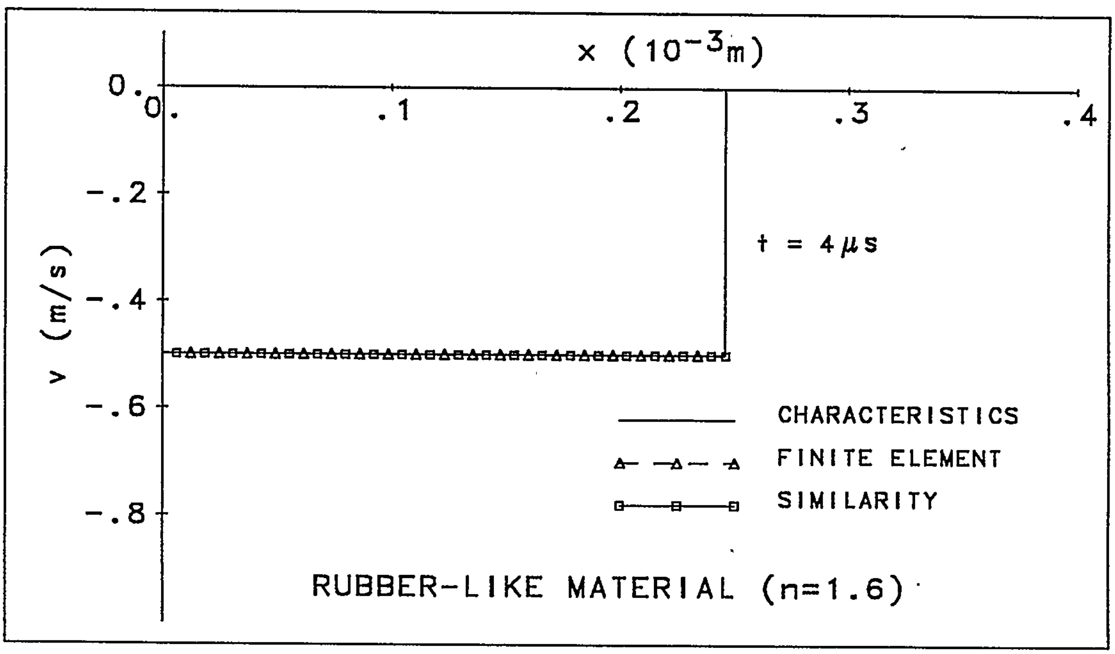

FIG. 6.26b VELOCITY RESPONSE OF A STRING OF A RUBBER-LIKE MATERIAL (n = 1.6) TO v(0,t) = - 0.5 m/s

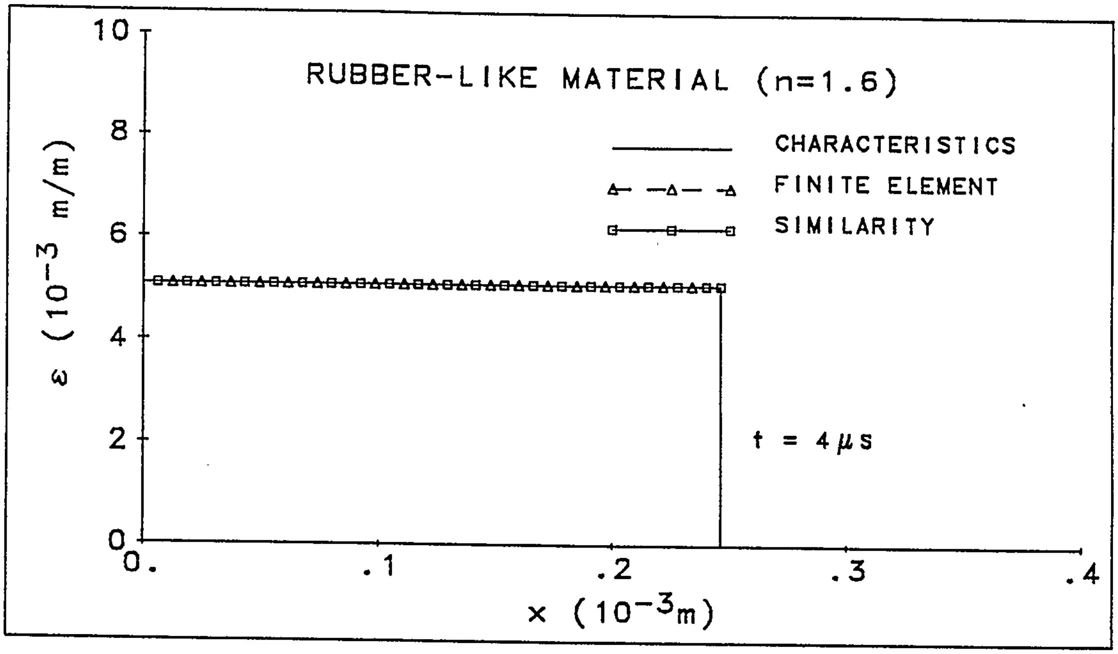

FIG. 6.26c STRAIN RESPONSE OF A STRING OF A RUBBER-LIKE MATERIAL (n = 1.6) TO $v(0,t) = -0.5$ m/s

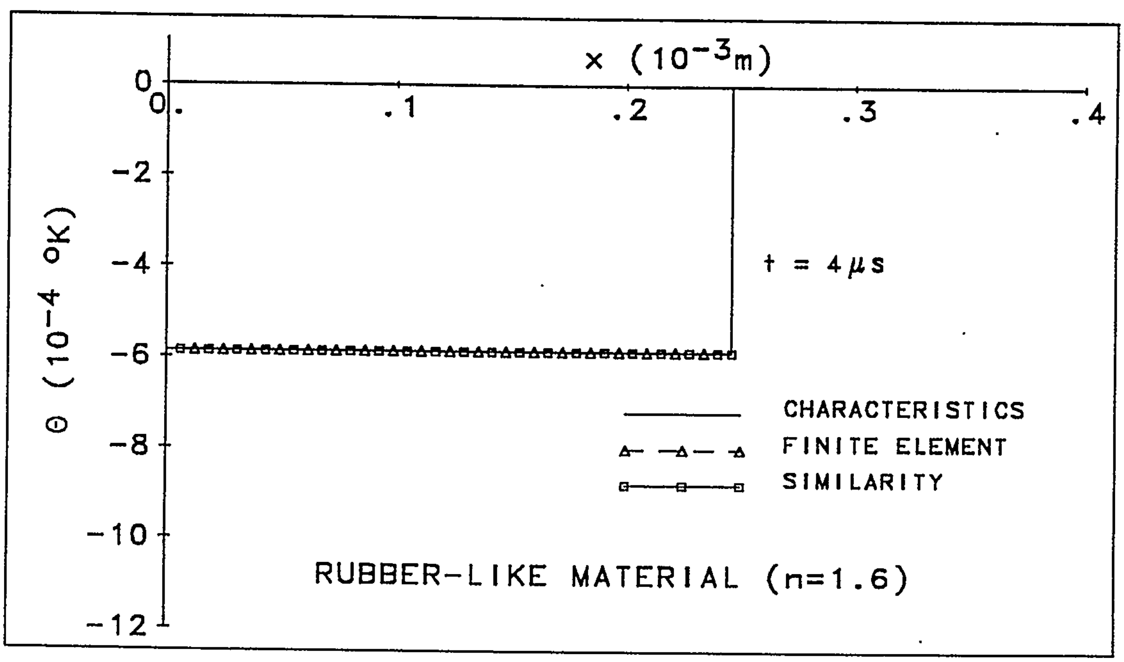

FIG. 6.26d TEMPERATURE RESPONSE OF A STRING OF A RUBBER-LIKE MATERIAL (n = 1.6) TO $v(0,t) = -0.5$ m/s

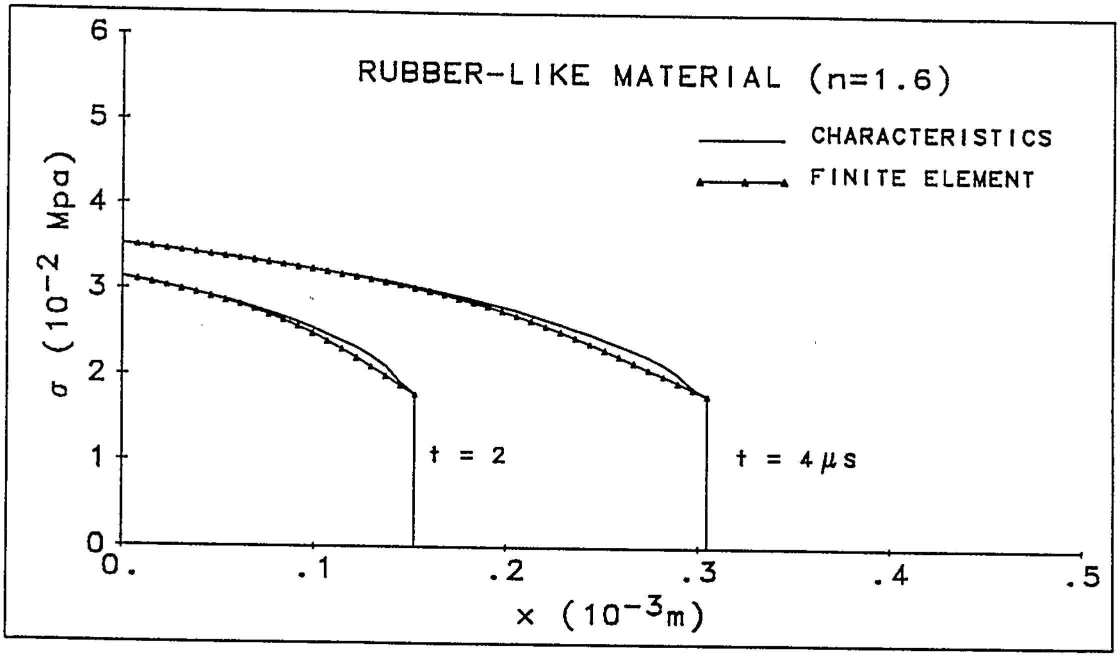

FIG. 6.27a STRESS RESPONSE OF A STRING OF A RUBBER-LIKE MATERIAL (n = 1.6) TO $v(0,t) = -5 \times t^{0.2}$ m/s

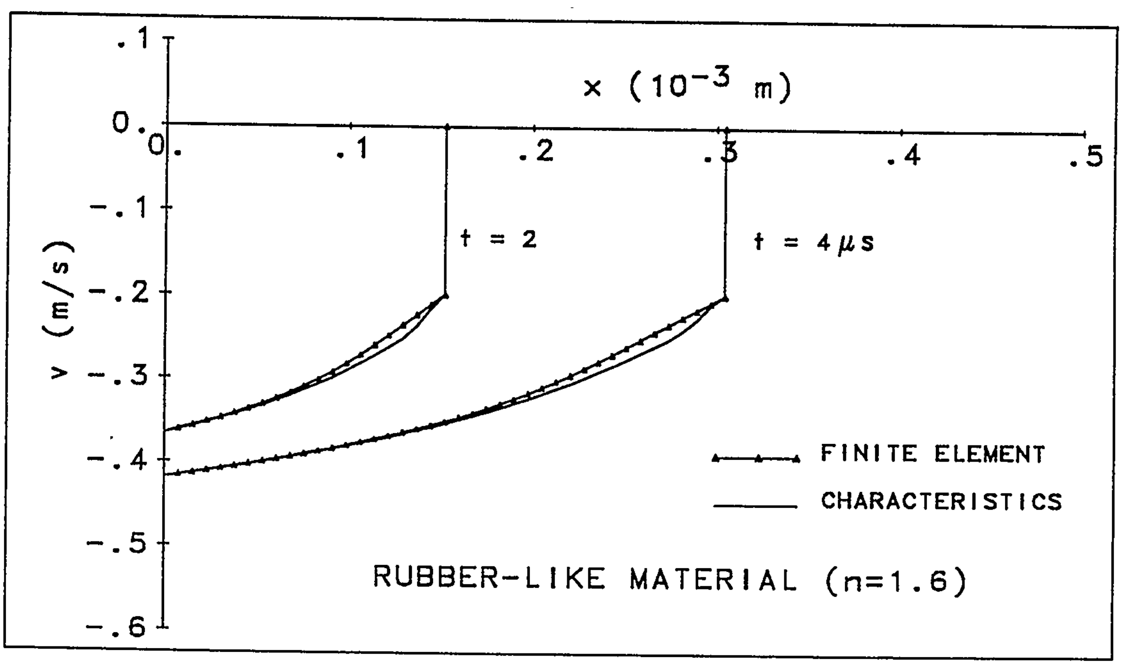

FIG. 6.27b VELOCITY RESPONSE OF A STRING OF A RUBBER-LIKE MATERIAL (n = 1.6) TO $v(0,t) = -5 \times t^{0.2}$ m/s

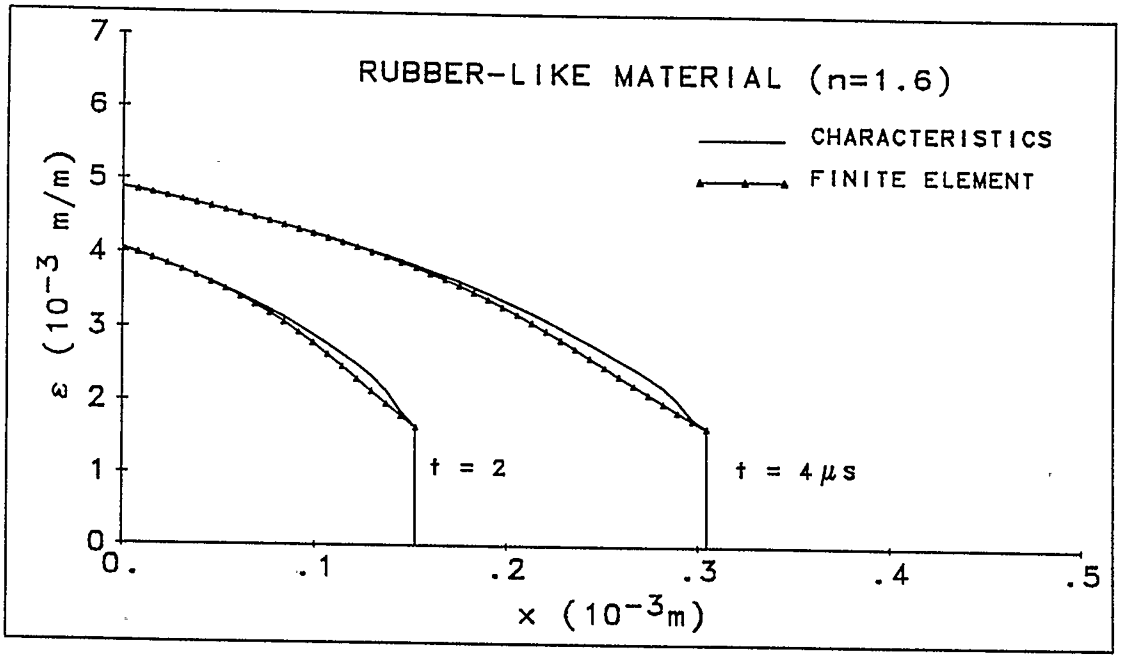

FIG. 6.27c STRAIN RESPONSE OF A STRING OF A RUBBER-LIKE MATERIAL (n = 1.6) TO $v(0,t) = -5 \times t^{0.2}$ m/s

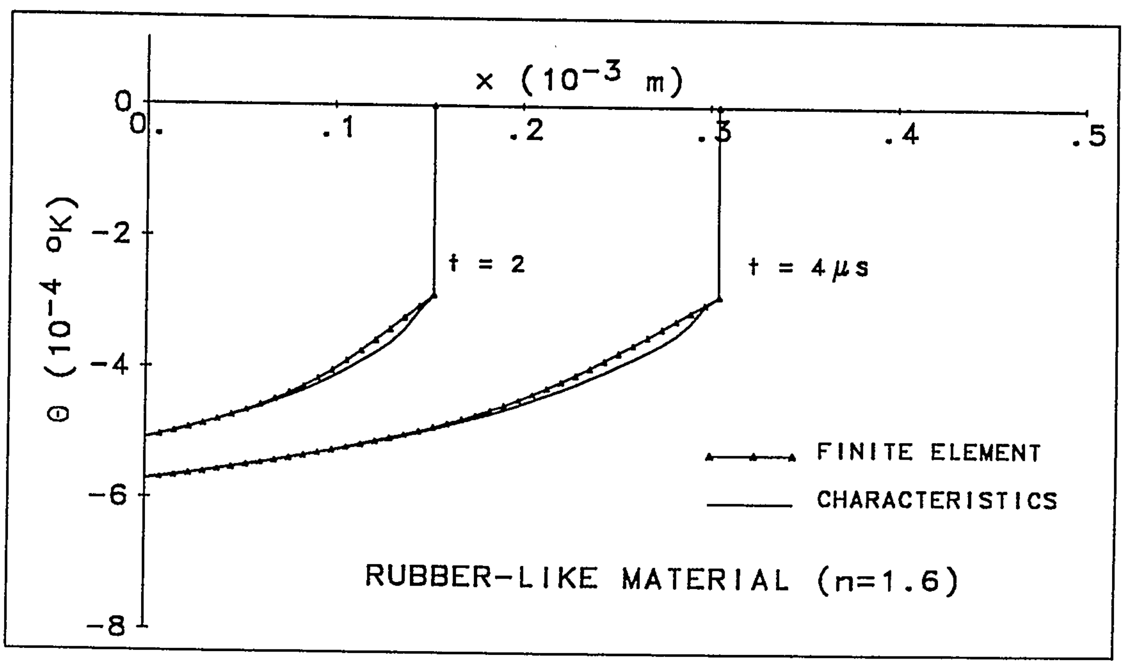

FIG. 6.27d TEMPERATURE RESPONSE OF A STRING OF A RUBBER-LIKE MATERIAL (n = 1.6) TO $v(0,t) = -5 \times t^{0.2}$ m/s

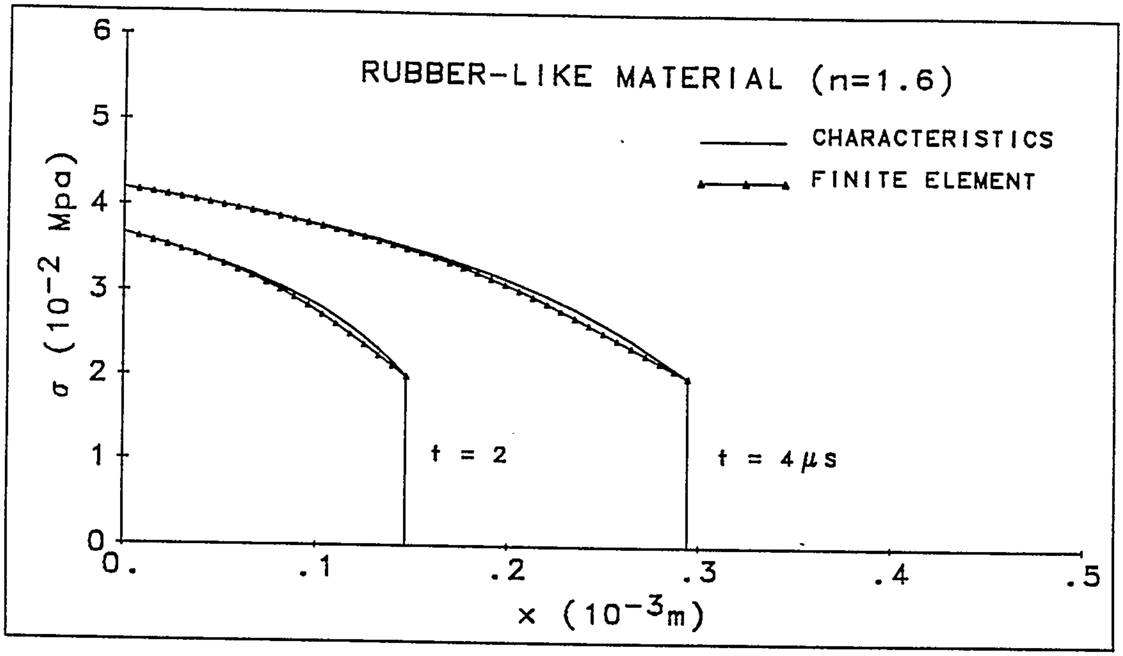

FIG. 6.28a STRESS RESPONSE OF A STRING OF A RUBBER-LIKE MATERIAL (n = 1.6) TO $\sigma(0,t) = 0.5 \times t^{0.2}$ MPa

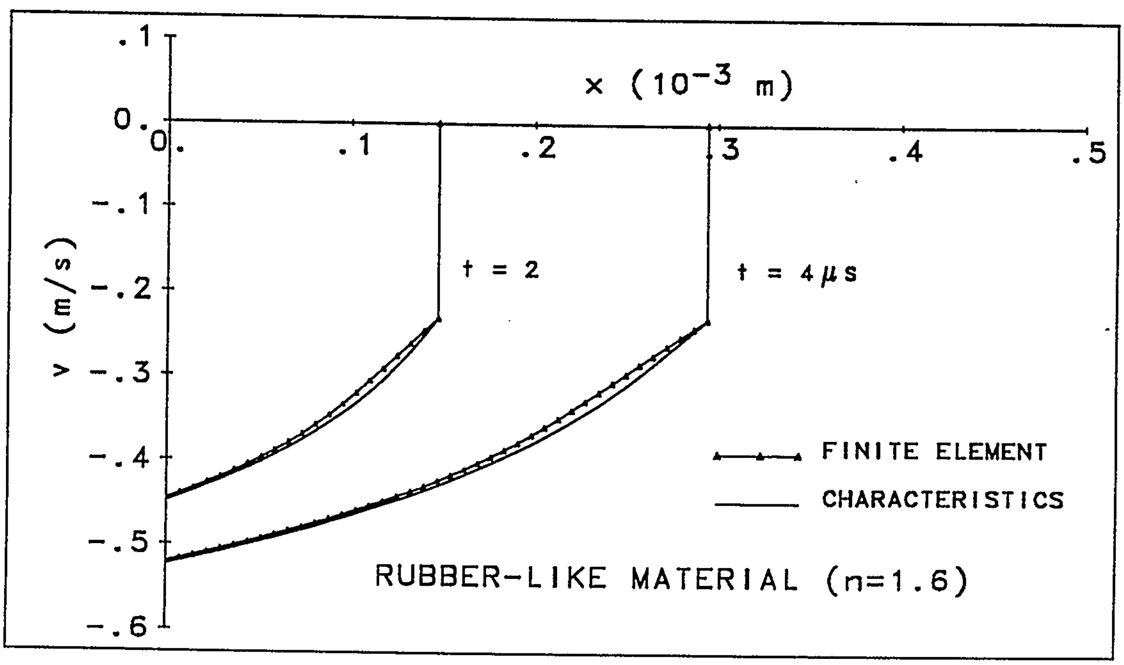

FIG. 6.28b VELOCITY RESPONSE OF A STRING OF A RUBBER-LIKE MATERIAL (n = 1.6) TO $\sigma(0,t) = 0.5 \times t^{0.2}$ MPa

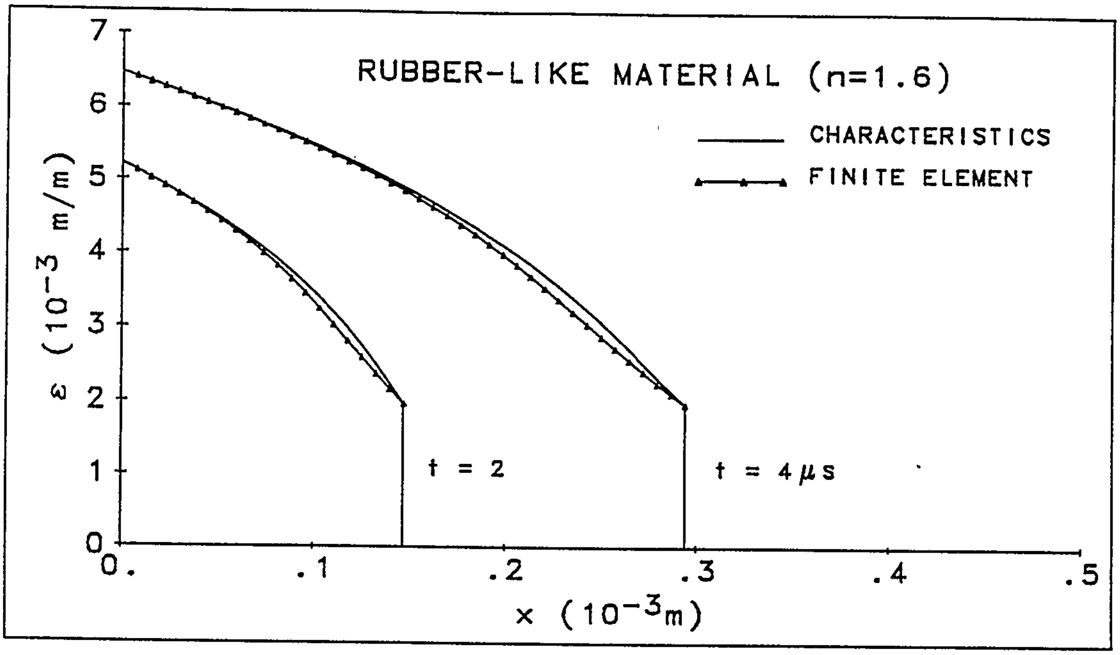

FIG. 6.28c STRAIN RESPONSE OF A STRING OF A RUBBER-LIKE MATERIAL (n = 1.6) TO $\sigma(0,t) = 0.5 \times t^{0.2}$ MPa

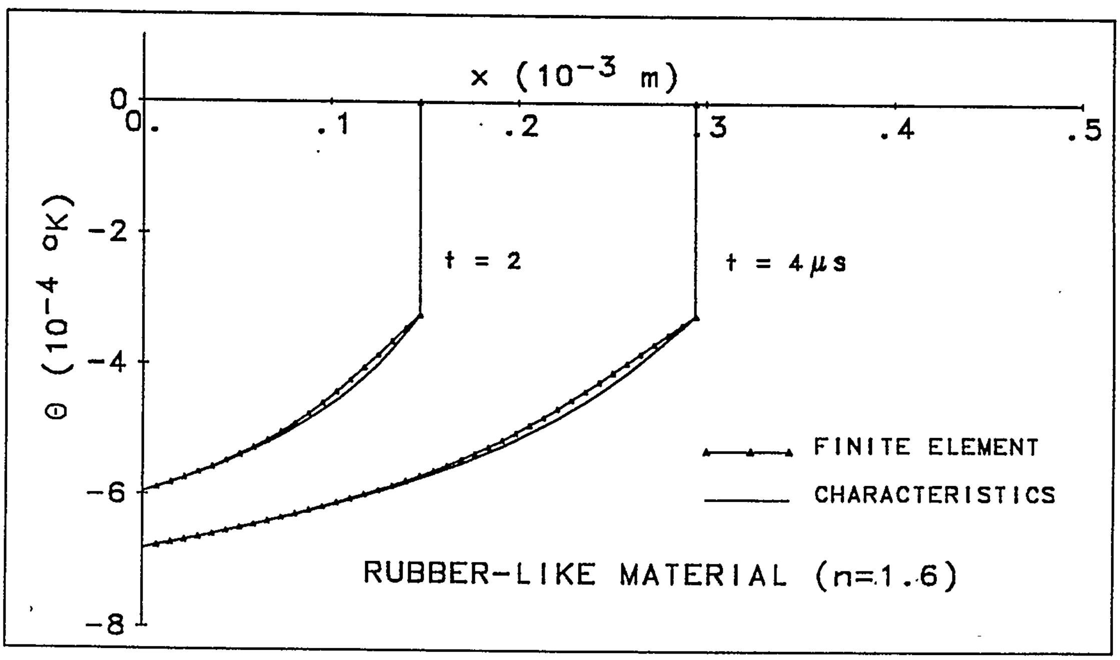

FIG. 6.28d TEMPERATURE RESPONSE OF A STRING OF A RUBBER-LIKE MATERIAL (n = 1.6) TO $\sigma(0,t) = 0.5 \times t^{0.2}$ MPa

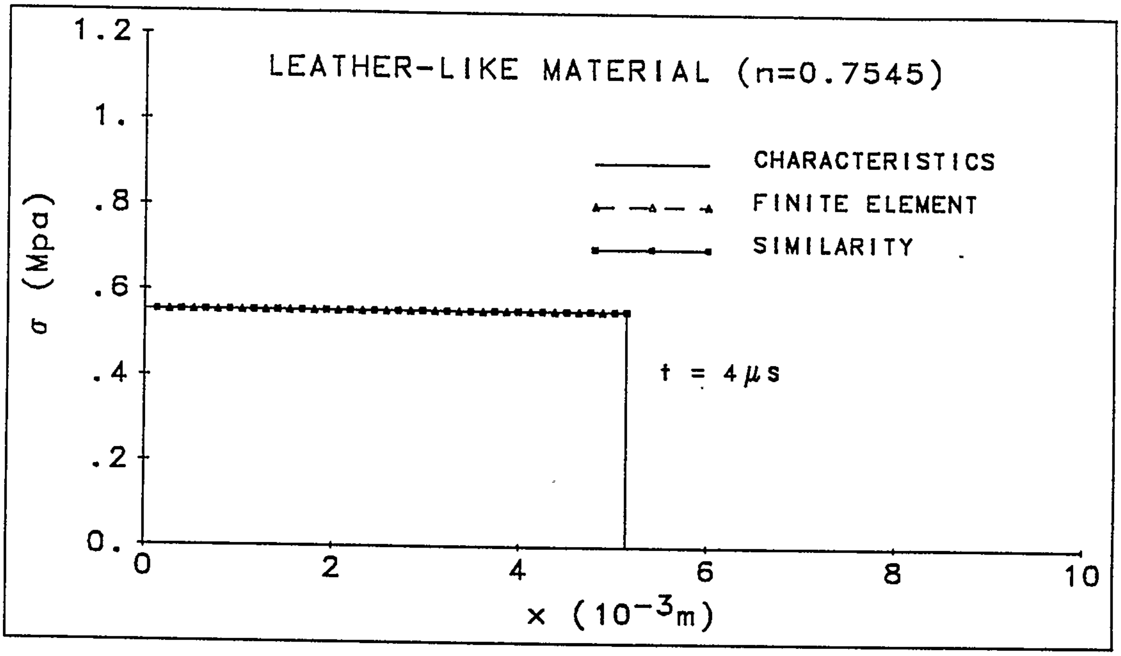

FIG. 6.29a STRESS RESPONSE OF A STRING OF A LEATHER-LIKE MATERIAL (n = 0.7545) TO $v(0,t) = -0.5$ m/s

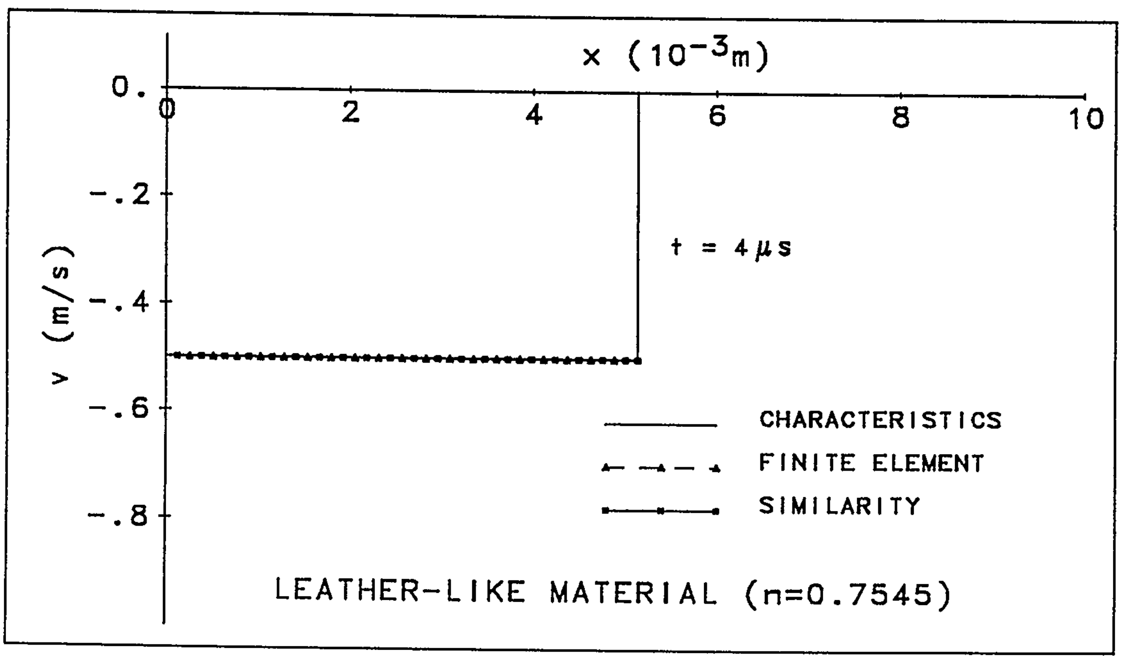

FIG. 6.29b VELOCITY RESPONSE OF A STRING OF A LEATHER-LIKE MATERIAL (n = 0.7545) TO $v(0,t) = -0.5$ m/s

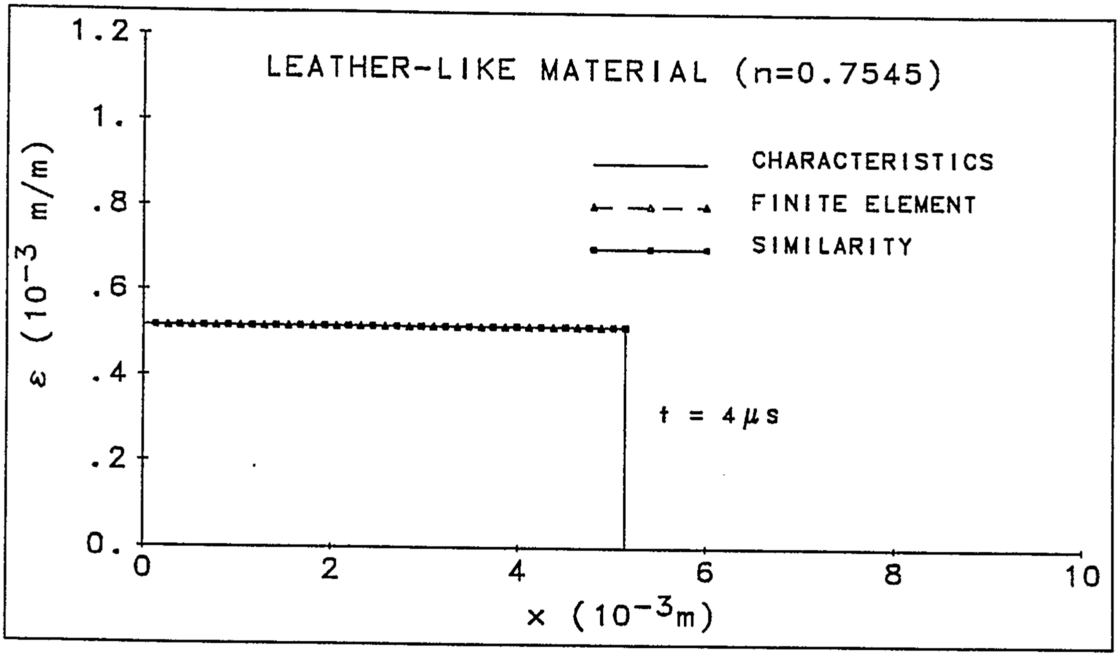

FIG. 6.29c STRAIN RESPONSE OF A STRING OF A LEATHER-LIKE MATERIAL (n = 0.7545) TO $v(0,t) = - 0.5$ m/s

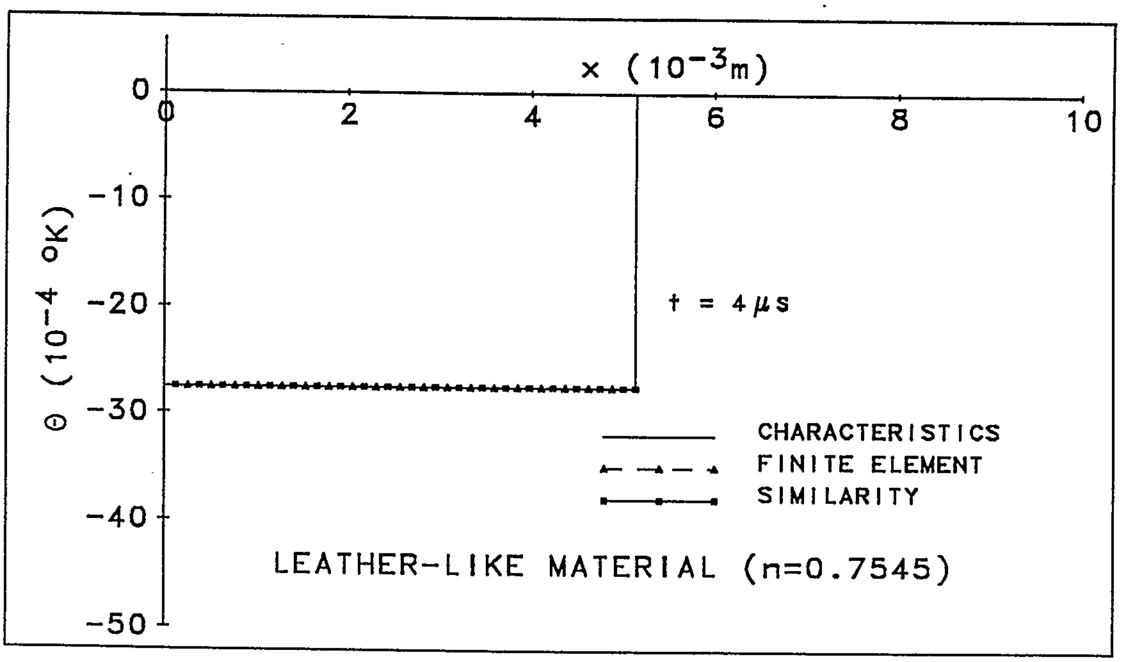

FIG. 6.29d TEMPERATURE RESPONSE OF A STRING OF A LEATHER-LIKE MATERIAL (n = 0.7545) TO $v(0,t) = - 0.5$ m/s

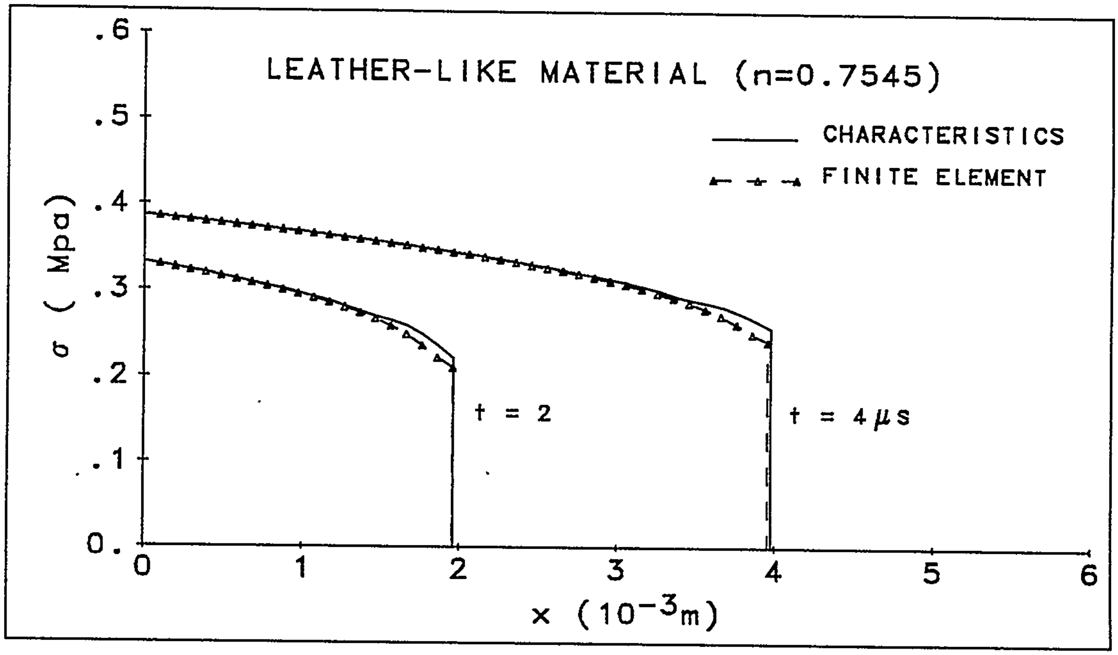

FIG. 6.30a STRESS RESPONSE OF A STRING OF A LEATHER-LIKE MATERIAL (n = 0.7545) TO $v(0,t) = -5 \times t^{0.2}$ m/s

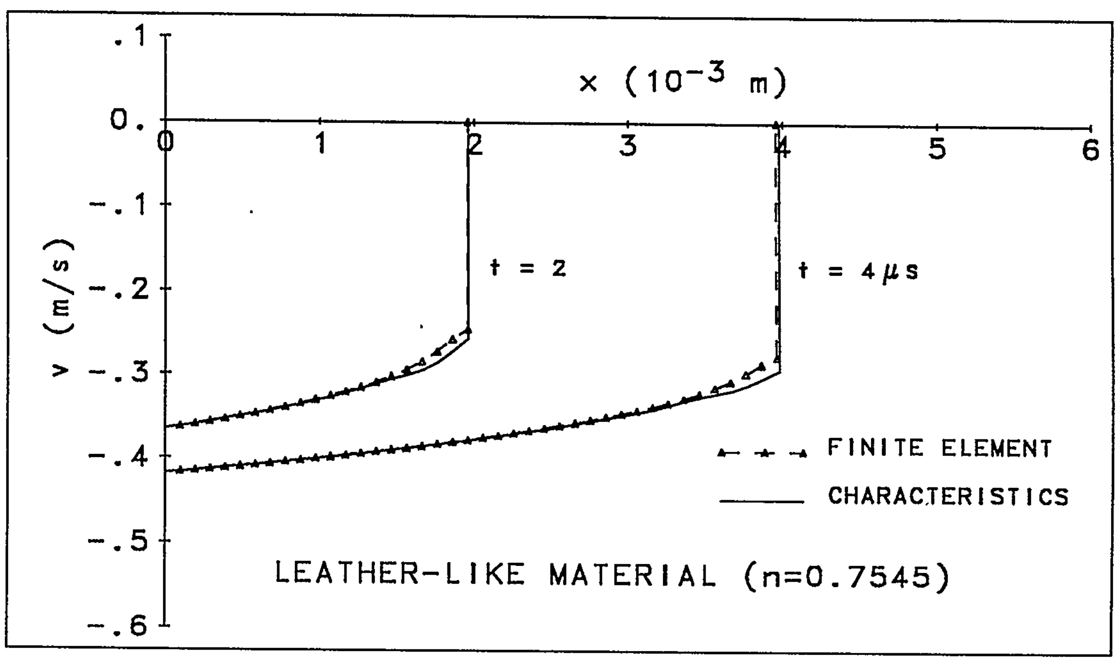

FIG. 6.30b VELOCITY RESPONSE OF A STRING OF A LEATHER-LIKE MATERIAL (n = 0.7545) TO $\sigma(0,t) = -5 \times t^{0.2}$ m/s

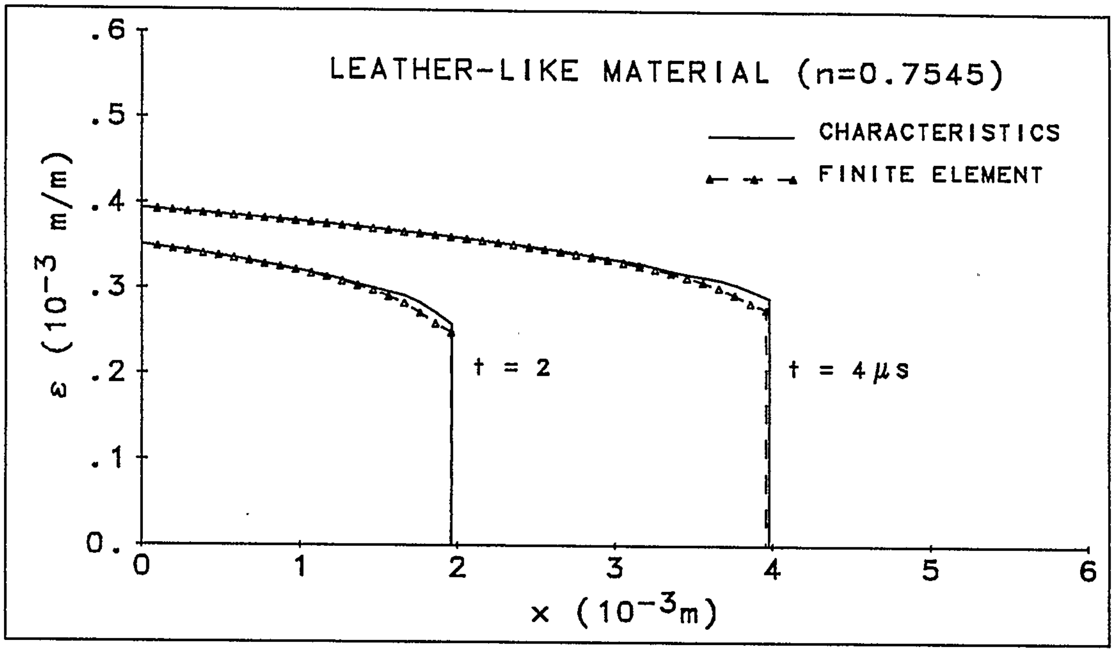

FIG. 6.30c STRAIN RESPONSE OF A STRING OF A LEATHER-LIKE MATERIAL (n = 0.7545) TO $v(0,t) = -5 \times t^{0.2}$ m/s

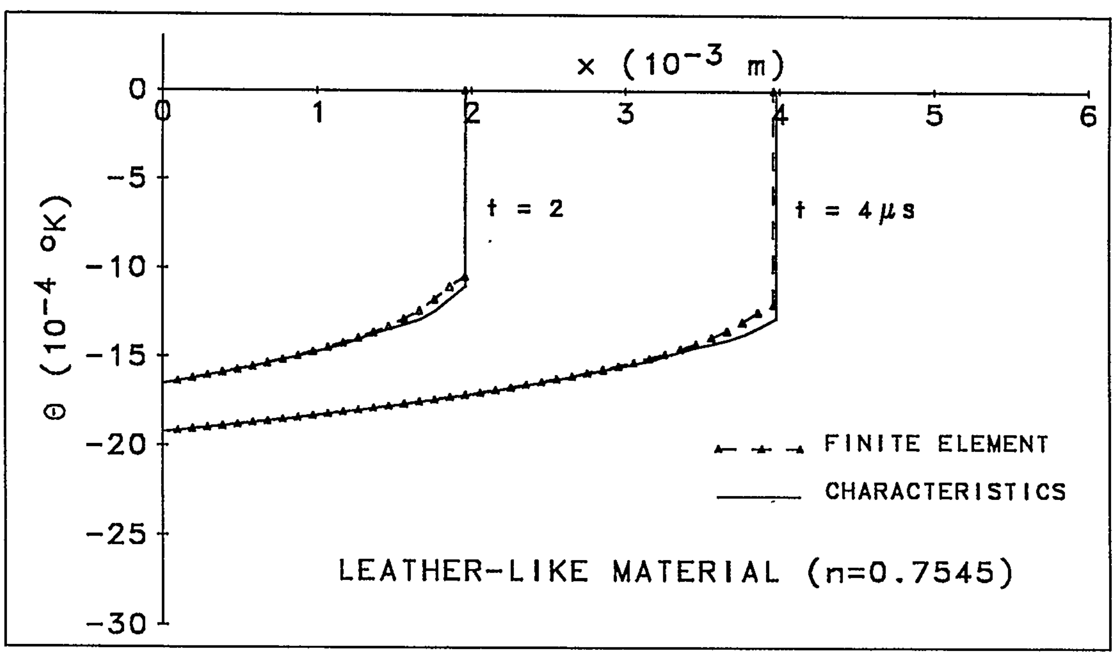

FIG. 6.30d TEMPERATURE RESPONSE OF A STRING OF A LEATHER-LIKE MATERIAL (n = 0.7545) TO $v(0,t) = -5 \times t^{0.2}$ m/s

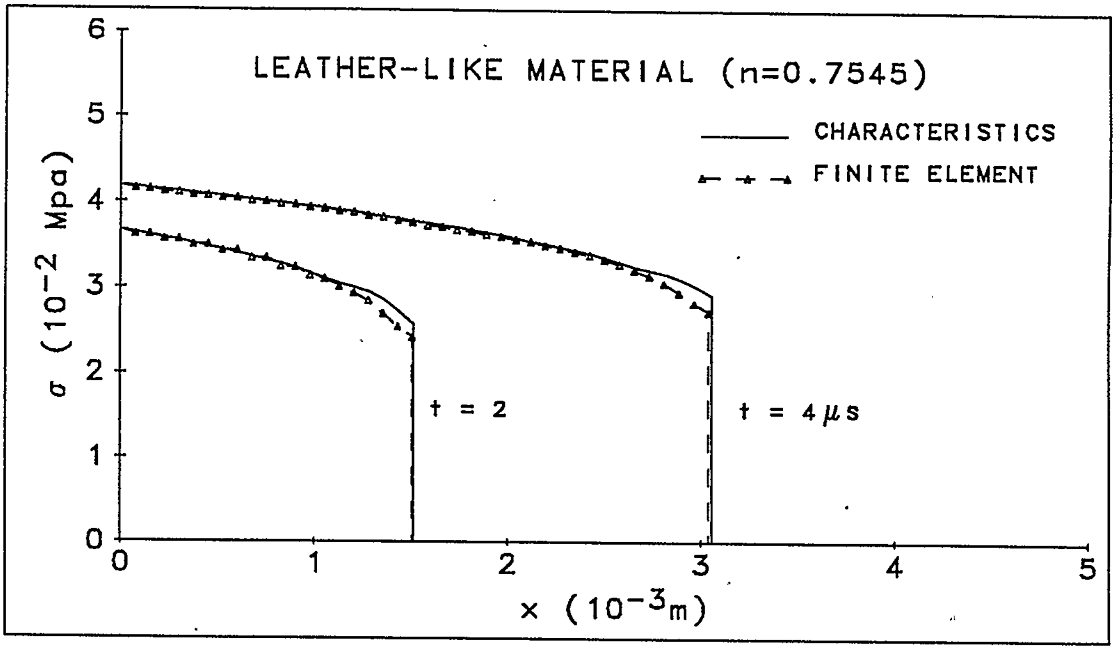

FIG. 6.31a STRESS RESPONSE OF A STRING OF A LEATHER-LIKE MATERIAL (n = 0.7545) TO $\sigma(0,t) = 0.5 \times t^{0.2}$ MPa

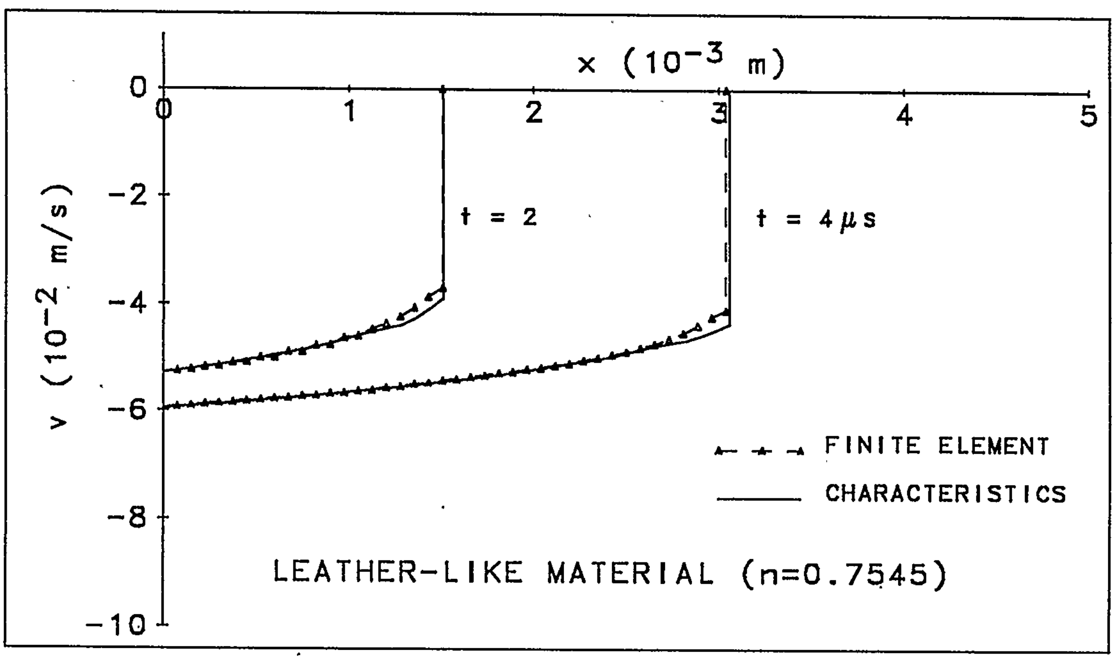

FIG. 6.31b VELOCITY RESPONSE OF A STRING OF A LEATHER-LIKE MATERIAL (n = 0.7545) TO $\sigma(0,t) = 0.5 \times t^{0.2}$ MPa

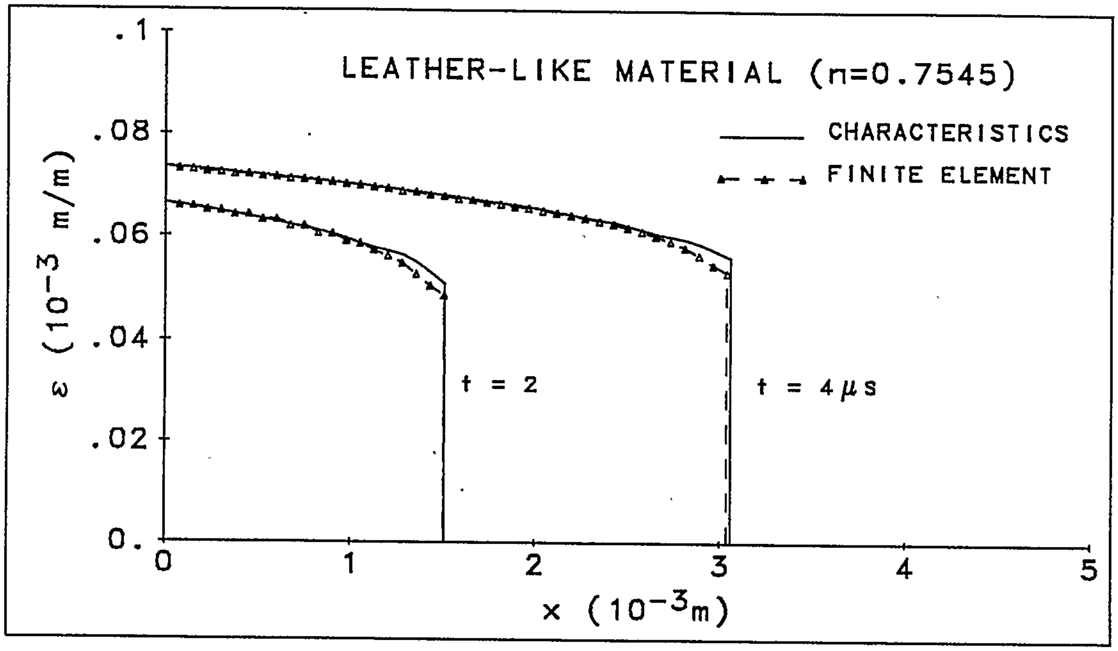

FIG. 6.31c STRAIN RESPONSE OF A STRING OF A LEATHER-LIKE MATERIAL ($n = 0.7545$) TO $\sigma(0,t) = 0.5 \times t^{0.2}$ MPa

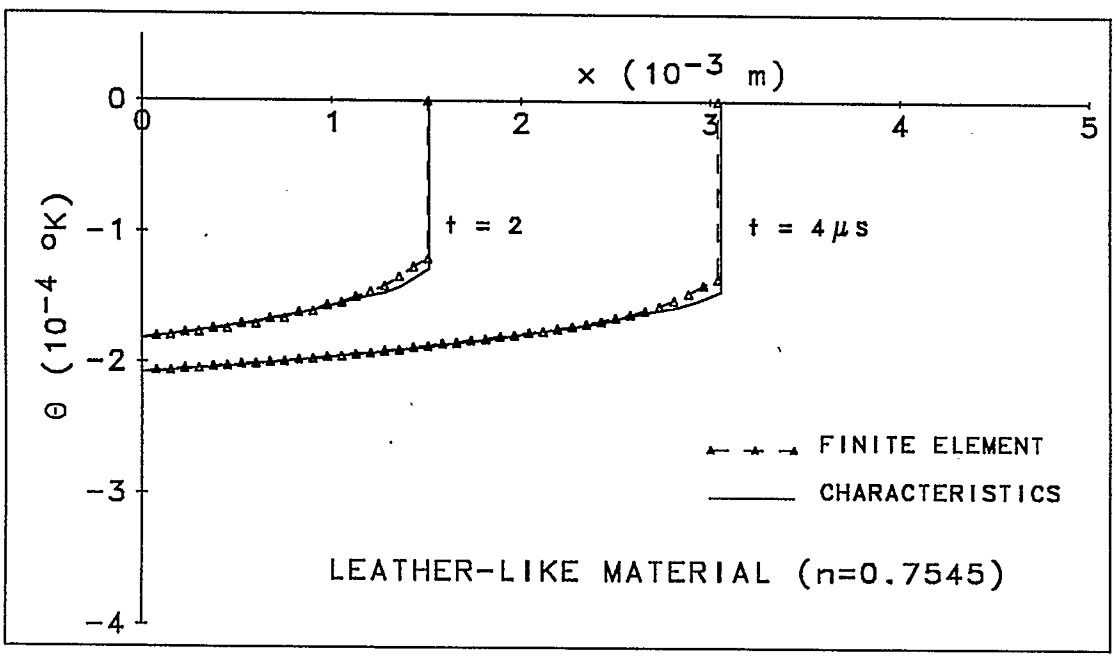

FIG. 6.31d TEMPERATURE RESPONSE OF A STRING OF A LEATHER-LIKE MATERIAL ($n = 0.7545$) TO $\sigma(0,t) = 0.5 \times t^{0.2}$ MPa

CHAPTER 7
DISCUSSIONS AND CONCLUSION

7.1 DISCUSSIONS OF RESULTS

7.1.1 For Conducting Materials

Before examining or discussing the dynamic response of non-linear thermoelastic materials, a physical property of linear and non-linear thermoelastic materials is compared on the basis of numerical calculation.

For illustration, copper is selected as a sample and has the stress-strain relation in an isothermal condition as shown in Figure 6.5. The three curves of stress vs strain represent three different cases of the material such as: (i) linear relation with E = 110 GPa, (ii) non-linear relation with $n = 1.047$ and $\mu = 78.35$ GPa, and (iii) linear relation with E = 120 GPa. As illustrated in the figure, within the range of stress (0-50 MPa), the non-linear curve of stress-strain relation lies between two linear ones.

In Figures 6.6 (a,b,c,d) and Figures 6.7 (a,b,c,d), we can see the discrepancies of the unknowns v, σ, θ and q for the above three cases along the rod whose free end is subjected to constant velocity impact and its temperature is kept at the initial value T_o. As expected that the dynamic response of the non-linear copper rod lies between the other linear ones. Not only by the characteristic method but also by the finite element method, the results obtained indicate that the non-linear relation has a good agreement with the one having the lower Young's modulus. Should the deviation be neglected among the curves, the model of non-linear thermoelasticity can be approximated by a linear one when the value of power n is very close to unity.

Figures 6.8a-d to Figures 6.25a-d present the distributions of dependent variables along the thin rods made of steel, cast iron or copper. Under the two types of boundary conditions such as mechanical impact and thermal impact, the propagation of waves in the medium is examined at the two time intervals of 2×10^{-12} second and 4×10^{-12} second .

a. Mechanical Impact :

(i) With identical boundary conditions of which either constant or time dependent velocity impact and the unchanged temperature are suddenly applied to the end of the rod, it is apparent that the stress response in the steel rod gives the largest magnitudes as shown in Figures 6.8a to 6.13a. Whereas the temperature produced in the copper rod is generally higher than that produced in steel or cast iron. The results are plotted in Figures 6.8c,6.9c and 6.10c or 6.11c,6.12c and 6.13c for easy comparisons.

It may be noted that, the heat flux in the steel rod gives the highest magnitude when its end is subjected to constant velocity impact as illustrated in Figure 6.8d. On the other hand, the largest heat flux is obtained in the copper rod when the time-dependent velocity is applied to the boundary (x = 0).

It is also to be noted that under the constant velocity impact, the heat flux is decreasing along the boundaries of three rods as shown in Figures 6.8d, 6.9d and 6.10d. However, the increase of heat flux can be seen in the case of cast iron and copper whose ends are subjected to time-dependent velocity impact.

(ii) The second type of mechanical impact , the constant stress impact (or time-dependent stress impact) and zero temperature are applied to the boundary, the results are represented in Figures 6.14a-d to 6.19a-d .

As expected, velocity response of cast iron yields the largest magnitudes - compare, for example, Figures 6.14b, 6.15b and 6.16b or Figures 6.17b, 6.18b and 6.19b. Whereas the temperature and heat flux produced in the copper rod give the highest values as seen in Figures 6.16c,d and 6.19c,d.

Together with the mechanical disturbances applied to the boundary, the negative values of difference temperature θ as shown in Figures 6.8(c) to 6.19(c) lead us to conclude that the elastic rods are "cooled" under a tensile load [6.7]. Moreover, the applied tensile force at the end of the rod also causes the temperature having the tendency to drop at the boundary, and thus heat must be continuously added at $x = 0$ to maintain θ at zero.

b. <u>Thermal Impact</u> :

The medium is, in turn, subjected to the thermal disturbances, namely the negative applied step temperature and either the zero velocity input or the zero stress input. The dynamic response of dependent variables distributing along the rods is illustrated in Figures 6.20a-d to 6.25a-d.

(i) Zero velocity and constant temperature impact : As illustrated in Figures 6.20a,b to 6.22a,b, the results obtained reveal that the stress and velocity distributed along the steel rod yield the largest magnitudes. On the other hand, the heat flux response gives the lowest values at the boundary of the copper rod.

Under this type of boundary conditions, the stresses are positive along the rods and changing with time at the boundaries ($x=0$). Since the constant temperature impact is negative, the heat flux must take place in the direction from the rod to the boundary. As seen in Figures 6.20d, 6.21d and 6.22d, the heat flux has a negative value and is increasing with time at $x = 0$.

(ii) Zero stress and constant temperature impact : Similar to case (i), the response of steel rod yields the largest stress and velocity at the leading wavefront. However, unlike the case (i), the stress response is negative at those points close to the boundary; two regions are clearly separated between the boundary and the leading wavefront such as compression and tension as shown in Figures 6.23a, 6.24a and 6.25a.

Also, it should be mentioned that the power term n of stress in the constitutive law causes much trouble in numerical computation whenever values of stress vanish. Because of that reason, we have applied a small value of stress at the boundary instead of zero as assumed theoretically . In calculation, the non-zero value of stress is taken as 1 Pa applied at $x = 0$.

General observation, under either the mechanical impact or thermal impact, we can say that :

(i) The mechanical wave propagates fastest in the steel rod.

(ii) The jumps in dependent variables at the leading wavefront as well as its location in the rods are clearly shown in each figure.

(iii) The values of stress along the leading wavefront at two different examing time $t = 2\times10^{-12}$ second and $t = 4\times10^{-12}$ second are almost the same in each rod. Thus, the assumption of the leading wavefront propagating along the characteristic curve C_1^+ having a positive slope seems to be valid when the numerical computation is performed.

7.1.2 For Non-Conducting Materials

In order to illustrate the phenomena of wave motion in this kind of material, leather and rubber are chosen as specimens in numerical computation. Regardless of the complexities of their microstructures, these materials are assumed to be homogeneous and isotropic. Furthermore, under a small load applied, the extension of rubber is considered to be an infinitesimal deformation whenever strain ε is very small as compared with unity. Their mechanical properties given in Table 6.2 are, thus, kept constant through the course of investigation.

The results of dynamic response in these two materials is recorded in Figures 6.26a-d to 6.31a-d wherein the examing time has the values of 2 μs and 4 μs.

As mentioned in Chapter 3 and Chapter 5, the wave behaviors may be simple waves or shock waves depending upon the prescribed boundary conditions or the stress-strain diagrams represented by the power n.

Under a constant velocity impact, only simple waves propagating in the medium irrespective of the value of power n . The results of this type of impact applied at the end of a string of a rubber-like or leather-like material are shown in Figures 6.26(a,b,c,d) or Figures 6.29(a,b,c,d). The response of dependent variables distributed along the string is maintained as constant . This is because the entropy $\mathcal{S}$ is constant throughout the disturbed region bounded by a single wavefront and the Ot-axis.

The adiabatic process occurs in each part of the body, consequently, the energy is conserved and with no heat loss or gain, kept unchanged in the region of a simple wave.

The extensive solutions of simple waves are also illustrated in Figures 6.27(a,b,c,d) and 6.28(a,b,c,d) where a string of a rubber-like material is subjected to time-dependent velocity impact and time-dependent stress impact, respectively. Carefully examining these curves, the results reveal that the jumps in stress at the wavefront separately located at two elapsed times are the same. Other velocity, strain and temperature jumps are observed in a similar manner as well. The characteristics in the direction of wave propagation, therefore, are straight lines because the conditions along them are constant [6.8].

The above situation will be different when shock waves are involved in the problem. The two identical boundary conditions prescribed above are now applied to the string of leather-like material which, as expected, contains a shock since its value of power n is less than unity (Table 6.2). The jump in stress and strain are increasing along the shockfront whereas the jumps in velocity and temperature difference are decreasing as shown in Figures 6.30(a,b,c,d) and 6.31(a,b,c,d). This can be explained as follows. Under a tensile load, the elastic energy e_M acquired by the material is numerically equal to the area under the stress-strain curve and expressible as :

$$e_M = \int_0^{\varepsilon} \sigma d\varepsilon \quad . \tag{7.1}$$

Because the strain ε is a function of stress, the equation (7.1) can be written in an equivalent form:

$$e_M = \sigma\varepsilon - \int_0^{\sigma} \varepsilon d\sigma \quad . \tag{7.2}$$

The total internal energy e, according to Chen [3.12], consisting of the thermal energy, e_T, of the material subjected to a shock is given by:

$$\|e\| = \frac{1}{2}(\sigma^- + \sigma^+)\,\|\varepsilon\| \quad . \tag{7.3}$$

With the assumption that the medium is initially at rest, the equation (7.3) yields:

$$e = \frac{1}{2}\sigma\varepsilon \quad . \tag{7.4}$$

It can be shown that $e > e_M$ whenever the power n is less than unity. Therefore, the material is always heated by a shock wave and its entropy increases. The stress is then increasing along the shockfront as a result.

7.2 CONCLUSION

In this thesis, the problem of combined thermal and mechanical effects on non-linear elastic wave propagation has been considered from two different points of view:

(i) a mathematical model of constitutive law is developed from the basics of continuum thermodynamics.

(ii) numerical computation taking into account the real materials is performed on the new meshes, namely combination meshes systematically constructed in the disturbed region.

It is evident from the analysis given in the preceding chapters that the non-linear thermoelastic theory contains mathematical development which tends to clarify the main features of the wave motion. It appears, that non-linear effects will become important whenever the linearized mechanics of constitutive relations of materials are invalid, and for many purposes non-linear thermoelastic theory should provide an adequate model of wave propagating in the medium.

The numerical results obtained have shown good agreement among the methods especially when applying them to the problems of non-conductors. One of the weaknesses of the method of characteristics as conventionally applied to the combination meshes is that the unstable values of unknowns at points close to the lagging wavefront cannot be controlled. The inability of the method, thus, has strongly affected the entire solution of the problem since the unknowns are determined from point to point throughout the disturbed region.

The finite element method, in contrast, has yielded smooth solutions in general. The main advantage of this method that it is unnecessary to employ an artificial viscosity term as in the case of finite difference method . However, the program of finite element method usually requires much more time on the computer.

With the use of combination meshes, the location of the leading wavefront (or single wavefront) and the jumps in unknowns across it have been fully determined. Another advantage is that the undisturbed region is not involved in numerical computation, and as a result, the time needed for executing the program would be reduced.

Besides, the technique of similarity representation has also given the results as exact as those obtained by the other methods. The results are specified in simple forms which can be computed by a pocket calculator. In spite of that this technique has not been extensively applied yet. The limitation of the material used as well as the boundary conditions prescribed has resulted in the weakness of similarity analysis. As shown in chapter 5, the solutions of the system of equations expressing the wave motion in a non-conducting material in terms of invariant variables are valid only when δ must have a value of zero. Moreover, the similarity method is restricted in the wave problem which contains only one wavefront. The extending similarity solutions of the problems having more than one wavefront such as wave motion in conducting materials are still within the investigation.

7.3 SUGGESTIONS FOR FURTHER WORK

Since the numerical computation based on the non-linear model of constitutive law is limited by the published data, supplementary experiments on other real materials for obtaining stress-strain relations within the elastic range are strongly recommended.

Even though the results obtained in the case of wave motion in conducting materials are fairly acceptable, apparently locating the lagging wavefront as well as exactly determining the jumps in unknowns across it would be an interesting area of research.

In this thesis, only one particular case of simple waves involved in the problem of non-conductors whose boundary is subjected to constant velocity impact is analyzed by the group theoretic technique. The extensive solutions of shock waves in terms of similarity transformations appear to be open for investigation.

In summary, the author believes that the model of constitutive law developed in this dissertation would be an additional step for searching the behavior of non-linear thermoelastic materials. Moreover, the modified method of numerical computation as developed in chapters 4 and 5 may be an appropriate numerical technique for solving the problems of wave propagation.

REFERENCES

1.1 Housner, G.W. and Vreeland, T., Jr., The Analysis of Stress and Deformation, The Macmillan Company, New York, 1966.

1.2 Kolsky, H., Stress Wave in Solids, Dover Publication, Inc., New York, 1963.

1.3 Miklowitz, J., Elastic Wave Propagation, Applied Mechanic Surveys, Spartan Books, 1966.

1.4 Mindlin, R.D. and Herrman, G., "A One-Dimensional Theory of Compressional Waves in an Elastic Rod", Proceeding of the First U.S. National Congress of Applied Mechanics, Chicago, pp. 187-191, 1951.

1.5 Wasley, R.J., Stress Wave Propagation in Solids, North-Holland, Amsterdam, 1973.

1.6 Achenbach, J.D., Wave Propagation in Elastic Solids, North-Holland, Amsterdam, 1973.

1.7 Johnson, W., Impact Strength of Materials, Edward Arnold, London, 1972.

1.8 Bell, J., "The Experimental Foundation of Solid Mechanics", in Encyclopedia of Physics, S. Flugge, Ed., Vol. VIa/1, Springer-Verlag, Berlin, 1973.

1.9 Frydrychowicz, W. and Singh, M.C., "Group Theoretic Technique for the Similarity Solution of a Non-Linear Elastic Rod Subjected to Velocity Impact", Theoretical Mechanics, Warsaw, Vol. 23, pp. 19-37, 1985

1.10 Elzanowski, M. and Epstein, M., "Decay of Strong Shocks in Non-Linear Elasticity", J. Sound and Vibration, Vol. 103, pp. 371-378.

1.11 Joule, J.P., "On Some Thermo-Dynamic Properties of Solids", Phil. Trans. Roy. Soc. London, Vol. 149, pp. 91-131, 1859.

1.12 Nowacki, W., Dynamic problems of Thermoelasticity, PWN-Polish Scientidic Publishers, Warszawa, 1975.

1.13 Kovalenko, A.D., Thermoelasticity, Wolters & Noordhoff, Growingen, 1969.

1.14 Fung, F.C., Foundations of Solid Mechanics, Prentice-Hall, Inc., New Jersey, 1965.

1.15 Boley, B.A., "Thermal Stress Today", Proceedings of the Seventh U.S. National Congress of Applied Mechanics, Chicago, PP. 99-102, 1974.

1.16 Danilovskaya, V.I., "Thermal Stresses in an Elastic Half-Space Due to a Sudden Heating of Its Boundary", Prikl. Mat. Mekh., Vol. 14, pp. 316-318, 1950.

1.17 Nowacki, W., "Some Three Dimensional Problems of Thermoelasticity", J. Applied Math. and Mech., Vol. 23, pp. 456-467, 1959.

1.18 Sternberg, E. and Chakravorty, J.G., "On Inertia Effects in a Transient Thermoelastic Problem", J. Appl. Mech., Vol. 26, pp. 503-509, 1959

1.19 Michael, J.E., "Thermally Induced Elastic Wave Propagation in Slender Bars", Proceedings Third U.S. National Congress on Applied Mechanics, Brown University, pp. 209-213, 1958.

1.20 Das, B.R., "Note on Thermoelastic Stresses in a Thin Semi-Infinite Rod Due to Some Time Dependent Temperature Applied to Its Free End", Indian J. Theoretical Physics, Vol. 9, No. 3, pp. 49-55, 1961.

1.21 Chattopadhyay, N.C., "Note on Thermoelastic Stresses in a Thin Semi-Infinite Rod Due to Some Time-Dependent Temperature Applied to Its Free End", Indian J. Theoretical Physics, Vol. 15, No. 2, pp. 49-55, 1961.

1.22 Roy Choudhuri, S.K., "Note on the Thermoelastic Stress in a Thin Rod of Finite Length Due to Some Constant Temperature Applied to Its Free End, the Other End Being Fixed and Insulated", Indian J. Theoretical Physics, Vol. 19, No. 3, pp. 99-106, 1968.

1.23 Roy Choudhuri, S.K., "Thermoelastic Stress in a Rod Due to Distributed Time-Dependent Heat Sources", J. Appl. Mech., Vol. 10, pp. 531-533, 1972.

1.24 Sneddon, I.N., "The Propagation of Thermal Stresses in Thin Metallic Rods", Proceeding of the Royal Society of Edinburgh, Series A, Vol. 35, pp. 121-143, 1958.

1.25 Dillon, O.W., Jr., "Thermoelasticity When the Material Coupling Parameter Equals Unity", J. Appl. Mech., 32, pp. 378-382, 1965.

1.26 Nickell, R.E. and Sackman, J.L., "Approximate Solution in Linear Coupled Thermoelasticity", J. Appl. Mech., Vol. 26, pp. 255-256, 1968.

1.27 Nickell, R.E. and Sackman, J.L., "Variational Principles for Linear Coupled Thermoelasticity", Quart. Appl. Math., Vol. 26, pp. 11-26, 1968.

1.28 Soler, A.J. and Chen, H.C., "On the Solution to Transient Coupled Thermoelastic Problems by Perturbation Techniques", J. Appl. Mech., Vol. 23, pp. 389-399, 1965.

1.29 Ting, E.C. and Chen, H.C., "A Unified Numerical Approach for Thermal Stress Waves", Computers and Structures, Vol. 5, pp. 165-175, 1982.

1.30 Gładysz, J., "Propagation of a Plane Wave in a Thermoelastic Half-Space Under Smooth Heating of Its Boundary", J. Thermal Stresses, Vol. 8, pp. 227-234, 1985.

1.31 Fan, H.T., Chen, K.K. and Sun, N.S., "Numerical Analysis of Uncoupled Dynamic Problem of Thermoelasticity", J. Thermal Stresses, Vol. 7, pp. 149-161, 1984.

1.32 Hetnarski, R., "Solution of the Coupled Problem of Thermoelasticity in the Form of Series of Functions", Arch. Mech. Stos., Vol. 16, pp. 919-940, 1964.

1.33 Achenbach, J.D., "Approximate Transient Solutions for the Coupled Equations of Thermoelasticity", J. Acoustical Soc. Am., Vol. 36, pp. 10-18, 1964.

1.34 Daimaruya, M. and Ishikawa, H., "On the Propagation of Thermoelastic Waves According to the Coupled Thermoelastic Theory", Bulletin of the JSME, Vol. 17, pp. 991-999, 1974.

1.35 Dhaliwal, R.S. and Shanker, M.U., "Coupled Thermoelastic Problem for an Infinite Medium with a Cylindrical Hole", Arch. Mech. Stos., Vol. 5, pp. 531-546, 1970.

1.36 Wilms, E.V., "On Coupling Effects in Transient Thermoelastic Problems", J. Appl. Mech, Vol. 31, pp. 719-722, 1964.

1.37 Rogge, T., "A Coupled Thermoelastic Problem", SIAM Review, Vol. 11, pp. 277-282, 1969.

1.38 Ackerman, C.C., Bertman, B., Fairbank, H.A., Guyer, R.A., "Second Sound in Solid Helium", Phys. Rev. Letters, Vol. 16, pp. 789-791, 1966.

1.39 Ackerman, C.C., Overton, W.C. Jr., "Second Sound in Solid Helium-3", Phys, Rev. Letters, Vol. 22, pp. 764-766, 1969.

1.40 Jackson, H. and Walker, C., "Second Sound in NaF", Phys. Rev. Letters, Vol. 25, pp. 26-28, 1970.

1.41 Nayfeh, A.H., "Transient Thermo-Elastic Waves in a Half-Space with Thermal Relaxation", J. Appl. Math. Phys. (ZAMP), Vol. 23, pp. 50-68, 1972.

1.42 Nayfeh, A.H., "Propagation of Thermoelastic Disturbances in Non-Fourier Solids", AIAA Journal, Vol. 15, pp. 957-960, 1977.

1.43 Chardrasekharaiah, D.S., "Wave Propagation in a Thermoelastic Half-Space", Indian J. Pure Appl. Math., Vol. 12, pp. 266-241, 1981.

1.44 Green, A.E. and Lindsay, K.A., "Thermoelasticity", J. Elasticity, Vol. 2, pp. 1-7, 1972.

1.45 Chandrasekharaiah, D.S., "Thermoelasticity with Second Sound: A Review", Appl. Mech. Rev., Vol. 39, pp. 355-376, 1986.

2.1 Boley, B.A. and Weiner, J.H., Theory of Thermal Stresses, John Wiley and Sons, New York, 1960.

2.2 Nowacki, W., Thermoelasticity, Pergamon Press, Warszawa, 1962

2.3 Parkus, H., Thermoelasticity, Blaisdell Publishing Co., Waltham, Mass., 1968.

2.4 Carlson, D.E., "Linear Thermoelasticity", in Encyclopedia of Physics, S. Flugge, Ed., Vol. VIa/2, Springer-Verlag, Berlin, 1972

2.5 Nowacki, W. and Sneddon, I.N., Thermomechanics in Solids, Springer-Verlag, New York, 1977.

2.6 Nowinski, J.L., Theory of Thermoelasticity with Applications, Sijthoff & Noordhoff, Alphen Ain Den Rijn, 1978.

2.7 Gurtin, M.E., "The Linear Theory of Elasticity" in Encyclopedia of Physics, S. Flugge, Ed., Vol. VIa/2, Springer-Verlag, Berlin, 1972

2.8 Onsager, L., "Reciprocal Relation in Irreversible Processes I", Phys. Rev., Vol. 37, pp. 405-426, 1931.

2.9 Onsager, L., "Reciprocal Relation in Irreversible II", Phys. Rev., Vol. 38, pp. 2265-2279, 1931.

2.10 Eckart, C., "Thermodynamics of Irreversible Processes IV, Theory of Elasticity and Anelasticity", Phys. Rev., Vol. 73, pp. 373-382, 1948.

2.11 Biot, M.A., "Theory of Stress-Strain Relations in Anisotropic Viscoelasticity and Relaxation Phenomena", J. Appl. Phys., Vol. 25, pp. 1385-1391, 1953.

2.12 Biot, M.A., "Variational Principles in Irreversible Thermodynamics with Application to Viscoelasticity", Phys. Rev., Vol. 97, pp. 1463-1469, 1955.

2.13 Coleman, B.D. and Mizel, V.J., "Existence of Caloric Equations of State in Thermodynamics", J. Chemical Physics, Vol. 40, pp. 1116-1125, 1964.

2.14 Biot, M.A., "Thermoelasticity and Irreversible Thermodynamics", J. Appl. Phys., Vol 27, pp. 240-253, 1956.

2.15 Coleman, B.D. and Gurtin, M.E., "Thermodynamics with Internal State Variables", J. Chemical Phys., Vol. 47, pp. 597-613, 1967.

2.16 Gol'denblat, I.I., Some Problems of the Mechanics of Deformable Media, Noordhoff, Groningen, 1962.

2.17 Lord, H.W. and Shulman, Y., "A Generalized Dynamical Theory of Thermoelasticity", J. Mech. Phys. Solid, Vol. 15, pp. 299-309, 1967.

2.18 Takeuti, Y., "Foundations for Coupled Thermoelasticity", J. Thermal Stress, Vol. 2, pp. 323-339, 1979.

2.19 Lebon, G., "A Generalized Theory of Elasticity", J. Tech. Phys., Vol. 23, pp. 37-46, 1982.

2.20 Stojanovitch, R., "On the Stress Relation in Non-Linear Thermoelasticity", Int. J. Non-Linear Mechanics, Vol. 4, pp. 217-233, 1969.

2.21 Gurtin, M.E., "Thermodynamics and the Possibility of Spatial Interaction in Elastic Materials", Arch. Rational Mech. Anal., Vol. 19, pp. 339-351, 1965.

2.22 Schappery, R.A. "Further Development of a Thermodynamic Constitutive Theory: Stress Formulation", Purdue University Report AA & ES 69-2, 1969.

2.23 Lubiner, J., "On the Thermodynamic Foundations of Non-Linear Solid Mechanics", Int. J. Non-Linear Mechanics, Vol. 7, pp. 237-245, 1972.

2.24 Chang, W.P. and Cozzarelli, F.A., "On the Thermodynamics of Non-linear Single Integral Representations for Thermoviscoelastic Materials with Applications to One-Dimensional Wave Propagation", Acta Mechanica, Vol. 25, pp. 187-206, 1977.

2.25 Malvern, L.P., Introduction to the Mechanics of a Continuous Medium, Prentice Hall, New Jersey, 1969.

2.26 Bargmann, H., "Recent Developments in the Field of Thermally Induced Waves and Vibrations", Nuclear Engineering and Design, Vol. 27,pp. 372-385, 1984.

2.27 Dillon, O.W., Jr., "Coupled Thermoelasticity of Bars", J. Appl. Mech., Vol. 34, pp. 137-145, 1967.

2.28 Boley, B.A. and Tolins, I.S., "Transient Coupled Thermoelastic Boundary Value Problems in the Half-Space", J. of Appl. Mech., Vol. 29, pp. 637-646, 1962.

2.29 Achenbach, J.D., "The Influence of Heat Conduction on Propagating Stress Jumps", J. Mech. Phys. Solids, Vol. 16, pp. 273-282, 1968.

2.30 Dillon, O.W. Jr. and Tauchert, T.R., "The Experimental Technique for Observing the Temperatures Due to the Coupled Thermoelastic Effect", Int. J. of Solids and Structures, Vol. 2, pp. 385-391, 1966.

2.31 Thurston, R.N., "Wave in Solids", in Encyclopedia of Physics, S. Flugge, Ed., Vol. VIa/4, Springer-Verlag, Berlin, 1974.

2.32 Nettleton, R.E., "Relaxation Theory of Thermal Conduction in Liquids", Phys. Fluids, Vol. 3, pp. 216-225, 1960.

2.33 Gibbings, J.C., Thermomechanics: The Governing Equations, Pergamon Press, London, 1970.

2.34 Lord, H.W. and Lopez, A.A., "Wave Propagation in Thermoelastic Solids at Very Low Temperature", Acta Mechanica, Vol. 10, pp. 85-97, 1970.

2.35 Norwood, F.R. and Warren, W.E., "Wave Propagation in the Generalized Dynamical Theory of Thermoelasticity", Quart. J. Mech. and Appl. Math., Vol. 22, pp. 283-290, 1969.

2.36 Popov, E.B., "Dynamic Coupled Problem of Thermoelasticity for a Half-Space Taking Account of the Finiteness of the Heat Propagation Velocity", J. Appl. Math. Mech., (PMM), Vol. 31, pp. 349-355, 1967.

2.37 Sawatzky, R.P. and Moodie, T.B., "On Thermoelastic Transients in a General Theory of Heat Conduction with Finite Wave Speeds", Acta Mechanica, Vol. 56, pp. 165-187, 1985.

2.38 Lebon, G. and Lambermont, J., "A Consistent Thermodynamic Formulation of the Field Equations for Elastic Bodies Removing the Paradox of Infinite Speed of Propagation of Thermal Signals", Journal de Mechanique, Vol. 15, pp. 579-594, 1976.

2.39 Chester, M., "Second Sound in Solids", Phys. Rev., Vol. 131, pp. 2013-2015, 1963.

2.40 Maurier, M.J., "Relaxation Model for Heat Conduction in Metals", J. Appl. Phys., Vol. 40, pp. 5123-5130, 1969.

2.41 Francis, P.H., "Thermo-Mechanical Effects in Elastic Wave Propagation: A Survey", J. Sound and Vibration, Vol. 21, pp. 181-192, 1972.

2.42 Mengi, Y. and Turhan, D., "The Influence of the Retardation Time of the Heat Flux on Pulse Propagation", J. Appl. Mech., Vol. 45, pp. 433-435, 1978.

2.43 Dillon, O.W., Jr., "A Nonlinear Thermoelasticity Theory", J. Mech. Phys. Solids, Vol. 10, pp. 123-131, 1962.

2.44 Jekot, T., "Nonlinear Thermoelastic Problems of Homogeneous and Isotropic Media Under Great Temperature Gradients", **Arch. Mech. Stos.**, Vol. 36, pp. 33-47, 1984.

3.1 John, F., **Partial Differential Equations**, Springer-Verlag, New York, 3rd Ed., 1978.

3.2 Mengi, Y. and Turhan, D., "Transient Response of Inhomogeneous Thermoelastic Media to a Dynamic Input", **J. Appl. Math. and Phys.**, (ZAMP), Vol. 29, pp. 561-576, 1978.

3.3 Kosinski, W., "Behaviour of the Acceleration and Shock Waves in Materials with Internal State Variables", **Int. J. Non-Linear Mech.**, Vol. 9, pp. 481-499, 1974.

3.4 Kosinski, W., "One-Dimensional Shock Waves in Solids with Internal State Variables", **Arch. of Mechanics**, Vol. 27, pp. 445-458, 1975.

3.5 Bland, D.R., **Nonlinear Dynamic Elasticity**, Blaisdell, Waltham, Mass., 1969.

3.6 Cristescu, N., **Dynamic Plasticity**, North-Holland, Amsterdam, 1967.

3.7 Eringen, A.C. and Suhubi, E.S., **Elastodynamics**, Vol. 1, Academic Press, New York, 1974.

3.8 Dejuhasz, K.J., "Graphical Analysis of Impact of Bars Stress Above the Elastic Range", **J. of Franklin Institute**, Vol. 248, Part I, pp. 15-48; Part II, pp. 113-142, 1949.

3.9 Hwang, S.H. and Davis, N., "Graphical Analysis of the Formation of Shock Fronts in Materials", **J. Mech. Phys. Solids**, Vol. 8, pp. 52-65, 1960.

3.10 Whiteman, G.B., **Linear and Nonlinear Waves**, Wiley-Interscience, New York, 1974.

3.11 Courant, R. and Friedricks, K.O., **Supersonic Flow and Shock Waves**, Springer-Verlag, New York, 1974.

3.12 Chen, P.J., "One-Dimensional Shock Waves in Elastic Non-Conductors", **Arch. Rational Mech. Anal.**, Vol. 43, pp. 350-361, 1971.

3.13 Chen, P.J. and Gurtin, M.E., "On the Growth of One-Dimensional Shock Waves in Materials with Memory", **Arch. Rational Mech. Anal.**, Vol. 36, pp. 33-46, 1970.

3.14 Ting, T.C.T., "Further Study on One-Dimensional Shock Waves in Non-linear Elastic Media", **Quart. J. Applied Math.**, Vol. 37, pp. 421-429, 1980.

3.15 Johnson, A.F., "Pulse Propagation in Heat-Conducting Elastic Materials", **J. Mech. Phys. Solids**, Vol. 23, pp. 55-75, 1975.

4.1 Lopez, A.A., "A Study of Thermoelastic Waves by the Method of Characteristics", Development in Theoretical and Applied Mech., Vol. 5, pp. 417-447, 1971.

4.2 Lee, C., Chang, W.P. and Cozzarelli, F.A., "Some Results on the One-Dimensional Coupled Nonlinear Thermoviscoelastic Wave Propagation Problem with Second Sound", Acta Mechanica, Vol. 37, pp. 111-120, 1980.

4.3 Jeffrey, A., Quasilinear Hyperbolic Systems and Waves, Pitman Publishing, London, 1976.

4.4 Jeffrey, A. and Tanuiti, T., Non-Linear Wave Propagation, Academic Press, New York, 1964.

4.5 Ames, W.F., Numerical Methods for Partial Differential Equations, Academic Press, New York, 1977.

4.6 Chou, P.C. and Mortimer, R.W., "Solution of One-Dimensional Elastic Wave Problem by the Method of Characteristics", J. Appl. Mech., Vol. 34, pp. 745-750, 1967.

4.7 Francis, P.H., "The Response of a Thin Elastic Rod to Combined Thermal and Mechanical Impulse", J. Appl. Math. Phys., (ZAMP), Vol. 19, pp. 113-127, 1968.

4.8 Campbell, J.D. and Taylor, D.B., "On the Numerical Solution of a Wave Propagation Problem in the Theory of Dislocation Motion", in Stress Waves in Anelastic Solids, Kolsky, H. and Prager, W., (Eds.), pp. 54-68, IUTAM Symposium Providence 1963, Springer-Verlag, Berlin, 1964.

4.9 Wood, E.R. and Phillips, A., "On the Theory of Plastic Wave Propagation in a Bar", J. Mech. Phys. Solids, Vol. 15, pp. 241-254, 1967.

4.10 Fox, L., Numerical Solution of Ordinary and Partial Differential Equations, Pergamon Press, Mass., 1968.

4.11 Lister, M., "The Numerical Solution of Hyperbolic Partial Differential Equations by the Method of Characteristics", in Mathematical Methods for Digital Computers, Ralston, A. and Wilf, H.S. (Eds.), pp. 165-179, John Wiley & Sons, New York, 1960.

4.12 Orisamolu, I.R., Continuum Thermodynamics Formulation on Numerical Simulation of the Propagation of Coupled Thermomechanical Waves in Inelastic Solids, Ph.D. Dissertation, University of Calgary, 1988.

4.13 Li, Y.Y, Ghoneim, H. and Chen, Y., "A Numerical Method in Solving a Coupled Thermoelastic Equation and Some Results", J. Thermal Stresses, Vol. 6, pp. 253-280, 1983.

4.14 Fost, R.B., Wellford, L.C., Jr. and Oden, J.T., "A Finite Element Analysis of Shocks and Finite Amplitude Waves in One-Dimensional Hyperelastic Bodies at Finite Strain", **Int. J. Solids Structures**, Vol. 11, pp. 377-401, 1975.

4.15 Prevost, J.H. and Tao, D., "Finite Element Analysis of Dynamic Coupled Thermoelasticity Problems with Relaxation Times", J. Appl. Mech., Vol. 50, pp. 817-822, 1983.

4.16 Huyakorn, P.S., "Solution of Steady-State, Convective Transport Equation Using an Upwind Finite Element Scheme", **Appl. Math. Modelling**, Vol. 1, pp. 187-195, 1977.

4.17 Gray, W. and Pinder, G.F., "An Analysis of the Numerical Solution of the Transport Equation", **Water Resources Research**, Vol. 12, pp. 547-555, 1976.

4.18 Fletcher, C.A.J., "The Group Finite Element Formulation", **Comp. Method Appl. Mech. Engg.**, Vol. 37, pp. 225-243, 1982.

4.19 Lucchi, W.C., "Improvement of Mac Cormack's Scheme for Burgers' Equation Using a Finite Element Method", **Int. J. Num. Meth. Engg.**, Vol. 15, pp. 537-555, 1980.

4.20 Fletcher, C.A.J., **Computational Galerkin Methods**, Springer-Verlag, New York, 1984.

4.21 Morton, K.W., "Generalized Galerkin Methods for Hyperbolic Problems", **Comp. Meth. Appl. Mech. Engg.**, Vol. 52, pp. 847-871, 1985.

4.22 Morton, K.W., "Finite Element Methods for Hyperbolic Equations", **Comp. Physics Reports**, Vol. 6, pp. 189-207, 1987.

4.23 Morton, K.W. and Griffiths, D.F., "Generalized Galerkin Methods for First-Order Hyperbolic Equations", J. **Computational Physics Reports**, Vol. 36, pp. 249-270, 1980.

4.24 Duncan, D.B. and Griffiths, D.F., "The Study of a Petrov-Galerkin Method for First-Order Hyperbolic Equations", **Comp. Meth. Appl. Mech. Engg.**, Vol. 45, pp. 147-166, 1984.

4.25 Sanz-Serna, J.M. and Christie, I., "Petrov-Galerkin Methods for Non-linear Dispersive Waves", J. **Computational Physics**, Vol. 39, pp. 94-102, 1981.

4.26 Lapidus, L. and Pinder, G.F., **Numerical Solution of Partial Differential Equations in Science and Engineering**, John Wiley & Sons, New York, 1982.

4.27 Oden, J.T., "Finite Element Analysis of Nonlinear Problems in the Dynamical Theory of Coupled Thermoelasticity", **Nuclear Engg. and Design**, Vol. 10, pp. 465-475, 1969.

4.28 Gottlieb, D. and Turkey, E., "Boundary Conditions in Finite Difference Methods for Time Dependent Equations", J. Comp. Phys., Vol. 26, pp. 181-196, 1974.

4.29 Chu, C.K. and Sereny, A., "Boundary Conditions in Finite Difference Fluid Dynamic Codes", J. Comp. Phys., Vol. 15, pp. 476-491, 1974

5.1 Aboudi, J. and Yako, B., "One-Dimensional Amplitude Wave Propagation in a Compressible Elastic Half-Space", Int. J. Solids Structures, Vol 9, pp. 363-378, 1973.

5.2 Fost, R.B., Wellford, L.C. and Oden, J.T., "A Finite Element Analysis of Shocks and Finite-Amplitude Waves in One-Dimensional Hyperelastic Bodies at Finite Strain", Int. J. Solids Structures, Vol. 11, pp. 377-401, 1975.

5.3 Hanegud, S.V. and Abhyankar, N.S., "A Numerical Scheme for the Study of Poynting Effect in Wave Propagation Problems with Finite Boundaries", Int. J. Non-Linear Mechanics, Vol. 19, pp. 507-524, 1984.

5.4 Lapidus, A., "A Detached Shock Calculation by Second-Order Finite Differences", J. Computational Physics, Vol. 2, pp. 154-177, 1967.

5.5 Von-Newman and Richtmyer, R.D., "A Method for Numerical Calculation of Hydrodynamic Shocks", J. of Appl. Physics, Vol. 21, pp. 232-237, 1950.

5.6 Brode, H.L., "Numerical Solutions of Spherical Blast Waves" J. Applied Physics, Vol. 26, pp. 766-775, 1955.

5.7 Sod, G.A., "A Survey of Several Finite Difference Methods for Systems of Nonlinear Hyperbolic Conservation Laws", J. Computational Physics, Vol. 27, pp. 1-31, 1978.

5.8 Bailey, P.B. and Chen, J., "An Accurate Implicit Finite Difference Algorithm for shocks in Non-Linear Wave Propagation - One Dimension", Wave Motion, Vol. 6, pp. 279-287, 1984.

5.9 Sedov, L.I., Similarity and Dimensional Method in Mechanics, Academic Press, 1959.

5.10 Ames, W.F., Nonlinear Partial Differential Equations in Engineering, Vol. 2, Academic Press, New York, 1972.

5.11 Hansen, A.G., Similarity Analysis of Boundary Value Problems in Engineering, Prentice-Hall, New jersey, 1964.

5.12 Seshadri, R. and Na, T.Y., Group Invariance in Engineering Boundary Value Problems, Springer-Verlag, New York, 1985.

5.13 Seshadri, R., **Group Theoretic Methods of Similarity Analysis Applied to Nonlinear Impact Problems**, Ph.D. Thesis, University of Calgary, Alberta, Canada, 1973.

5.14 Birkhoff, G., **Hydrodynamics**, 2nd Edition, Princeton University Press, Princeton, New Jersey, 1960.

5.15 Moran, M.J. and Gaggioli, R.A., "Reduction of the Number of Variables in Systems of Partial Differential Equations with Auxiliary Conditions", **SIAM J. Appl. Math.**, Vol. 16, pp. 202-215, 1968.

5.16 Moran, M.J. and Marshek, K.M., "Some Matrix Aspects of Generalized Dimensional Analysis", **J. of Engg. Mathematics**, Vol. 6, pp. 291-303, 1972.

5.17 Frydrychowicz, W. and Singh, M.C., "Similarity Representation of Wave Propagation in a Non-Linear Viscoelastic Rod on a Group Theoretic Basis", **Appl. Math. Modelling**, Vol. 10, pp. 284-293, 1986.

5.18 Frydrychowicz, W. and Singh, M.C., "Group Theoretic and Similarity Analysis of Hyperbolic Partial Differential Equations", **J. Math. Anal. Appl.**, Vol. 114, pp. 75-99, 1986.

5.19 Seshadri, R. and Singh, M.C., "Similarity Analysis of Wave Propagation in Nonlinear Rods", **Arch. Mech.**, Vol. 32, pp. 933-945, 1980.

6.1 Richtmyer, R. and Morton, K.W., **Difference Methods for Initial-Value Problems**, Wiley, New York, 2nd Ed., 1967.

6.2 Sucec, J., **Heat Transfer**, WCB, Iowa, 1985.

6.3 White, F.M., **Heat Transfer**, Addison-Wesley, 1984.

6.4 Gere, J.M. and Tiomshenko, S.P., **Mechanics of Materials**, Brooks/Cole Engineering Division, California, 2nd Ed., 1984.

6.5 Bolz, R.E. and Tuve, G.L., **Handbook of Tables for Applied Engineering Science**, The Chemical Rubber Co., Cleveland, 1970.

6.6 Weir, C.E., "Expansivity of Leather and Collagen", **Am. Leather Chemist Association**, Vol. 44, pp. 79-90, 1949.

6.7 Swalin, R.A., **Thermodynamics of Solids**, John Wiley & Sons, New York, 2nd Ed., 1972.

6.8 Lee, E.H., "Some Recently Developed Aspects of Plastic Wave Analysis", in **Wave Propagation in Solids**, The American Society of Mechanical Engineers, New York, pp. 115-128, 1969.

APPENDIX A

DETERMINING THE UNKNOWNS AT THE ORIGIN FOR THE CASE OF CONDUCTING MATERIALS

Generally, assuming that the end of the rod is subjected to a set of prescribed boundary conditions as follows:

Case (i)

$$\begin{cases} \sigma(0,t) = \sigma_o t^\delta \quad ; \quad t > 0 \quad , & \text{(A.1a)} \\ \theta(0,t) = \theta_o \quad ; \quad t > 0 \quad . & \text{(A.1b)} \end{cases}$$

Recalling the jump conditions discussed in part A of Chapter 3:

$$V_1 \rho \| v \|_1 = - \| \sigma \|_1 \quad , \tag{A.2a}$$

$$V_2 \rho \| v \|_2 = - \| \sigma \|_2 \quad , \tag{A.2b}$$

$$V_1 \tau_o \| q \|_1 = K \| \theta \|_1 \quad , \tag{A.2c}$$

$$V_2 \tau_o \| q \|_2 = K \| \theta \|_2 \quad , \tag{A.2d}$$

$$\rho V_1 C_\sigma \| \theta \|_1 + V_1 \alpha T_o \| \sigma \|_1 = \| q \|_1 \quad , \tag{A.2e}$$

$$\rho V_2 C_\sigma \| \theta \|_2 + V_2 \alpha T_o \| \sigma \|_2 = \| q \|_2 \quad . \tag{A.2f}$$

The equations (A.2c,d) imply that:

$$\| q \|_1 = \frac{K}{V_1 \tau_o} \| \theta \|_1 \quad , \tag{A.3a}$$

$$\| q \|_2 = \frac{K}{V_2 \tau_o} \| \theta \|_2 \quad . \tag{A.3b}$$

Substituting equation (A.3a) into equation (A.2e) and simplifying, we obtain:

$$\|\theta\|_1 = \frac{\alpha T_o V_1^2 \tau_o}{(K-\rho C_\sigma \tau_o V_1^2)} \|\sigma\|_1 \quad . \tag{A.4a}$$

Similarly, substituting equation (A.3b) into equation (A.2f) yields

$$\|\theta\|_2 = \frac{\alpha T_o V_2^2 \tau_o}{(K-\rho C_\sigma \tau_o V_2^2)} \|\sigma\|_2 \quad . \tag{A.4b}$$

Adding (A.4a) to (A.4b)

$$\|\theta\|_1 + \|\theta\|_2 = \theta(0,0) = \frac{\alpha T_o V_1^2 \tau_o}{(K-\rho C_\sigma \tau_o V_1^2)} \|\sigma\|_1 + \frac{\alpha T_o V_2^2 \tau_o}{(K-\rho C_\sigma \tau_o V_2^2)} \|\sigma\|_2 \tag{A.5}$$

which leads to

$$\|\sigma\|_2 = \frac{K-\rho C_\sigma \tau_o V_2^2}{\alpha T_o V_2^2 \tau_o} \left\{ \theta(0,0) - \frac{\alpha T_o V_1^2 \tau_o}{(K-\rho C_\sigma \tau_o V_1^2)} \|\sigma\|_1 \right\} \quad . \tag{A.6}$$

Also, from Chapter 3

$$\sigma(0,0) = \|\sigma\|_1 + \|\sigma\|_2 \quad . \tag{A.7}$$

Substituting equation (A.6) in equation (A.7) and manipulating, we have :

$$\|\sigma\|_1 = \frac{V_2^2(\rho C_\sigma \tau_o V_1^2 - K)}{K(V_1^2 - V_2^2)} \sigma(0,0) + \frac{(\rho C_\sigma \tau_o V_1^2 - K)(\rho C_\sigma \tau_o V_2^2 - K)}{\alpha T_o \tau_o K(V_1^2 - V_2^2)} \theta(0,0) \quad . \tag{A.8}$$

After determining the jump in stress across the leading wavefront, other unknowns can be found as follows:

$$\|\sigma\|_2 = \sigma(0,0) - \|\sigma\|_1 \quad , \tag{A.9a}$$

$$\|v\|_1 = -\frac{1}{\rho V_1} \|\sigma\|_1 \quad , \tag{A.9b}$$

$$\|v\|_2 = -\frac{1}{\rho V_2} \|\sigma\|_2 \quad , \tag{A.9c}$$

$\|\theta\|_1$ and $\|\theta\|_2$ are calculated from (A.4a,b), respectively. $\|q\|_1$ and $\|q\|_2$ are then found from (A.3a,b).

Finally,

$$v(0,0) = \|v\|_1 + \|v\|_2 \quad , \tag{A.9d}$$

$$q(0,0) = \|q\|_1 + \|q\|_2 \quad . \tag{A.9e}$$

Case (ii)

$$\begin{cases} v(0,t) = V_o t^{\delta} \quad ; \quad t > 0 \quad , & \text{(A.10a)} \\ \theta(0,t) = \theta_o \quad . & \text{(A.10b)} \end{cases}$$

The procedure is performed as above, however, the value of stress $\sigma(0,0)$ in this case is defined by :

$$\sigma(0,0) = \frac{K(V_1^2-V_2^2)V_1V_2}{V_1^3(K-\rho C_\sigma \tau_o V_2^2) + V_2^3(\rho C_\sigma \tau_o V_1^2-K)} \left\{ -\rho v(0,0) + \left(\frac{1}{V_2} - \frac{1}{V_1}\right) \times \frac{(\rho C_\sigma \tau_o V_1^2-K)(\rho C_\sigma \tau_o V_2^2-K)}{K\alpha T_o \tau_o (V_1^2-V_2^2)} \theta(0,0) \right\} \quad . \tag{A.11}$$

APPENDIX B

DETERMINING THE MASS MATRIX AND STIFFNESS MATRIX FOR A FINITE ELEMENT SCHEME

Recalling the trial function for one element:

$$\phi_1(x) = 1 - \frac{x}{h_I} \quad ; \quad 0 \le x \le h_I \quad , \tag{B.1a}$$

$$\phi_2(x) = \frac{x}{h_I} \quad ; \quad 0 \le x \le h_I \quad . \tag{B.1b}$$

And, the test functions are defined by:

$$w_1(x) = \phi_1(1-\xi_1) + \xi_1 \left[2(2-3\xi_2) - 6(1-2\xi_2)\frac{x}{h_I}\right] \quad , \tag{B.2a}$$

$$w_2(x) = (1-\xi_1)\,\phi_2 \quad , \tag{B.2b}$$

where $0 \le x \le h_I$.

The coefficients of the submatrix of elemental mass matrix $[K_1]_i$ are given as:

$$a_{11} = \int_{h_I}^{h_I} \phi_1 w_1 dx$$

$$= \int_0^{h_I} \left\{\phi_1^2(1-\xi_1) + \xi_1\left[2(2-3\xi_2) - 6(1-2\xi_2)\frac{x}{h_I}\right]\phi_1\right\} dx$$

$$= \left[\frac{1}{3}(1+2\xi_1) - \xi_1\xi_2\right] h_I \quad , \tag{B.3a}$$

$$a_{12} = \int_0^{h_I} \phi_2 w_1 dx$$

$$= \int_0^{h_I} (1-\xi_1)\ \phi_1\phi_2 dx + \int_0^{h_I} \xi_1 \left[2(2-3\xi_2) - 6(1-2\xi_2)\ \frac{x}{h_I}\right] \phi_2\ dx$$

$$= \left[\frac{1}{6}\ (1-\xi_1) + \xi_1\xi_2\right]\ h_I \quad , \tag{B.3b}$$

$$a_{21} = \int_0^{h_I} \phi_1 w_2 dx$$

$$= \int_0^{h_I} (1-\xi_1)\ \phi_1\phi_2\ dx$$

$$= \frac{1}{6}\ (1-\xi_1)h_I \quad , \tag{B.3c}$$

$$a_{22} = \int_0^{h_I} \phi_2 w_2 dx$$

$$= \int_0^{h_I} (1-\xi_1)\ \phi_2\phi_2\ dx$$

$$= \frac{1}{3}\ (1-\xi_1)h_I \quad . \tag{B.3d}$$

For one element, the matrix $[K_1]_i$ is written as:

$$[K_1]_i = \begin{bmatrix} \left\{\frac{1}{3}(1+2\xi_1) - \xi_1\xi_2\right\}h_I & \left\{\frac{1}{6}(1-\xi_1) + \xi_1\xi_2\right\}h_I \\ \frac{1}{6}(1-\xi_1)h_I & \frac{1}{3}(1-\xi_1)h_I \end{bmatrix} . \quad (B.4)$$

When $N_J = 2$, where N_J is number of elements at the level J on the Ot-axis. The mass matrix $[K_1]$ is then assembled as:

$$[K_1]= \begin{bmatrix} \left\{\frac{1}{3}(1+2\xi_1)-\xi_1\xi_2\right\}h_1 & \left\{\frac{1}{6}(1-\xi_1)+\xi_1\xi_2\right\}h_1 & 0 \\ \frac{1}{6}(1-\xi_1)h_1 & \frac{1}{3}(1-\xi_1)h_1+\left\{\frac{1}{3}(1+2\xi_1)-\xi_1\xi_2\right\}h_2 & \left\{\frac{1}{6}(1-\xi_1)+\xi_1\xi_2\right\}h_2 \\ 0 & \frac{1}{6}(1-\xi_1)h_2 & \frac{1}{3}(1-\xi_1)h_2 \end{bmatrix}$$

(B.5)

The stiffness matrix $[K_2]$ is also constructed in the similar manner. The coefficients of the submatrix of elemental stiffness matrix $[K_2]_i$ are:

$$b_{11} = \int_0^{h_I} \frac{d\phi_1}{dx} w_1 \, dx$$

$$= -\frac{1}{h_I}\int_0^{h_I} \left\{\phi_1(1-\xi_1) + \xi_1\left[2(2-3\xi_2) - 6(1-2\xi_2)\frac{x}{h_I}\right]\right\} dx$$

$$= -\frac{1}{2}(1+\xi_1) \quad , \quad (B.6a)$$

$$b_{12} = \int_0^{h_I} \frac{d\phi_2}{dx} w_1 \, dx$$

$$= \frac{1}{h_I} \int_0^{h_I} \left\{\phi_1(1-\xi_1) + \xi_1\left[2(2-3\xi_2) - 6(1-2\xi_2)\frac{x}{h_I}\right]\right\} dx$$

$$= \frac{1}{2}(1+\xi_1) \quad , \tag{B.6b}$$

$$b_{21} = \int_0^{h_I} \frac{d\phi_1}{dx} w_2 \, dx$$

$$= \int_0^{h_I} - \frac{1}{h_I}(1-\xi_1)\,\phi_2 \, dx$$

$$= -\frac{1}{2}(1-\xi_1) \quad , \tag{B.6c}$$

$$b_{22} = \int_0^{h_I} \frac{d\phi_2}{dx} w_2 \, dx$$

$$= \int_0^{h_I} \frac{1}{h_I}(1-\xi_1)\,\phi_2 \, dx$$

$$= \frac{1}{2}(1-\xi_1) \quad . \tag{B.6d}$$

The element matrix $[K_2]_i$ is written as:

$$[K_2]_i = \frac{1}{2}\begin{bmatrix} -(1+\xi_1) & (1+\xi_1) \\ -(1-\xi_1) & (1-\xi_1) \end{bmatrix} , \tag{B.7}$$

and the stiffness matrix $[K_2]$, when $N_J = 2$, is

$$[K_2] = \frac{1}{2}\begin{bmatrix} -(1+\xi_1) & (1+\xi_1) & 0 \\ -(1-\xi_1) & -2\xi_1 & (1+\xi_1) \\ 0 & -(1-\xi_1) & (1-\xi_1) \end{bmatrix} . \tag{B.8}$$